

LA-UR-17-31268

Approved for public release; distribution is unlimited.

Title: Characterization of Shear Properties for APO/MBI Syntactic Foam

Author(s): Reser, Patrick M.

Lewis, Matthew W.

Clark, Jarod Ahuja, Nishant Lenke, Lary R.

Intended for: Report

Issued: 2017-12-14



CHARACTERIZATION OF SHEAR PROPERTIES FOR APO/BMI SYNTACTIC FOAM

Prepared for: Los Alamos National Laboratories Mailstop C926 Los Alamos, New Mexico 87545

Prepared by:

Patrick M. Reser Nishant Ahuja Lary R. Lenke

Revised by:

Matthew Lewis Patrick Reser Jarrod Clark

Department of Civil Engineering University of New Mexico Albuquerque, New Mexico 87131

TABLE OF CONTENTS

Chapter 1 Introduction and Background	1
1.1 Introduction	1
1.2 Nomenclature and Definitions	3
1.3 Specimen Description	5
Chapter 2 Tests Performed and Apparatus Used	7
2.1 Tests	7
2.2 Apparatus	7
2.3 Procedure	12
2.3.1 Uniaxial Compression Test	12
2.3.2 Hydrostatic Compression Test	13
2.3.3 Triaxial Compression Tests Under Various	
2.3.4 General Procedure for the Triaxial Compres	
2.3.5 General Procedure for the Tensile Tests	21
Chapter 3 Material Characteristics and Mechanical	Properties 24
3.1 Mechanical Properties derived from the Triaxia	Compression Tests 24
3.2 Mechanical Properties derived from the Tensile	
3.3 APO/BMI Material Properties and Characteristic	cs 27
Chapter 4 Conclusions	29
Bibliography	30
Appendix A Data Plots for APO/BMI Foam	Al
List of Figures	
Figure 2.1: Wykeham Farrance 1 ton Load Frame	9
Figure 2.2: Wykeham Farrance 10 ton Load Frame	9
Figure 2.3: Placement of Tape to Prevent Membrane D	
Figure 2.4: Placement of Rubber Membrane over Samp	•
Figure 2.5: Placement of O-Rings	14
Figure 2.6: Placement of Longitudinal LVDT Ring	15
Figure 2.7: Connection of Radial LVDT Ring	15
Figure 2.8: Assembled Displacement Apparatus	16
Figure 2.9: Zeroing Devices	16
Figure 2.10: Placement of Containment Rods	17
Figure 2.11: Assembled Triaxial Compression Cell	17
Figure 2.12: Triaxial Compression Cell & 2k Load France	
Figure 2.13: Data Acquisition	19
Figure 2.14: Fracture Angle for Sample 12of36	20
Figure 2.15: Modified Foam Specimen for Tensile Test	
Figure 2.16: Placing Superglue in End Cap	21

Figure 2.17: Placing End Cap on Sample			
Figure 2.18: Assembled Specimen for Tensile Test	22		
Figure 2.19: Tensile Failure of Sample 16of36	23		
Figure 3.1: Composite plot of q vs. ε_1 for APO/BMI Syntactic Foam	28		
Figure 3.2: Composite plot of q vs. p for APO/BMI Syntactic Foam	28		
List of Tables			
Table 1: APO-BMI Syntactic Foam	6		
Table 2.1: Triaxial Compression Tests Performed	7		
Table 2.2: Test Equipment	8		
Table 3.1: Tensile Test Results	27		
Table 3.2: Determined Hydrostatic Yield from Hydrostatic Compression Tests	27		

CHAPTER 1

INTRODUCTION AND BACKGROUND

1.1 INTRODUCTION

Triaxial compression testing is a means for mechanical characterization of a material. A unique feature of the triaxial compression test is the application of two different magnitudes of compressive pressures on the material simultaneously. The material behavior under these different compressive pressures can be monitored over time. Several important characteristics of the material, such as stress yield values and the shear failure envelope may then be determined. Also mechanical properties such as Poisson's ratio, Young's modulus and bulk modulus can be determined from the triaxial compression test.

The triaxial compression test was employed in this investigation to characterize the shear behavior, shear failure envelope, and mechanical properties of a syntactic foam. Los Alamos National Laboratory (LANL) supplied a total of 36 samples of APO-BMI syntactic foam to the University of New Mexico, Department of Civil Engineering for testing between December 2003 and May 2004.

Each sample had a diameter of 1.395 ± 0.005 in. $(3.543\pm0.013\text{cm.})$ and a length of 2.796 ± 0.004 in. $(7.102\pm0.010 \text{ cm.})$. The samples had an average density of 0.295 g/cm^3 . Additional information about the material tested in this investigation can be found in the "Specimen Description" section contained in Chapter 1. The nomenclatures used in this study is presented in Chapter 1.

In addition to designing and implementing triaxial compression tests capable of up to 2,000 psi. confining pressure (minor principal stress) and roughly 13,000 psi. in axial pressure (major principal stress), a pure tension test was designed and conducted on the foam material. The purpose of this pure tension test was to obtain maximum tensile stress values to enhance the characterization of the shear envelope in the stress space. The sampling procedure and specimen preparation for a standard test can be found in the American Society for Testing Materials (ASTM) D 5379/D 5379-93. The above tests mentioned and their procedures are discussed in Chapter 2.

Chapter 2 contains the types of tests performed and the apparatus used for testing the material. Chapter 2 also has a brief explanation of the equipment and the procedures used for conducting the tests. In Chapter 3, the material characteristics and mechanical properties obtained from the tests are described; composite plots of deviatoric vs. mean stress and deviatoric stress vs. longitudinal strain are also included. The plots of deviatoric stress vs. mean

stress clearly identify the shear envelope for the material. Chapter 4 summarizes the vital information obtained from the tests and the conclusions made.

All the necessary plots and the data generated during the testing have been included in the Appendix. The information in the appendix includes plots of: Strain vs. Time, Stress vs. Time, Stress vs. Strain, Mean Stress vs. Volumetric Strain, Lateral Strain vs. Longitudinal Strain, and q vs. p. Bulk modulus, Poisson's ratio, and Young's modulus are displayed in the appropriate plots in each appendix.

1.2 NOMENCLATURE AND DEFINITIONS*

Hydrostatic Yield (σ_{HY}) – Determined yield stress of the foam material under hydrostatic compression.

Major Principal Stress (Major Effective Stress) (σ_1) – The pressure applied to the specimen in the longitudinal direction by a piston and the hydraulic fluid within the triaxial compression cell.

Minor Principal Stress (Minor Effective Stress, Confining Pressure) (σ_3) – The pressure applied to the specimen by hydraulic fluid in triaxial compression cell.

Major Principal Strain (ε_1) – Change in length (longitudinal) divided by the original length.

Gauge Length (L_g) – Original length of the specimen, used to calculate the major principal strain (ϵ_1) .

Minor Principal Strain (ε_3) – Change in radius divided by the original radius.

Gauge Radius (R_g) – Original radius of the specimen used to calculate the minor principal strain (ε_3).

Poisson's Ratio (ν) – The ratio of the radial (lateral) strain to the longitudinal strain.

Young's Modulus (E) – The ratio of stress to strain.

Mean Stress (p) – Average of the stresses acting on the specimen.

Deviatoric Stress (q) – The difference between the major principal stress and the minor principal stress.

Volumetric Strain (ε_v) – The sum of the major principal strain and twice the minor principal strain.

Bulk Modulus (k) – Ratio of the mean stress to volumetric strain

Piston Load (P) – The load applied longitudinally on the specimen by the piston.

Piston Diameter (ϕ_{PD}) – The diameter of the piston used for applying pressure to the specimen in the longitudinal direction.

Specimen Diameter (ϕ_{SD}) – The diameter of the foam specimen.

Radius of Specimen (r_s) – Average radius of the foam specimen.

Pore Pressure (\mathbf{u}) – The back pressure generated from the specimen if moisture is present within it's pores.

Sample Area (A_s) – The cross sectional area of the specimen.

Stress Concentration Factor (**K**) – Stress concentration factor, for the "dog bone" shaped sample, used to calculate the maximum stress from the average stress in the tensile test.

Average Tensile Stress (σ_{AVG}) – The measured average tensile stress from the tensile test.

Area of Sample (A_m) – The cross sectional area of the specially designed tensile test specimen at mid length.

Max Tensile Force (W) – The tensile force that caused the specimen to fail in tension.

Maximum Tensile Stress (σ_{MAX}) – Calculated maximum tensile stress from K and σ_{AVG} .

Linear Variable Differential Transducer (LVDT) – An Electronic device used to measure the voltage difference that is then converted to the actual displacements using calculated sensitivities.

American Society of Testing Materials (ASTM)

^{*}Note: all positive values reference compression testing.

1.3 SPECIMEN DESCRIPTION

Syntactic foams are composite materials formed by mechanically combining manufactured material bubbles or micro-spheres with a binder phase. They are referred to as syntactic because the micro-spheres are arranged together in this process while conventional foam or blown foam is created by injecting gas into a liquid slurry of resin.

The APO/BMI syntactic foam tested consists of carbon microballoons and a thermosetting resin binder phase. It is different from most other syntactic foams because of the high void volume fraction in the binder phase. The desired dimensions for all the samples were 7.112 cm (2.8 in.) in length and 3.556 cm (1.4 in.) in diameter. The actual length, diameter and mass of all the APO-BMI syntactic foam samples were measured prior to testing and these measurements are displayed in Tables 1. The diameter was measured in two orthogonal directions and the average diameter was calculated. Densities and volumes were calculated using standard formulas.

Various triaxial compression tests were performed on these foam samples in an effort to probe the stress space and develop a representative shear failure envelope. In addition, tension tests were also performed to generate a better determination of the shear envelope for the foam material. The test matrix for the foam samples is illustrated in Table 1 (for additional information about the test matrix see Chapter 2). Also displayed in the table is the test date, the measured mass, calculated density and volume of each sample. Before conducting the tests on the foam samples, they were numbered and randomly selected to determine test category. This is explained in more depth in Chapter 2 but is mentioned here because of its relevance to Table 1.

In this study, the specimen had three principal directions, the major principal direction and two minor principal directions. Each direction was orthogonal to the others; however, due to the limitations of the pressure application apparatus in the triaxial compression test the applied minor principal stresses were always equal. The major principal direction coincides with the longitudinal direction of the specimen while the minor principal directions coincide with radial directions orthogonal to the longitudinal axis. The minor principal stress is applied radially to the sample and is referred to as σ_3 while the major principal stress is applied longitudinally and is referred to as σ_1 . The same is true for the minor and major principal strains that are referred to as ε_3 and ε_1 respectively.

Table 1 APO-BMI Syntactic Foam

Bag	Sample	Test	Weight	Height	Mid Dia.	Mid Dia.	Avg. Dia.	Density	Volume
		Number	(g)	(cm.)	1 (cm.)	2 (cm.)	(cm.)	(g/cm^3)	(cm ³)
	1	12	20.513	7.117	3.556	3.556	3.556	0.290	70.683
	2	33	20.463	7.112	3.548	3.548	3.548	0.291	70.330
	3	8	20.440	7.112	3.533	3.541	3.537	0.293	69.878
	4	11	20.597	7.109	3.553	3.551	3.552	0.292	70.456
Bag 1	5	35	20.434	7.109	3.569	3.556	3.562	0.288	70.860
	6	32	20.355	7.107	3.571	3.561	3.566	0.287	70.986
	7	23	20.509	7.117	3.543	3.541	3.542	0.292	70.129
	8	7	20.369	7.112	3.543	3.546	3.545	0.290	70.179
	9	3	20.411	7.097	3.543	3.543	3.543	0.292	69.979
	10	25	21.244	7.107	3.543	3.543	3.543	0.303	70.079
	11	6	21.153	7.104	3.541	3.541	3.541	0.302	69.953
	12	17	21.365	7.094	3.543	3.543	3.543	0.305	69.954
	13	28	21.383	7.107	3.538	3.538	3.538	0.306	69.878
Bag 2	14	19	21.389	7.109	3.541	3.541	3.541	0.306	70.003
	15	21	21.150	7.112	3.541	3.541	3.541	0.302	70.028
	16	34	21.203	7.087	3.541	3.541	3.541	0.304	69.778
	17	14	21.471	7.117	3.538	3.541	3.539	0.307	70.028
	18	5	21.274	7.099	3.541	3.543	3.542	0.304	69.954
	19	26	20.441	7.109	3.533	3.526	3.529	0.294	69.552
	20	16	20.461	7.112	3.538	3.538	3.538	0.293	69.928
	21	1	20.625	7.112	3.546	3.543	3.545	0.294	70.179
D 2	22	4	20.402	7.112	3.548	3.548	3.548	0.290	70.330
Bag 3	23	31	20.467	7.112	3.541	3.541	3.541	0.292	70.028
	24	27	20.323	7.109	3.543	3.543	3.543	0.290	70.104
	25	20	20.553	7.112	3.543	3.538	3.541	0.293	70.028
	26	15	20.522	7.112	3.543	3.543	3.543	0.293	70.129
	27	13	20.041	7.112	3.536	3.523	3.529	0.288	69.577
	28	29	20.674	7.112	3.543	3.541	3.542	0.295	70.079
Bag 4	29	10	20.705	7.111	3.543	3.543	3.543	0.295	70.119
	30	36	20.114	7.084	3.546	3.546	3.546	0.287	69.964
	31	2	20.598	7.115	3.543	3.543	3.543	0.294	70.154
	32	30	20.701	7.104	3.541	3.543	3.542	0.296	70.004
	33	18	20.845	7.109	3.541	3.543	3.542	0.298	70.054
	34	9	20.448	7.115	3.546	3.545	3.546	0.291	70.245
	35	22	20.768	7.112	3.541	3.538	3.539	0.297	69.978
	36	24	20.781	7.112	3.538	3.541	3.539	0.297	69.978

CHAPTER 2

EXPERIMENTAL METHODS

2.1 TESTS

In an effort to develop a shear envelope for the APO-BMI syntactic foam, different areas in the stress space were probed using numerous triaxial compression tests. Hydrostatic compression tests were performed on some foam samples first to obtain a hydrostatic yield for the material. A hydrostatic compression test applies equal pressures in all principal directions, resulting in the major and minor principal stresses being equal (Hibbeller). Based on the determined value of hydrostatic yield, the test matrix was specified. The matrix included several triaxial compression tests that were performed with the minor principal stress held constant at various percentages of the hydrostatic yield while increasing the major principal stress. For instance, for one test the confining pressure was increased gradually to 500 psi. then held constant while increasing the major principal stress. Table 2.1 illustrates the triaxial compression tests performed on the APO-BMI Foam samples.

Table 2.1 Triaxial Compression Tests Performed

Hydrostatic Test
Uniaxial
Confining pressure of 50 psi.
Confining pressure of 100 psi.
Confining pressure of 300 psi.
Confining pressure of 500 psi.
Confining pressure of 650 psi.
Confining pressure of 800 psi.

Throughout each of the triaxial compression tests the major and minor principal stresses and the strains were continuously monitored and recorded every second by the data acquisition system. The specifics of this data acquisition system and related apparatus are discussed in the following section.

2.2 APPARATUS

The equipment used to perform the triaxial compression and tensile tests is located in the Civil Engineering Materials Laboratory at the University of New Mexico (CEML-UNM). Table 2.2 contains the identification, description and serial numbers of every piece of equipment used in this study.

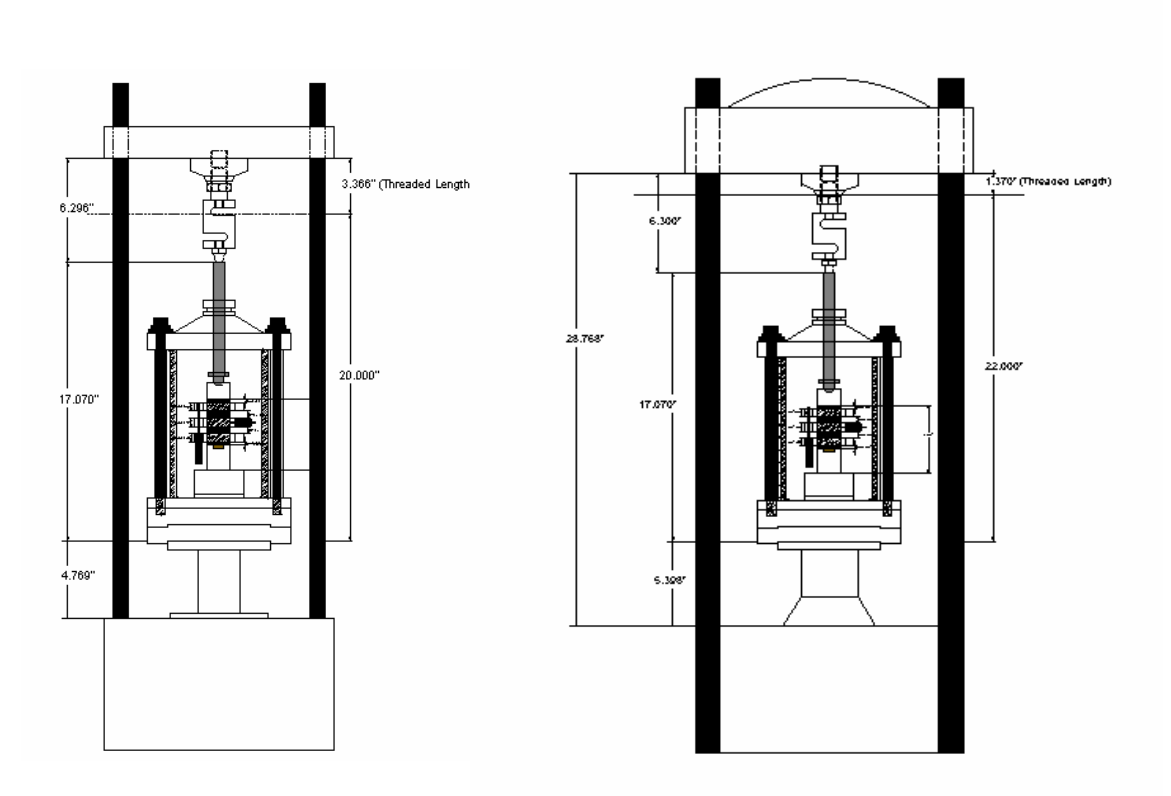
Table 2.2 Test Equipment

Item	Description	Serial Number(s)
Triaxial Compression Load Frame 10 ton	WYKEHAM FARRANCE 10 TON	136371
Triaxial Compression Load Frame 2 ton	WYKEHAM FARRANCE 1 TON	D2995/2
Pressure Gauge	Kulite 4449 (2000 psi)	N/A
	Sensate Pressure Gauge (10,000 psi)	379003
Pressure Gauge	STANDARD TEST GAUGE, 125 psi Model 2UH2	400
Pore Pressure Transducer	Kulite (500 psi)	N/A
Radial Linear Variable Transducer	Schaevitz LVDT Radial (±0.010 in)	J2871
	Schaevitz LVDT Radial (±0.010 in)	J2870
	Schaevitz LVDT Radial (±0.010 in)	J2857
	Schaevitz LVDT Radial (±0.010 in)	
Longitudinal Linear Variable Transducer	Schaevitz LVDT Longitudinal (±0.0250 in)	6676
Transducci	Schaevitz LVDT Longitudinal (±0.0250 in)	6690
	Schaevitz LVDT Longitudinal (±0.0250 in)	6676
Manual Pressure Pump	Used to apply confining pressure	N/A
Triaxial Pressure Cell		N/A
Hardware	National Instruments Data Acq. Card (2), PCI 6043E	
	National Instruments Strain Gauge Input Card (1), SC-2043-SG	
	Servo Console Model 447	
	Tektronic PS280 DC power supply	
Personal Computer w/ Digital Data Acquisition	HP Vectra Vli8 w/Pentium III (500 MHz), Windows NT	US95204538
Software	National Instruments Lab View (Windows NT)	N/A
Caliper (length and diameter)		
Platform Scale	Scale name	3822
	Scale name	14834302
Load Cells	Sensotronics 2K load cell model 60001A2k-1000	1169801
	Sensotronics 10K load cell model 60001A10k-1000	1169800
Tension End Caps	End caps used to hold sample for Tensile test	N/A

When conducting tests with low values of major principal stress, the Wykeham Farrance 1 ton machine (see Figure 2.1) was used and for high values of the major principal stress, the 10-ton machine was used (see Figure 2.2). A plexiglas shell was used for conducting the triaxial tests with confining pressures below 200 psi., an aluminum shell was required for tests above 200 psi. The Plexiglas allowed the observation of the foam sample in the triaxial compression cell. Apart from visually observing the progress of the test, Linear Variable Differential Transducers (LVDTs) were used to measure the longitudinal and radial displacement of the sample. The radial LVDT's had a range of \pm 0.10-inches while the longitudinal LVDT's had a range of \pm 0.25-inches. Both were connected to the data acquisition system via electronic feedthroughs located at the base of the testing apparatus. The LVDT displacements were recorded at second intervals throughout each test.

Figures 2.1 and 2.2 Wykeham Farrance 1 ton and 10 ton Load Frames for Triaxial Compression Testing

Fig.2.1 Fig.2.2



The data acquisition system used an HP Vectra PC with National Instrument's Labview software. A program was created in Labview to record the pressure and LVDT measurements as a data file. The load cells measured the axial load on the sample. This value was then used along with the confining pressure to calculate the major principal stress. The pressure gauges

were used to measure the confining pressure as well as the pore pressures which were further used to calculate the effective major and minor principal stresses. The LVDT's were used to measure the displacements of the samples. Each of the measurements was recorded in voltage and converted by the Labview program to the desired units using calculated sensitivities. Scales were used to measure the mass of each sample and calipers to measure the dimensions before and after the each test.

The triaxial compression cell was specifically designed to house specimens measuring 2.80 in. long and having a diameter of 1.40 in. Due to the electronics involved in this study, hydraulic fluid was used for applying the confining pressure rather than water. The pressure within the cell was increased and controlled manually using a hydraulic hand pump.

The high-pressure triaxial compression cell was made of aluminum (T6061). The cell height was 9.375 in. while the inner and outer diameters measured 5.25 and 6.00 in., respectively. This cell was suitable for use with confining pressures up to 2,000 psi. The cell contains an end cap with a means of applying an axial load to the specimen through a piston with a diameter of 0.75 in. The base plate of the cell contains 9 single pole electronic feedthroughs with fusite fittings that mate to the LVDT's. The base plate also contains feeder valves for inserting and regulating hydraulic fluid, monitoring cell pressure, and monitoring pore pressure.

The Sensotec 10,000 psi. pressure gauge and the Kulite 5,000 psi. pressure gauge were used for monitoring confining pressure. The 500 psi. Kulite pore pressure transducer was used to monitor the pore pressure and measure the fluid pressures within the specimen.

Wykeham Farrance 10 ton and 1 ton load frames capable of applying axial compression load at variable rates were used to increase the major principal stress to the specimen. Rates for this test vary from $6.0x10^{-3}$ in/min to $6.3x10^{-3}$ in/min corresponding to strain rates of $2.143x10^{-3}$ min⁻¹ to $2.250x10^{-3}$ min⁻¹. 10,000-lb and 2,000-lb Sensotronic load cells were used to measure the axial loads on the specimen applied by the Wykeham Farrance 10 ton and 1 ton load frames, respectively.

Longitudinal and radial (lateral) LVDT's were used to measure the sample's vertical and horizontal deformation. Three aluminum rings were used to hold and maintain the positions of the LVDT's around the sample.

Thin Teflon disks having the same diameter as the sample were placed on both ends between porous stones and the sample. The two porous stones, both having a diameter of 1.4-inches and thicknesses of 0.25 in. and 0.125 in., were used to separate the specimen from the pedestal and the end cap. A seamless rubber membrane in the form of a tube, open at both ends, of diameter equal to that of the specimen and of length approximately 2 in. greater than the height of the specimen was used to keep the specimen free of hydraulic fluid during the test. The thickness of the rubber membrane was approximately 0.012 in. The rubber membrane was

placed on the sample using a membrane stretcher to suit the size of the specimen. Four rubber Orings were used to fasten the rubber membrane to the end cap and pedestal and prevent the intrusion of hydraulic fluid. Six spacer blocks and knurled nuts were used to position the LVDT's consistently for each test, thus maintaining a longitudinal gauge length of 1.9 in.

2.3 PROCEDURE

The APO/BMI foam samples, having a diameter of 1.4 in. and length of 2.8 in., were delivered from LANL to CEML-UNM in a single shipment containing four bags of nine samples. The samples were immediately inspected for defects, measured, weighed, recorded and stored in sealed plastic bags at ambient temperature until testing. Their data were recorded. Each bag was numbered from 1 to 36 to properly identify and associate a given test with each sample. Randomly selecting and removing the labeled samples from the box containing them determined the order in which each sample would be tested. A matrix was developed to perform a series of triaxial compression, uniaxial compression, and tension tests in the same systematic and methodical manner that was used for testing CMB and Polyurethane foams in the past.

Prior to testing, each sample was again inspected, dimensioned, and weighed, the data were recorded. The volume and density of each sample was then calculated using conventional formulas for volume of a cylinder and density, shown in Equations 2.1 and 2.2 respectively.

Equation 2.1
$$V = \frac{h * (\pi * \phi_{SD}^2)}{4}$$

Equation 2.2
$$D = \frac{M}{V}$$

In the above equations h is the height of the specimen, π is the value of pi, D is density, M is mass of the specimen, and V is the volume of the specimen.

The types of compression tests performed included uniaxial compression, hydrostatic compression, and several triaxial compression tests under a variety of confining pressures. The tensile test was conducted to determine the average tensile stress present at failure and from that value along with the stress concentration factor the maximum stress was calculated. The description and general procedures used in performing these tests are included in the following sections.

2.3.1 UNIAXIAL COMPRESSION TEST

In the uniaxial compression test, the major principal stress was increased while the minor principal stress maintained a zero. No hydraulic fluid was used in the triaxial compression cell. Constant compression being applied to the sample from the base below and the load cell above increased the major principal stress. The pedestal maintained a constant vertical velocity of 0.006-inch/min and a strain rate of 2.143x10⁻³ min⁻¹.

2.3.2 HYDROSTATIC COMPRESSION TEST

Hydraulic fluid was used in the hydrostatic compression testing to maintain a constant pressure value in all directions. A hydraulic hand pump was used to increase the pressure within the triaxial compression cell at a constant rate, often stopping every 25, 50 or 100 psi. to equilibrate. The predetermined hydrostatic yield of the foam was then used to specify the triaxial compression test matrix. The matrix consisted of tests performed at confining pressures that were 90%, 65%, 37.5%, and 12% of hydrostatic yield.

2.3.3 TRIAXIAL COMPRESSION TESTS UNDER VARIOUS CONFINING PRESSURES

The triaxial compression test required the technician to initially obtain the desired confining pressure before applying the axial load. This was accomplished using the hydraulic hand pump as in the hydrostatic compression tests. Once the desired confining pressure was attained it was held constant while the axial load on the sample was increased at a strain rate of $2.143 \times 10^{-3} \, \text{min}^{-1}$, thus increasing the major principal stress until either the sample failed or a desired value was obtained. The axial load was then moved prior to releasing the hydrostatic pressure to a value of zero.

2.3.4 GENERAL PROCEDURE FOR THE TRIAXIAL COMPRESSION TESTS

Before any testing was conducted, test forms were prepared. Each form included filename, date, type of test being run, and dimensions of the sample, along with the test protocol. The specimen's diameter, length, and mass were measured. Then all hydraulic fluid was removed from pedestal and end cap with a cloth rag. The 0.25-in. thick porous stone was then placed on the pedestal followed by a Teflon pad and the foam specimen. A Teflon pad was then placed on top of the sample, followed by the 0.125 in. porous stone and the end cap. The intersection of the porous stones with the Teflon and the foam specimen were then wrapped with electrical tape to prevent a breach of the rubber membrane during a test (as depicted in Figure 2.3).

Figure 2.3 Placement of Tape to Prevent Membrane Damage



The rubber membrane was then placed in a suction device and over the sample, ensuring that the rubber membrane was centered longitudinally along the length of sample as in Figure 2.4.

Figure 2.4 Placement of Rubber Membrane over Sample



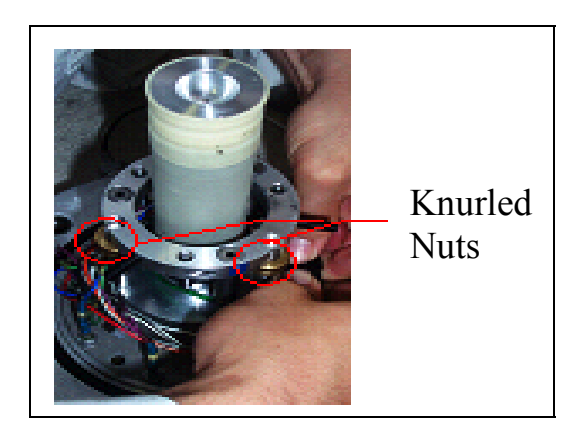
The rubber membrane was then removed from the suction device and unrolled along the sample. It was folded up from the base of pedestal to form a double layer of membrane extending from the base to about 1.75 in. in the vertical direction. The O-rings were stretched around the suction device and placed over membrane-covered sample before being slid into their respective pedestal grooves. In the same manner the membrane was folded from the top of the end cap downwards in order to have a little over an inch of double-layered membrane, which is illustrated in Figure 2.5.

Figure 2.5 Placement of O-rings



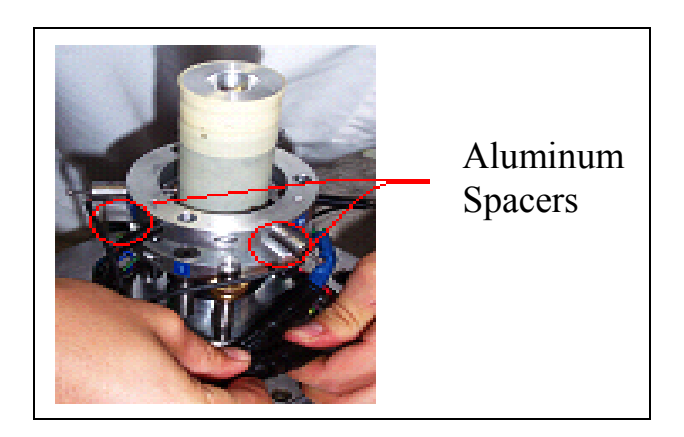
The knurled nuts were then placed on the positioning rod at 1.96 in. from bottom. This distance was measured from bottom resting position to the top of knurled nut using a caliper with a resolution of .001 in. The lower longitudinal LVDT ring was then placed on the knurled nuts, making sure the LVDT wires were connected and not obstructing LVDT cores as shown is Figure 2.6.

Figure 2.6 Placement of Longitudinal LVDT Ring



While pressing down lightly on LVDT ring with one hand, the spring plungers were tightened with the other hand. The ring spacers were then placed on top of the longitudinal LVDT's (equally spaced and not over LVDT cores) followed by lateral LVDT ring taking care to match holes on this ring to those used for longitudinal cores (Figure 2.7).

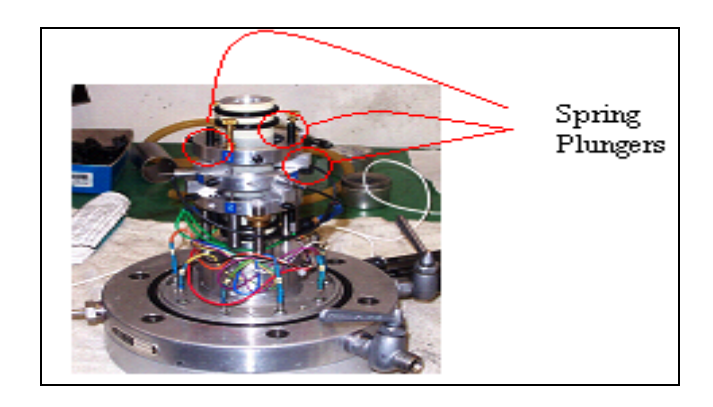
Figure 2.7 Connection of Radial LVDT Ring



The spring plungers were then tightened to the desired position. Another set of ring spacers were placed over the lateral (radial) LVDT ring in such a way that none would interfere with the longitudinal LVDT rods.

The next set of O-rings was then placed around the exterior of the suction device and placed on the end cap grooves over the rubber membrane. This was followed by the placement of the longitudinal LVDT ring (containing longitudinal rods and cores on spacers), taking care to align rods and cores to their respective LVDT's as shown in Figure 2.8.

Figure 2.8 Assembled Displacement Apparatus



The ring was centered on the sample and each spring plunger was tightened to the desired position. The LVDT's were then connected to the Servo Console Model 447 and data acquisition card (DAQ) card 2.

The knurled nuts were loosened and the centering rods and spacers were removed. The LVDT cores were then centered (adjusted until a value of zero was observed on the digital display of the Servo 447) to a tolerance of about 0.001 in. Zeroing of the lateral LVDT's was accomplished by adjusting the lateral cores individually in or out of the ring. Each longitudinal LVDT was adjusted using the corresponding "jam nut" on top of the longitudinal LVDT ring. Both of these devices are pointed out in Figure 2.9 below.

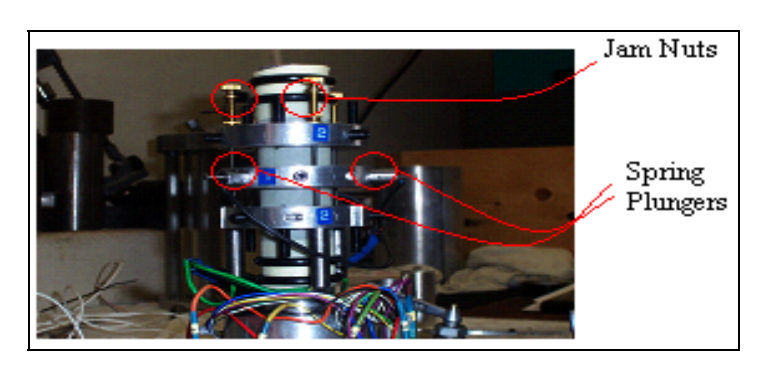


Figure 2.9 Zeroing Devices

Two triaxial cell rods were then placed directly across from one another into the base plate, leaving 11½ inches of rod protruding vertically from the base plate as shown in Figure 2.10.

Figure 2.10 Placement of Containment Rods



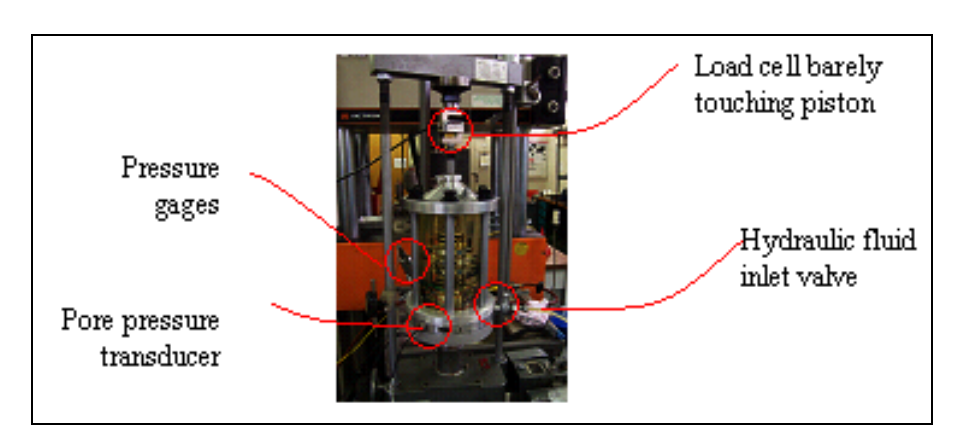
The slots in the triaxial cell cover were then matched with the two rods extruding from the base plate and slid down to the base of the rods. The remaining rods were then inserted and threaded to match the same height as the first two rods. Washers and nuts were then placed on each rod and tightened (using a torque wrench) to 30 ft-lbs as shown in Figure 2.11.

Figure 2.11 Assembled Triaxial Compression Cell



The bleeder valve on top of the triaxial cell was opened. The triaxial cell was then placed on the load frame. Then, the pressure gauges were connected to the base of the triaxial compression cell. The hydraulic fluid hose was then connected to the fill valve on the base and hydraulic fluid was transferred to the triaxial compression cell. Fluid was forced into the cell using compressed air until fluid escaped from the bleeder valve on top of the cell. This process is demonstrated in Figure 2.12.

Figure 2.12 Triaxial Compression Cell & 2k Load Frame

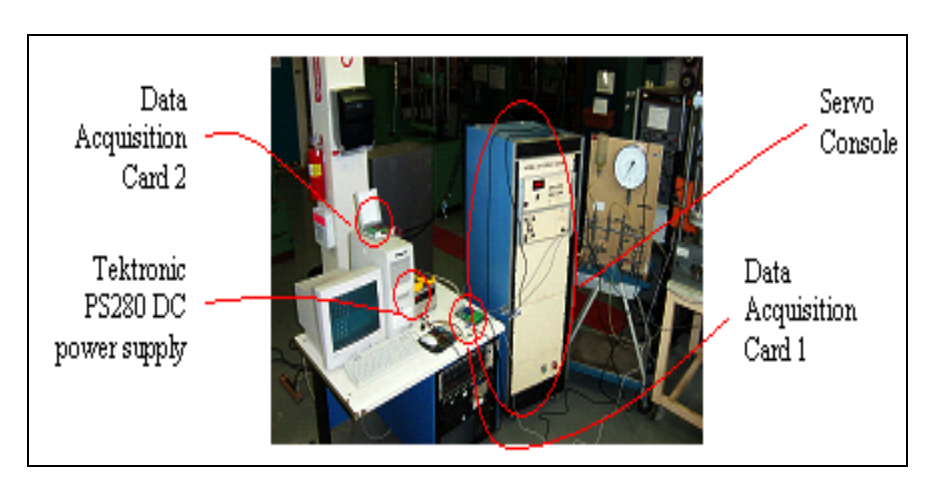


The Tektronic PS280 DC power supply was then connected to DAQ card 1 using positive and negative signal wires. At this point, the base was raised manually until the load cell was barely touching the protruding piston of the triaxial cell as shown in Figure 2.12.

The pressure gauge wires were then connected from the triaxial cell to their respective slots in DAQ card 1. The load cell wires were also connected to their respective slot in DAQ card 1 (The 10k-load cell was connected to channel 2, while the 2k-load cell was connected to channel 1, the Kulite 4449 and 4450 pressure gauges were connected to channels 4 and 5, respectively while the Sensotech pressure gauge was connected to channel 3. The Kulite pore pressure gauges 1 and 2 were connected to channels 6 and 7). Each channel consisted of four slots: negative excitation, negative signal, positive signal, and positive excitation. In our system, the black-coated wire was the negative excitation signal, the white-coated wire was negative signal, the green-coated wire was the positive signal and the red-coated wire was the positive excitation signal.

With the power supply engauged and the voltmeter connected to the power supply, the voltage output was monitored and refined to a voltage output that was as close to 10.000 volts as possible. DAQ card 1 was then turned on. The hydraulic hand pump was connected to the triaxial compression cell, at which point the Labview data acquisition software "LATTDataAcq1mod.vi" was opened and operated by selecting Operate, Run, and designating a file name to store collected data. The data acquisition system is shown in Figure 2.13.

Figure 2.13 Data Acquisition



The bleeder valve was closed on the top of the testing cell and all valves were double-checked to verify that all pertinent gauges were connected and their respective valves were open.

At this point the confining pressure was increased by equal increments every 2 minutes until the desired confining pressure was obtained for the triaxial shear test. If performing the hydrostatic test, the confining pressure was increased until the longitudinal LVDT's reached their maximum displacement value. If performing a uniaxial compression test, the only pressure involved is that from the load frame and no hydraulic fluid was necessary. The specimen was then loaded axially by engaging the load frame to begin applying the major principal stress. The sample was continuously loaded until the desired response was achieved. In most cases, loading continued until the longitudinal LVDT's reached their voltage limit of 10 volts. The load was then halted by disengaging the load frame followed by moving the load switch to "reverse" while maintaining a constant pressure. Once the major principal stress was equivalent to the minor principal stress, an additional amount of time was allotted before the confining pressure was decreased.

Next, the inline needle valve was closed and the valve on the hydraulic hand pump was opened slightly. The inline needle valve was then opened slightly until pressure began to be relieved from the triaxial compression cell at a desired rate. After all the confining pressure had been removed, the bleeder valve on top of the triaxial compression cell was removed.

The hydraulic fluid inlet line from hydraulic hand pump to testing cell was removed and the line used to drain the triaxial compression cell was connected. The valve connecting to this line was then opened and the hydraulic fluid drained. The pore pressure wire was disconnected from DAQ card 1 and the triaxial compression cell was moved from load frame to a table for disassembly.

All 6 retaining nuts were removed from the rods, and four opposing rods were unscrewed from base. Two opposing rods were left in place as a guide for sliding the cell up and off of the base. Once the cell was off, these rods were removed from the base.

The retaining screws from the top LVDT ring were unscrewed and the ring was slid up and off of the sample. A rag was used to remove excess hydraulic fluid from the ring. The middle LVDT ring connected to the base plate was disconnected and the retaining screws were unscrewed to remove the ring from the sample. The bottom LVDT ring was disconnected from the base plate and its retaining screws were unscrewed and removed. Using a sharp scalpel, an incision was made between the lower porous stone and the lower pedestal, cutting through the rubber membrane and electrical tape. The sample was then completely removed from the base plate and was prepared for inspection.

Using surgical scissors, the rubber membrane was carefully cut along its entire length from bottom to the top, taking care not to gouge the sample. Next, the rubber membrane was carefully removed from the sample, keeping hydraulic fluid from contaminating it. The sample was positioned on a white background that displayed the sample ID. Photos were then taken from various angles to display fracture angle, type of failure, etc. One of these photos is displayed in Figure 2.14 below. The sample was then placed in its original Ziploc bag and stored with remaining samples of the same batch.

Figure 2.14 Fracture Angle for Sample 12of36



2.3.5 GENERAL PROCEDURE FOR THE TENSILE TEST

The tensile test was conducted using a modified sample, shaped similar to an hour-glass (see Figure 2.15) designed to produce a maximum stress at the midsection of the sample. Each end of the sample was glued into an end cap using cyanoacrylite adhesive (super glue) and a spray-on accelerator.

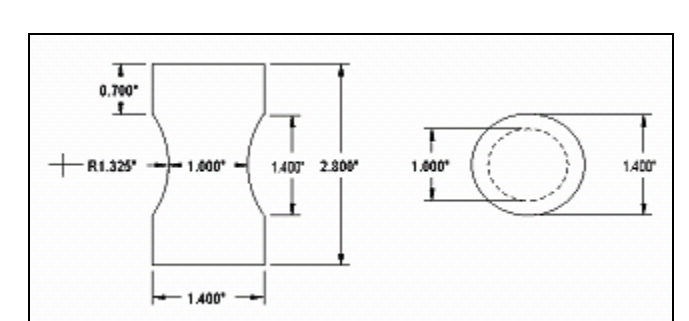


Figure 2.15 Modified Foam Specimen for Tensile test

Prior to applying glue, the ends of the specimen were sprayed with an accelerator. The purpose of the accelerator was to develop an instant bond between the two materials to ensure proper alignment. After 15 seconds the superglue was placed inside the end cap as shown in Figure 2.16, followed by the sample as in Figure 2.17.



Figure 2.16 Placing Superglue in End cap

Figure 2.17 Placing End cap on Sample



This was repeated for the opposite end of the specimen and the second end cap as shown in Figure 2.18.

Figure 2.18 Assembled Specimen for Tensile Test



In the tensile test, the specimen was suspended vertically by one end cap and weight was added slowly to the other end cap. Weight was continuously added until the specimen failed under tension, shown in Figure 2.19 on the following page.

Figure 2.19 Tensile Failure of Sample 16of36



The weight that caused the foam to fail was then measured and the average stress σ_{avg} calculated using this measured weight and the area at the fracture location. The specifics and equations for the calculation of σ_{avg} and the max stress σ_{max} are given in Chapter 3.

CHAPTER 3

MATERIAL CHARACTERISTICS & MECHANICAL PROPERTIES

3.1 MECHANICAL PROPERTIES DERIVED FROM THE TRIAXIAL COMPRESSION TESTS

The confining pressure applied to the sample was measured with the pressure gauge. Recall that all values are positive in compression. To determine the effective principal stress, the pore pressure, u, within the sample is subtracted as shown in Equation 3.1.

Equation 3.1
$$\sigma_3' = \sigma_3 - u$$

Three pressures make up the effective major principal stress, the confining pressure, the longitudinal pressure applied to the specimen by the load frame, and the pore pressure.

Equation 3.2
$$\sigma'_1 = \sigma_3 * \left(1 - \left(\frac{\phi_{PD}}{\phi_{SD}} \right)^2 \right) + \frac{P}{A_s} - u$$

The main contributor to the effective major principal stress is the confining pressure and the pressure applied to the specimen by the load frame, where P is the force applied by the load frame and A_s is the surface area over which this force acts. The values of the major and minor principal stress are needed to calculate other parameters. A measure of the deviatoric stress is twice the maximum shear stress. This value is denoted as q, as defined in Eq. 3.3. For the hydrostatic compression tests the q is zero because in this case $\sigma_1 = \sigma_3$. For the uniaxial test, $q = \sigma_1$.

Equation 3.3
$$q = |(\sigma_1 - \sigma_3)|$$

The mean stress p is the average of the 3 principal stresses applied to the sample. Due to the limitations of the triaxial compression tests the stresses in two of these principal directions are always equal. Thus, the effective minor principal stress is accounted for two times in Equation 3.4.

Equation 3.4
$$p = \frac{\left(\sigma_1 + 2 * \sigma_3\right)}{3}$$

Plots of p vs. q for are found in the Appendix while a composite plot of p vs. q is found in Figures 3.1 and 3.2.

The major principal strain was calculated using a gauge length L_{g} of 1.9-inches in Equation 3.5.

Equation 3.5
$$\epsilon_1 = \frac{\Delta L_g}{L_g}$$

Three major principal strains were calculated from the deformation values ΔL_g obtained from the three longitudinal Linear Variable Differential Transducers (LVDTs). These strains were then added together and divided by 3 to obtain the average major principal strain.

The minor principal strain was calculated using a measured gauge diameter D_g that was divided by 2 to obtain the gauge radius R_g of specimen. The change in R_g divided by the gauge radius is the minor principal strain, Equation 3.6.

Equation 3.6
$$\varepsilon_3 = \frac{\Delta R_g}{R_g}$$

Again, the three radial LVDTs were used to measure ΔR_g and to calculate three lateral strains and used to obtain the average minor principal strain.

The volumetric strain is calculated in much the same manner as the mean stress was but rather than use stress the strain is used, and the total is not divided by three.

Equation 3.7
$$\varepsilon_{v} = (\varepsilon_{1} + 2 * \varepsilon_{3})$$

From the volumetric strain and mean stress, the Bulk Modulus, k, can be calculated as shown in Equation 3.8.

Equation 3.8
$$k = \frac{p}{\varepsilon_v}$$

Young's Modulus, E, can be calculated from the effective major principal stress and the major principal strain, in a uniaxial compression test. The relevant equation is Eq. 3.9.

Equation 3.9
$$E = \frac{\sigma_1}{\varepsilon_1}$$

Poisson's ratio is equal to the magnitude of the ratio of lateral strain to longitudinal strain for a uniaxial test and is given by Equation 3.10.

Equation 3.10
$$v = \frac{\varepsilon_3}{\varepsilon_1}$$

The values obtained for k, E and v are displayed where applicable in the plots included in Appendix A.

3.2 MECHANICAL PROPERTIES DERIVED FROM THE TENSILE TEST

The tensile tests gave the maximum weight W the specimen could withstand in tension. This determined weight and the area of the specimen midway down the length of the sample, A_m , was used to calculate the average stress σ_{avg} experienced by the sample at the time of failure using Equation 3.11.

Equation 3.11
$$\sigma_{avg} = \frac{W}{A_m}$$

The max stress σ_{max} was then calculated using the determined stress concentration factor K for the dimensions of the prepared specimen (Pilkey). The value for K was 1.18 and the max stress was calculated by rearranging equation 3.12 and solving for σ_{max} .

Equation 3.12
$$K = \frac{\sigma_{max}}{\sigma_{avg}}$$

Equation 3.13
$$\sigma_{max} = K * \sigma_{avg}$$

In order to incorporate this value in p vs. q space, the corresponding values of q and p were calculated using Equations 3.3 and 3.4 where $\sigma_{max} = \sigma_1$. The values obtained for p were negative because the stress was tensile rather than compressive but q was positive because equation 3.3 incorporates an absolute value function. The max stress values obtained from the tensile test were plotted to the left of the vertical q axis. The values obtained from the tensile test are displayed in Table 3.1.

Table 3.1 Tensile Test Results

Sample ID	Tensile Force	Average Stress	K	Max Stress
	(lbs.)	(psi.)		(psi.)
4-6-04-T-16of36	118.58	77.03	1.18	90.90
4-7-04-T-5of36	173.82	112.94	1.18	133.27
4-12-04-T-30of36	162.00	105.26	1.18	124.21

Readily apparent from Table 3.1 is a drastic variation in the maximum stress values attained under the current design. We attribute this variation to the unparallel axes of the opposing specimen ends. When the sample ends are not parallel, a bending moment is initiated, thereby causing a stress concentration that is greater than 1.18 to develop and a failure that is not centrally located. Sample failure locations were inconsistent and outside of the gauge length. We will modify the current design to increase the central stress concentration factor. This will localize the major stress value at the center of each sample, thereby increasing the usability of the tensile test.

3.3 APO/BMI MATERIAL PROPERTIES AND CHARACTERISTICS

The performed triaxial compression tests provided a great deal of useful data to assist in the characterization of this foam. Primarily, the hydrostatic test was used to determine the hydrostatic yield, which is shown in Table 3.2.

Table 3.2 Determined Hydrostatic Yield from Hydrostatic Compression Tests

	Test $1,\sigma_{HY}$	Test 2, σ_{HY}	Test 3, σ_{HY}	Average, σ_{HY}
APO/BMI Foam	1050	1075	1080	1068

The determined hydrostatic yield was used to develop a test matrix for conducting the remaining triaxial compression tests as discussed in Chapter 2. An important relationship resulting from these tests was that between q and ϵ_1 . The composite plot of this relationship is provided in Figure 3.1. The test matrix was designed to probe stress space in different locations, thus providing necessary information to identify the shear envelope. The composite plots for q vs. p are provided along with a calculated/fitted shear envelope in Figure 3.2. Additional plots for each specimen are included in the Appendix. These include: Strain vs. Time, Stress vs. Time, Stress vs. Strain, Mean Stress vs. Volumetric Strain, Lateral Strain vs. Longitudinal Strain, and q vs. p. The plots for bulk modulus, Poisson's ratio, and Young's modulus are also included in the appendix.

Figure 3.1 Composite plot of q vs. ε_1 for APO/BMI Syntactic Foam

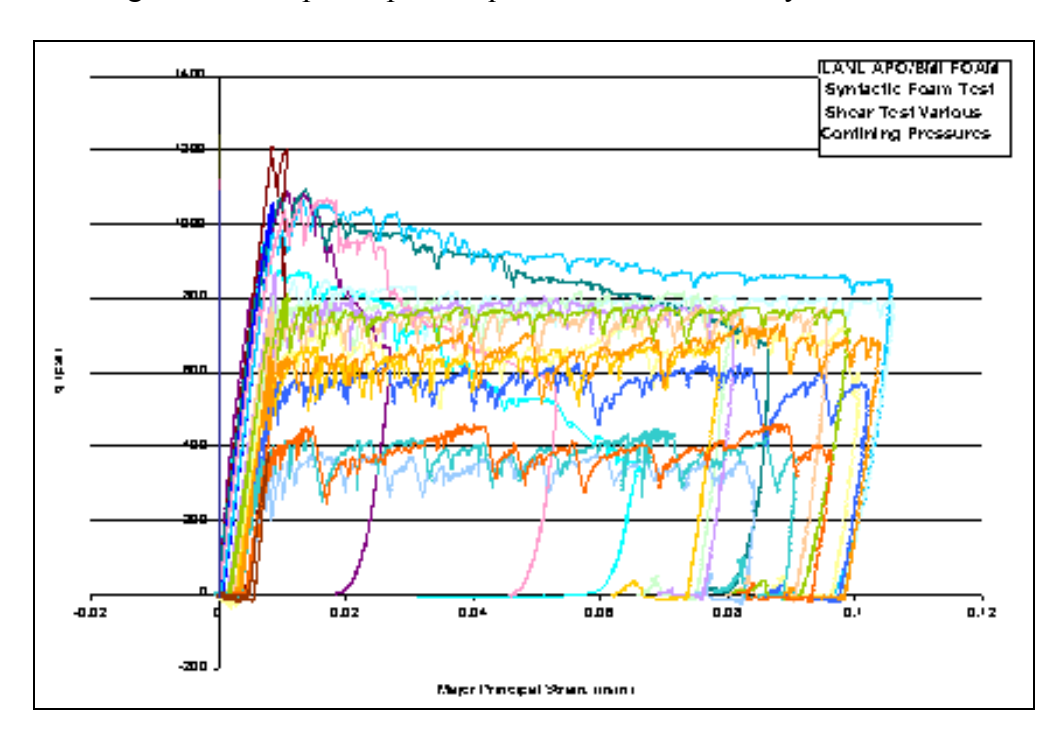
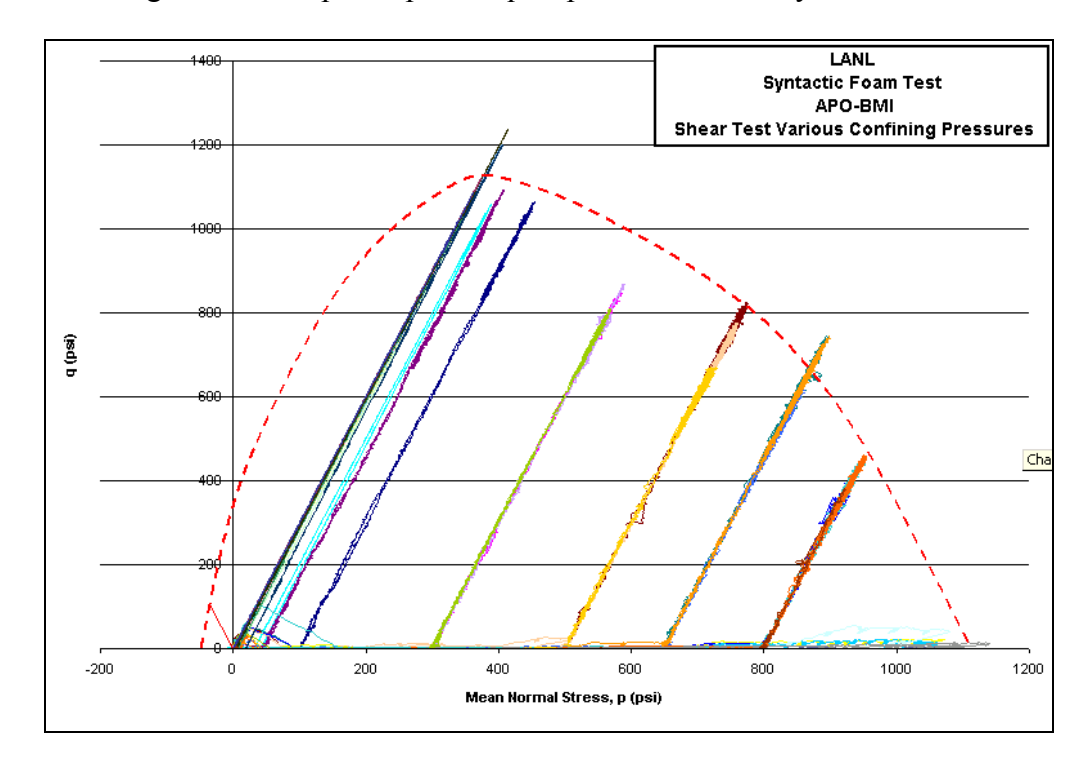


Figure 3.2 Composite plot of q vs. p for APO/BMI Syntactic Foam



CHAPTER 4

CONCLUSIONS

The scope of this work was to develop a shear failure envelop for APO/BMI syntactic foam. Our team successfully completed five hydrostatic compression, twelve uniaxial compression, sixteen triaxial compression, and three tension tests on this material over a span of six months. Material response data was recorded at second intervals throughout each experiment and converted into usable engineering units. The number of tests performed in this matrix was sufficient to acquire an estimate of the behavior of the material under a variety of loading conditions and to obtain various material characteristics.

Future experimentation would greatly benefit from the use of a scanning electron microscope (SEM) imaging apparatus to investigate the foam microstructure and propagation of the failure mechanism as it occurs. This would provide a means of comparing this material to similar syntactic foams that have been characterized previously.

BIBLIOGRAPHY

Erikson, R. "Mechanical Engineering", *January 1999*. http://www.memagazine.org/backissues/january99/features/foams/foams/html.

Hibbeler, R.C. Mechanics of Materials, 4th Ed. New Jersey: Prentice Hall. 2000.

ASTM D 5379/5379-93, Standard Test Method for Shear Properties of Composite Materials by the V-notched Beam Method, American Society of Testing Materials, West Conshohocken, PA, vol 8.01, 1993

Desai, C.S., H.J. Siriwardane. *Constitutive Laws for Engineering Materials with Emphasis on Geologic Materials*. New Jersey: Prentice Hall, 1984.

Roark, Raymond J., Warren C. Young. Formulas for Stress and Strain, 5th Ed. New York: McGraw-Hill, 1975.

Das, Braja M. Advanced Soil Mechanics, 2nd Ed. Washington: Taylor & Francis, 1997.

Bishop, Alan W., D.J. Henkel. *The Measurement of Soil Properties in the Triaxial Test.* London: Edward Arnold LTD, 1962.

Pilkey, Walter D. *Peterson's Stress Concentration Factors*, 2nd Ed. New York: John Wiley & Sons, Inc., 1997.

Beer, F.P., R. Johnston. *Mechanics of Materials*, 2nd Ed. New York: McGraw-Hill, 1992.

Amiss, John M., F.D. Jones, H.H. Ryffel. *Machinery's Handbook, 22nd Revised Ed.* New York: Industrial Press, 1984.

Levinson, Irving J. Machine Design. Reston: Reston Publishing Company, Inc., 1978.

APPENDIX A

APO/BMI SYNTACTIC FOAM

STRAIN vs. TIME and STRESS vs. TIME,

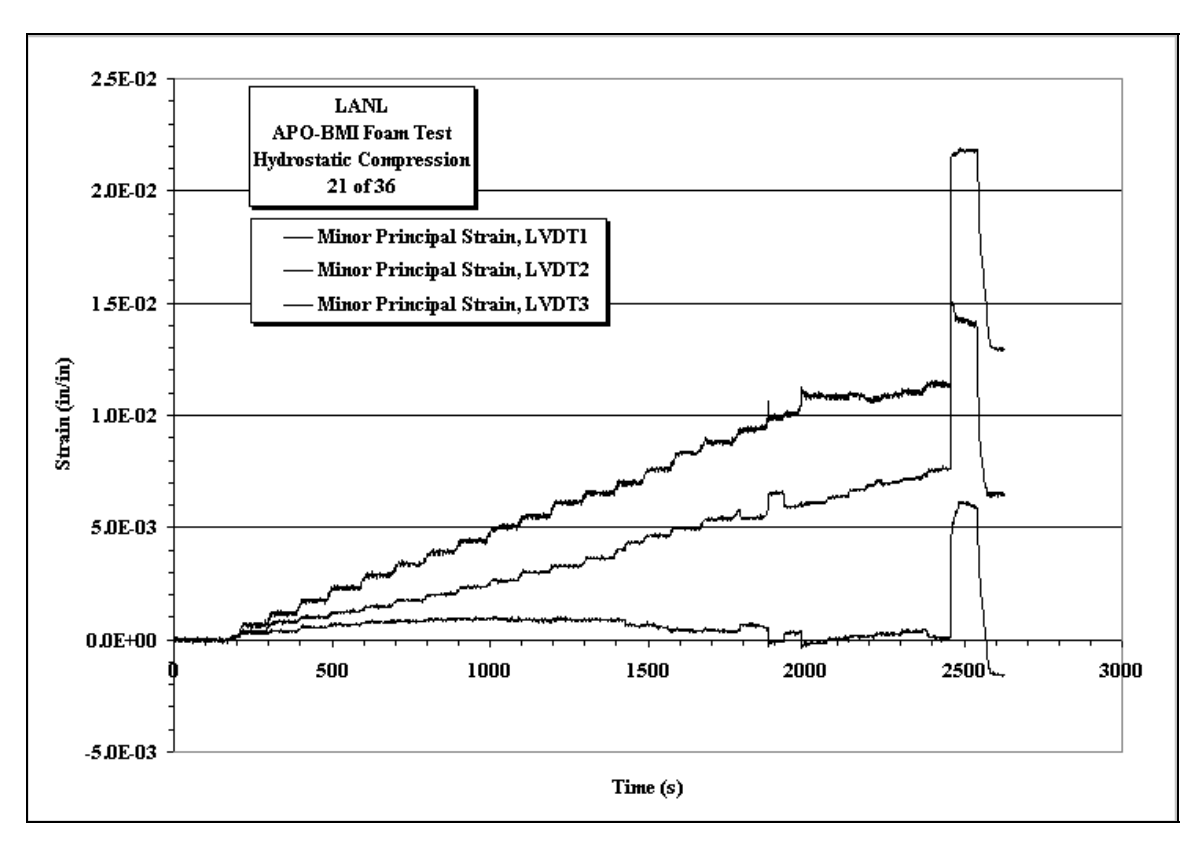
MAJOR and MINOR STRESS vs. MAJOR and MINOR PRINCIPAL STRAIN,

MEAN STRESS vs. VOLUMETRIC STRAIN,

POISSON'S RATIO (MINOR STRAIN vs. MAJOR STRAIN)

DEVIATORIC STRESS vs. MEAN STRESS

Contained within Appendix A are data plots from the twenty-one triaxial compression tests performed on the AOP/BMI foam. The test matrix for the triaxial compression tests performed in this investigation are outlined and explained in Chapter 2.



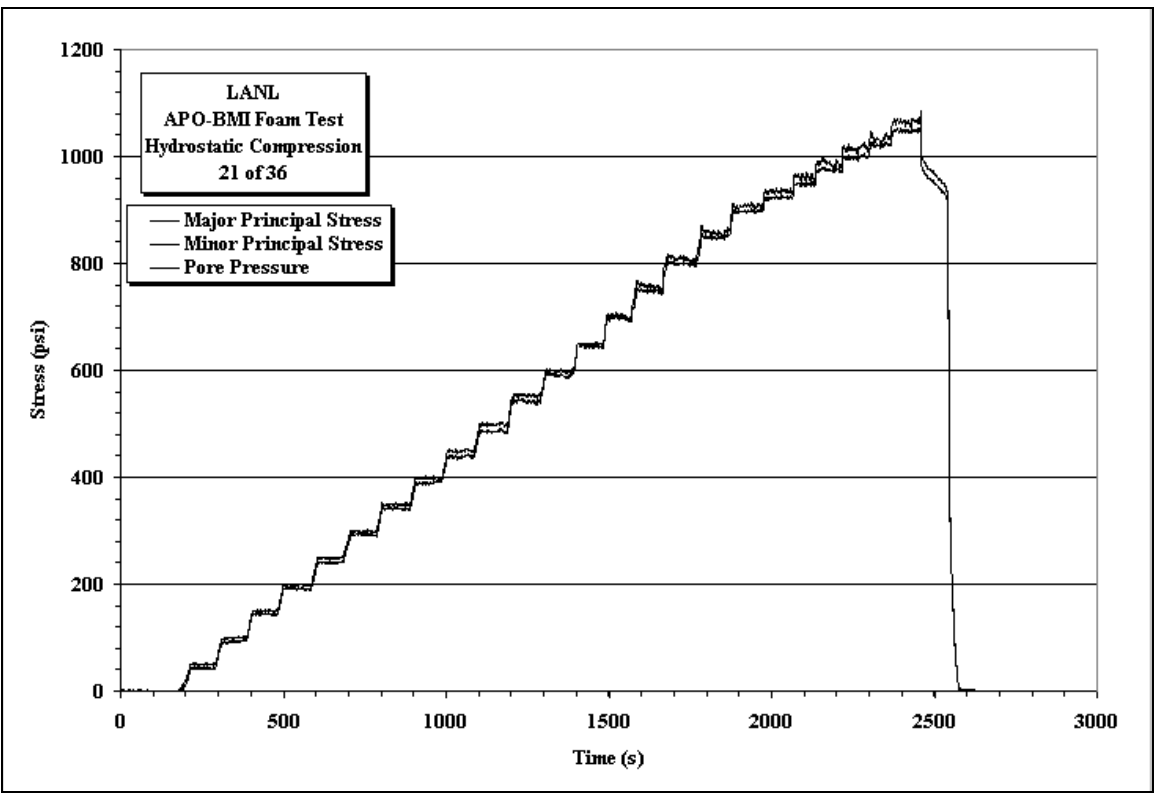
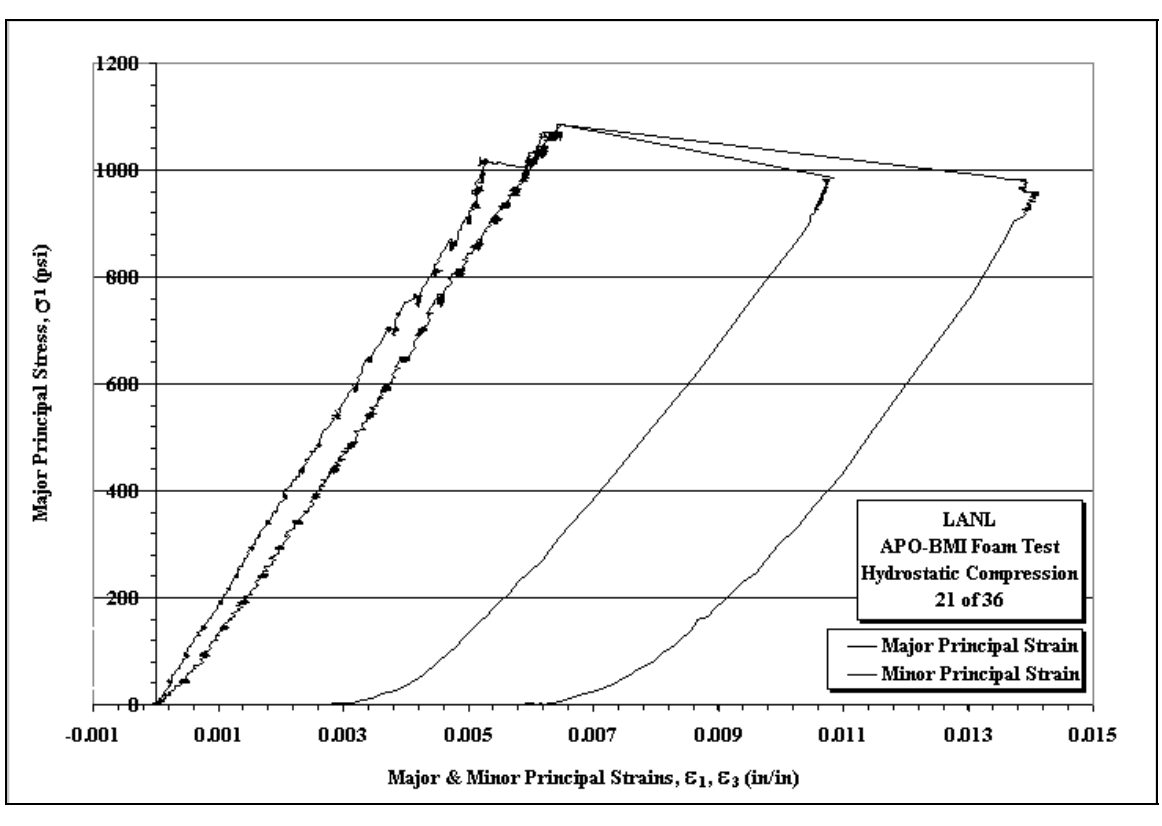


Figure A1. Strain vs. Time and Stress vs. Time plots for Sample 21of36 under an equivalent pressure applied in all directions.



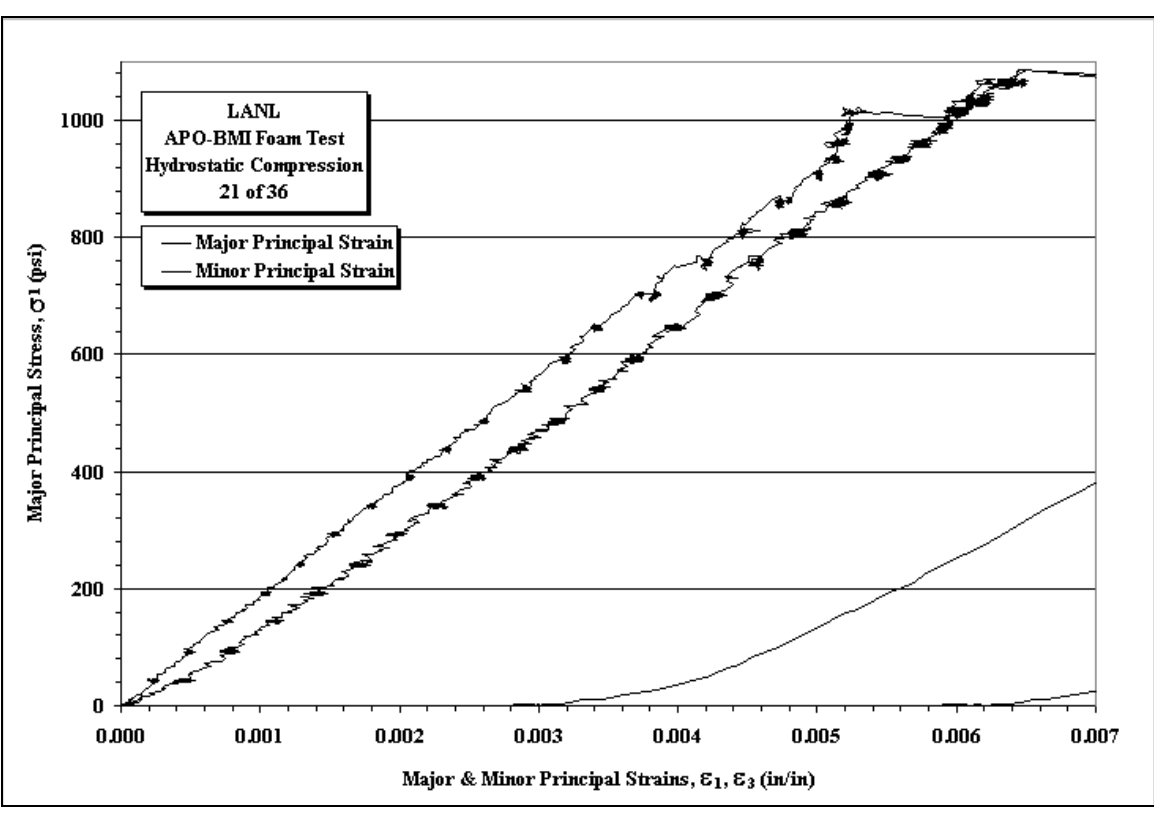
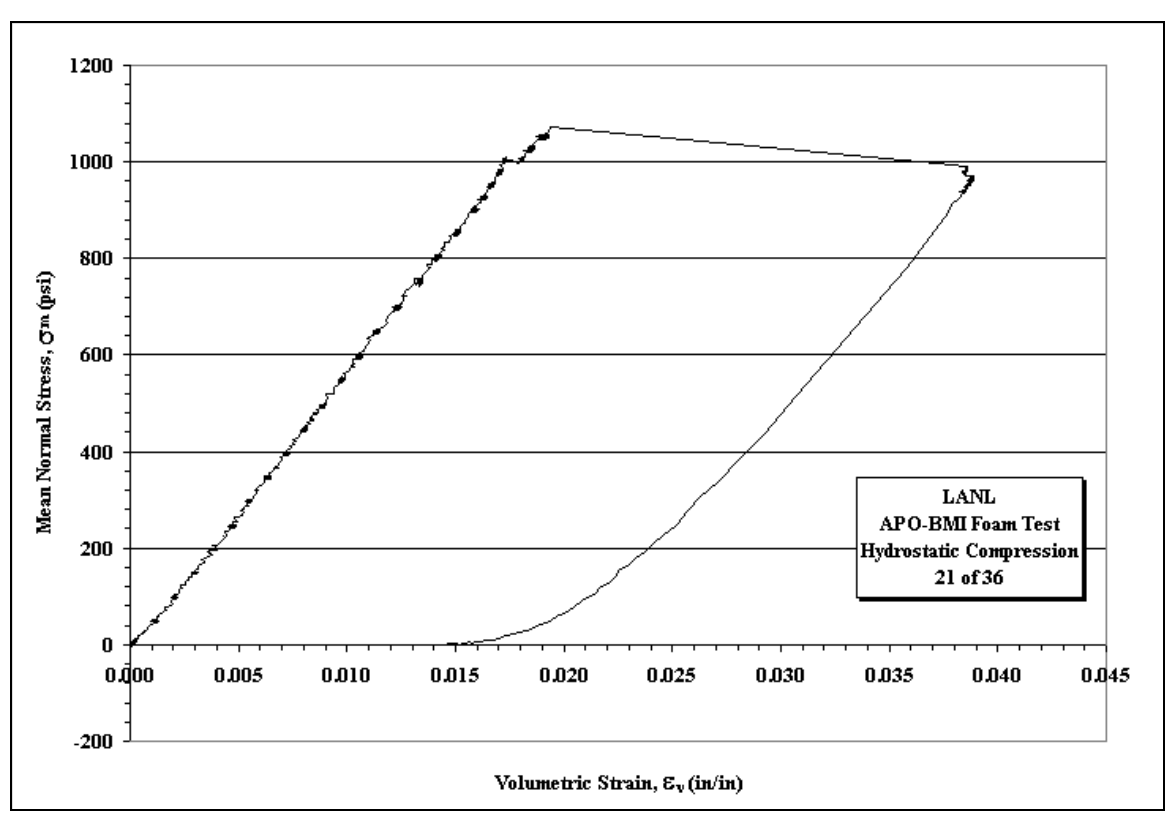


Figure A2. Stress vs. Strain plots for Sample 21of36 under an equivalent pressure applied in all directions.



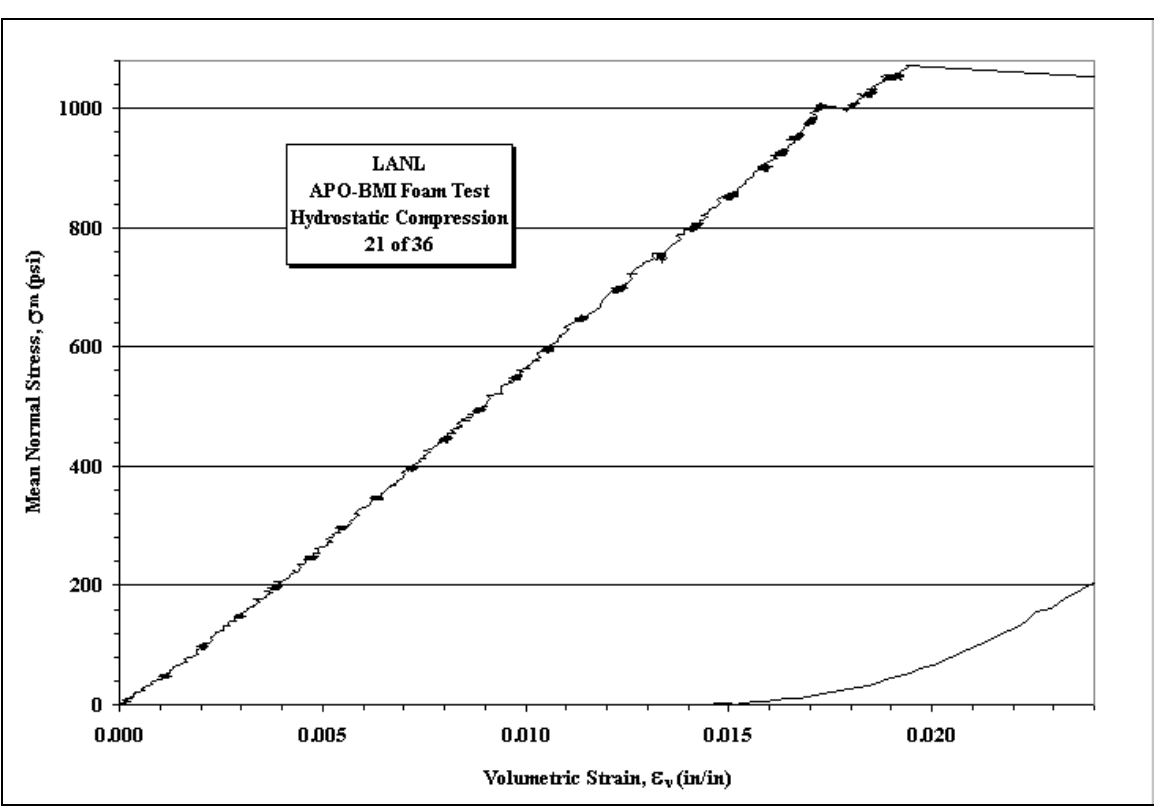
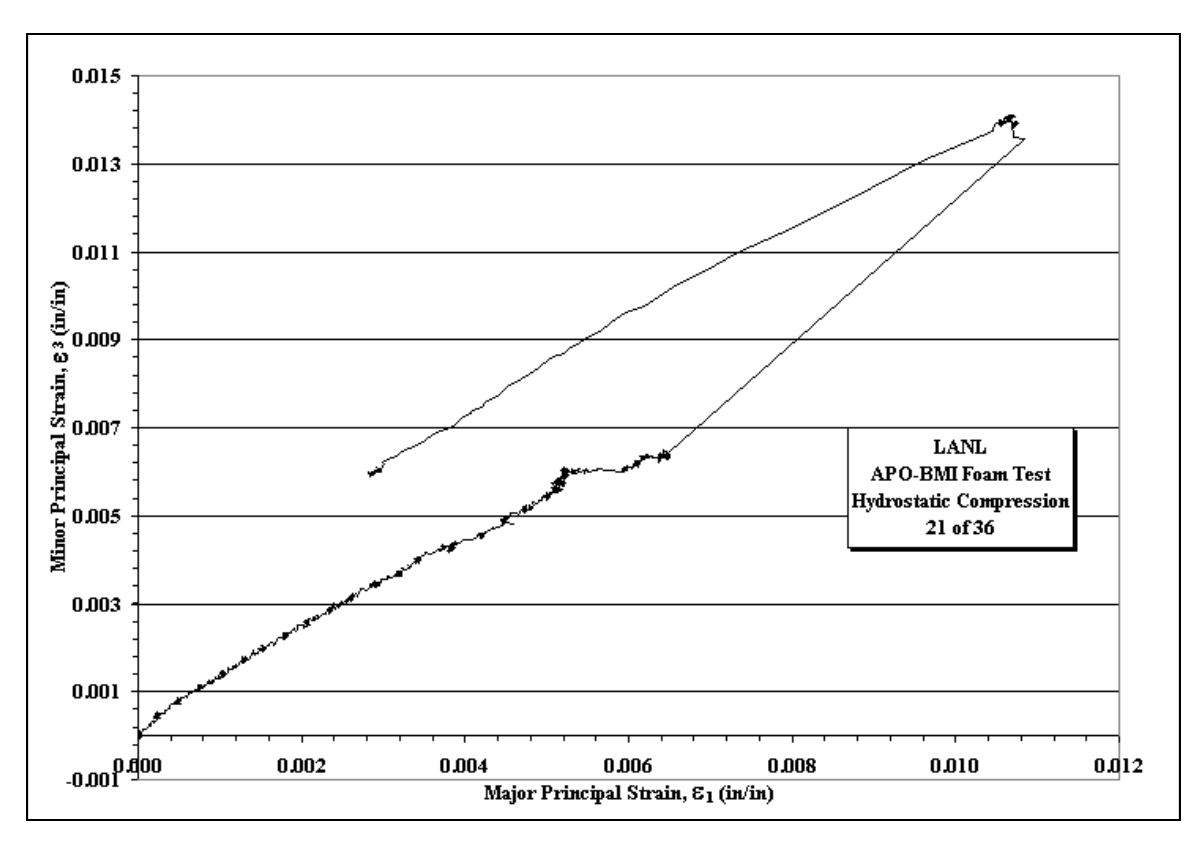


Figure A3. Mean Stress vs. Volumetric Strain plots for Sample 21of36 under an equivalent pressure applied in all directions.



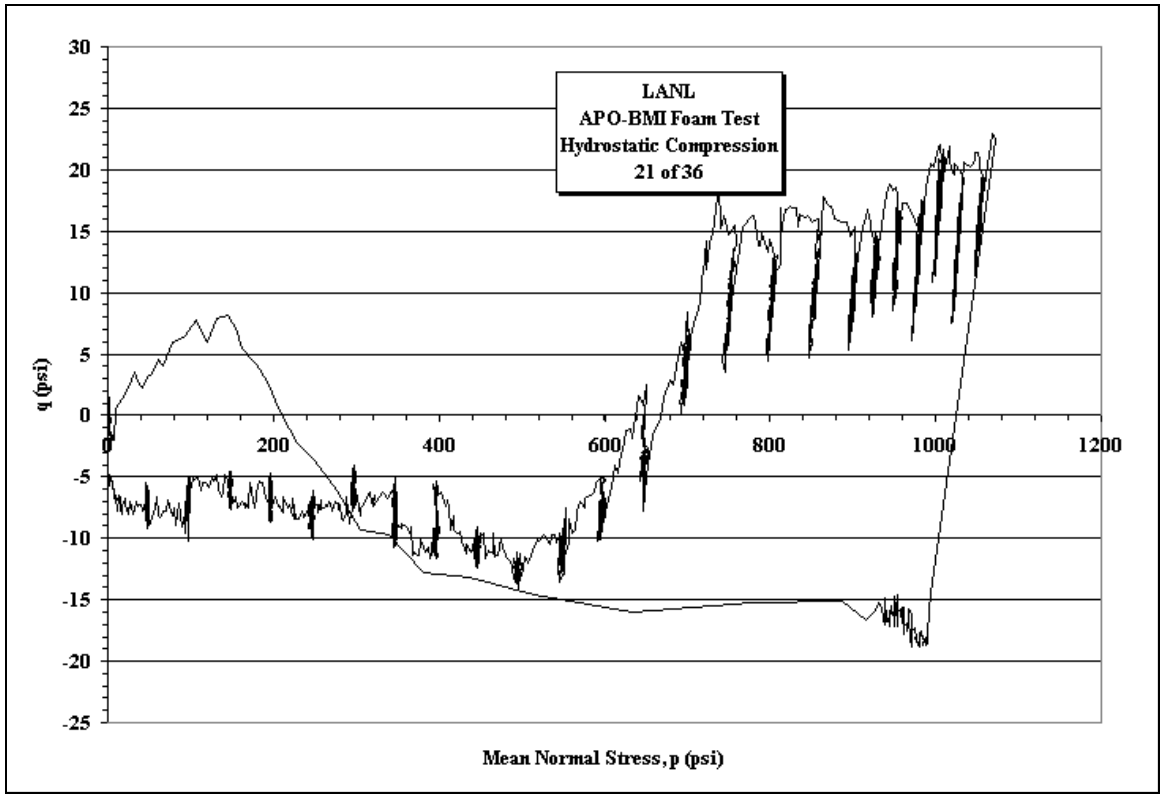
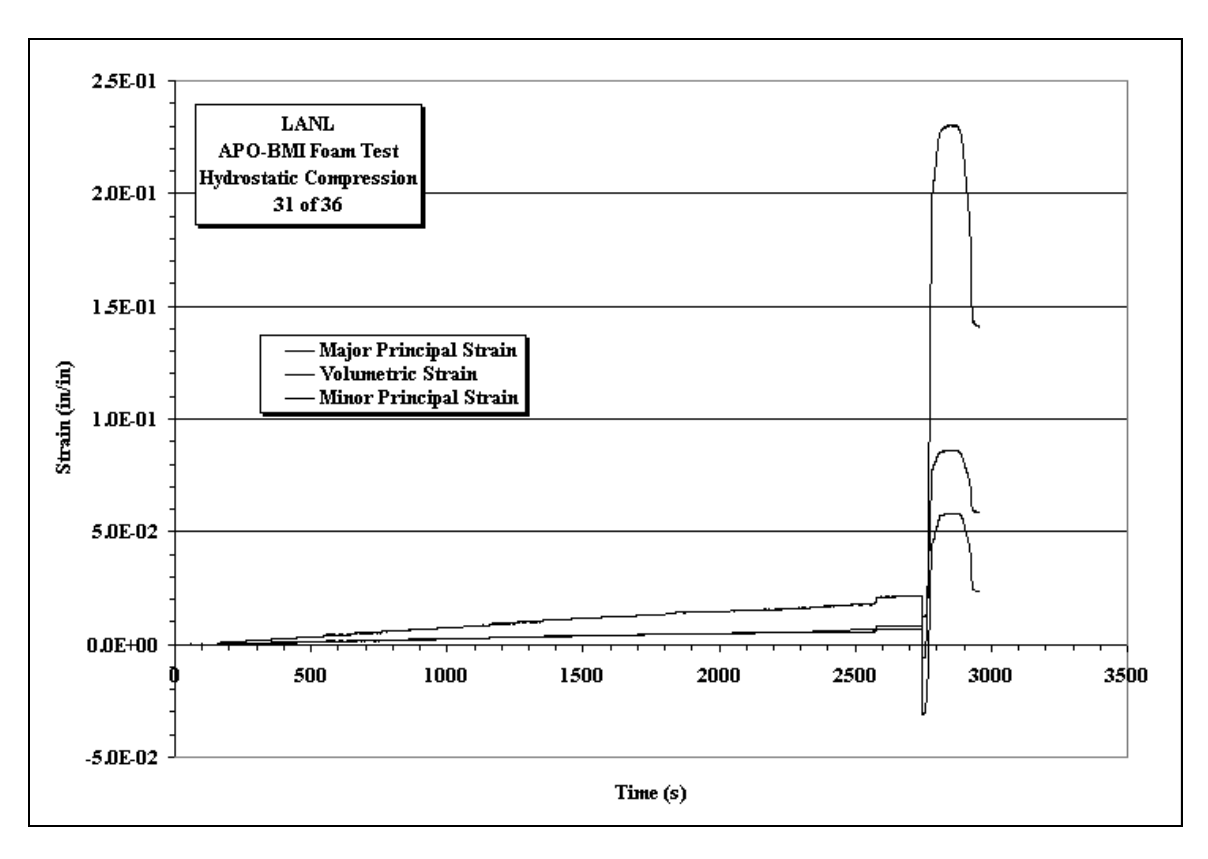


Figure A4. Minor Principle Strain vs. Major Principle Strain and Deviatoric Stress vs. Mean Stress plots for Sample 21of36 under an equivalent pressure applied in all directions.



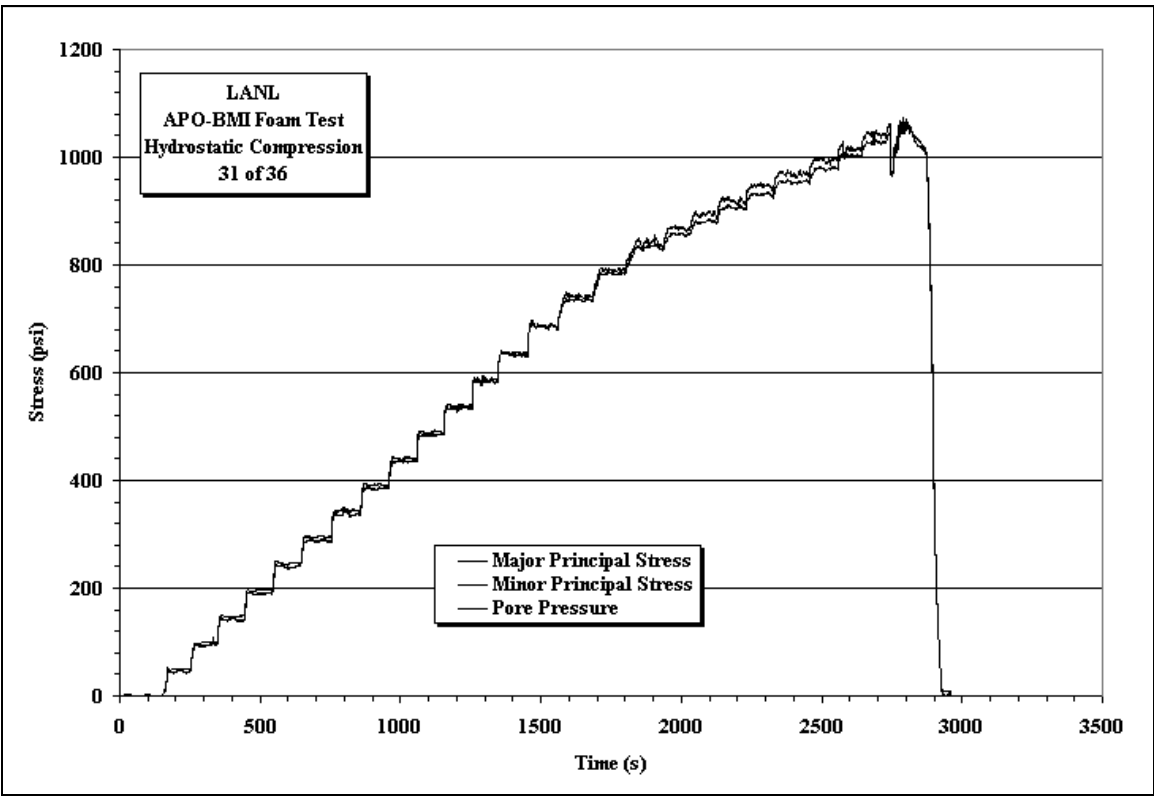
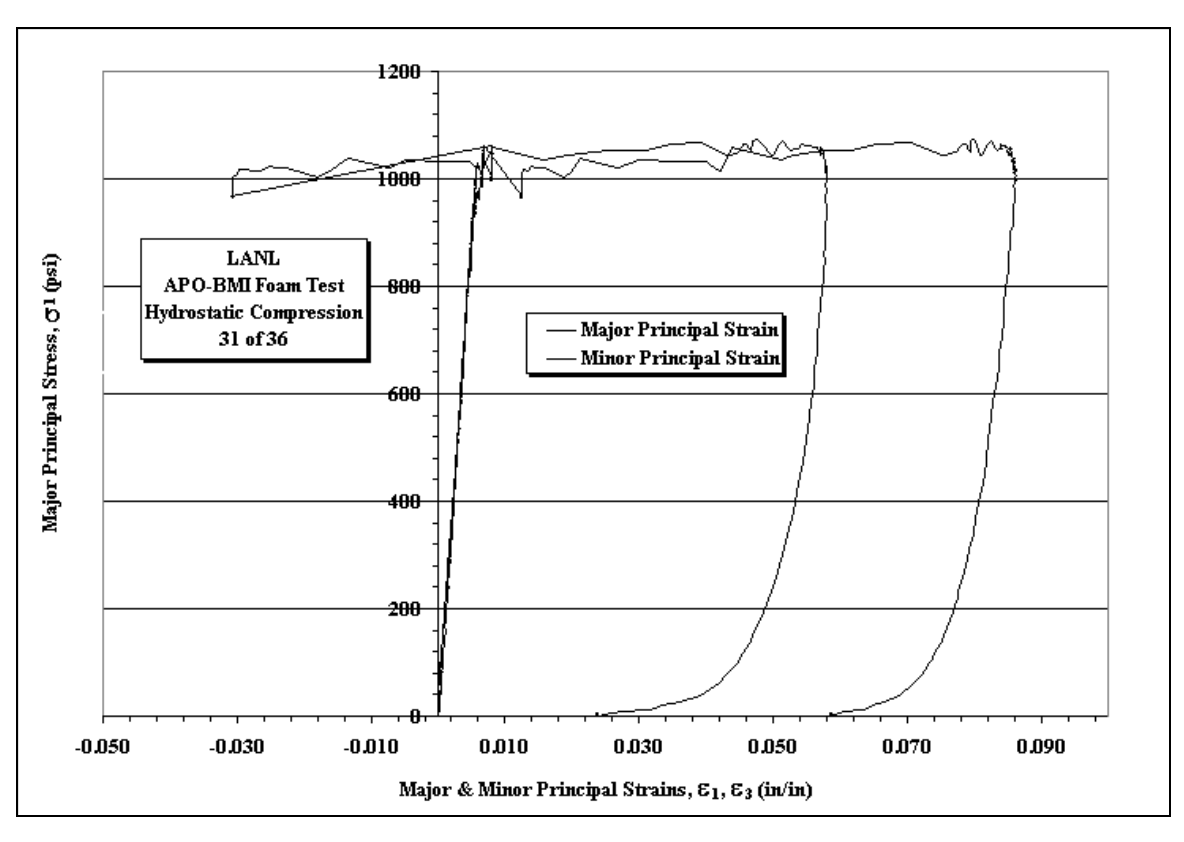


Figure A4. Minor Principle Strain vs. Major Principle Strain and Deviatoric Stress vs. Mean Stress plots for Sample 31of36 under an equivalent pressure applied in all directions.



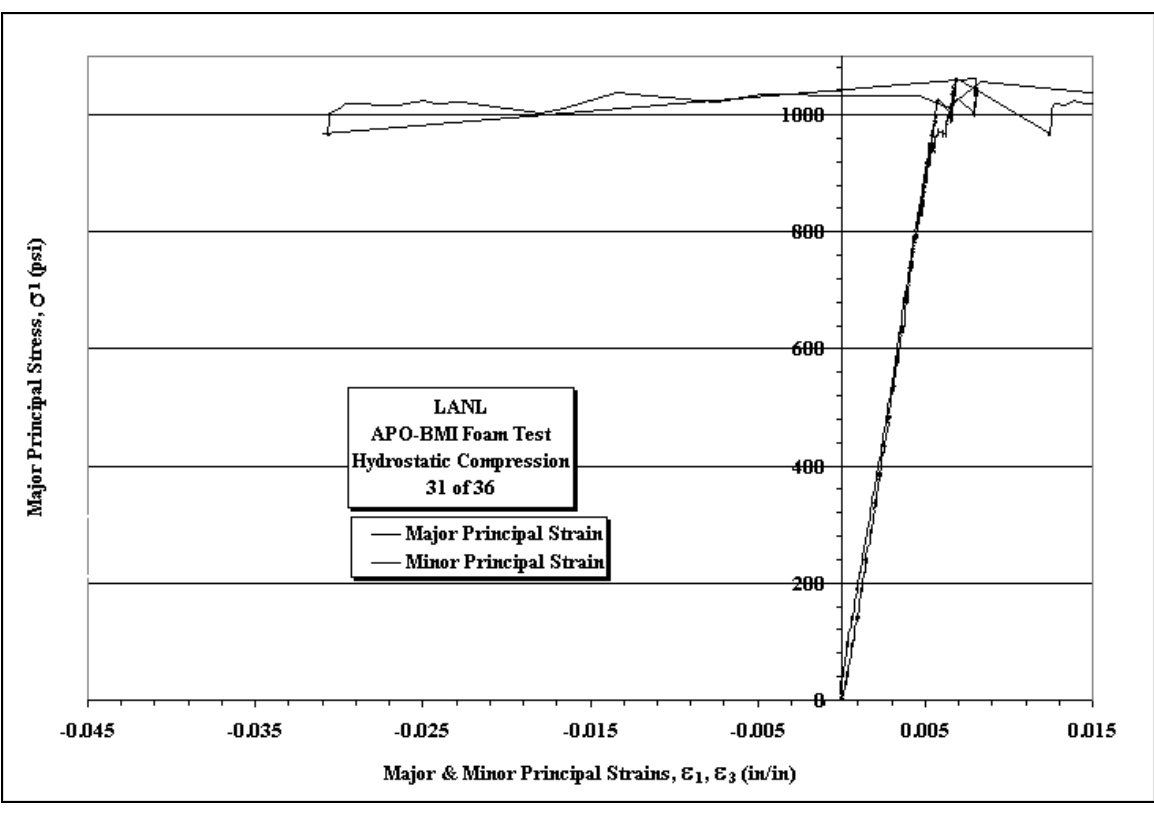
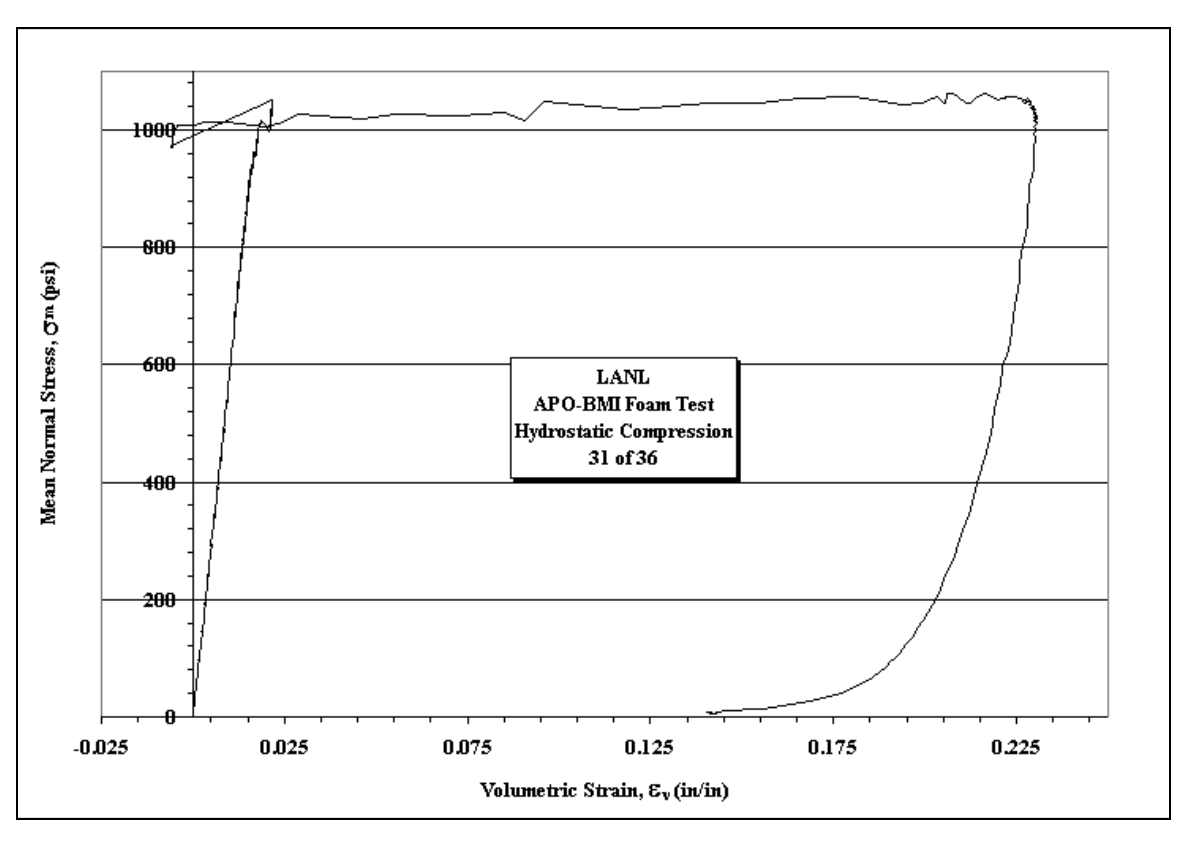


Figure A6. Stress vs. Strain plots for Sample 31of36 under an equivalent pressure applied in all directions.



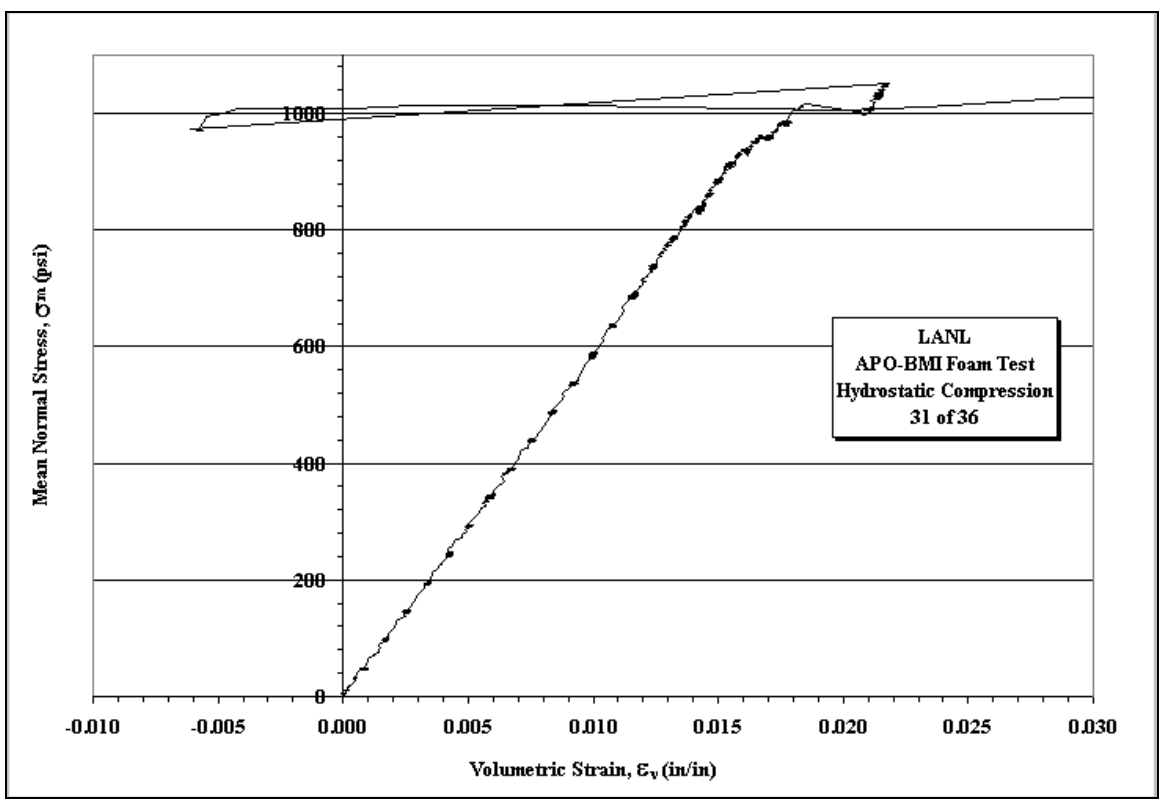
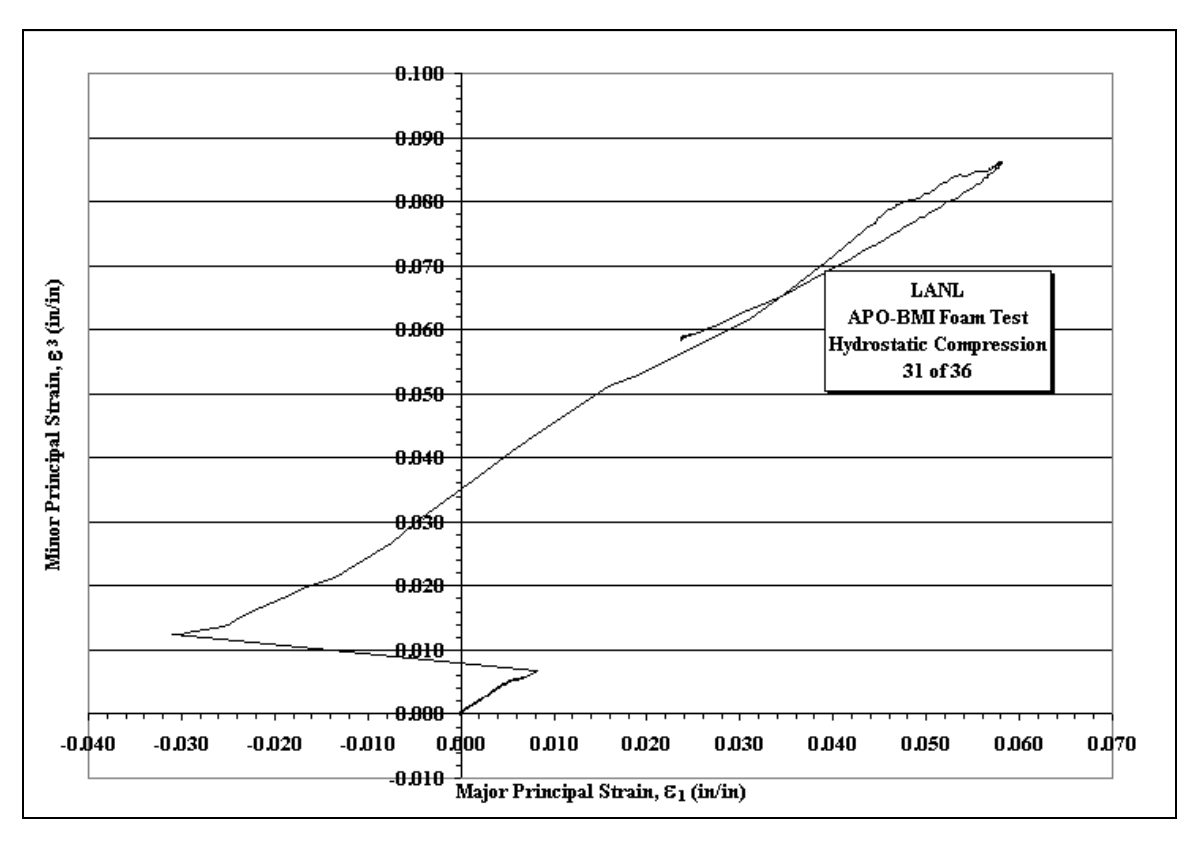


Figure A7. Mean Stress vs. Volumetric Strain plots for Sample 31of36 under an equivalent pressure applied in all directions.



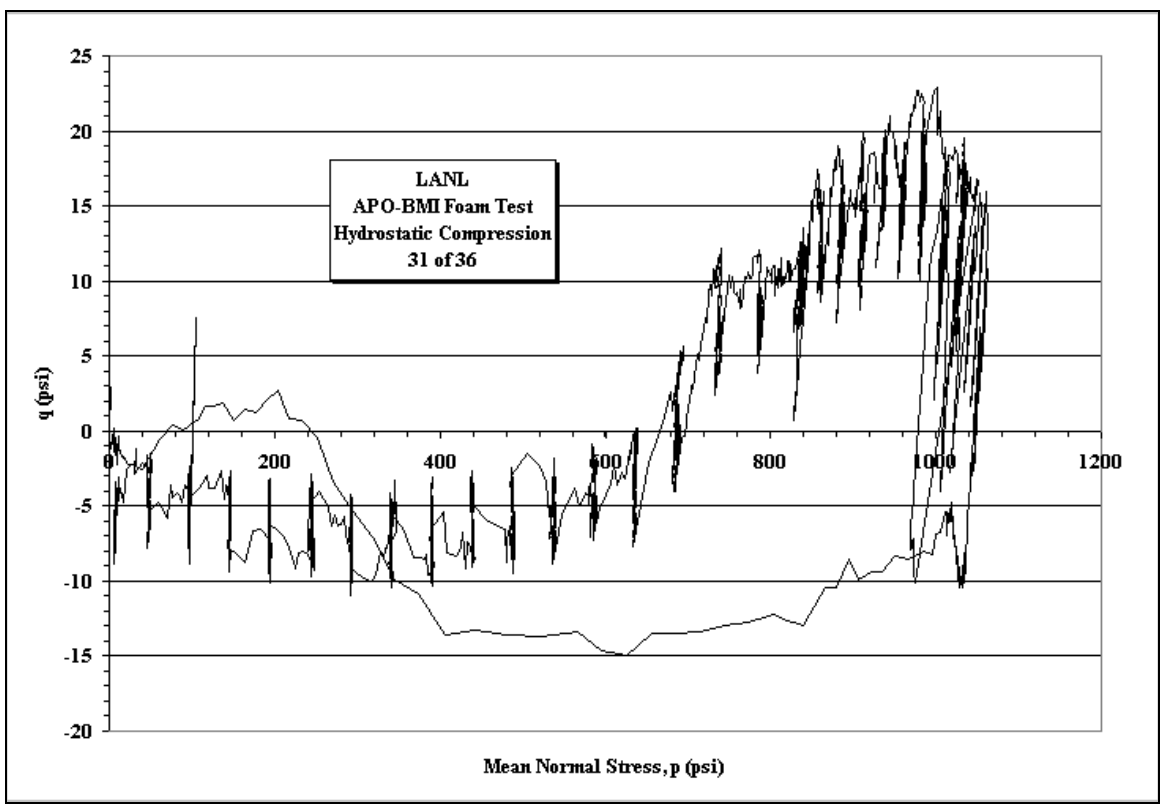
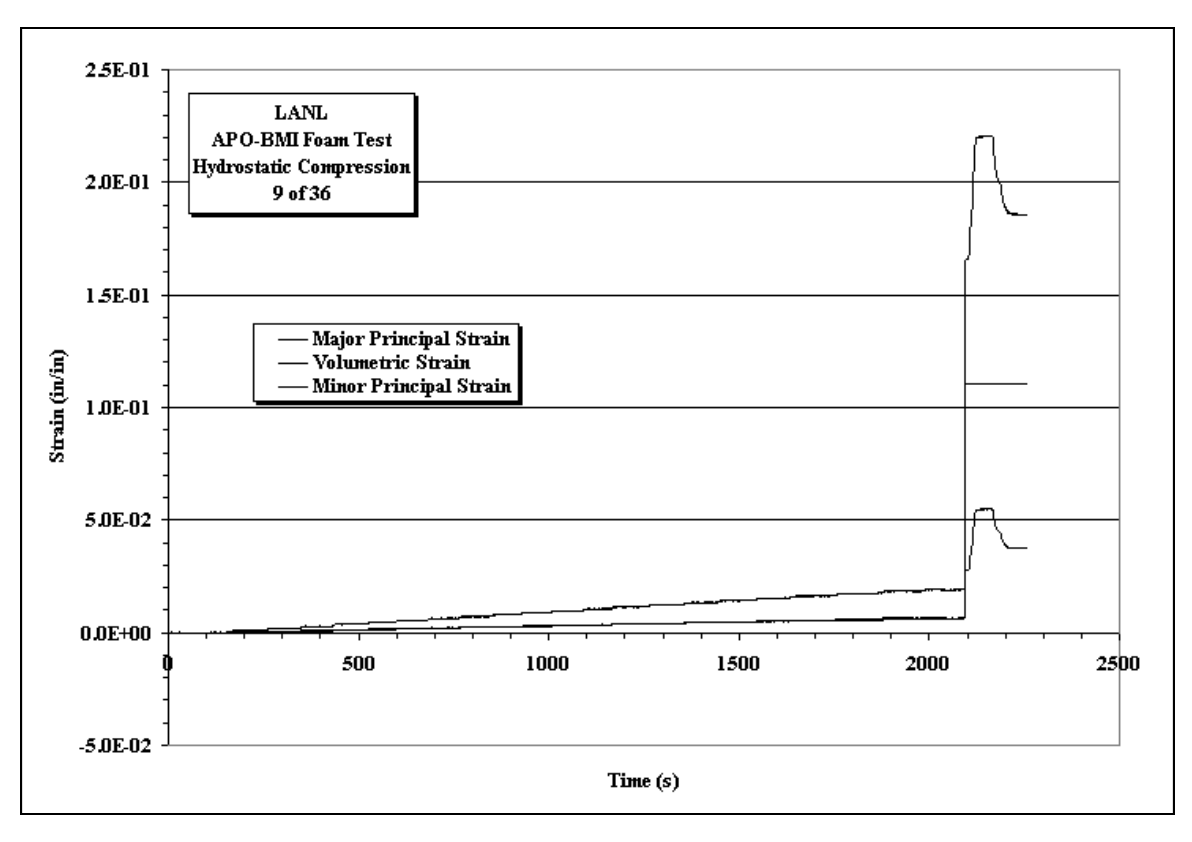


Figure A8. Minor Principle Strain vs. Major Principle Strain and Deviatoric Stress vs. Mean Stress plots for Sample 31of36 under an equivalent pressure applied in all directions.



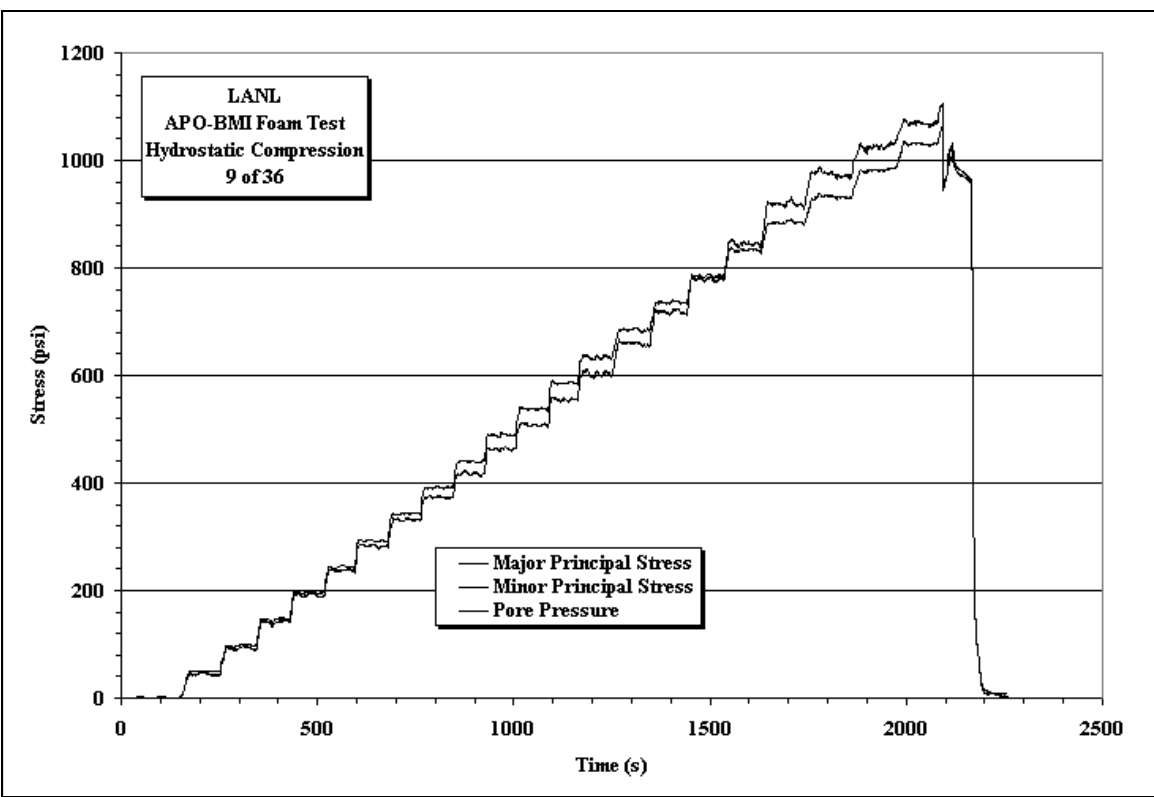
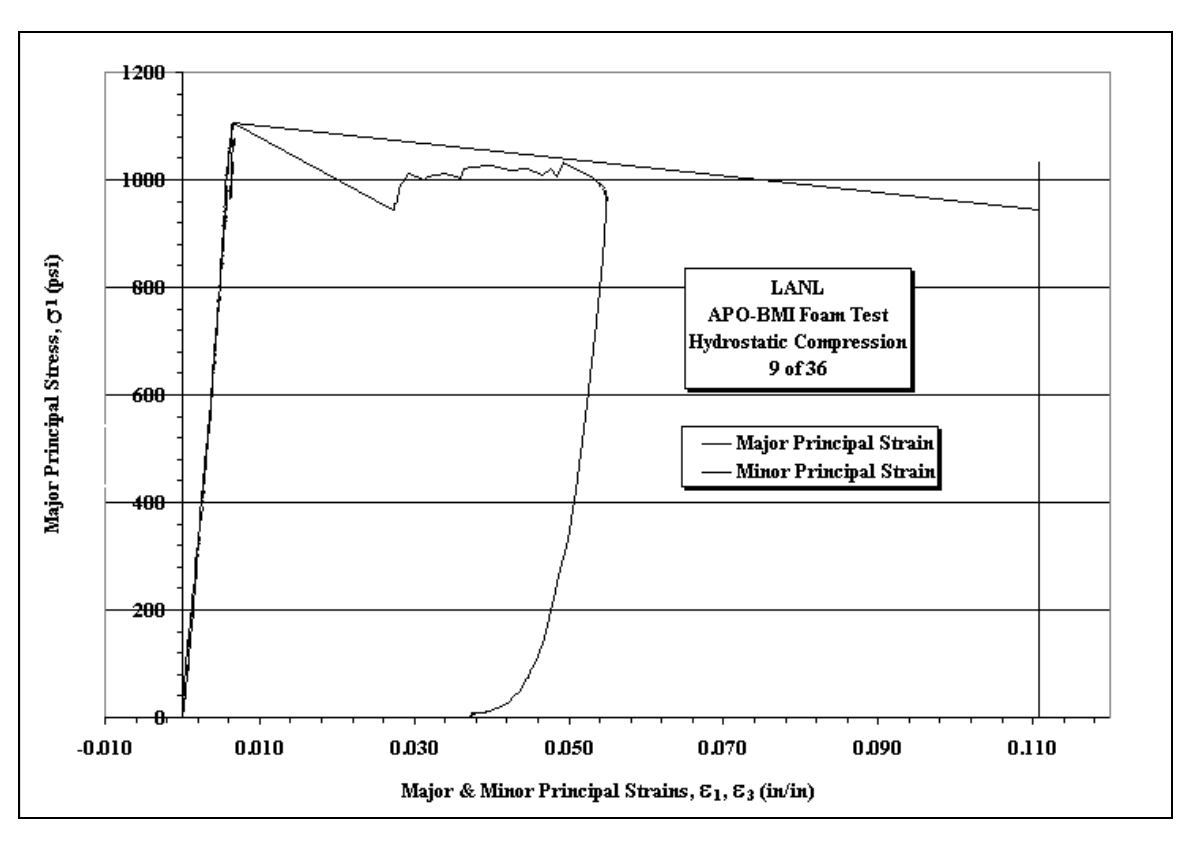


Figure A9. Minor Principle Strain vs. Major Principle Strain and Deviatoric Stress vs. Mean Stress plots for Sample 9of36 under an equivalent pressure applied in all directions.



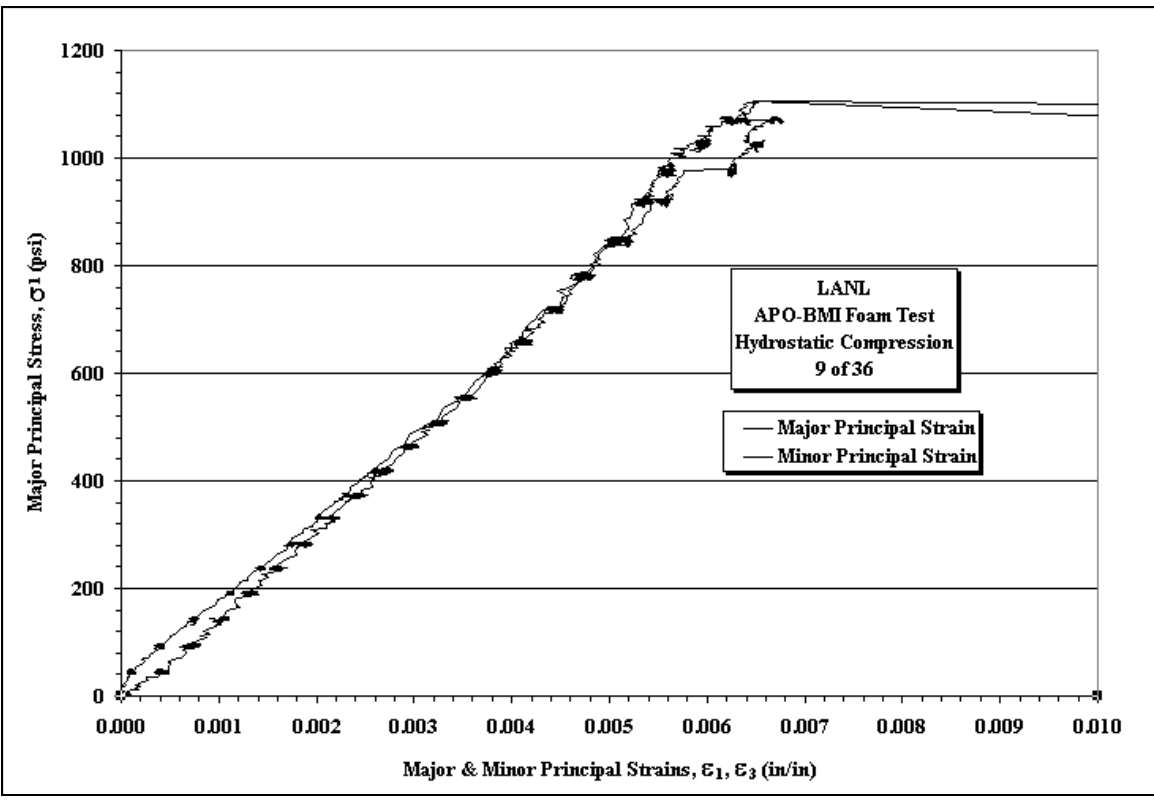
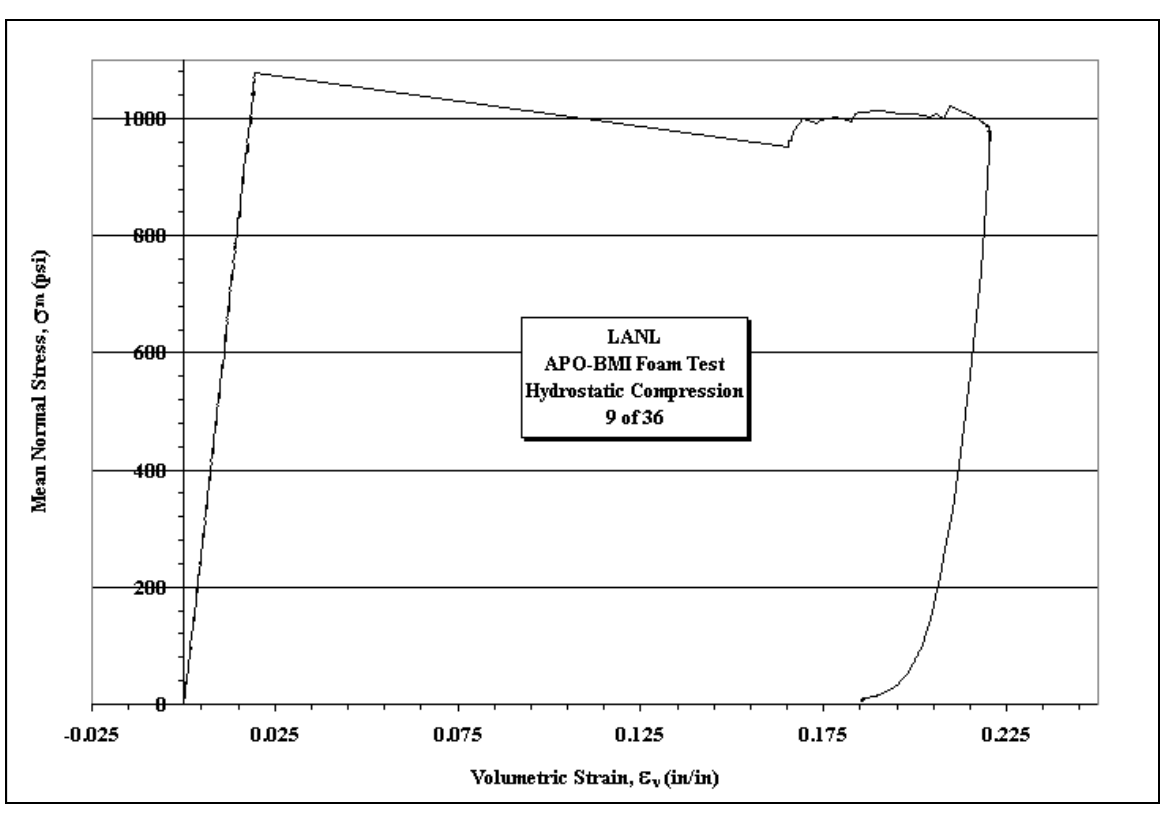


Figure A10. Stress vs. Strain plots for Sample 9of36 under an equivalent pressure applied in all directions.



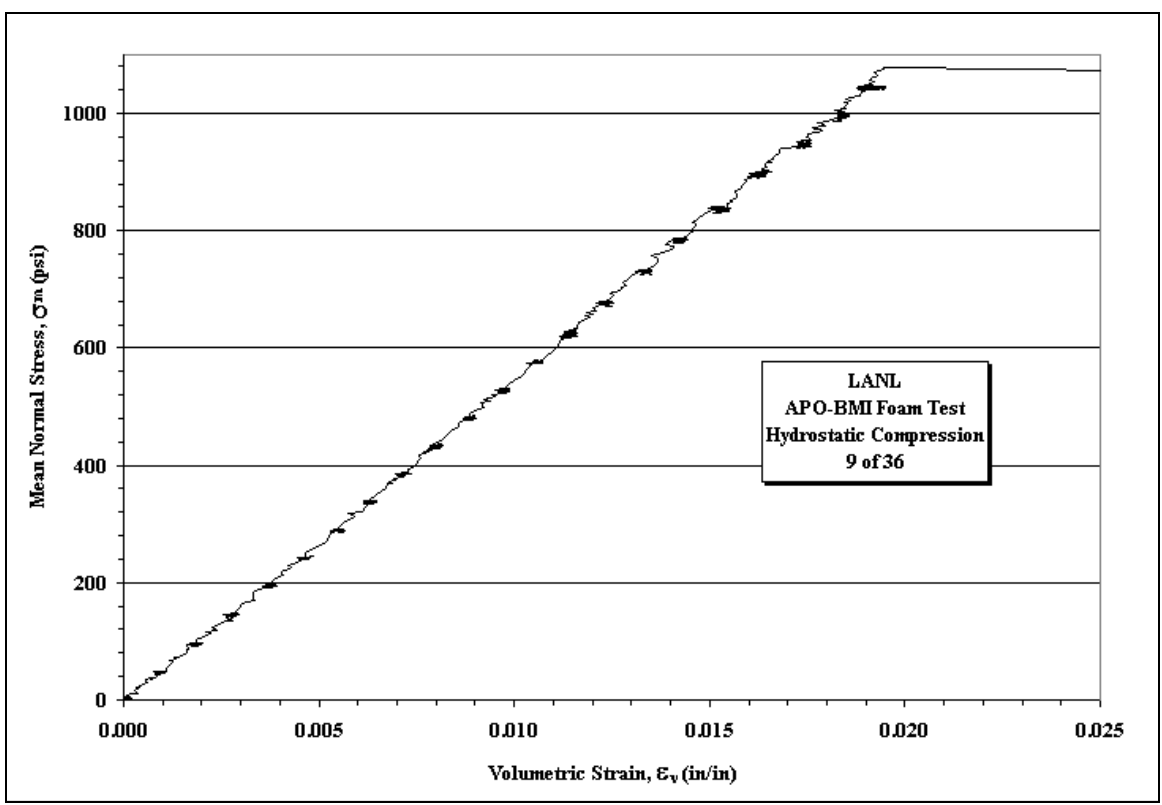
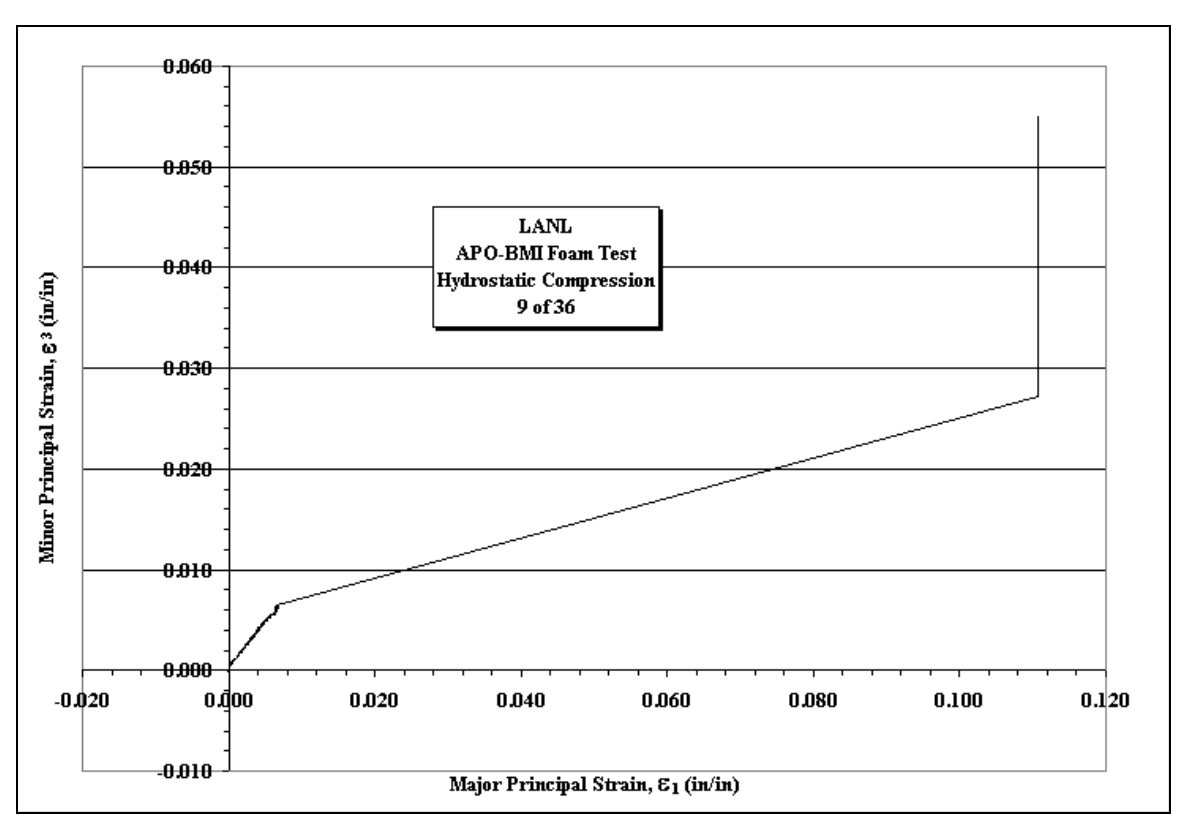


Figure A11. Mean Stress vs. Volumetric Strain plots for Sample 9of36 under an equivalent pressure applied in all directions.



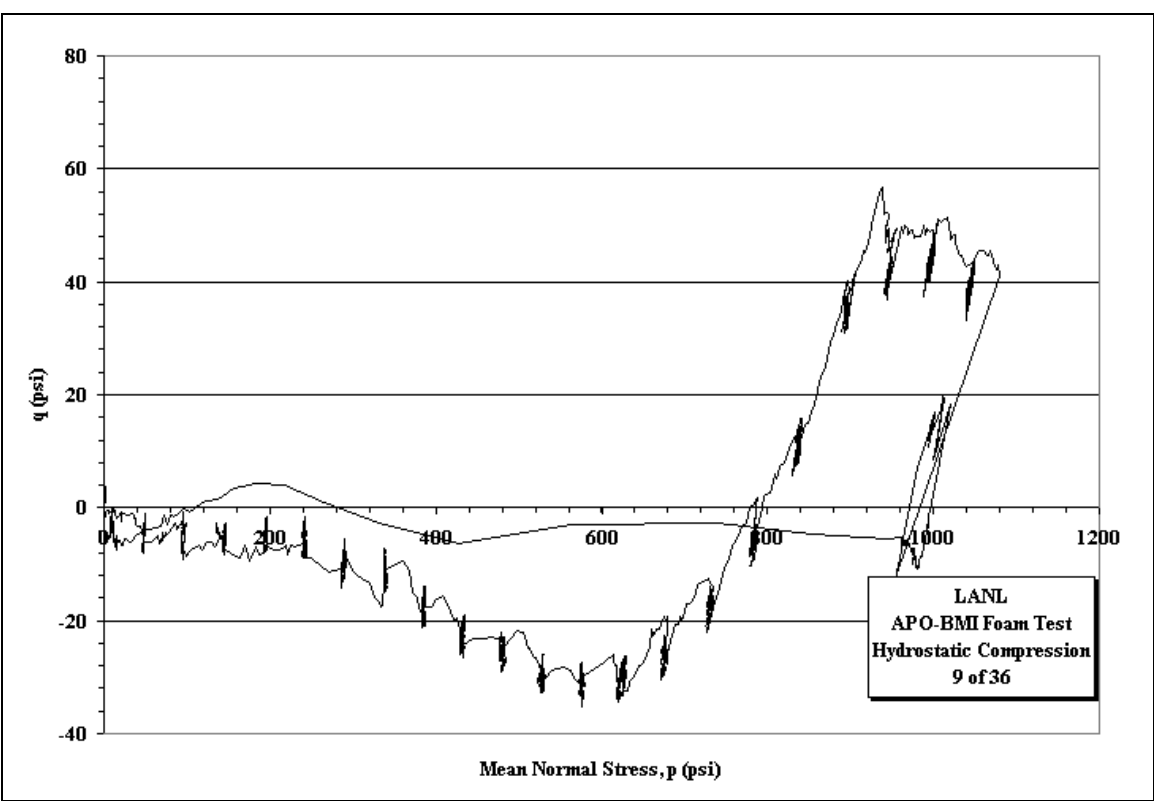
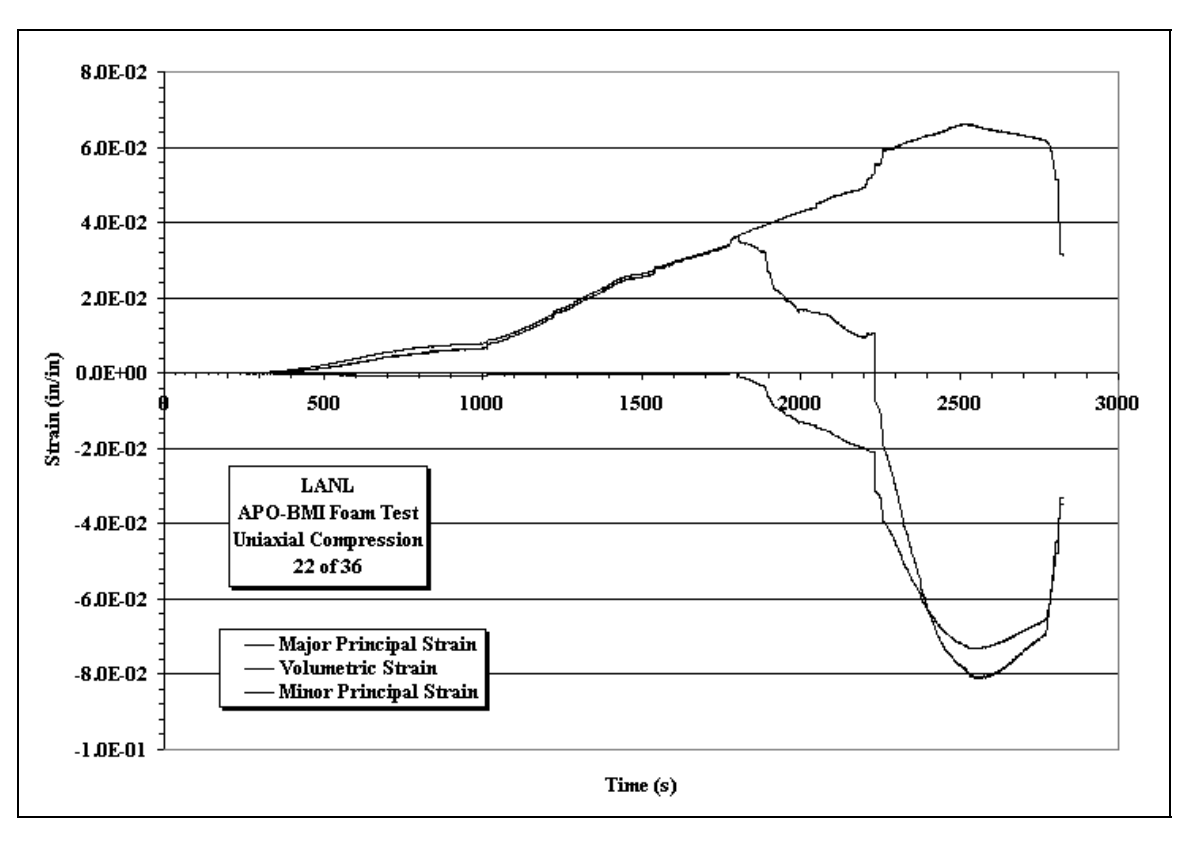


Figure A12. Minor Principle Strain vs. Major Principle Strain and Deviatoric Stress vs. Mean Stress plots for Sample 9of36 under an equivalent pressure applied in all directions.



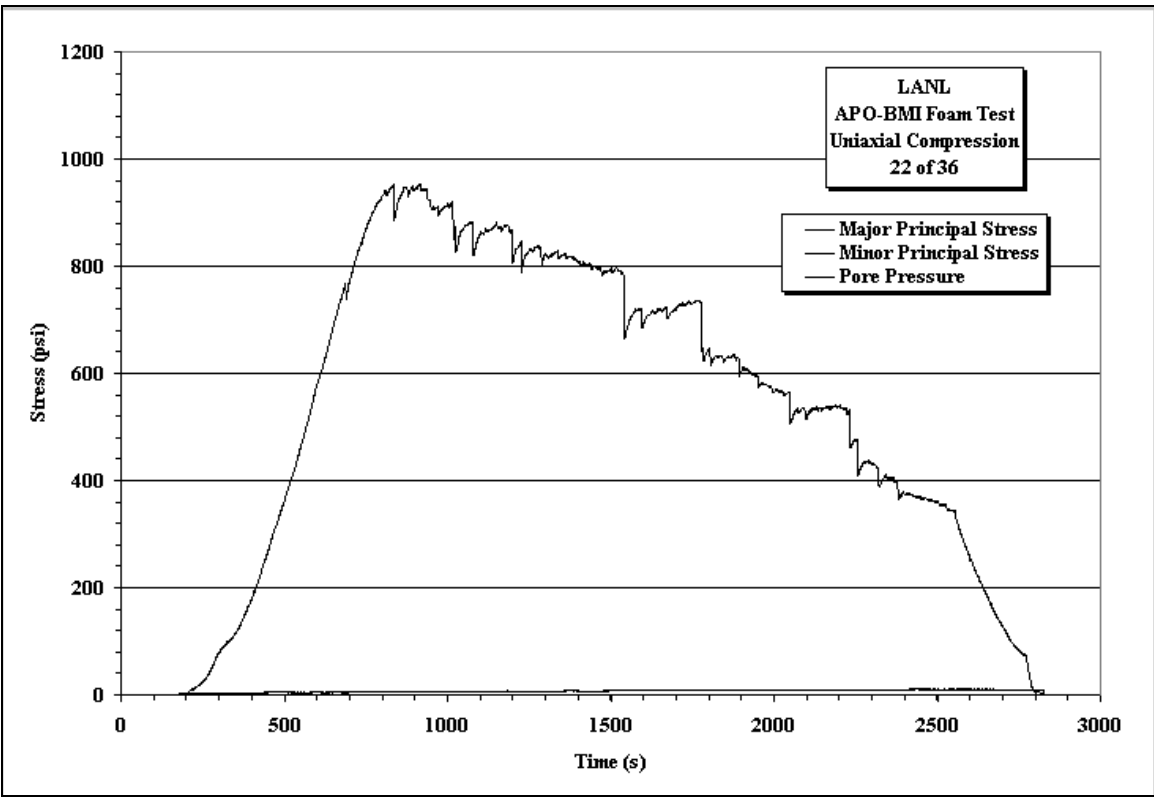
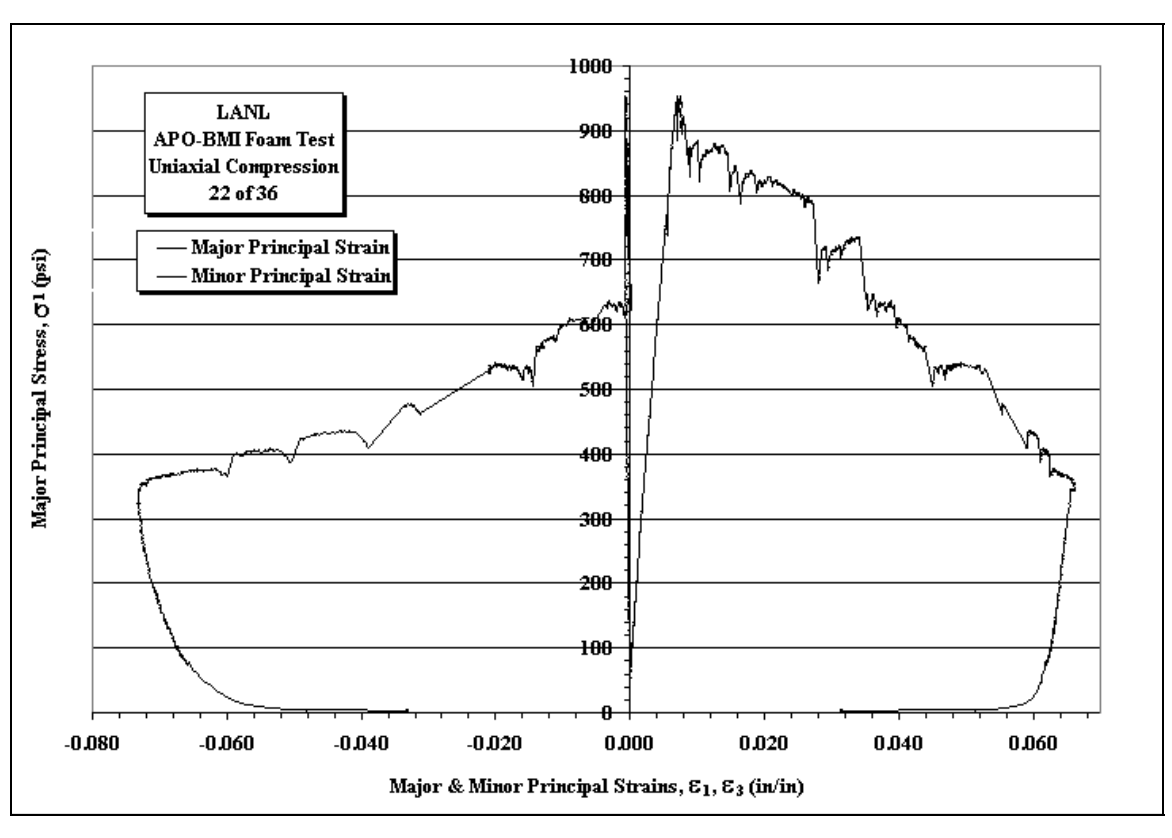


Figure A13. Minor Principle Strain vs. Major Principle Strain and Deviatoric Stress vs. Mean Stress plots for Sample 22of36 under a uniaxial pressure applied longitudinally on sample.



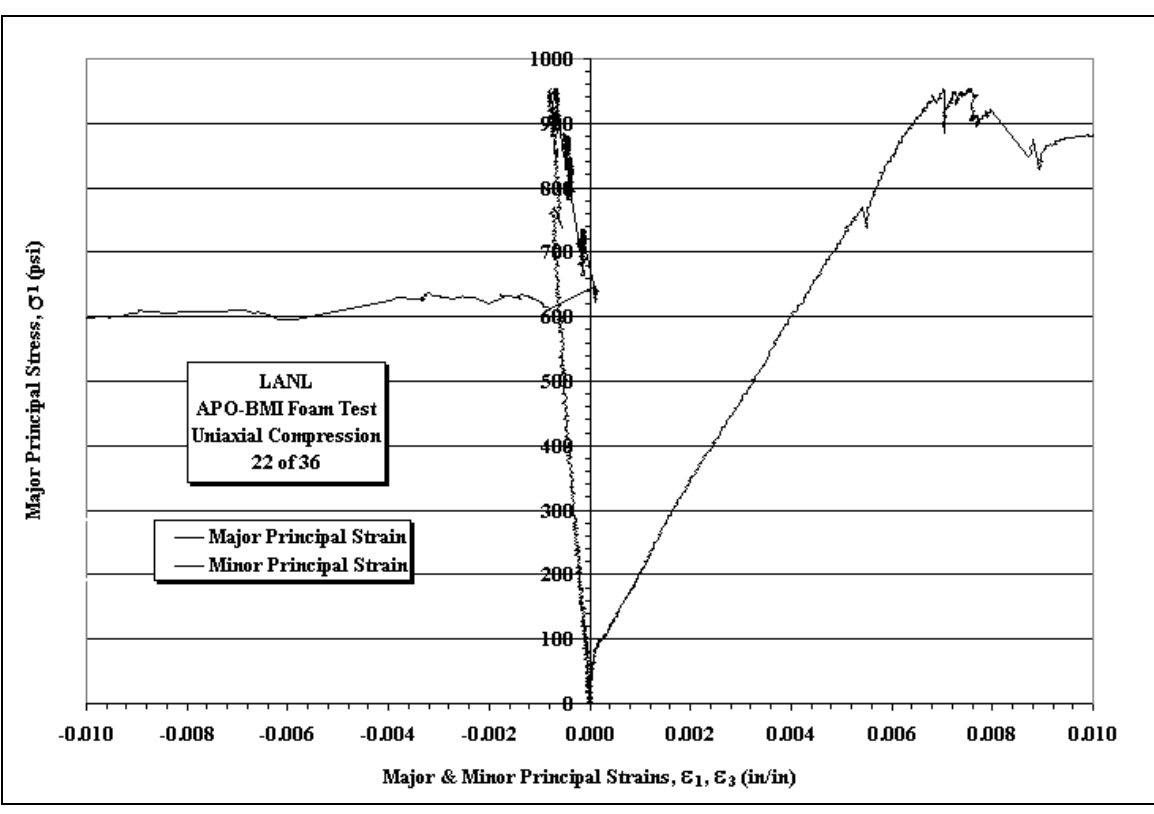
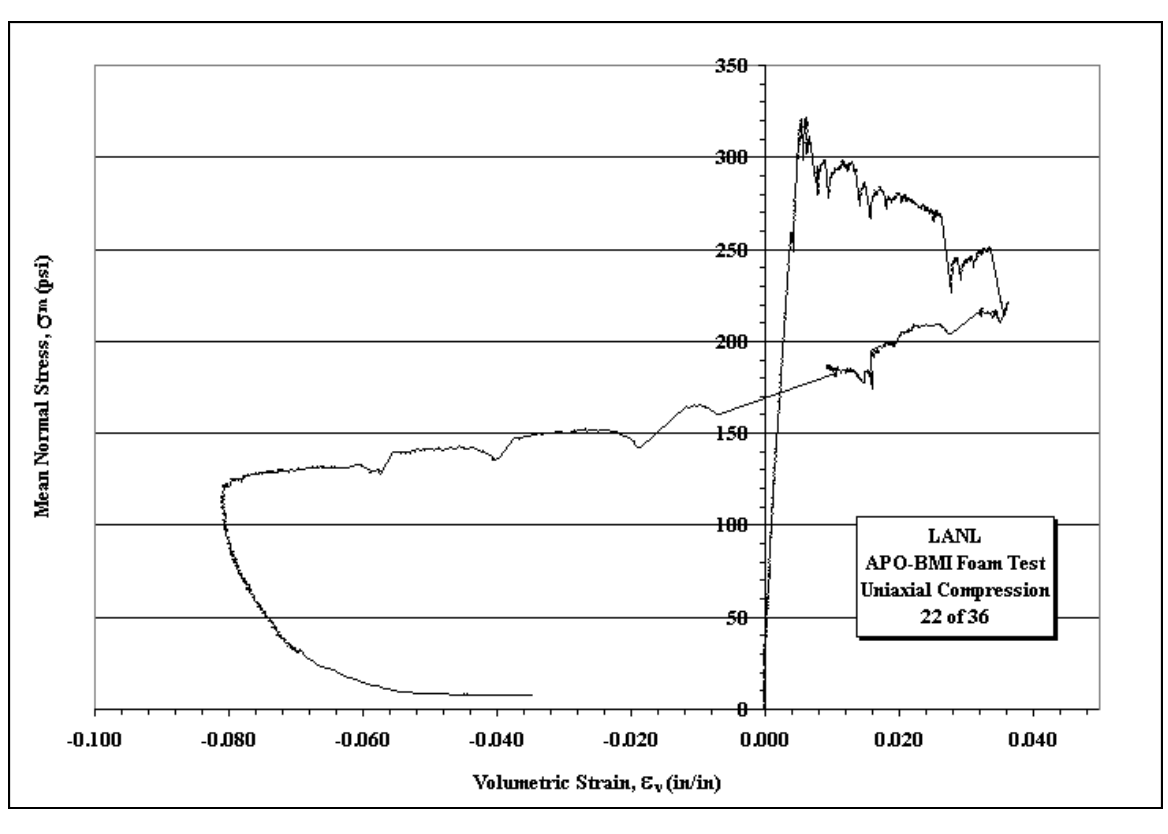


Figure A14. Stress vs. Strain plots for Sample 22of36 under a uniaxial pressure applied longitudinally on sample.



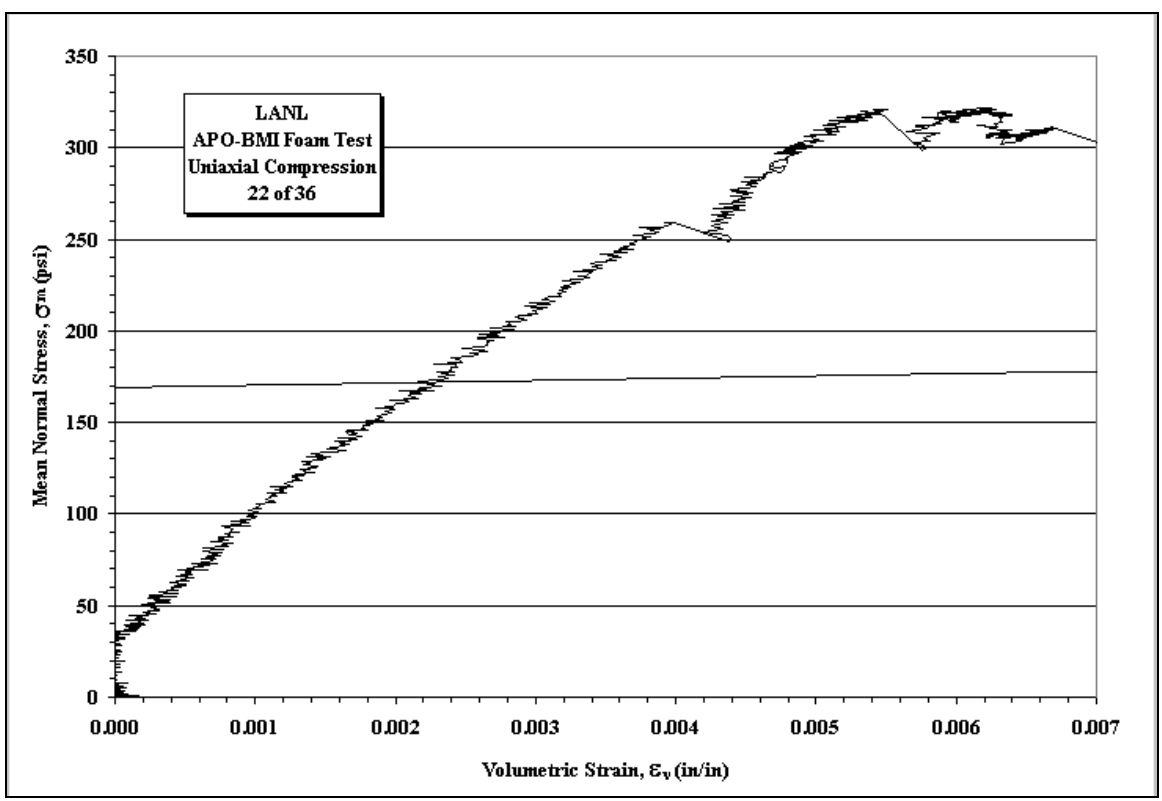
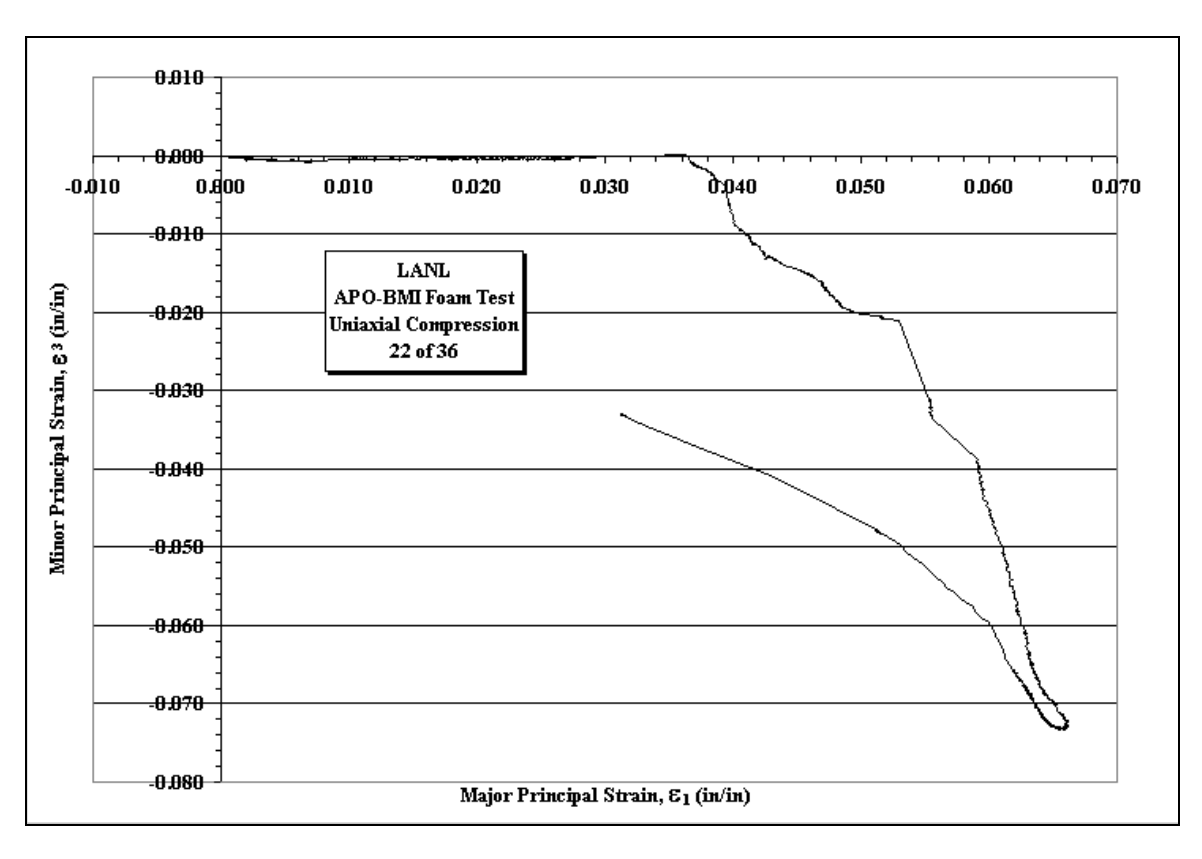


Figure A15. Mean Stress vs. Volumetric Strain plots for Sample 22of36 under a uniaxial pressure applied longitudinally on sample.



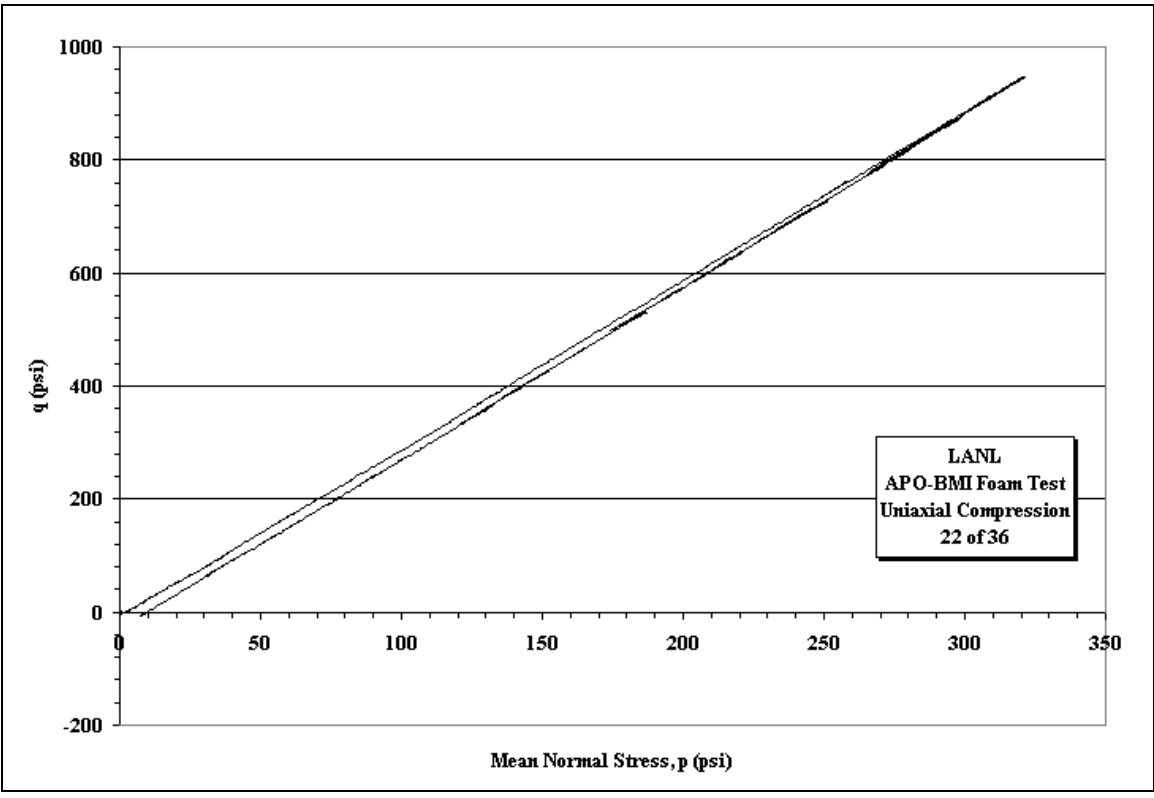
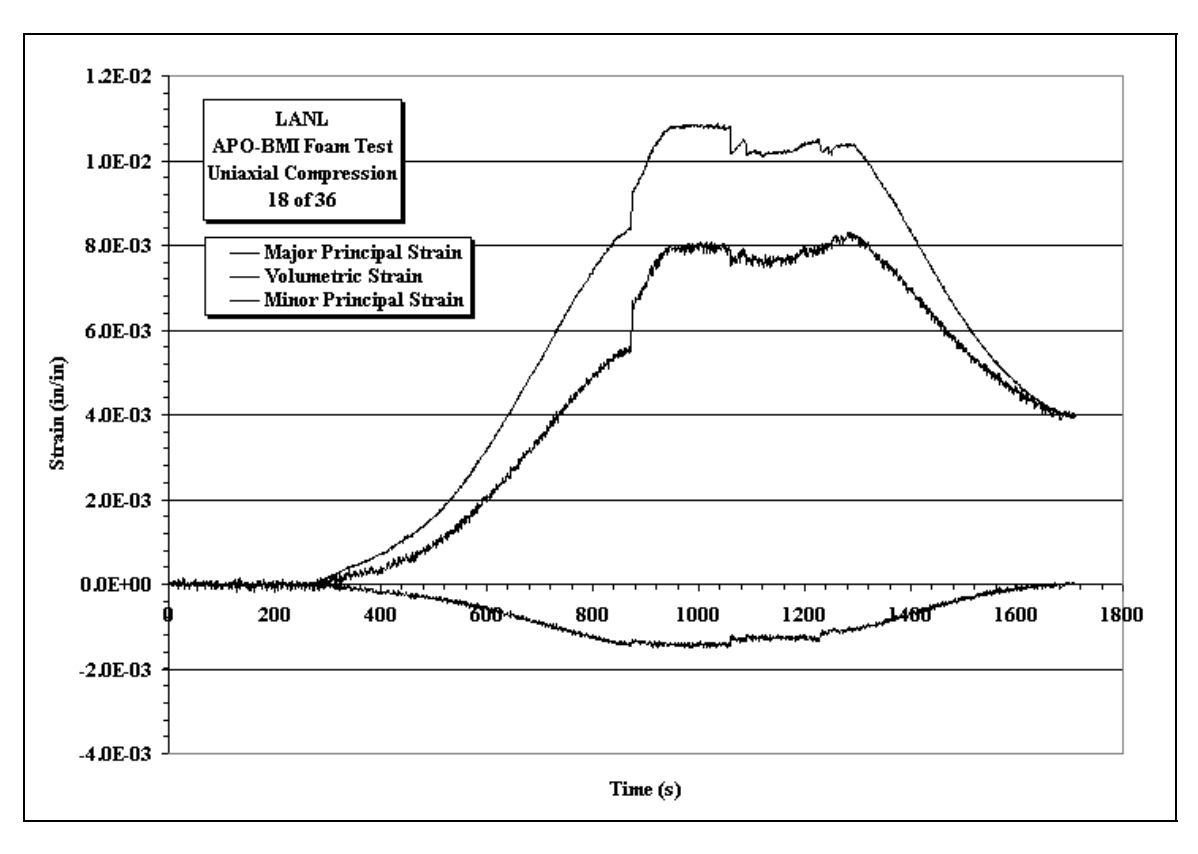


Figure A16. Minor Principle Strain vs. Major Principle Strain and Deviatoric Stress vs. Mean Stress plots for Sample 22of36 under a uniaxial pressure applied longitudinally on sample.



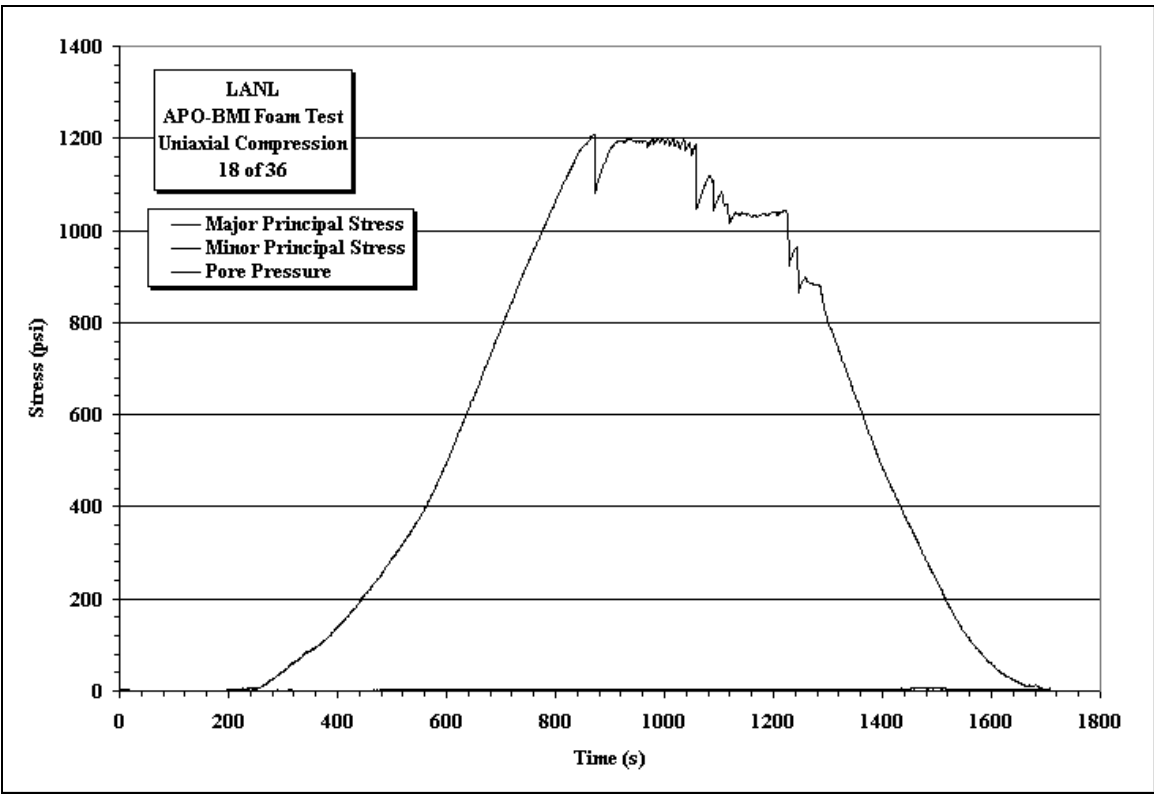
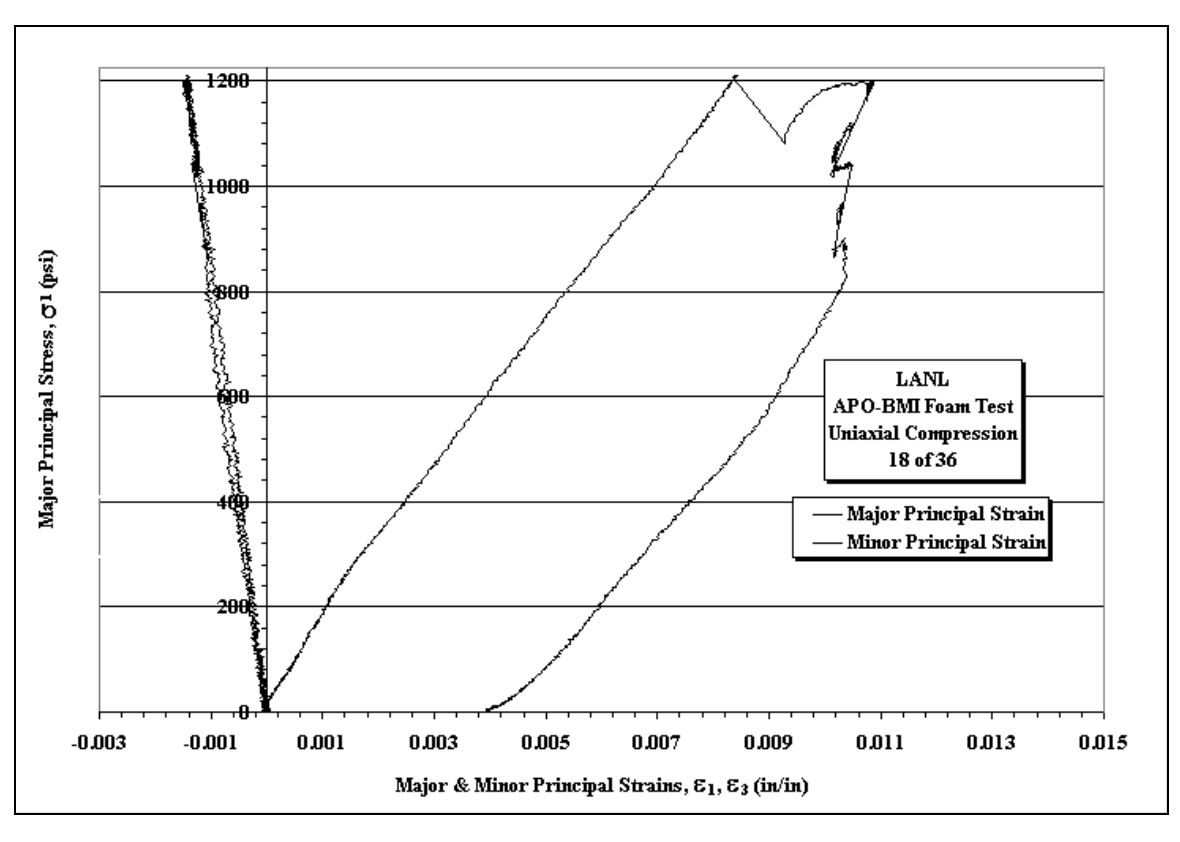


Figure A17. Minor Principle Strain vs. Major Principle Strain and Deviatoric Stress vs. Mean Stress plots for Sample 18of36 under a uniaxial pressure applied longitudinally on sample.



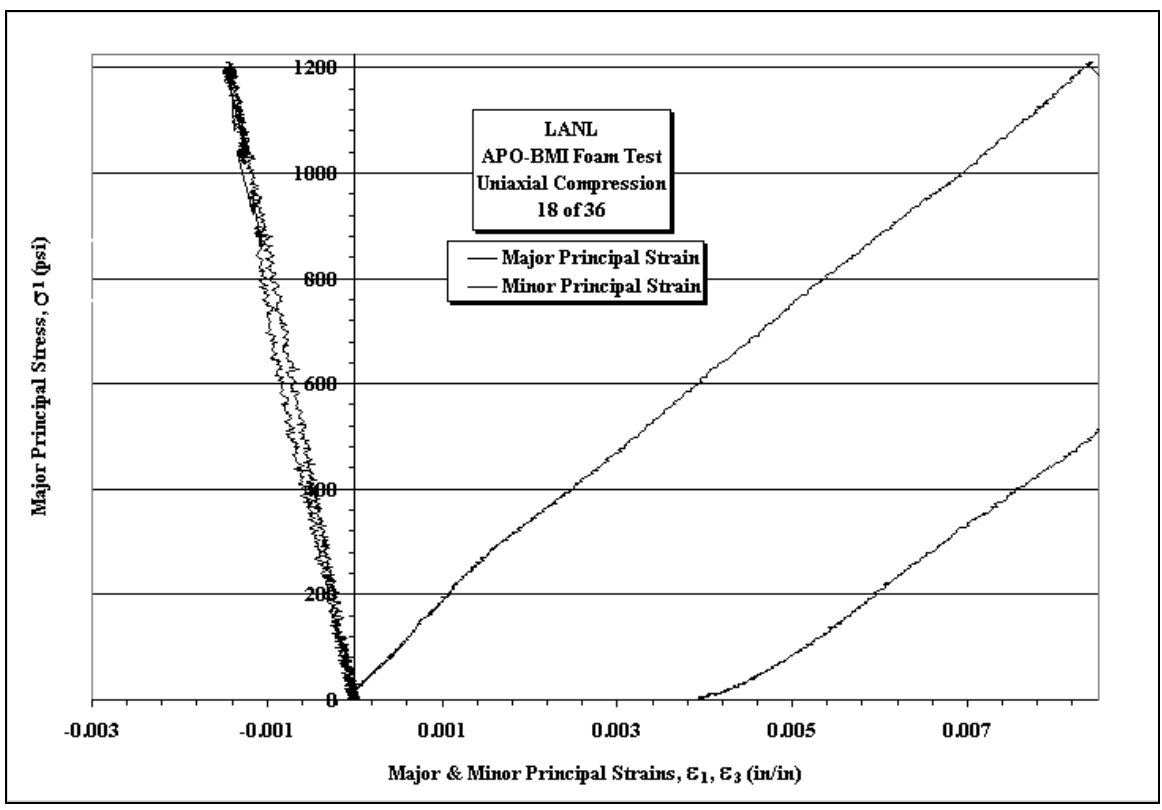
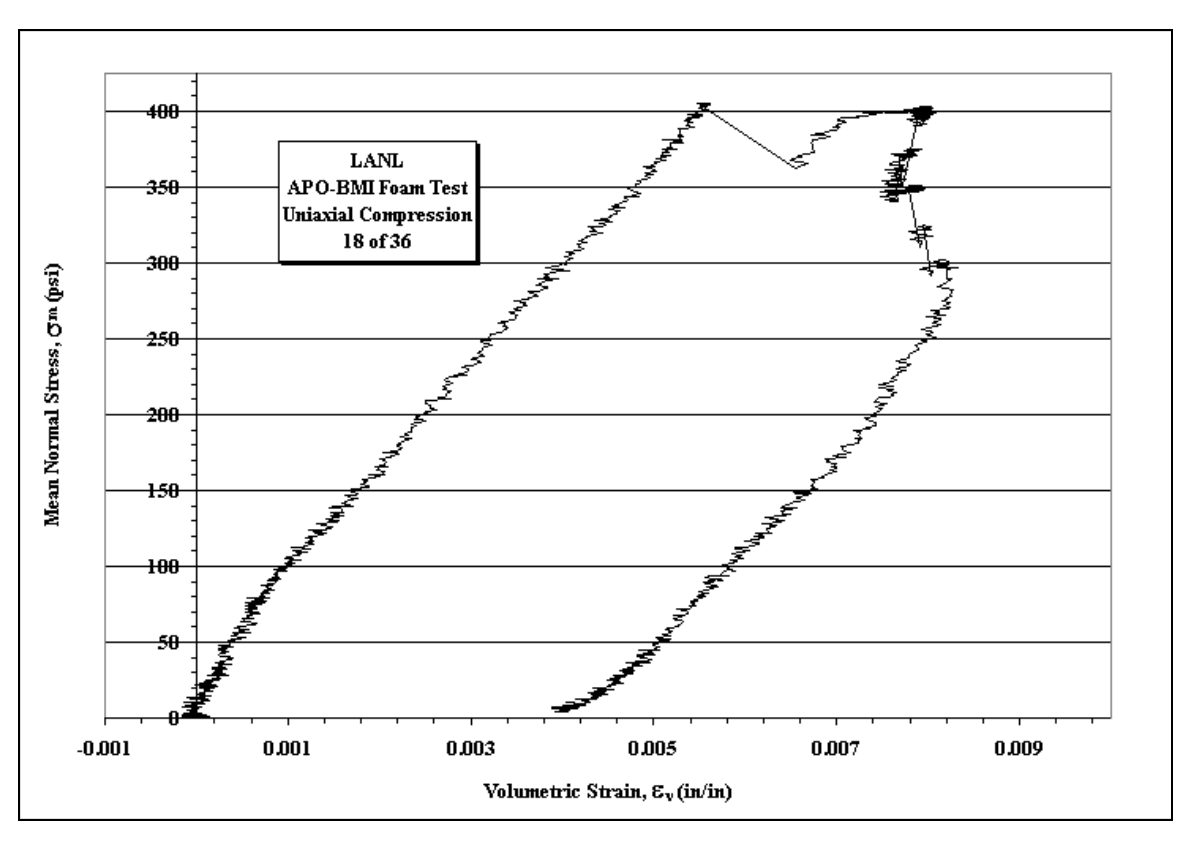


Figure A18. Stress vs. Strain plots for Sample 18of36 under a uniaxial pressure applied longitudinally on sample.



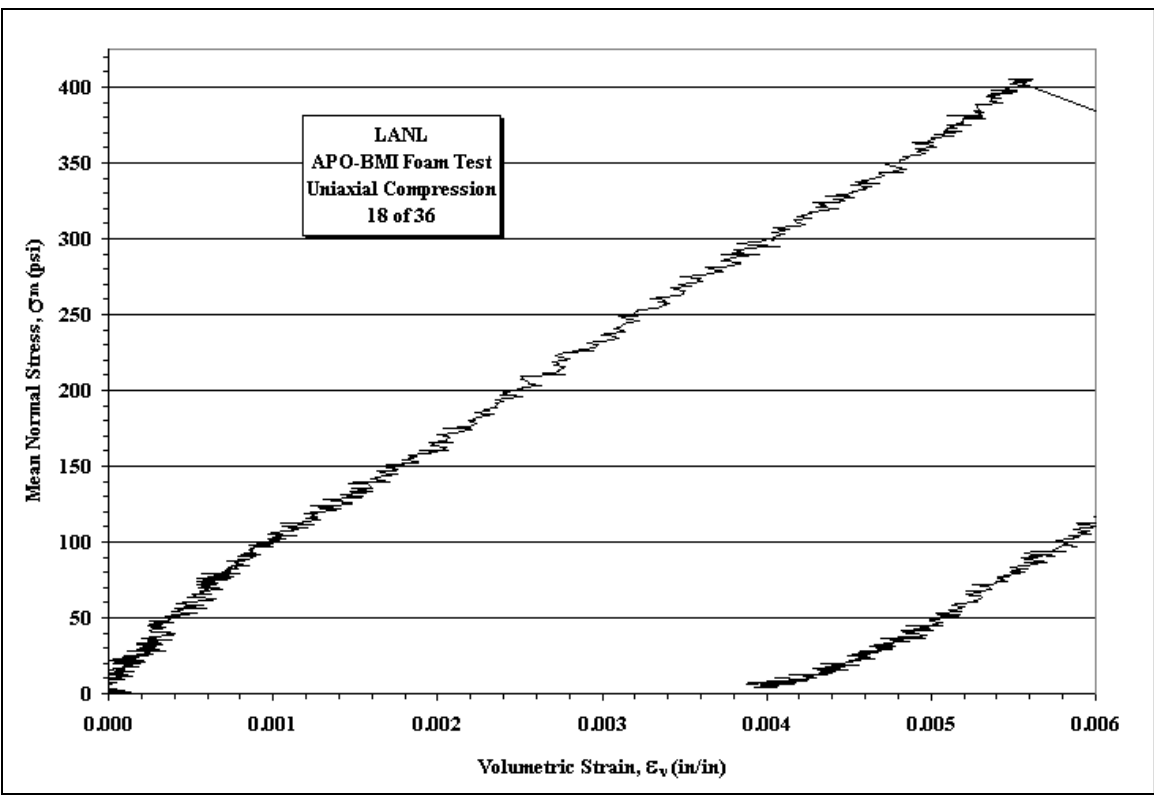
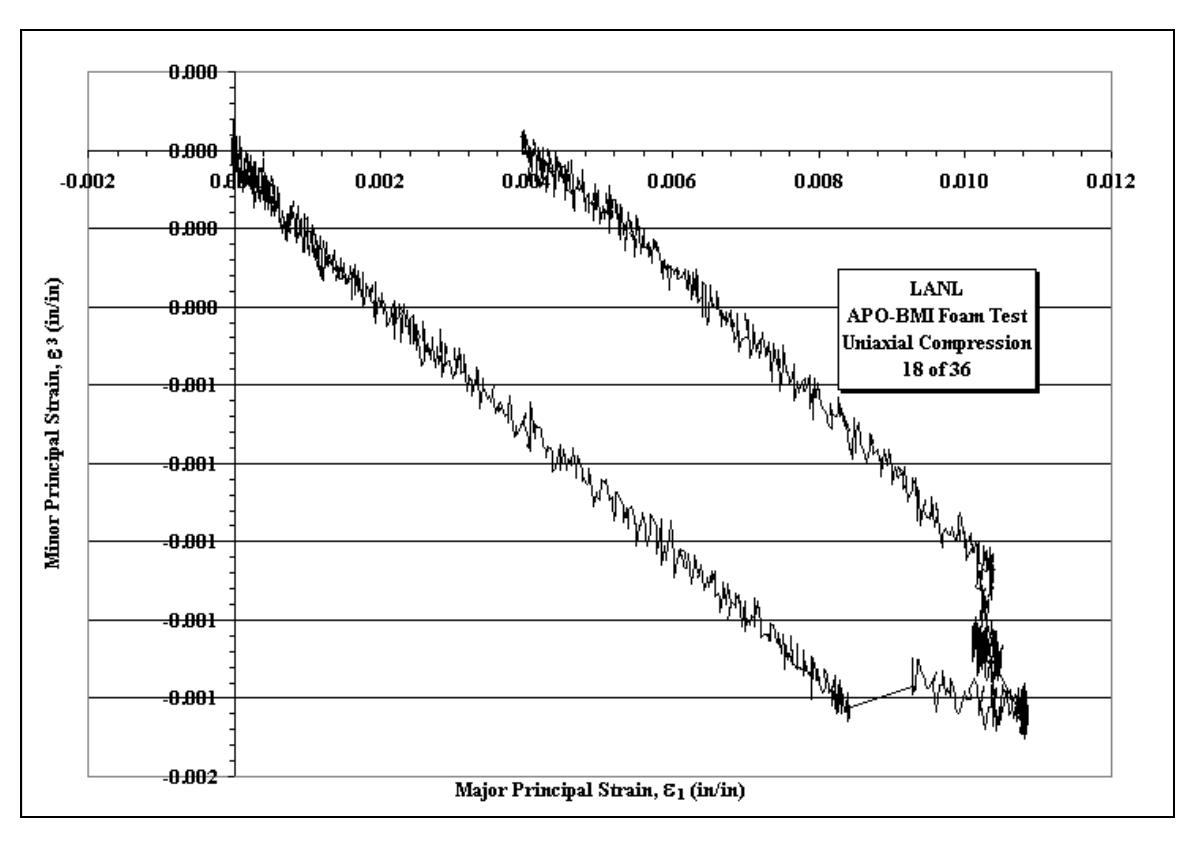


Figure A19. Mean Stress vs. Volumetric Strain plots for Sample 18of36 under a uniaxial pressure applied longitudinally on sample.



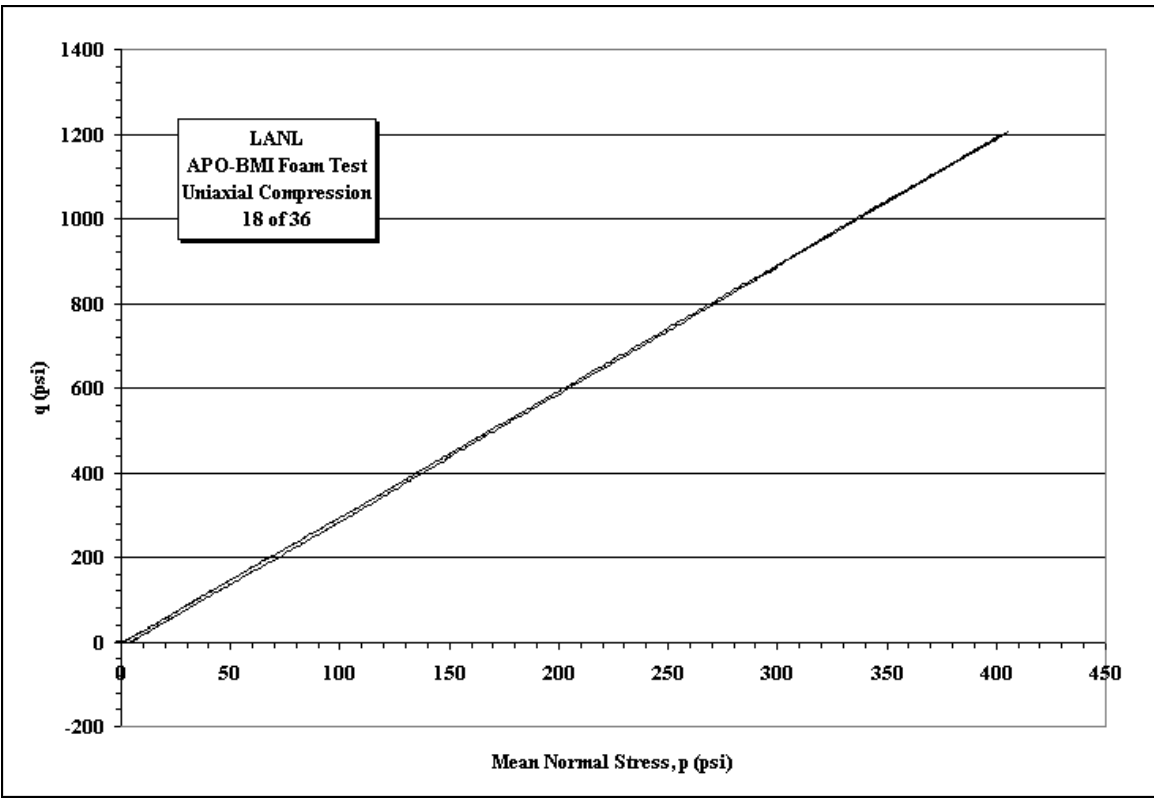
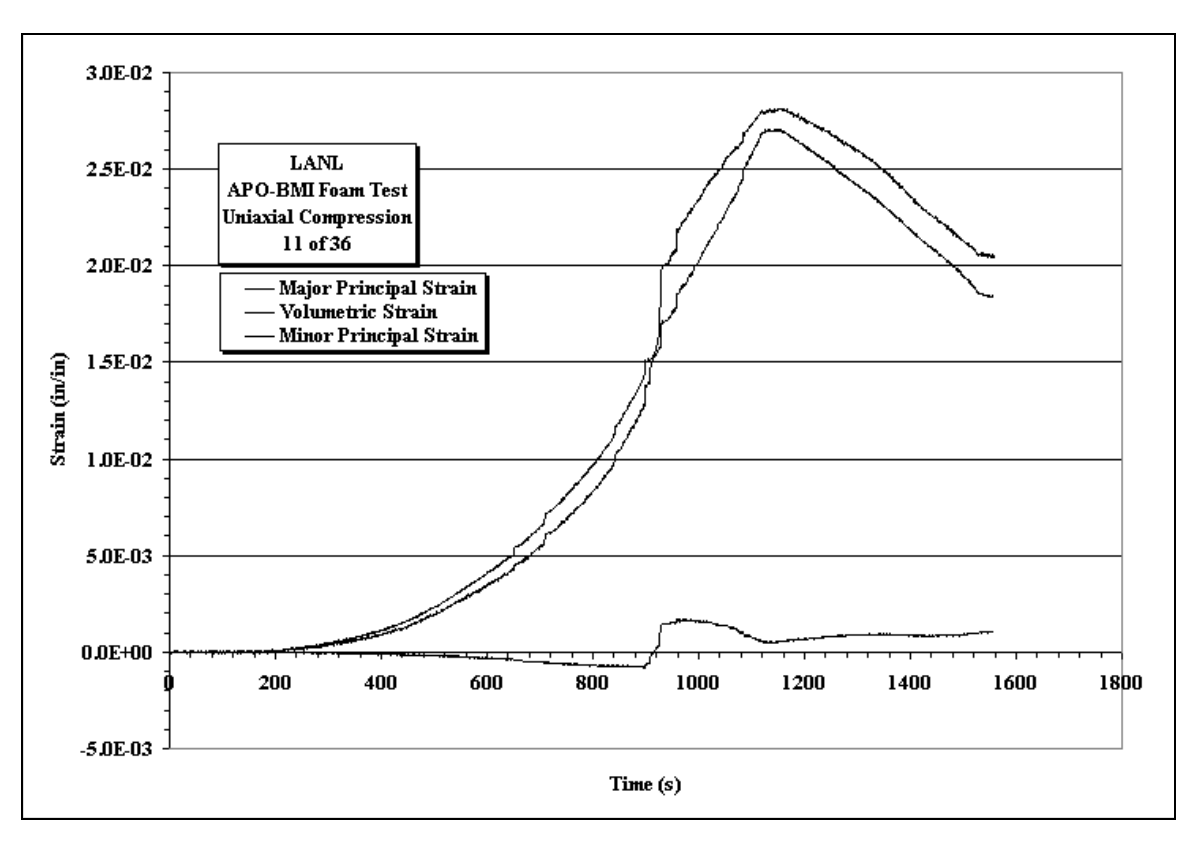


Figure A20. Minor Principle Strain vs. Major Principle Strain and Deviatoric Stress vs. Mean Stress plots for Sample 18of36 under a uniaxial pressure applied longitudinally on sample.



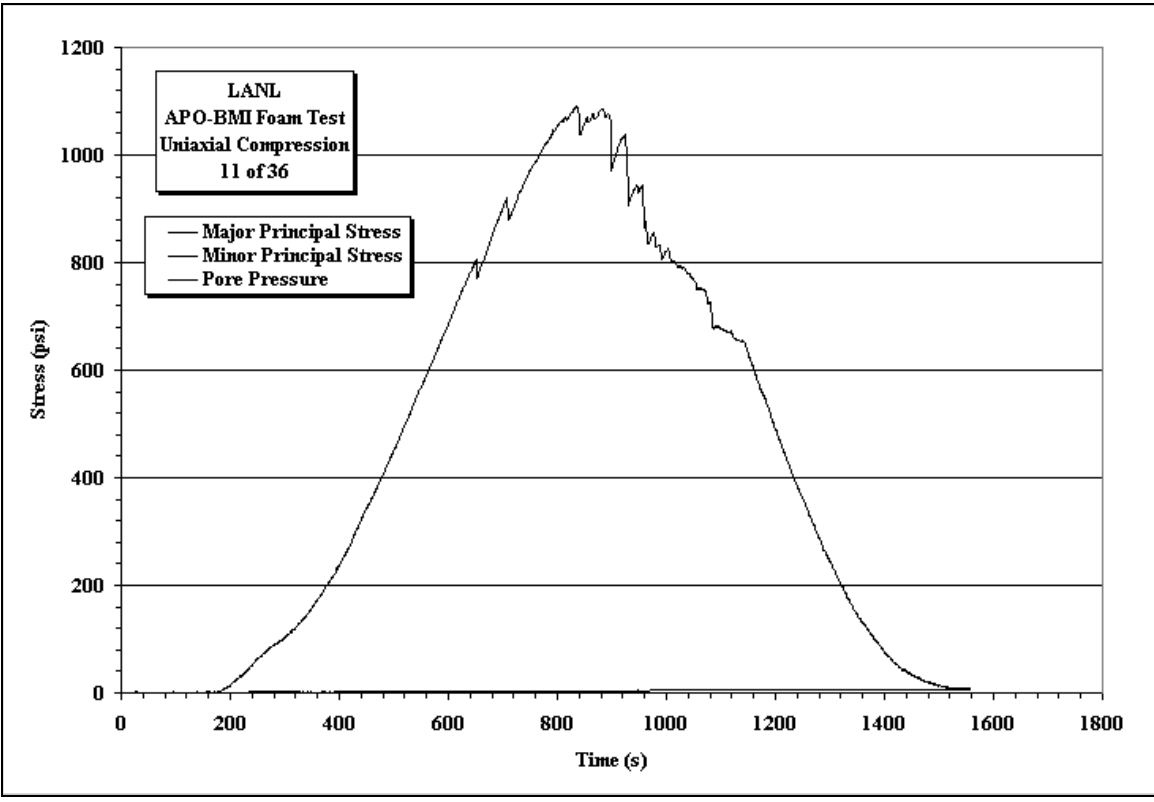
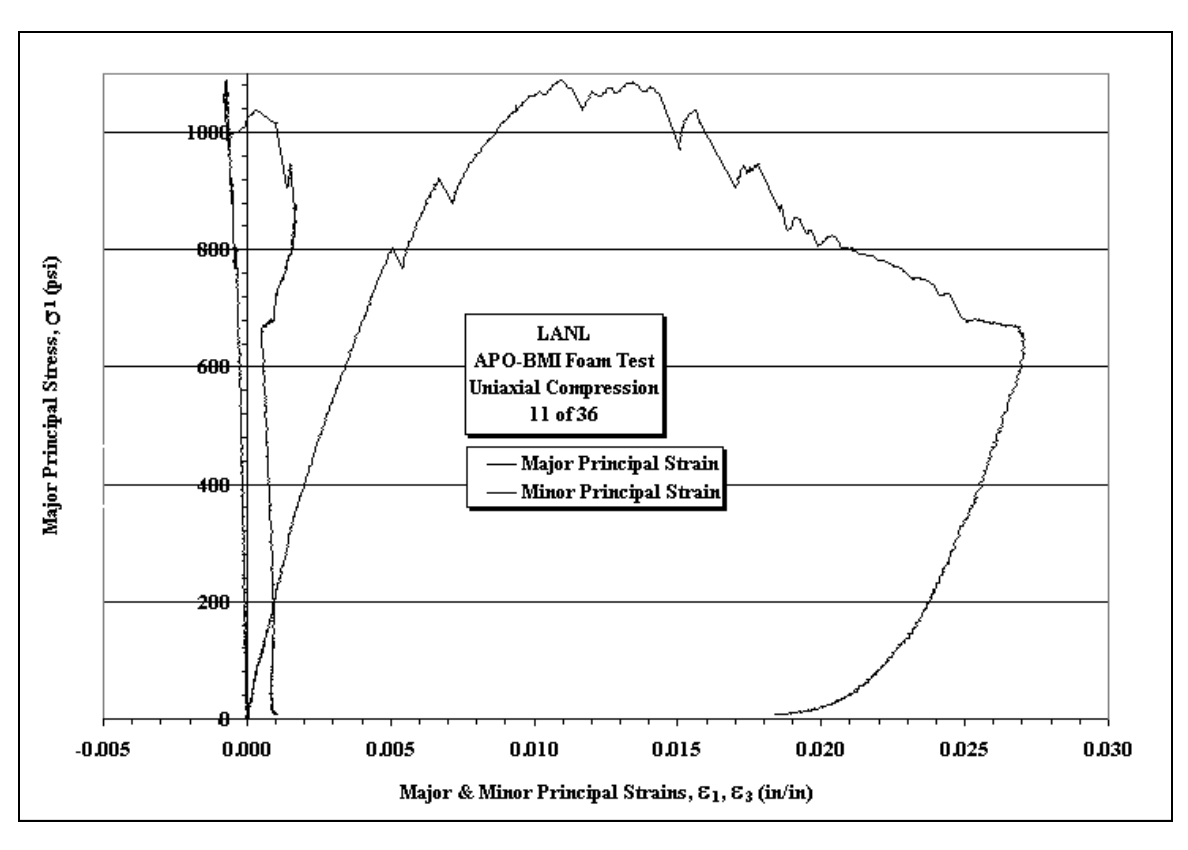


Figure A21. Minor Principle Strain vs. Major Principle Strain and Deviatoric Stress vs. Mean Stress plots for Sample 11of36 under a uniaxial pressure applied longitudinally on sample.



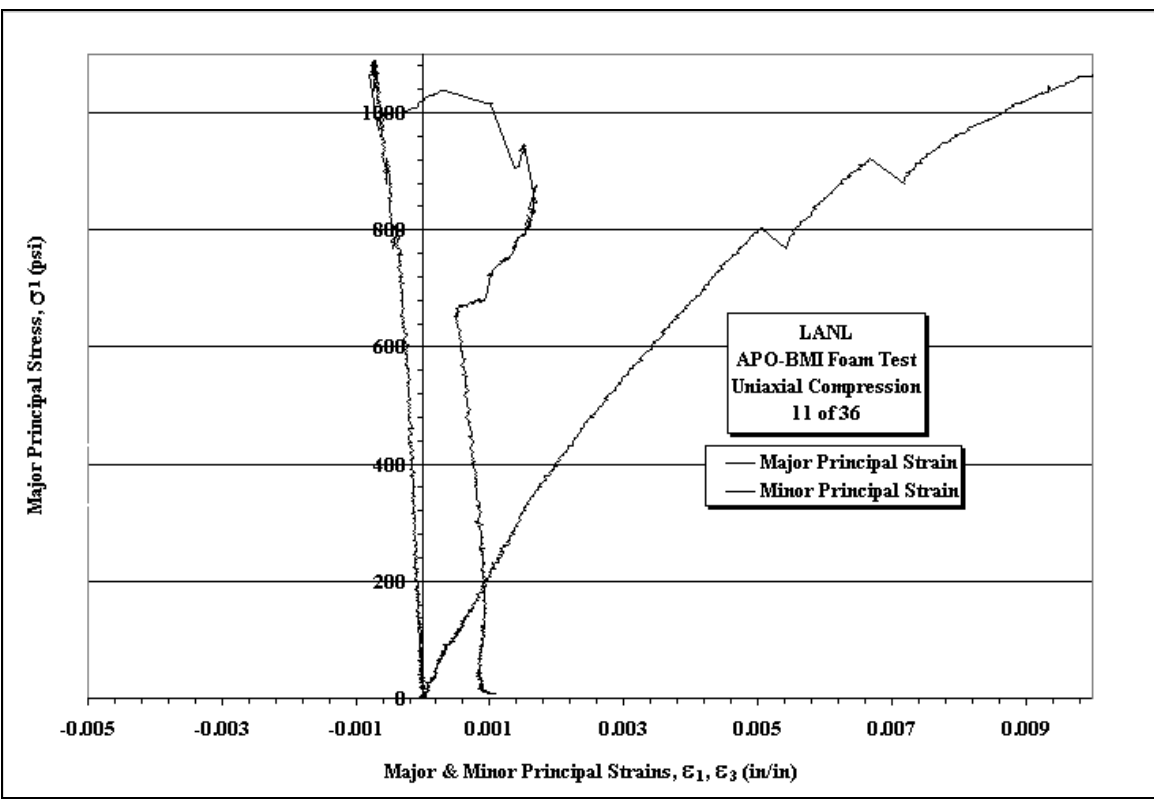
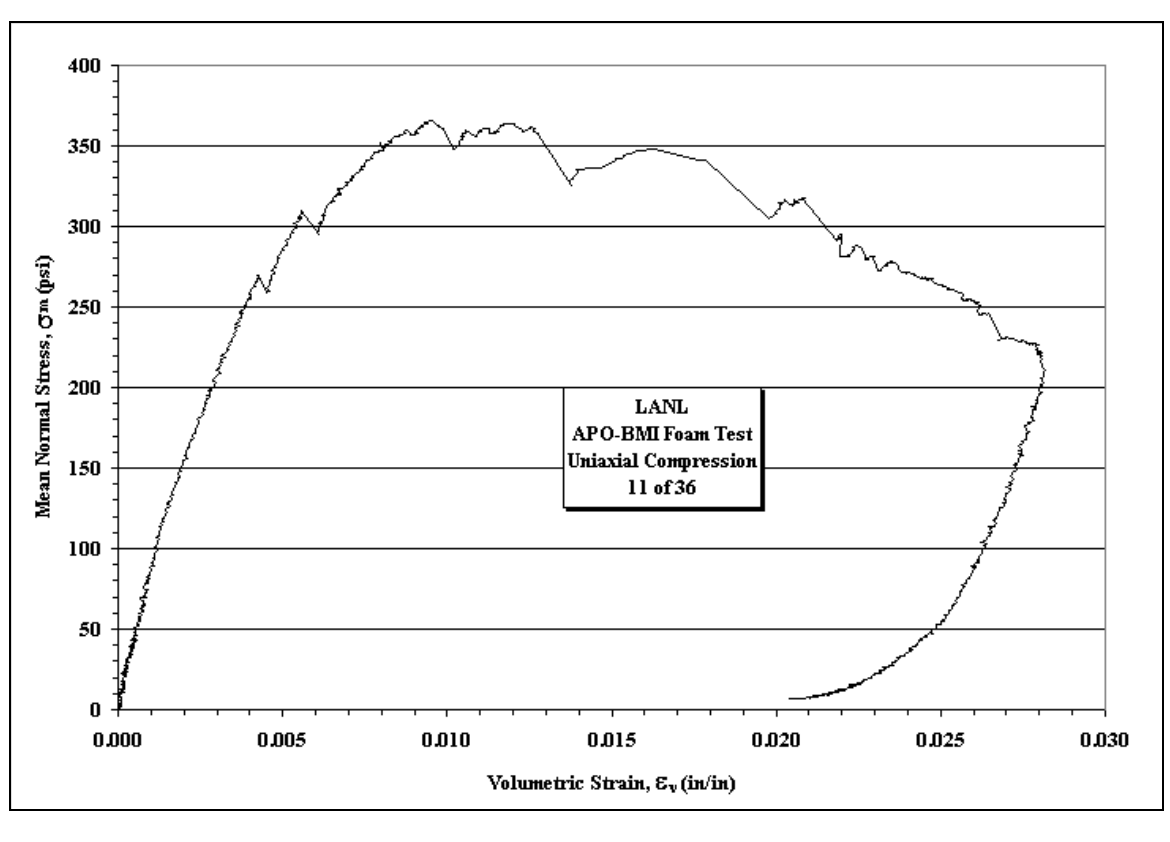


Figure A22. Stress vs. Strain plots for Sample 11of36 under a uniaxial pressure applied longitudinally on sample.



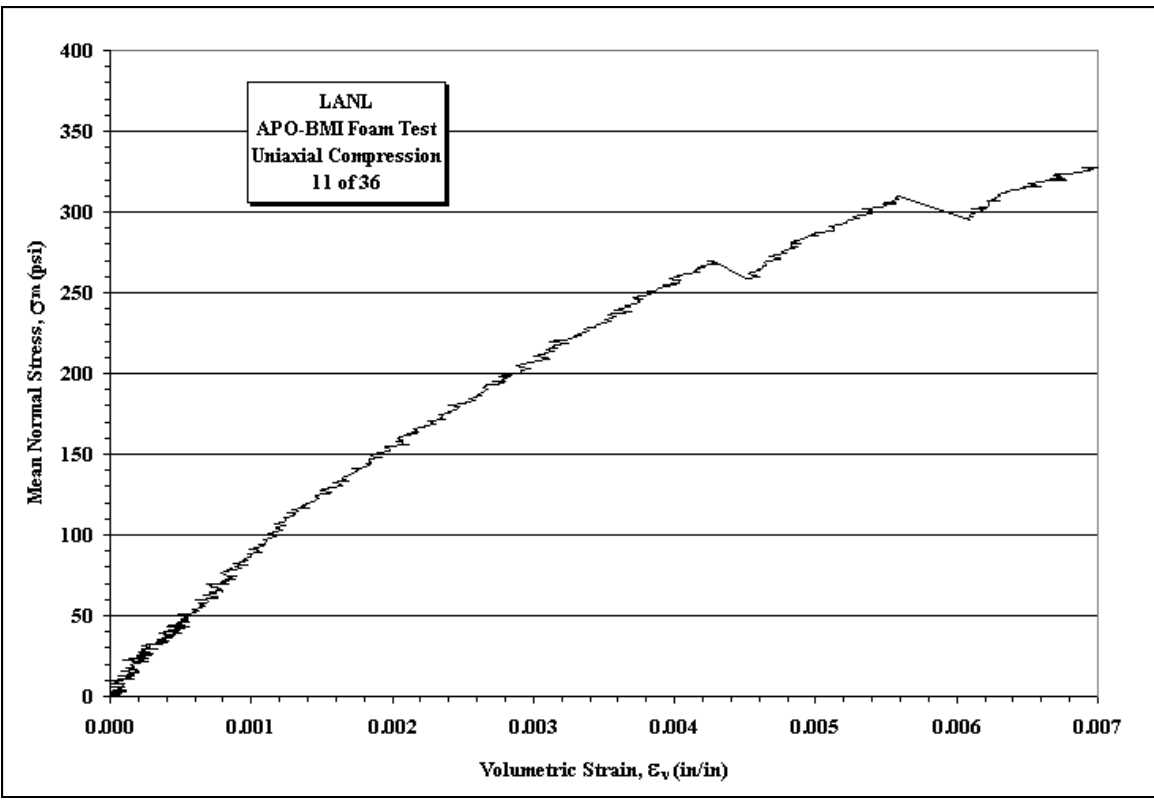
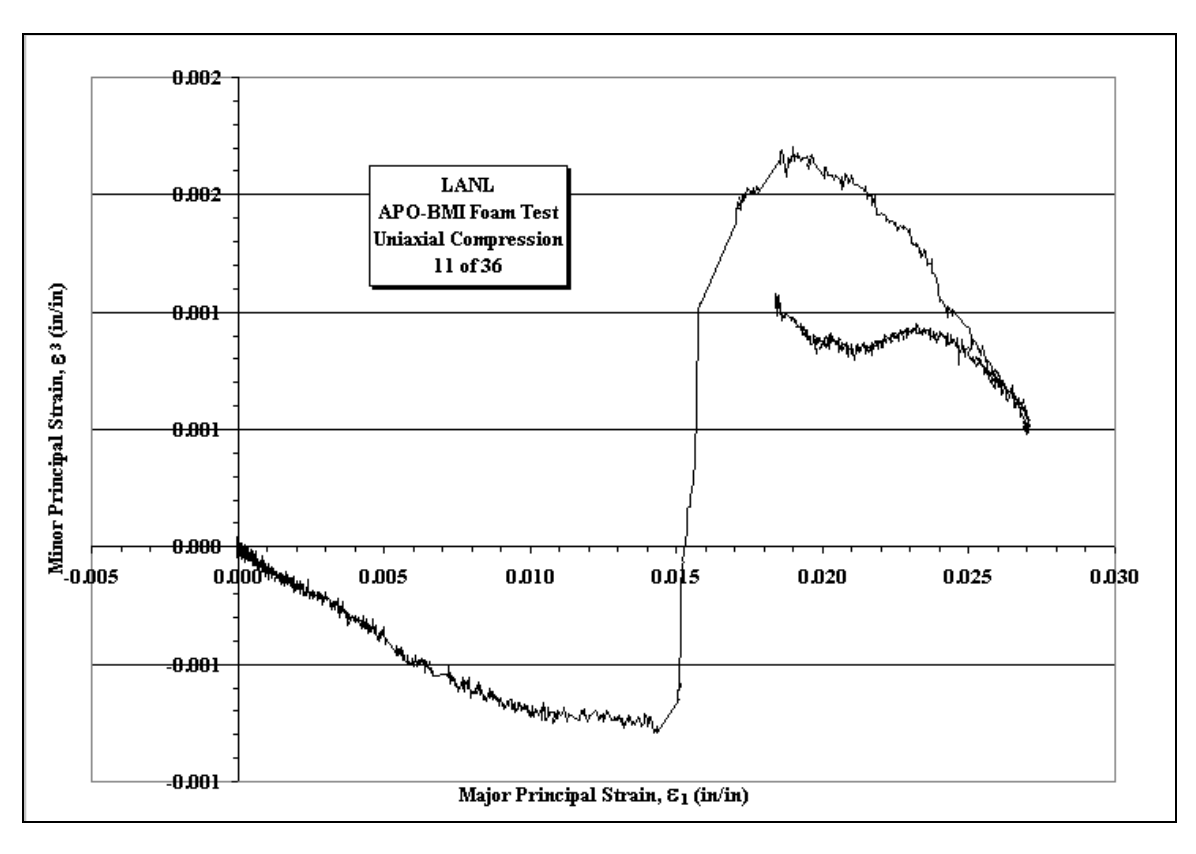


Figure A23. Mean Stress vs. Volumetric Strain plots for Sample 11of36 under a uniaxial pressure applied longitudinally on sample.



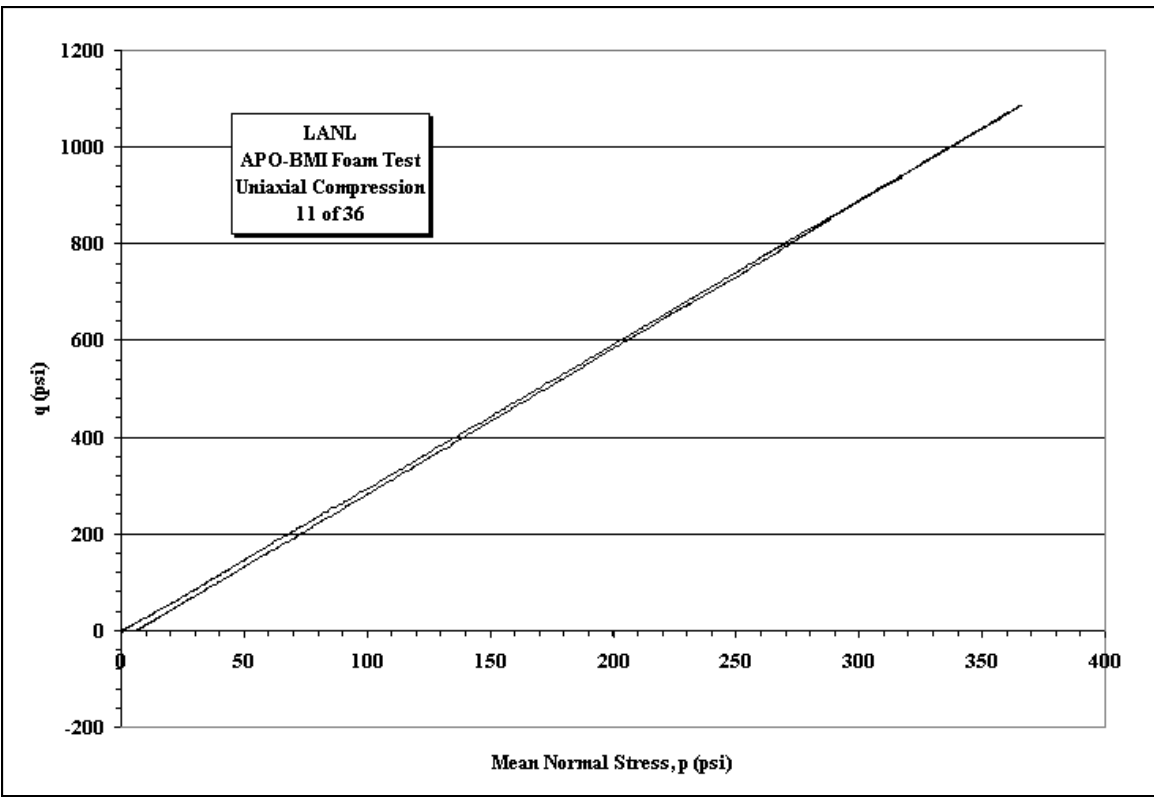
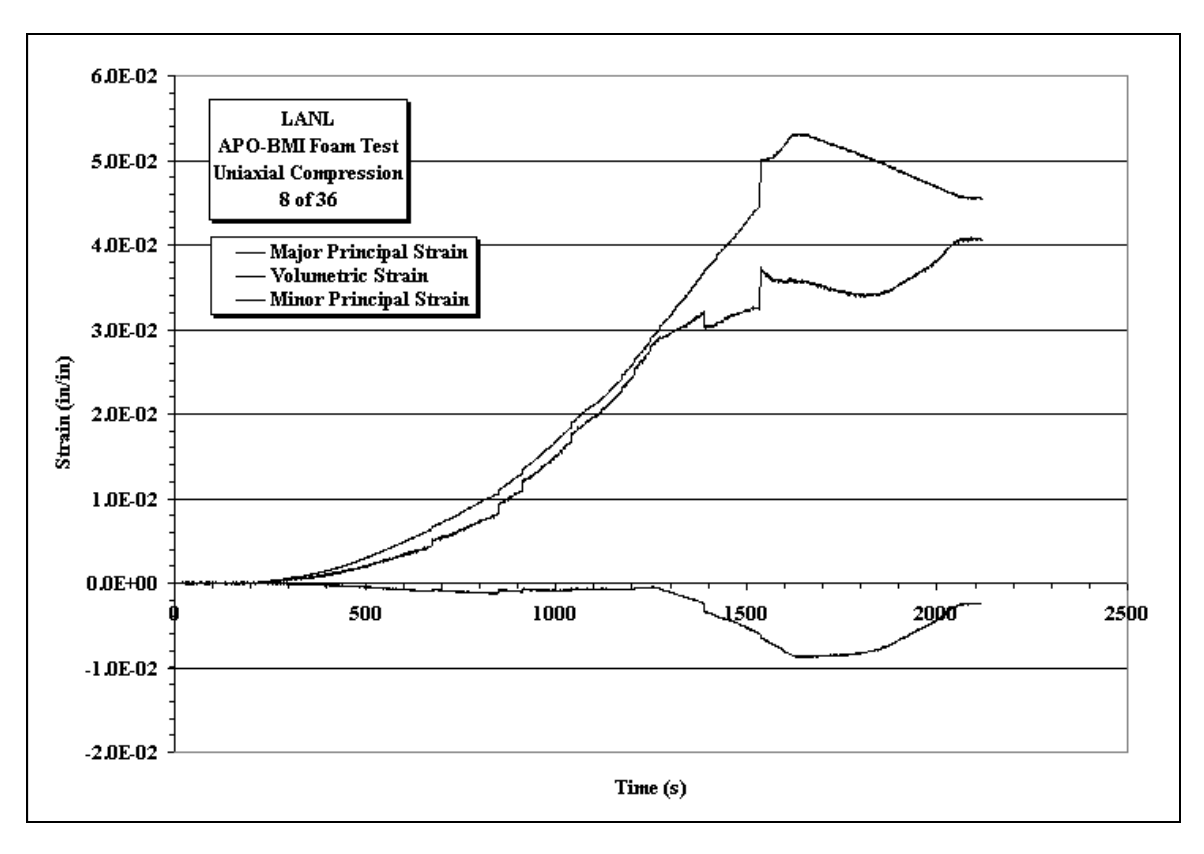


Figure A24. Minor Principle Strain vs. Major Principle Strain and Deviatoric Stress vs. Mean Stress plots for Sample 11of36 under a uniaxial pressure applied longitudinally on sample.



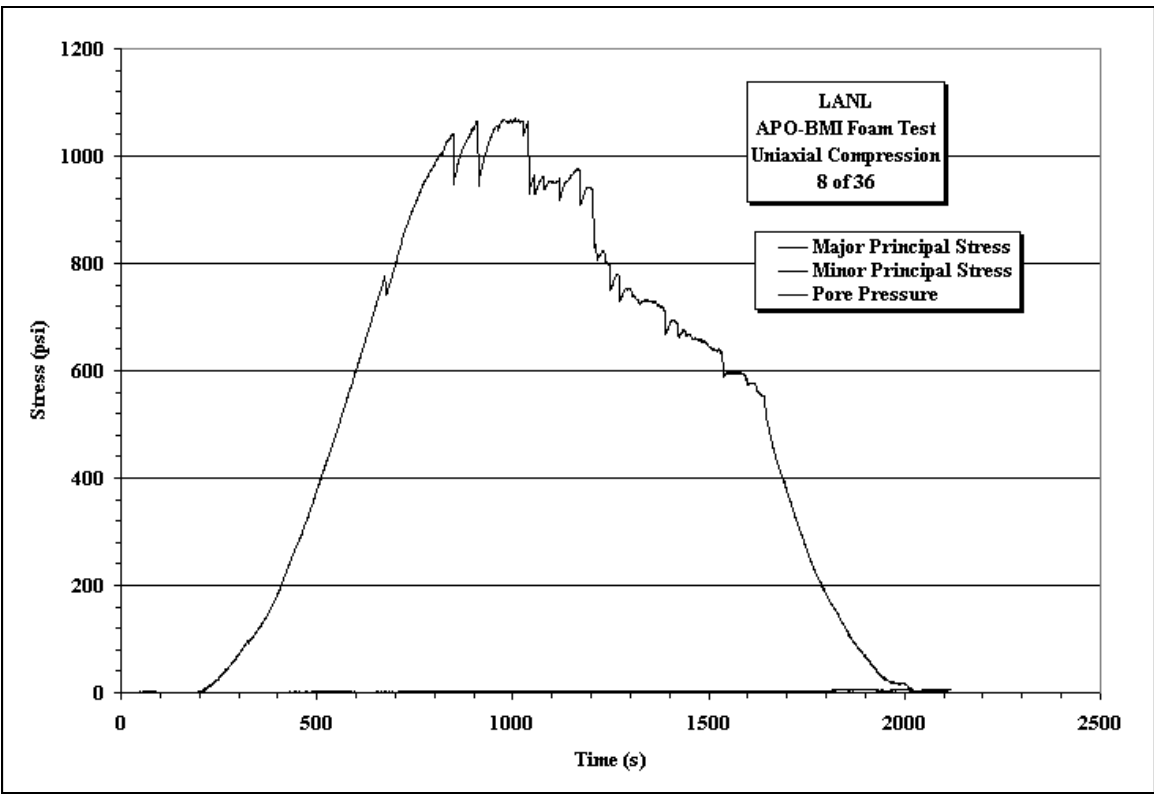
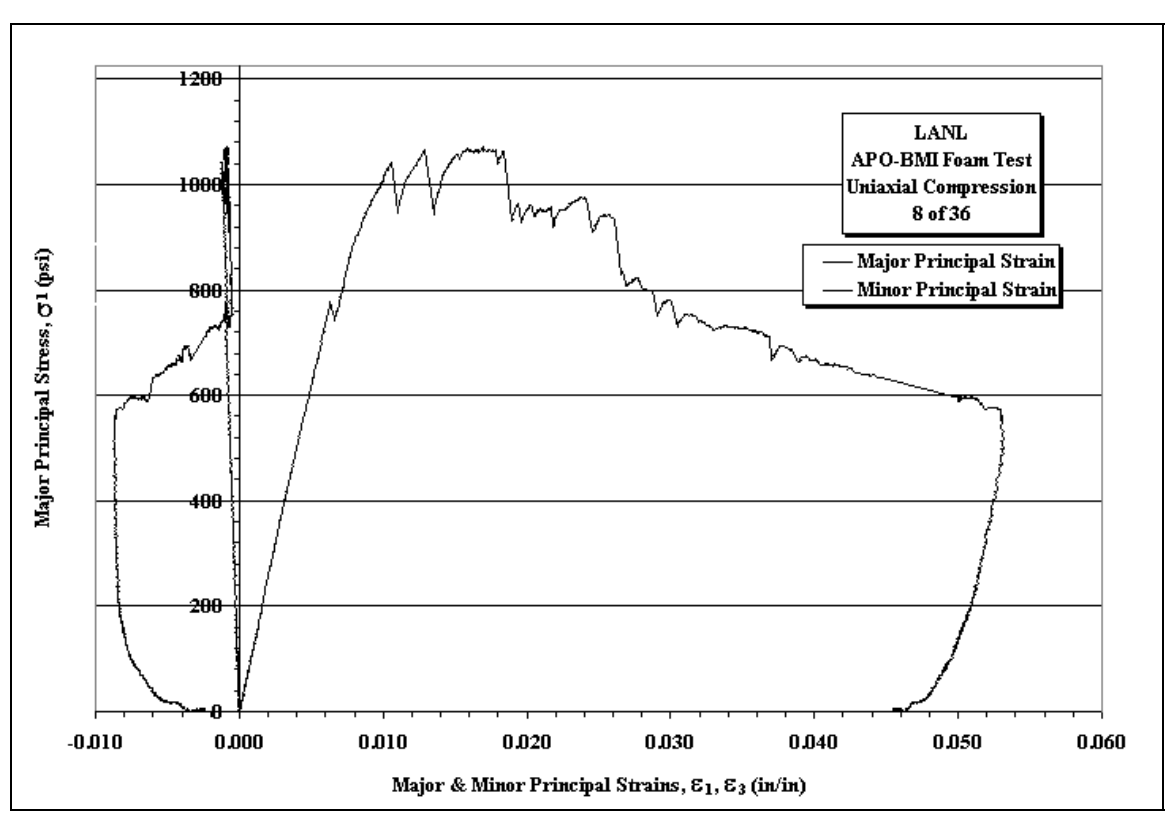


Figure A25. Minor Principle Strain vs. Major Principle Strain and Deviatoric Stress vs. Mean Stress plots for Sample 8of36 under a uniaxial pressure applied longitudinally on sample.



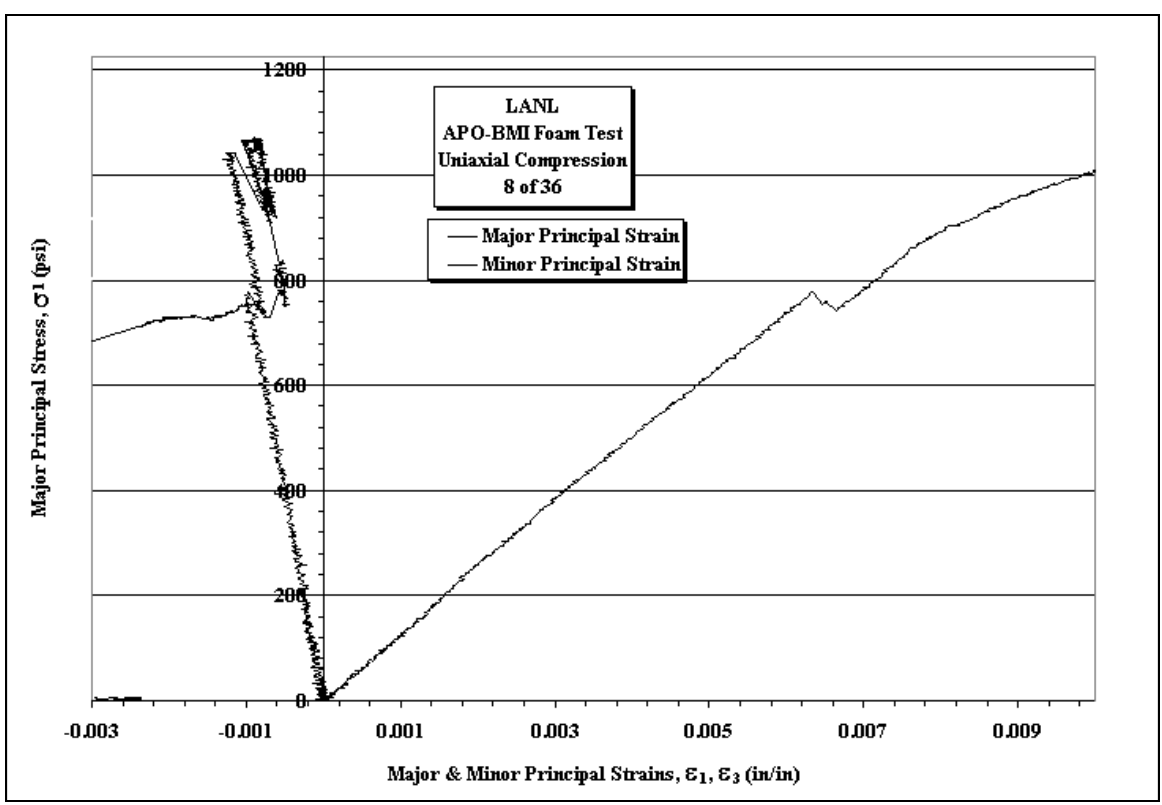
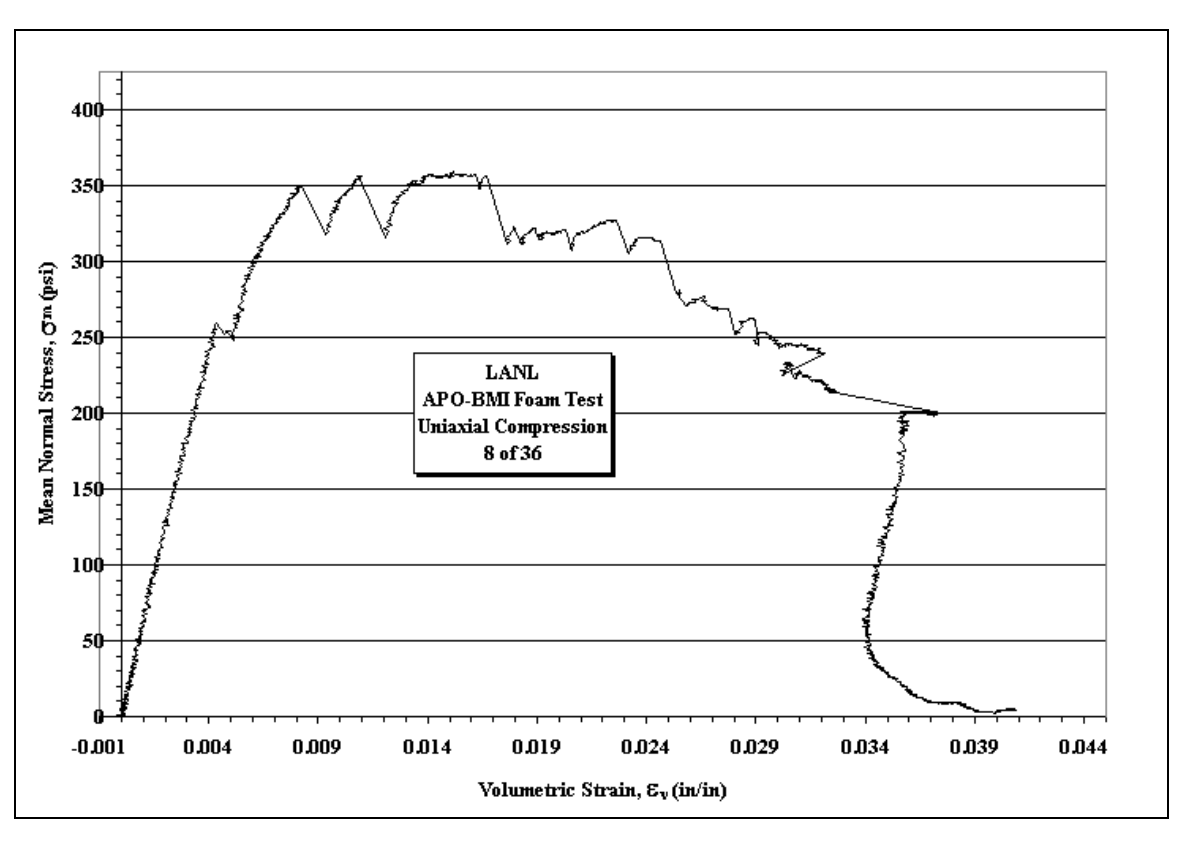


Figure A26. Stress vs. Strain plots for Sample 8of36 under a uniaxial pressure applied longitudinally on sample.



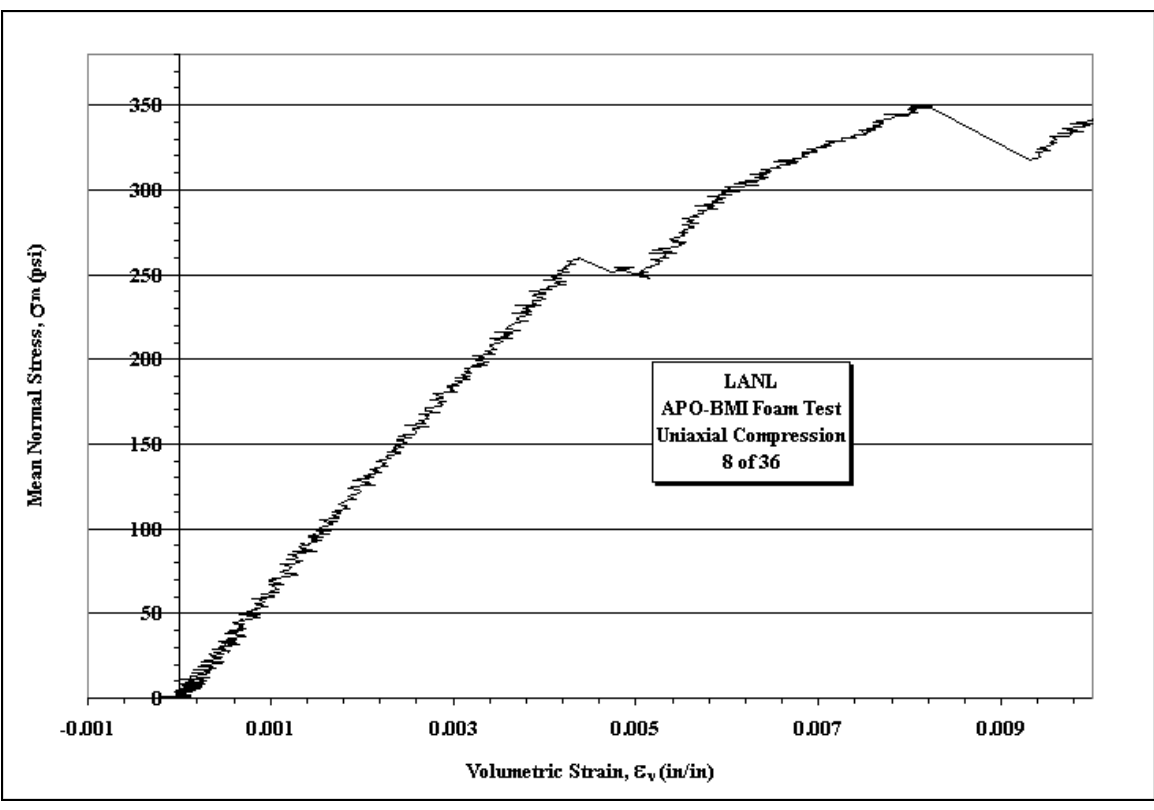
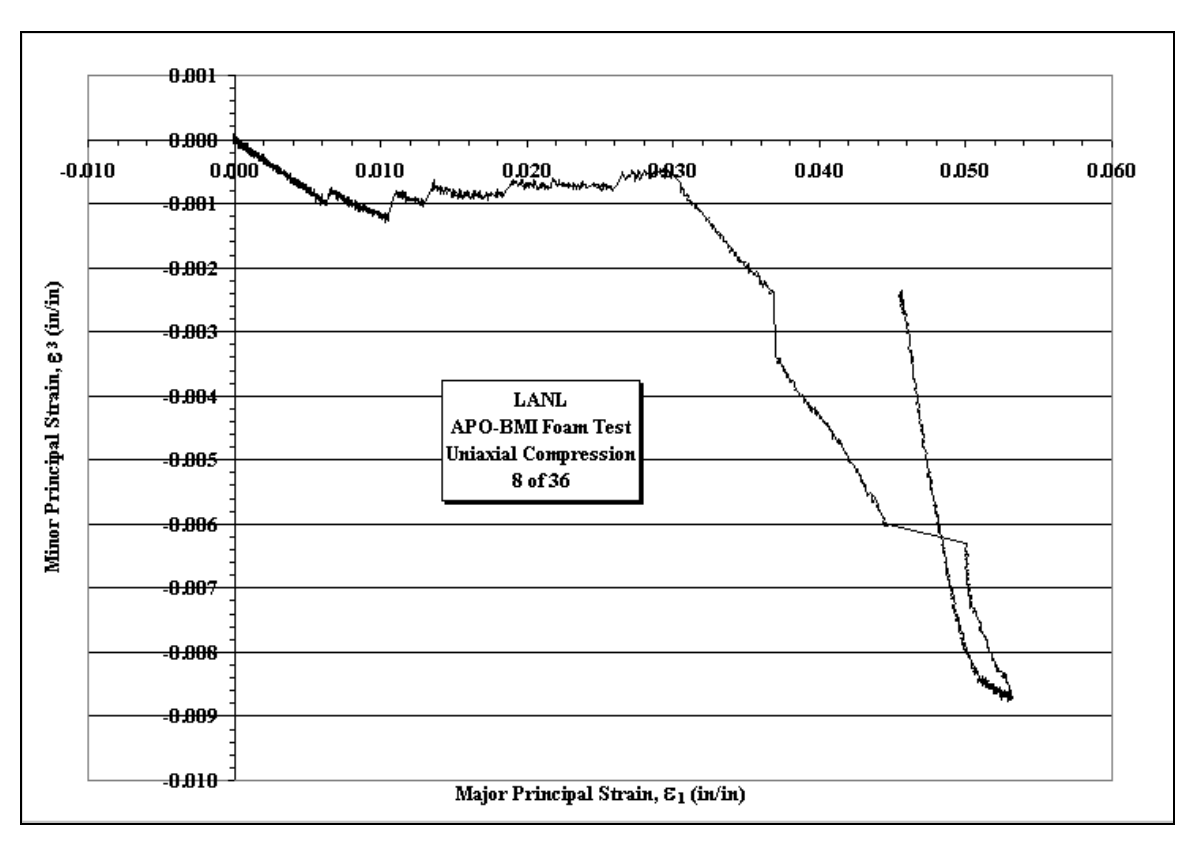


Figure A27. Mean Stress vs. Volumetric Strain plots for Sample 8of36 under a uniaxial pressure applied longitudinally on sample.



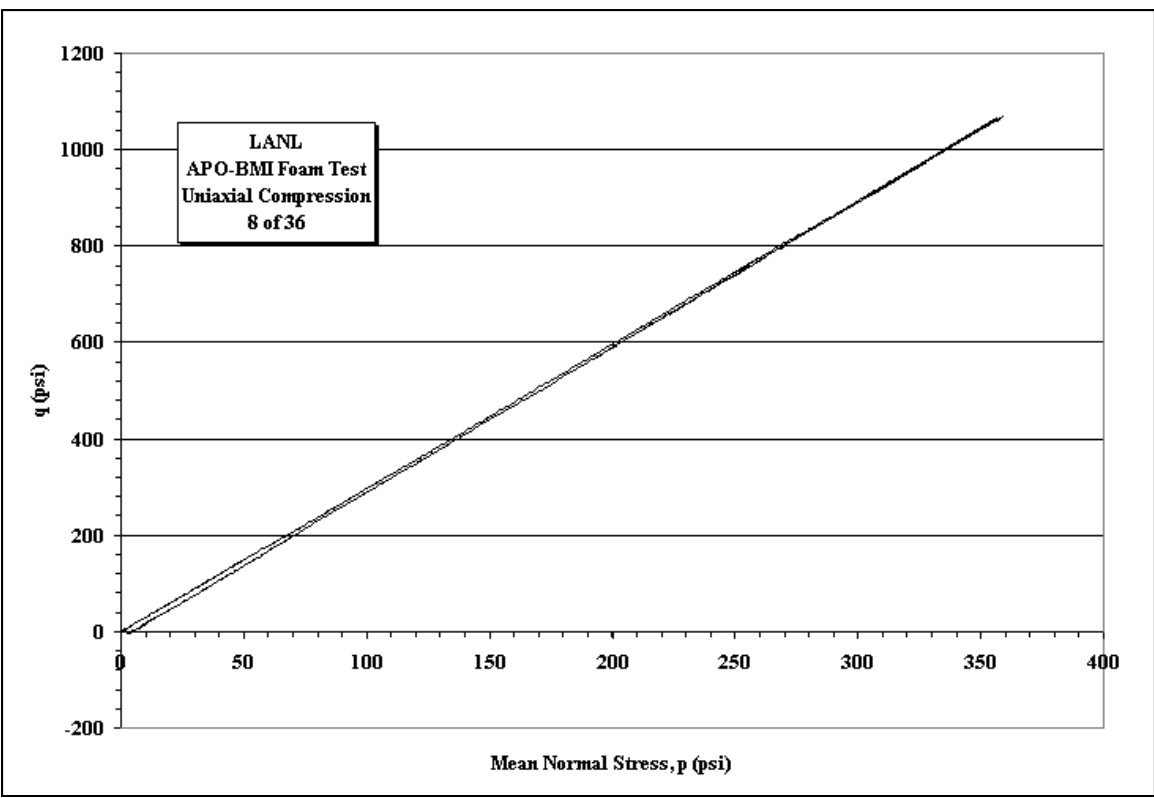
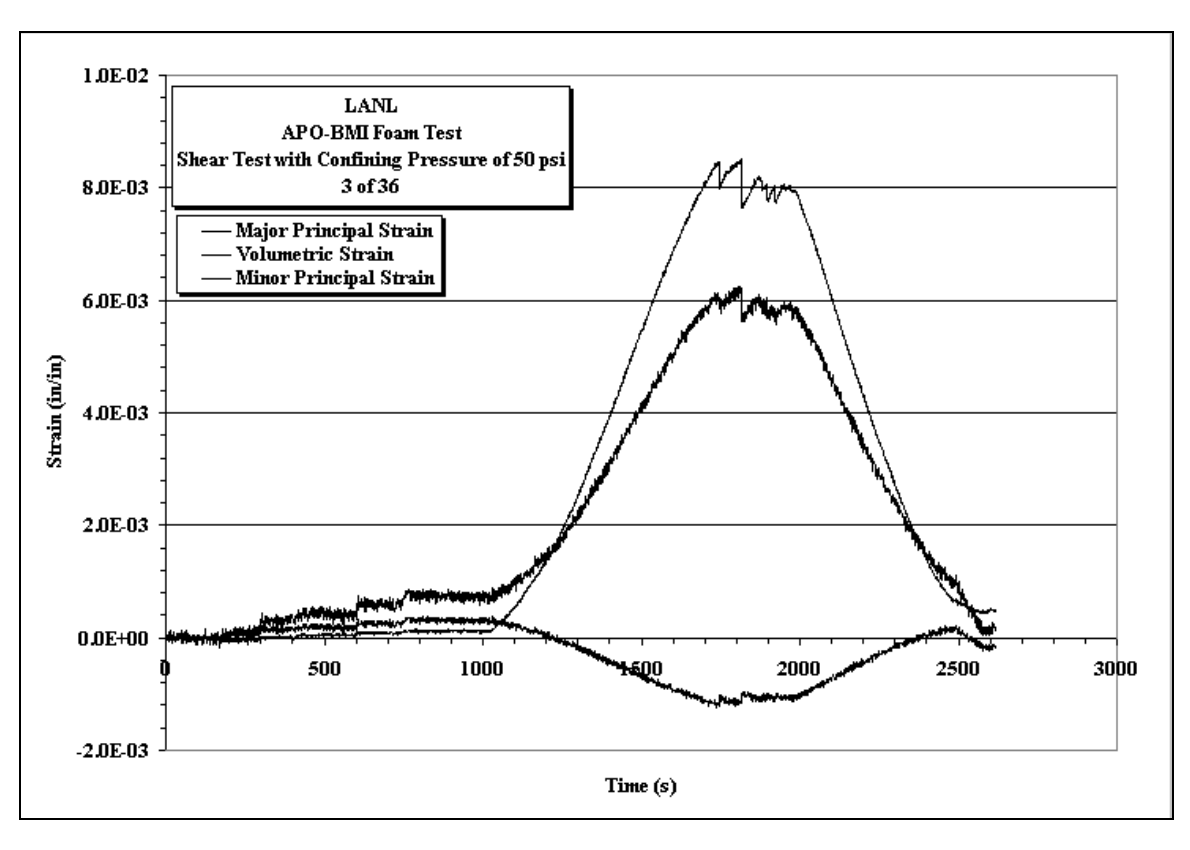


Figure A28. Minor Principle Strain vs. Major Principle Strain and Deviatoric Stress vs. Mean Stress plots for Sample 8of36 under a uniaxial pressure applied longitudinally on sample.



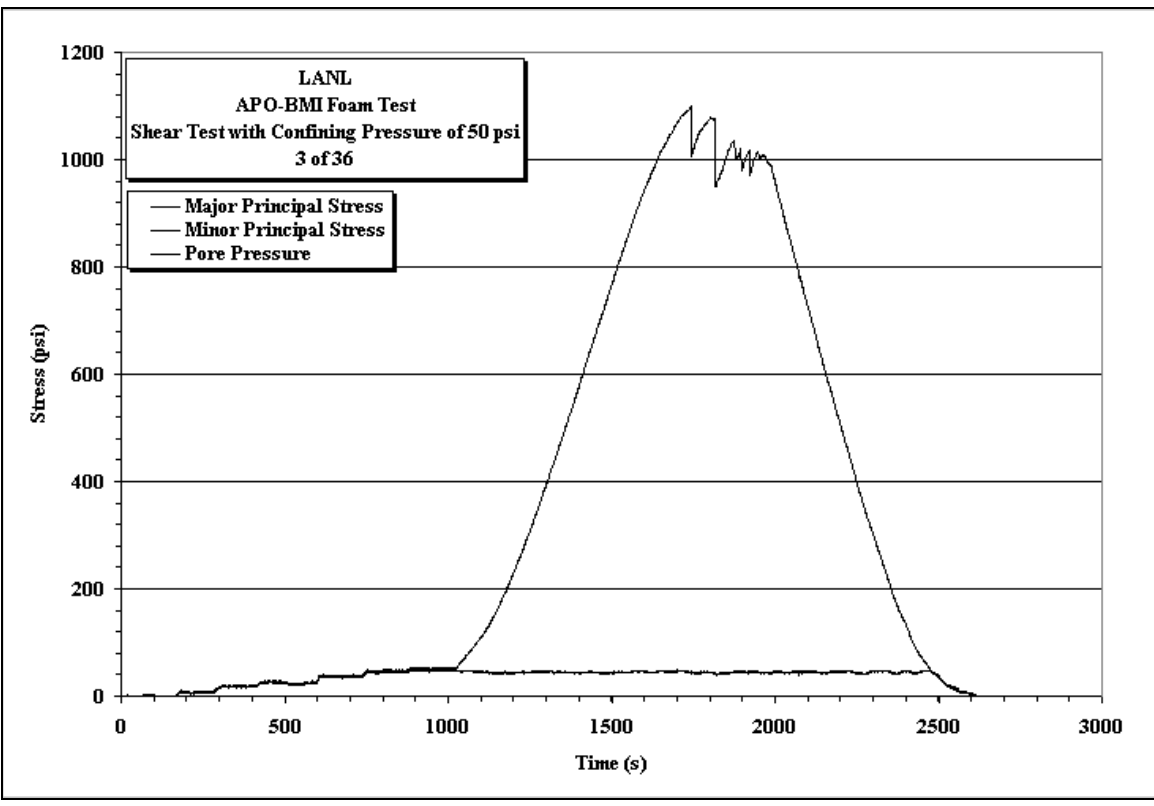
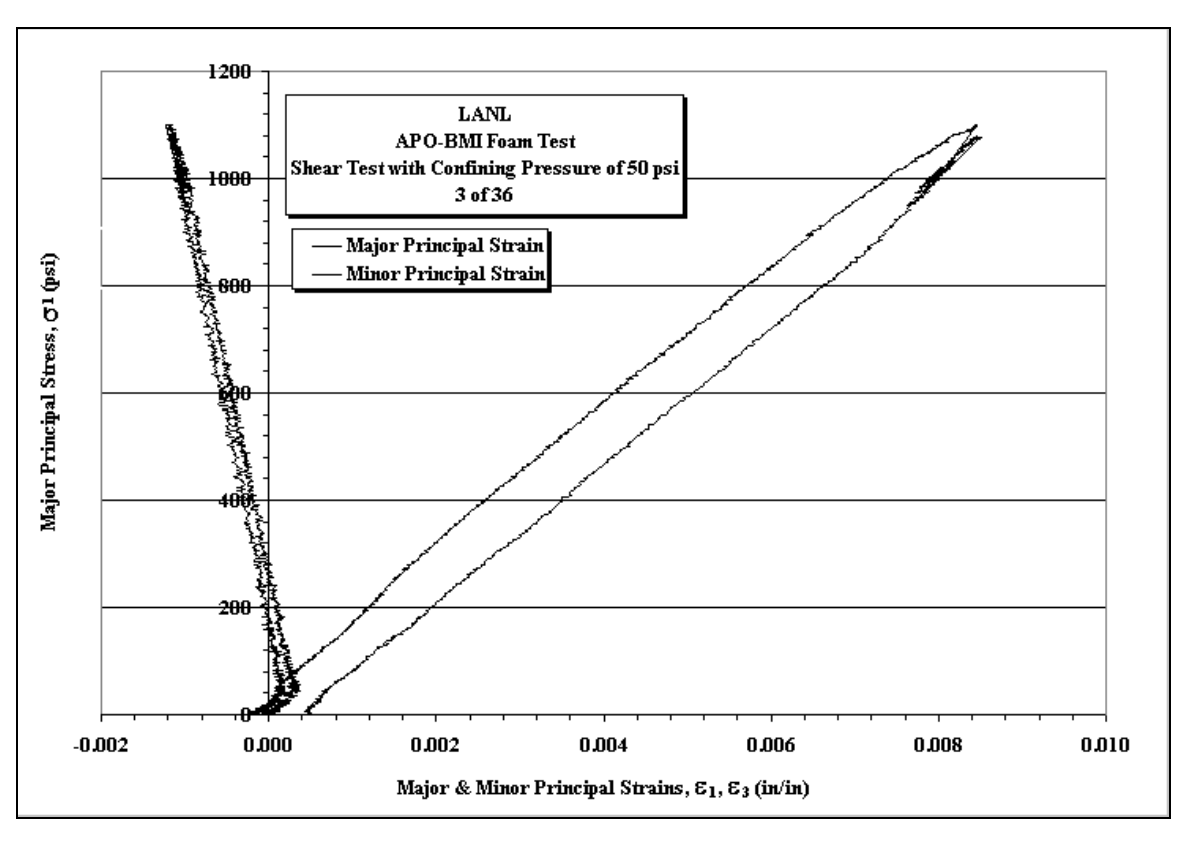


Figure A29. Minor Principle Strain vs. Major Principle Strain and Deviatoric Stress vs. Mean Stress plots for Sample 3of36 with a constant confining pressure of 50 psi.



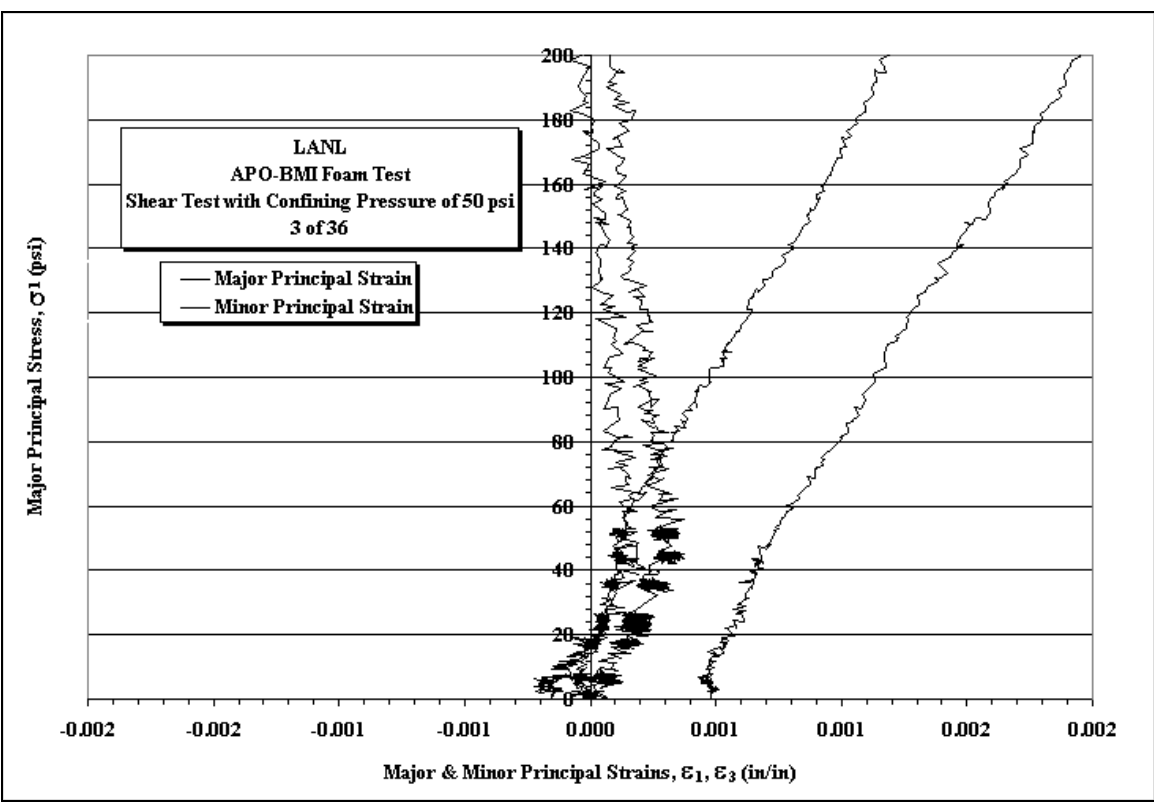
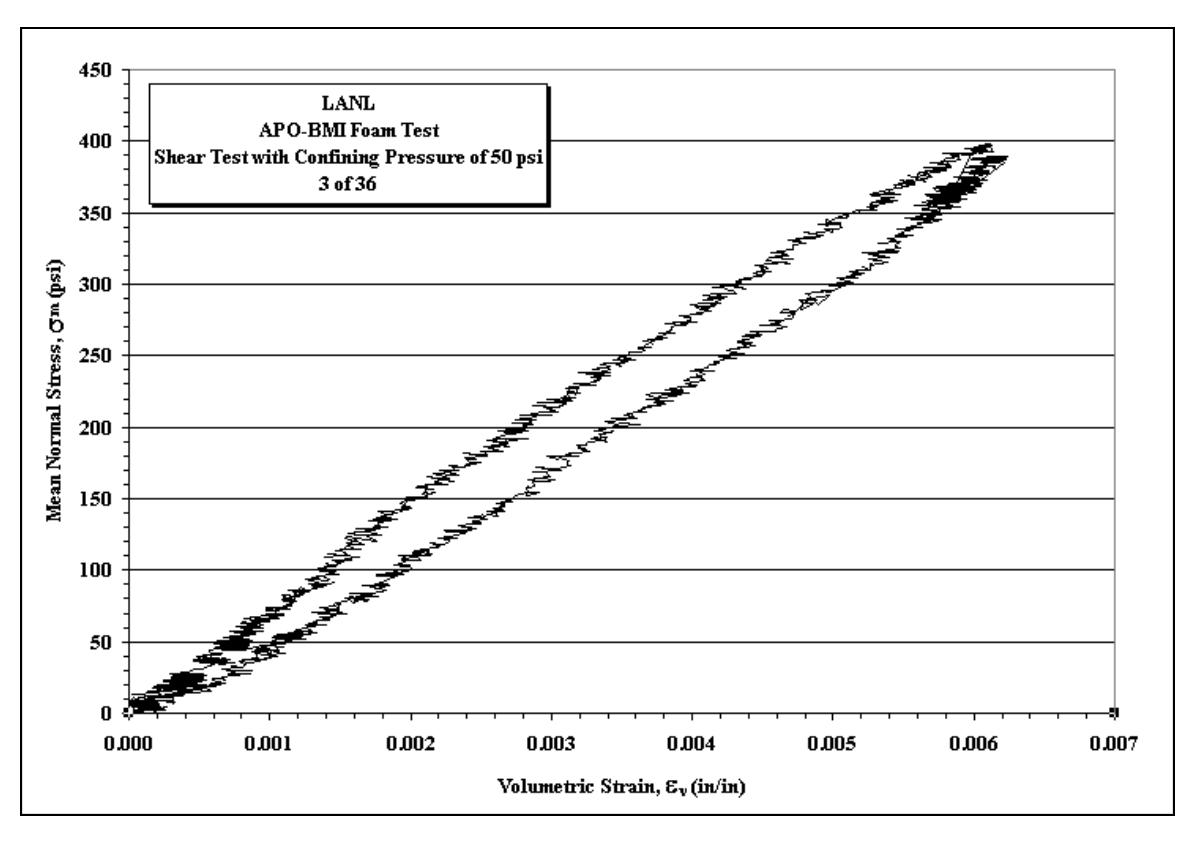


Figure A30. Stress vs. Strain plots for Sample 3of36 with a constant confining pressure of 50 psi.



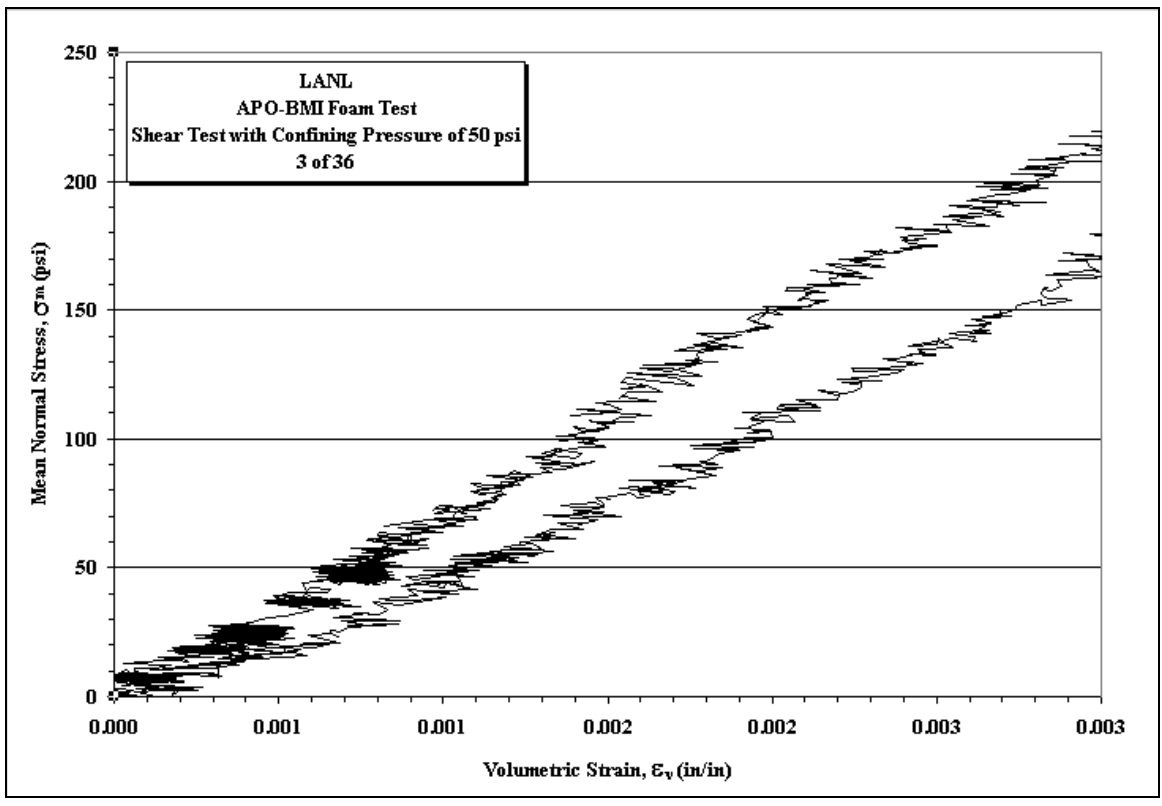
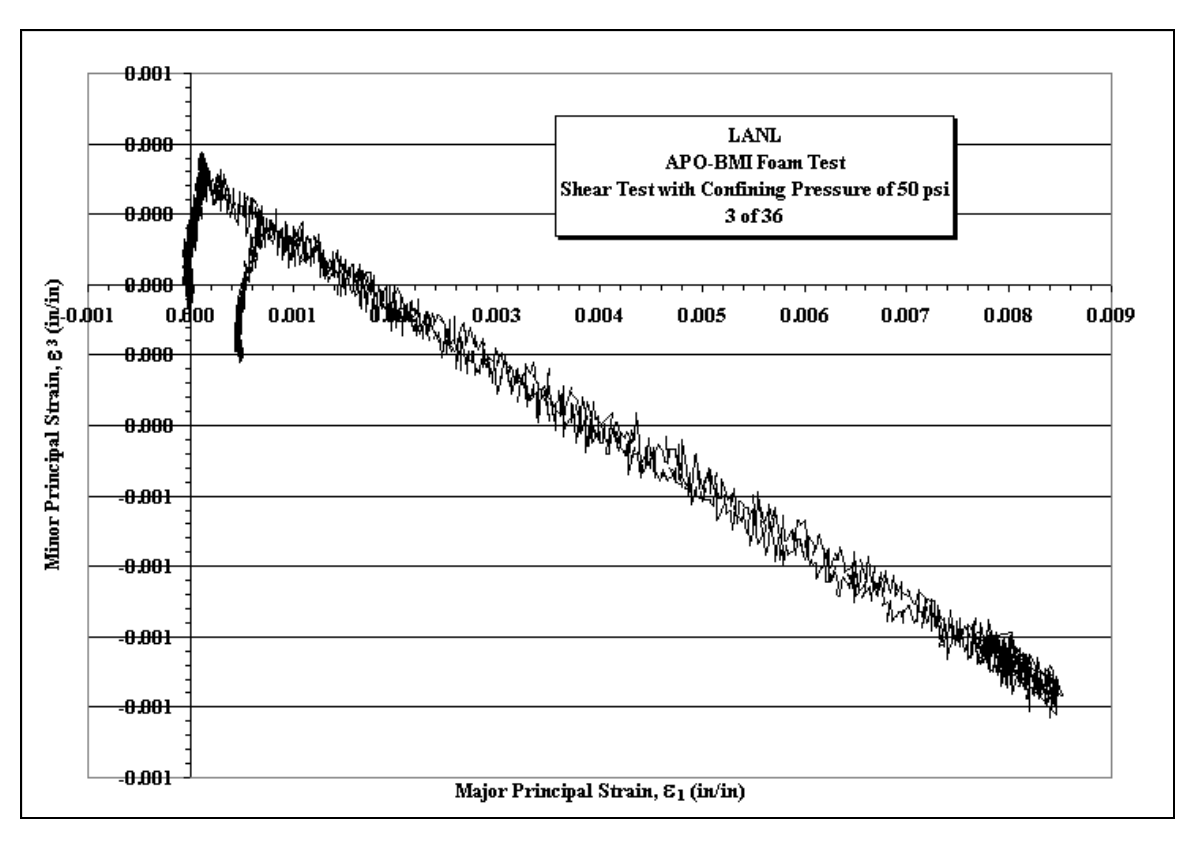


Figure A31. Mean Stress vs. Volumetric Strain plots for Sample 3of36 with a constant confining pressure of 50 psi.



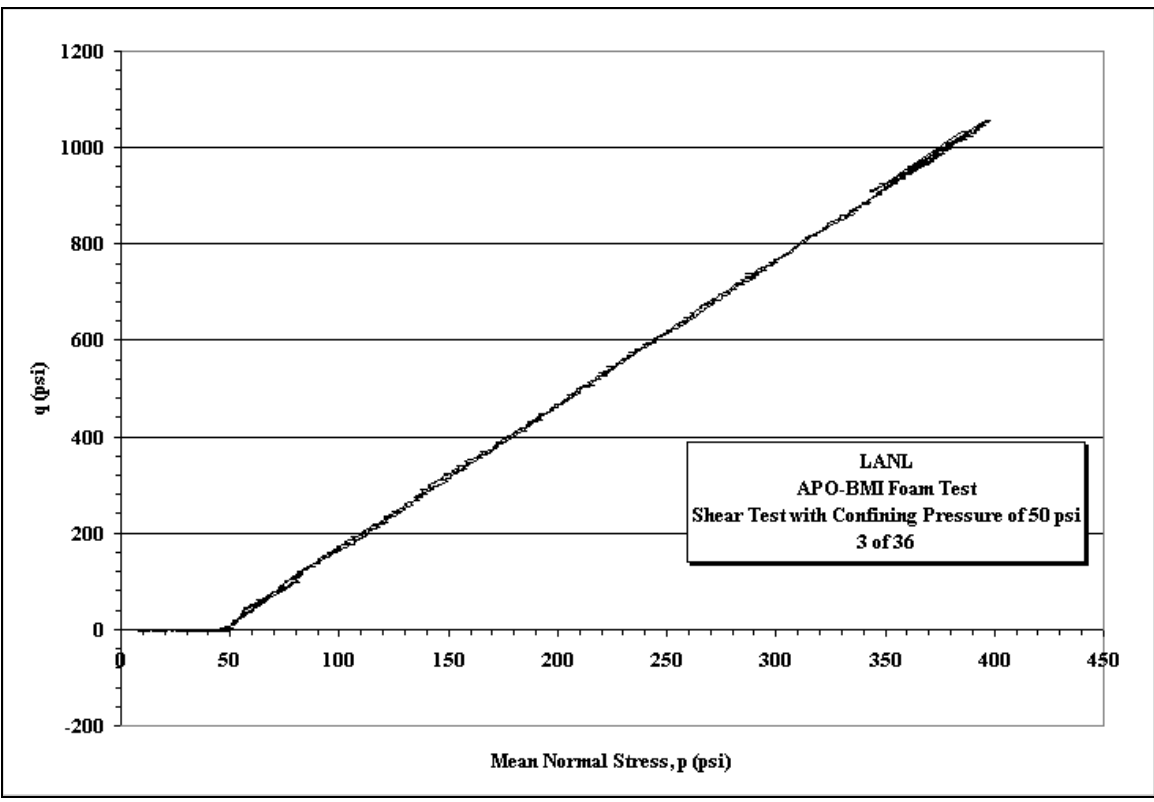
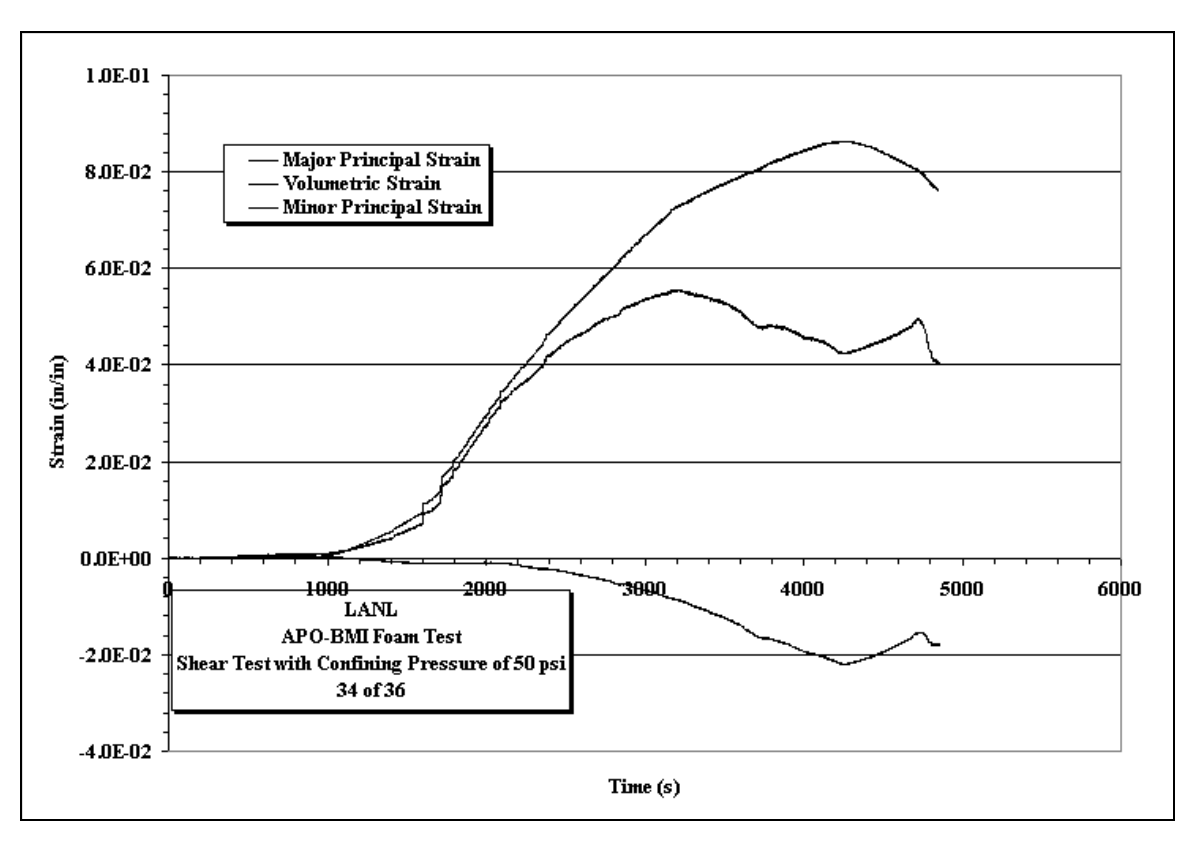


Figure A32. Minor Principle Strain vs. Major Principle Strain and Deviatoric Stress vs. Mean Stress plots for Sample 3of36 with a constant confining pressure of 50 psi.



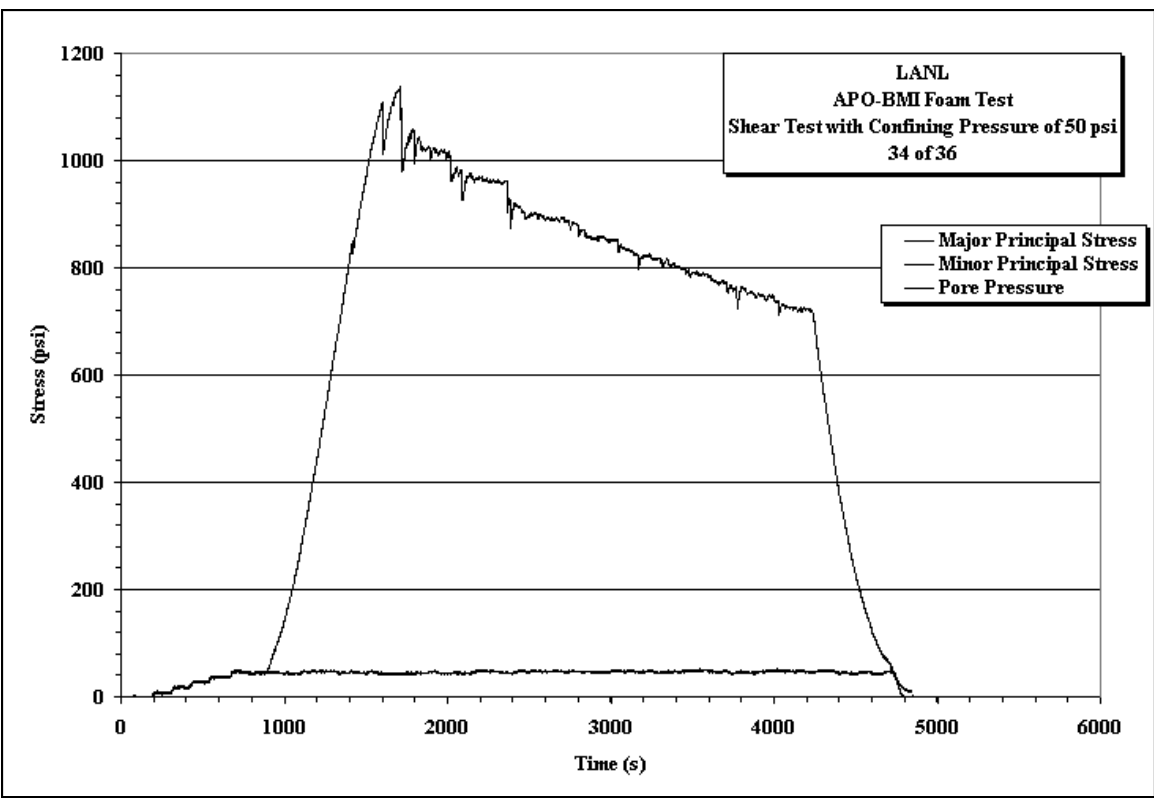
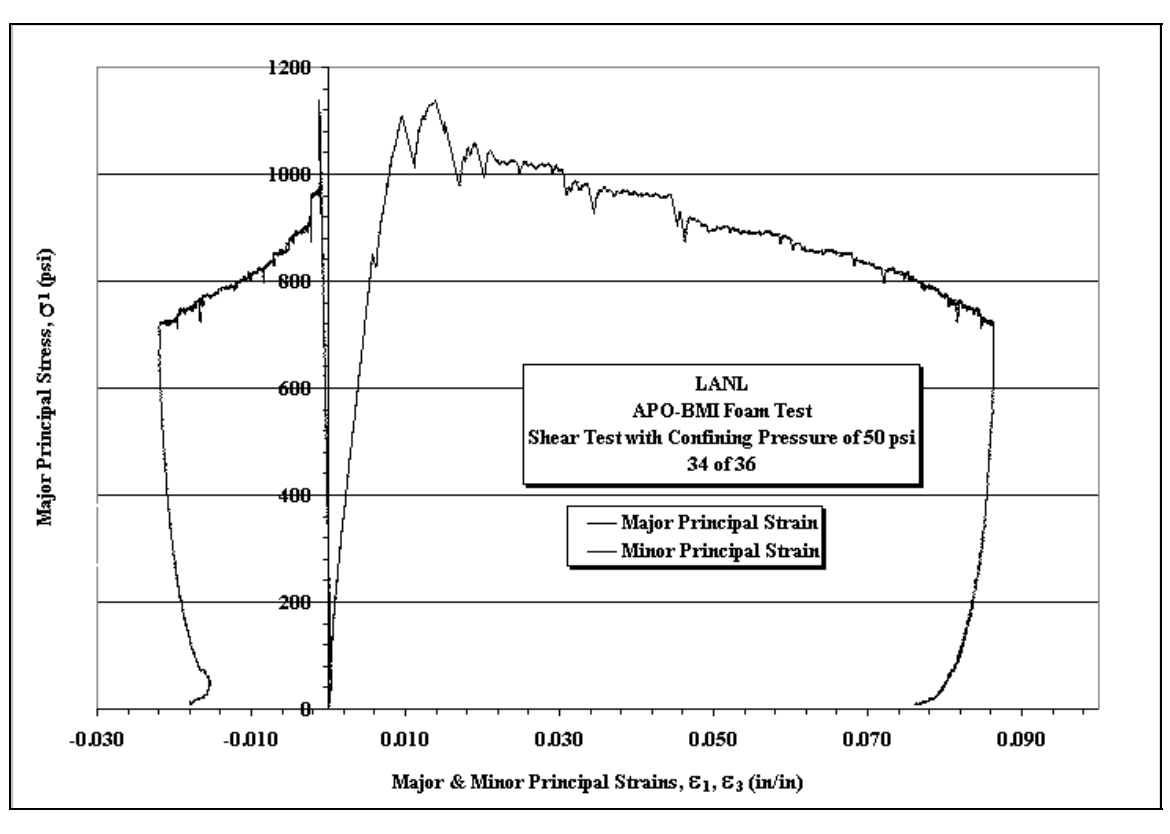


Figure A33. Minor Principle Strain vs. Major Principle Strain and Deviatoric Stress vs. Mean Stress plots for Sample 34of36 with a constant confining pressure of 50 psi.



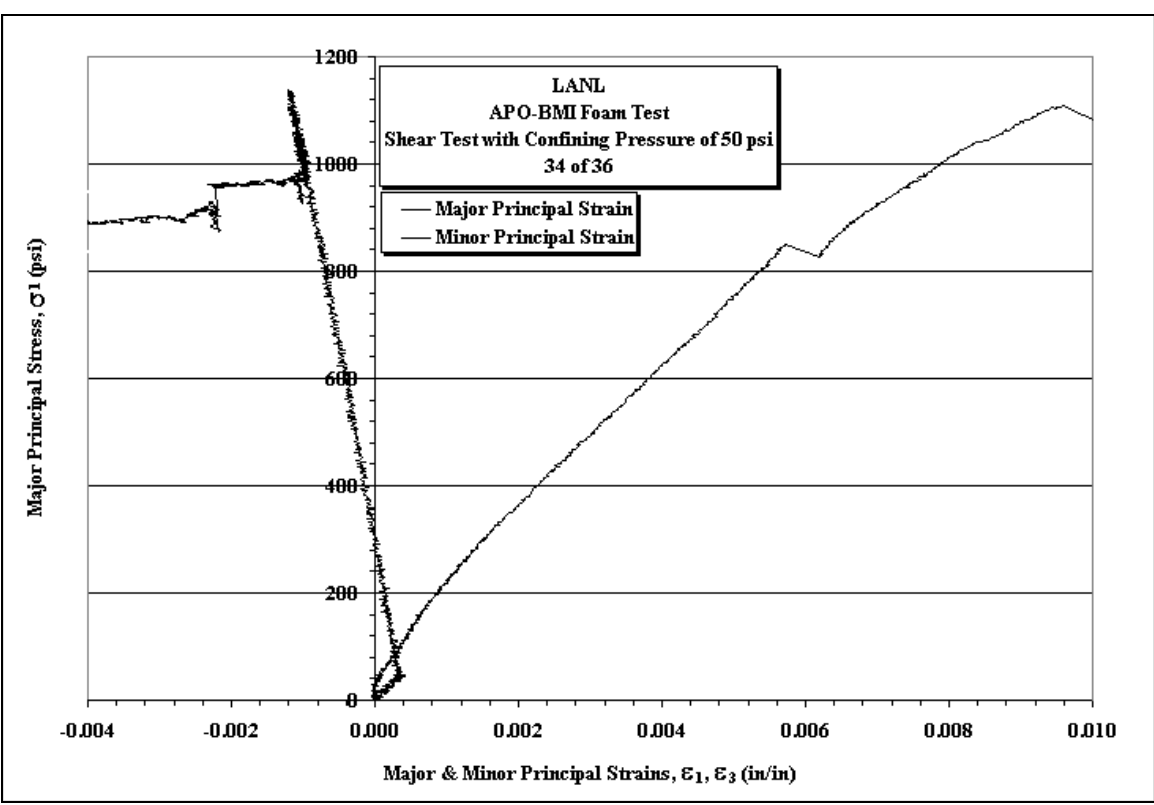
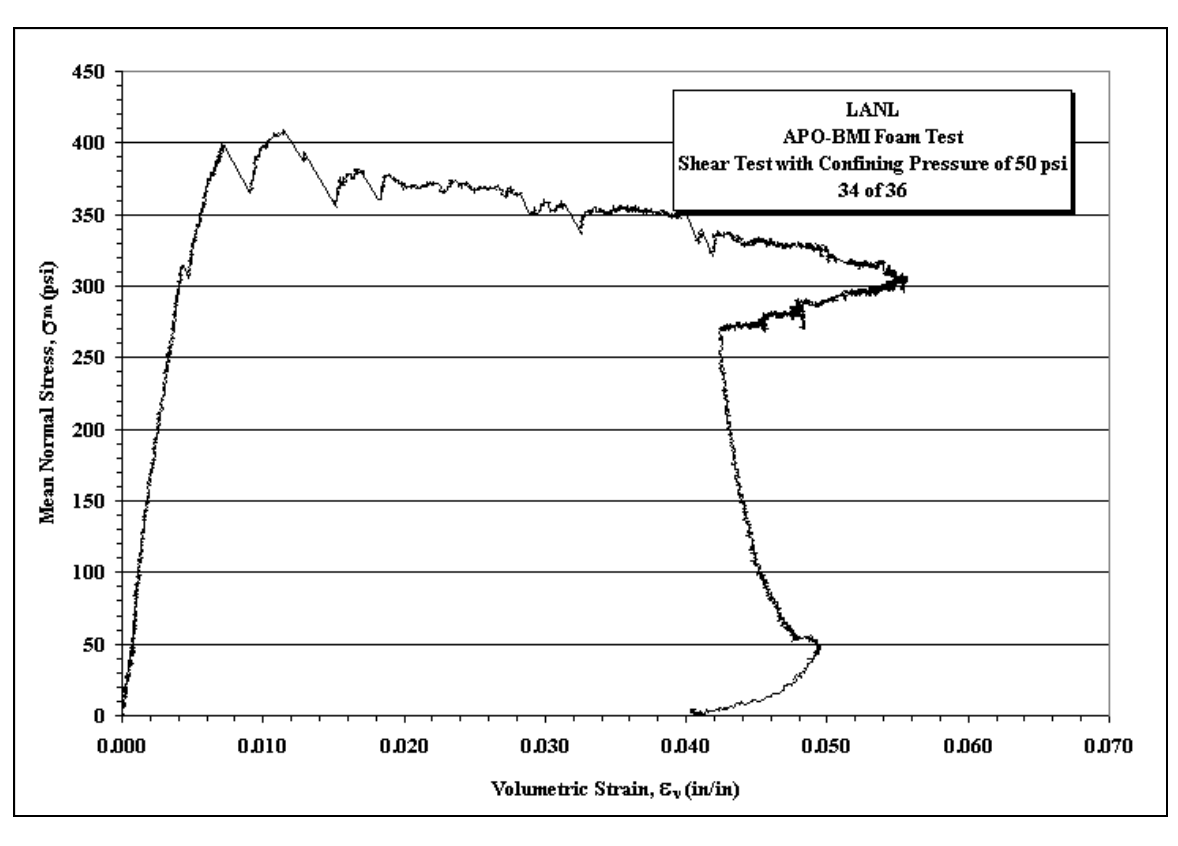


Figure A34. Stress vs. Strain plots for Sample 34of36 with a constant confining pressure of 50 psi.



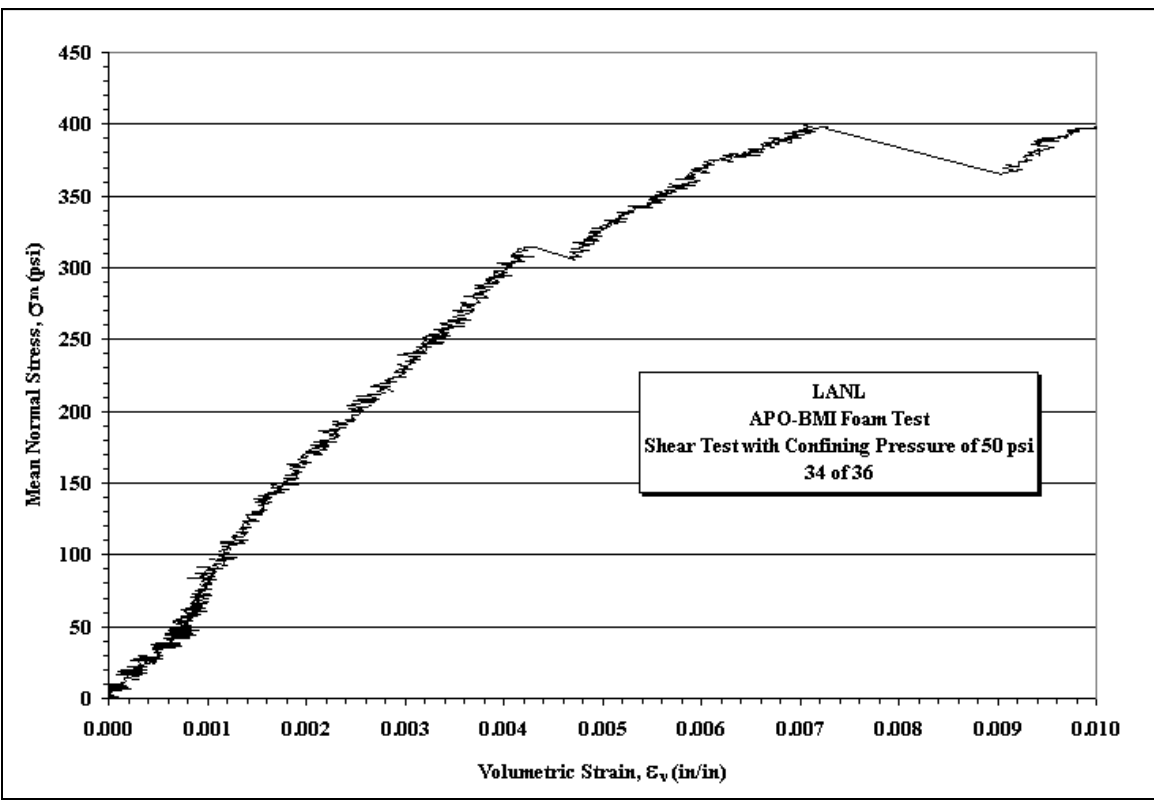
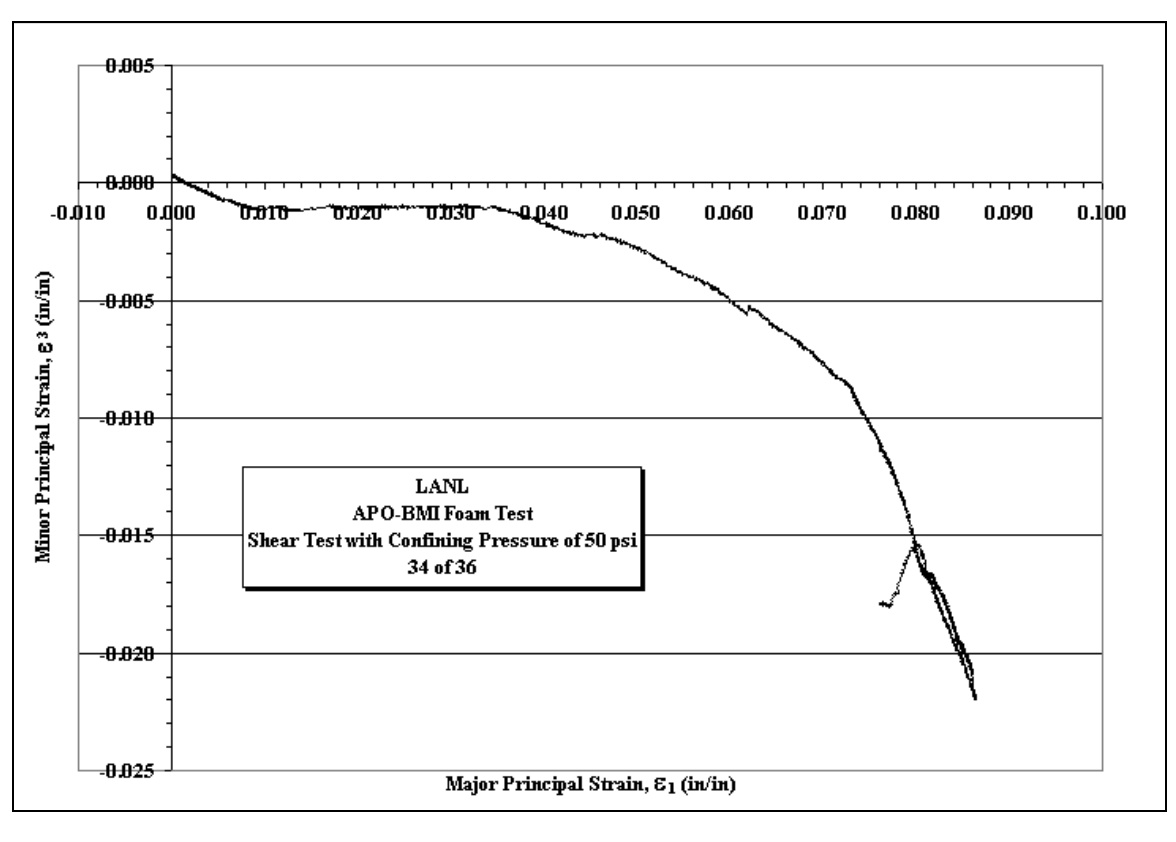


Figure A35. Mean Stress vs. Volumetric Strain plots for Sample 34of36 with a constant confining pressure of 50 psi.



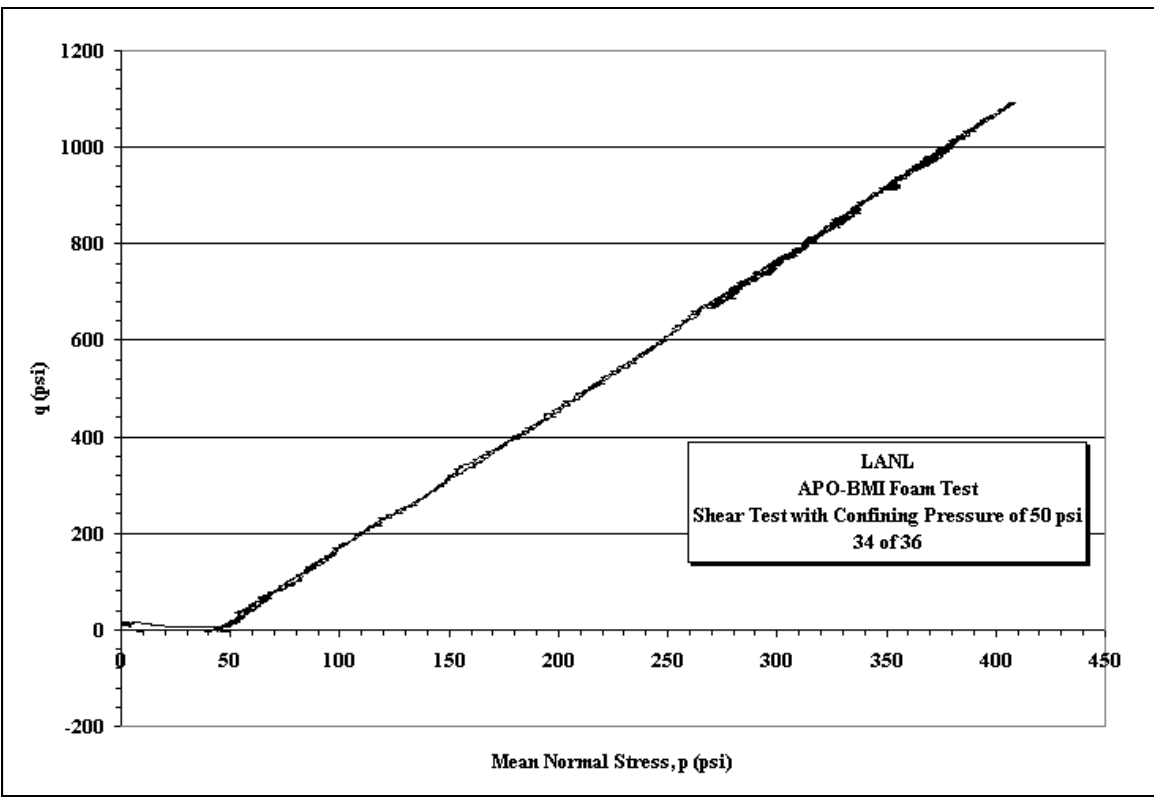
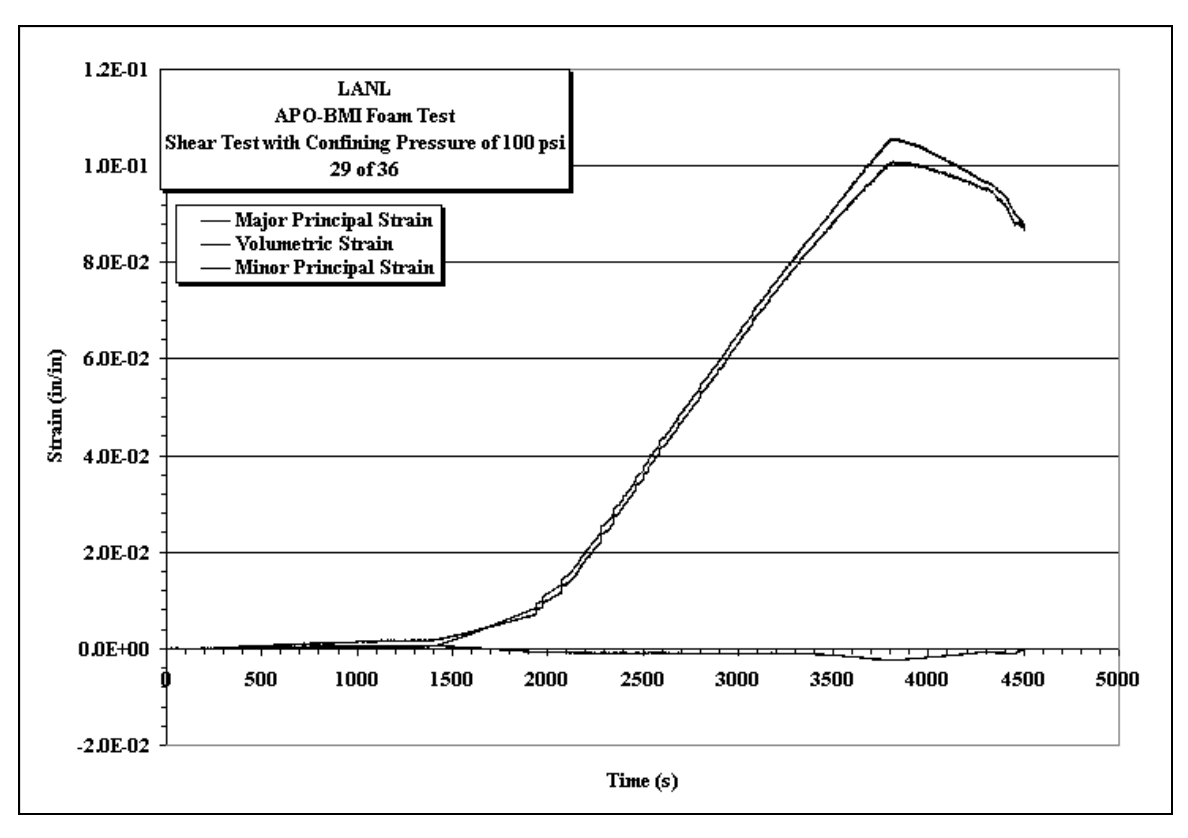


Figure A36. Minor Principle Strain vs. Major Principle Strain and Deviatoric Stress vs. Mean Stress plots for Sample 34of36 with a constant confining pressure of 50 psi.



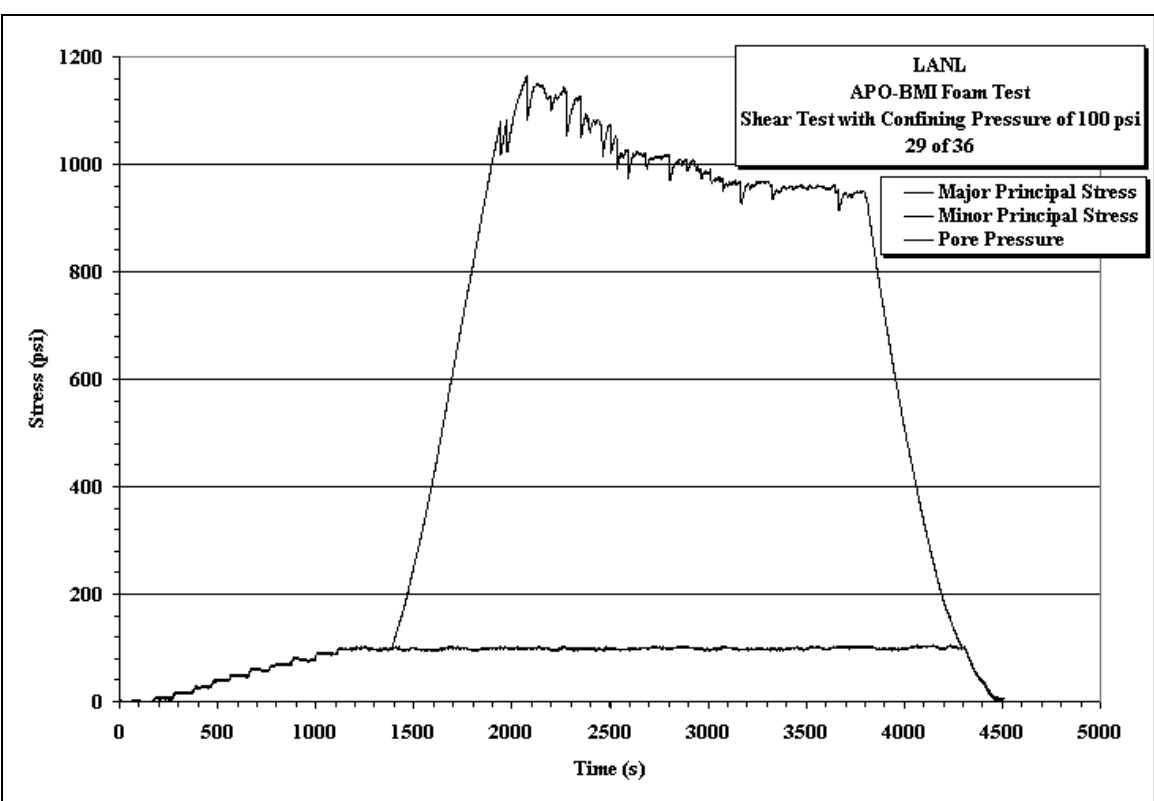
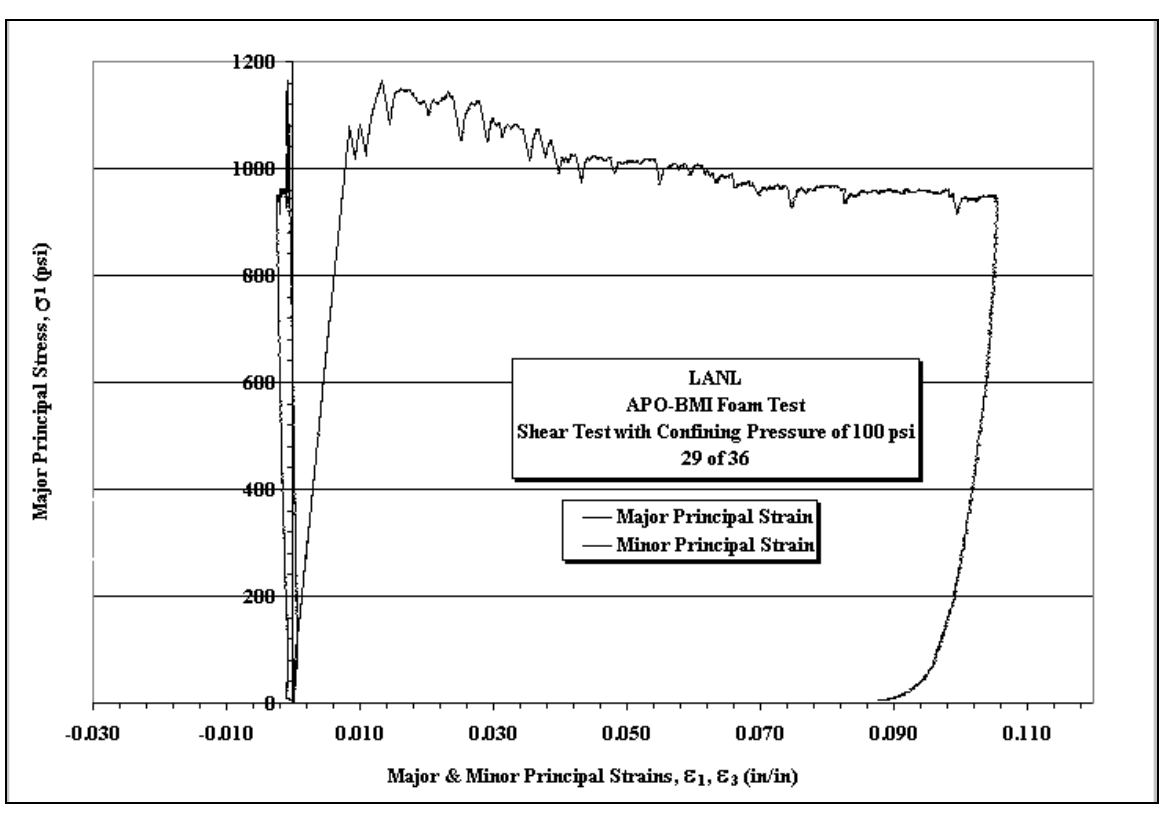


Figure A37. Minor Principle Strain vs. Major Principle Strain and Deviatoric Stress vs. Mean Stress plots for Sample 29of36 with a constant confining pressure of 100 psi.



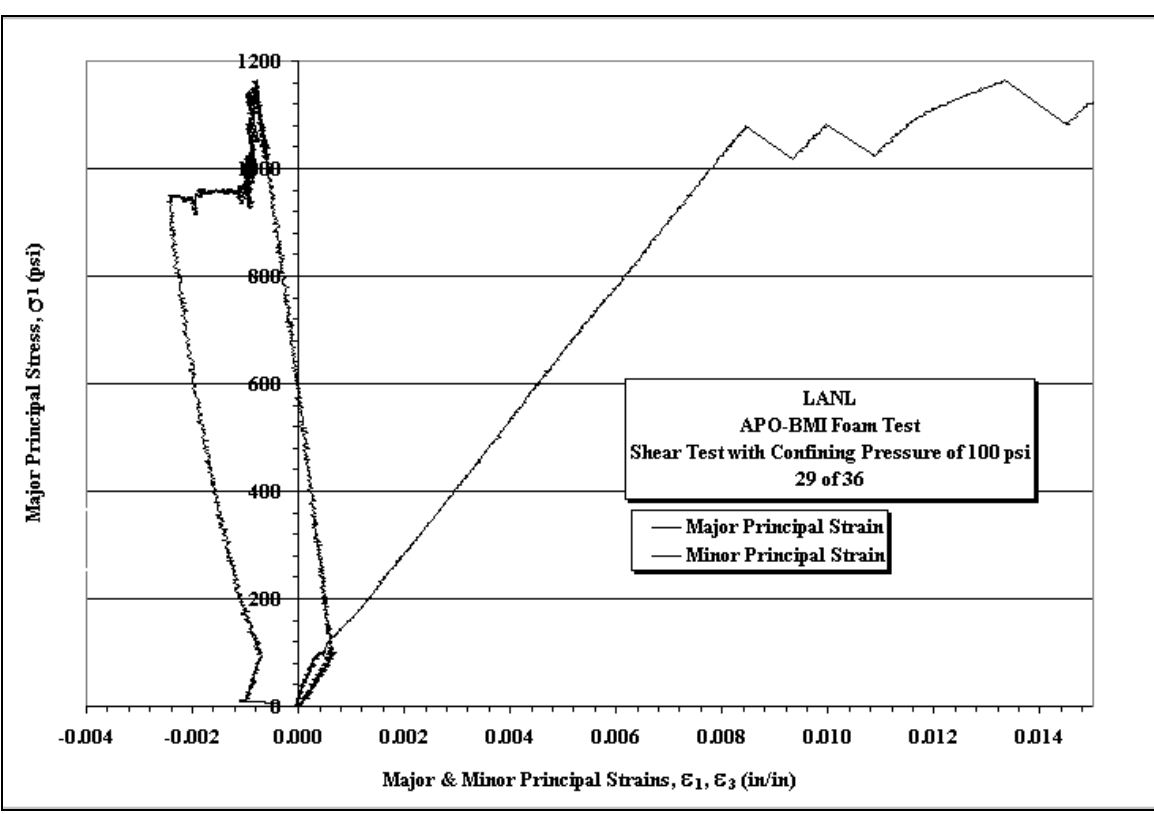
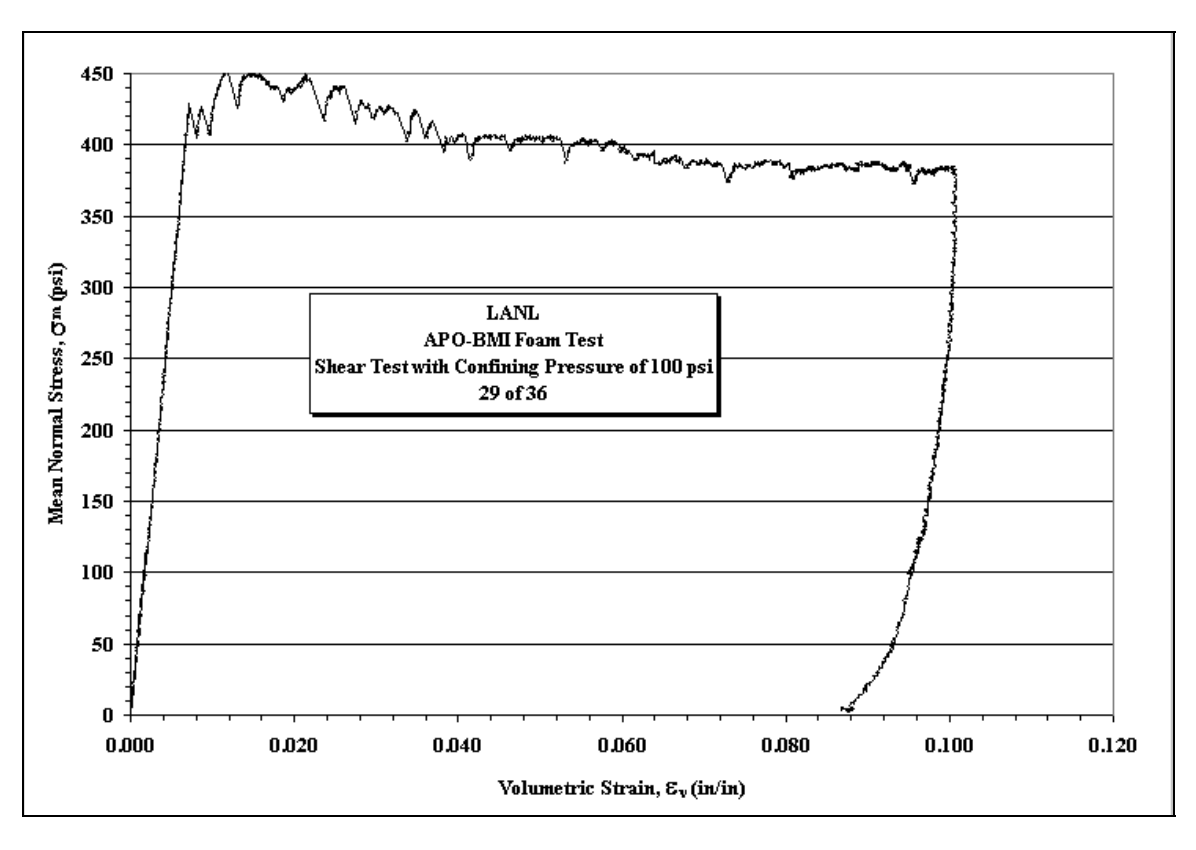


Figure A38. Stress vs. Strain plots for Sample 29of36 with a constant confining pressure of 100 psi.



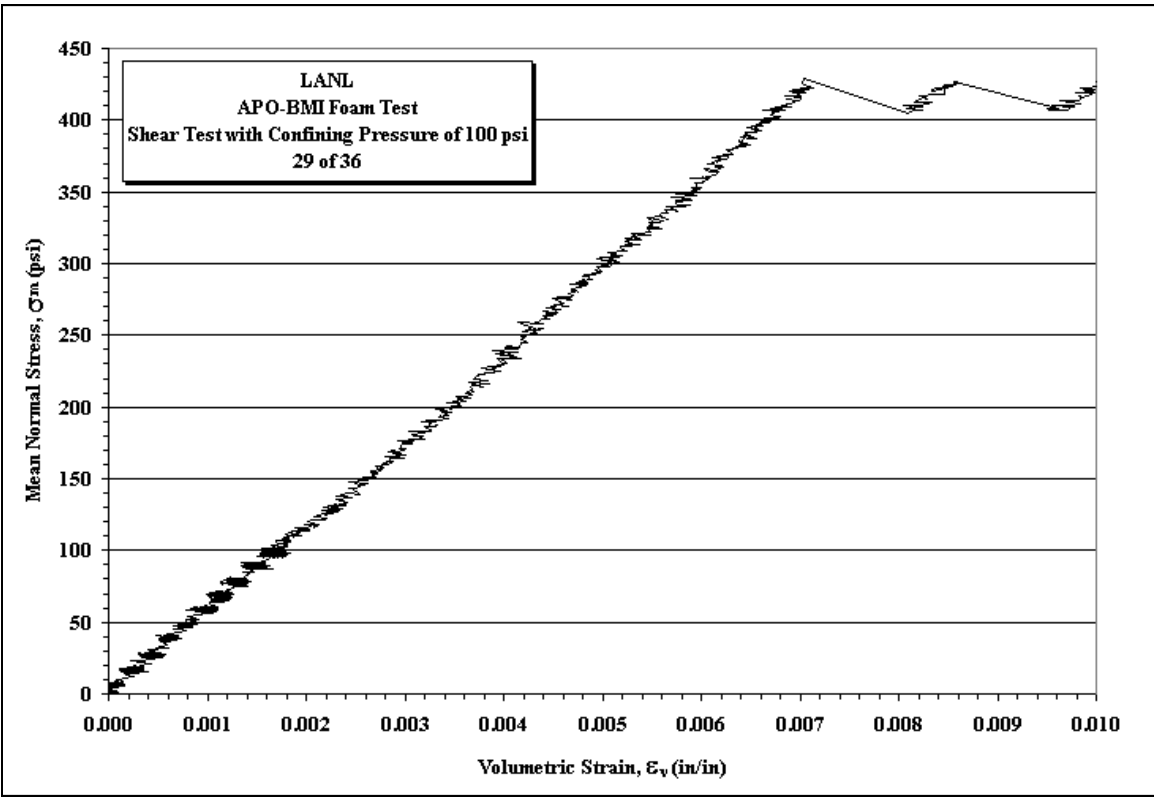
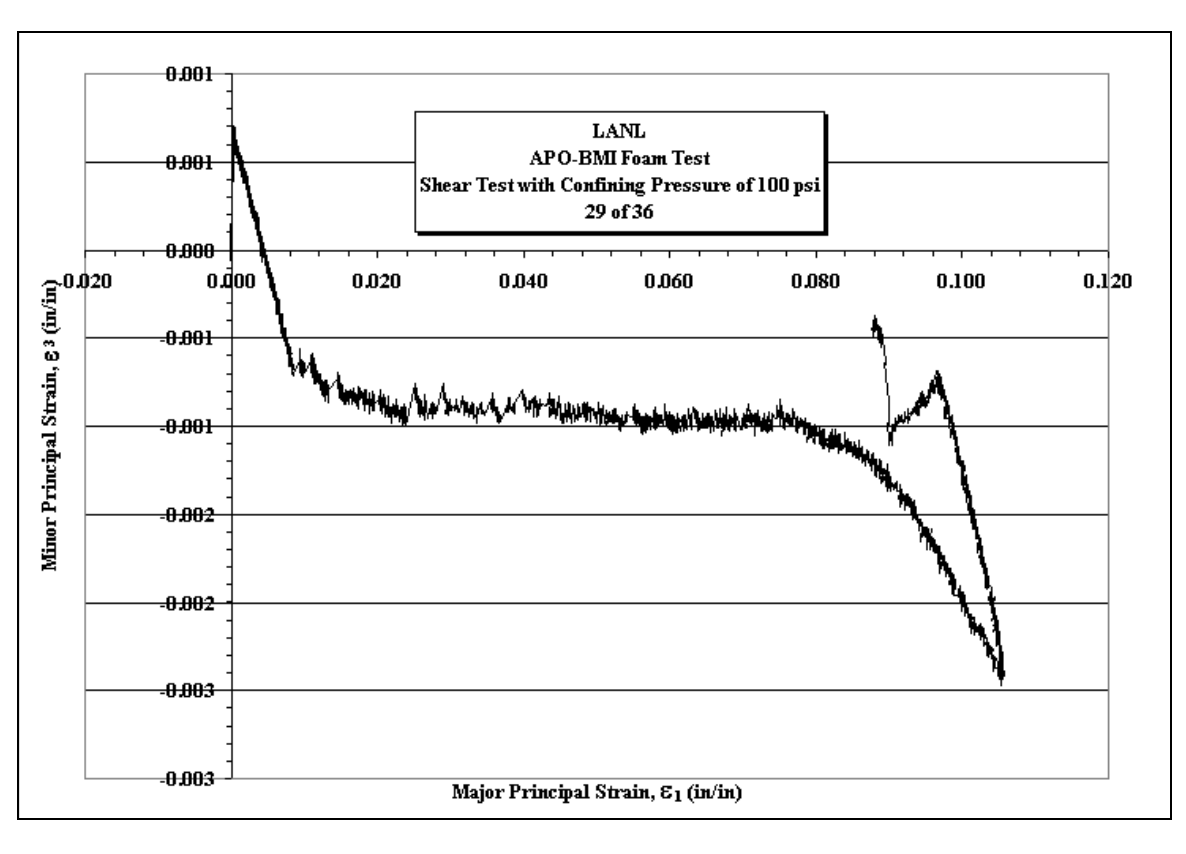


Figure A39. Mean Stress vs. Volumetric Strain plots for Sample 29of36 with a constant confining pressure of 100 psi.



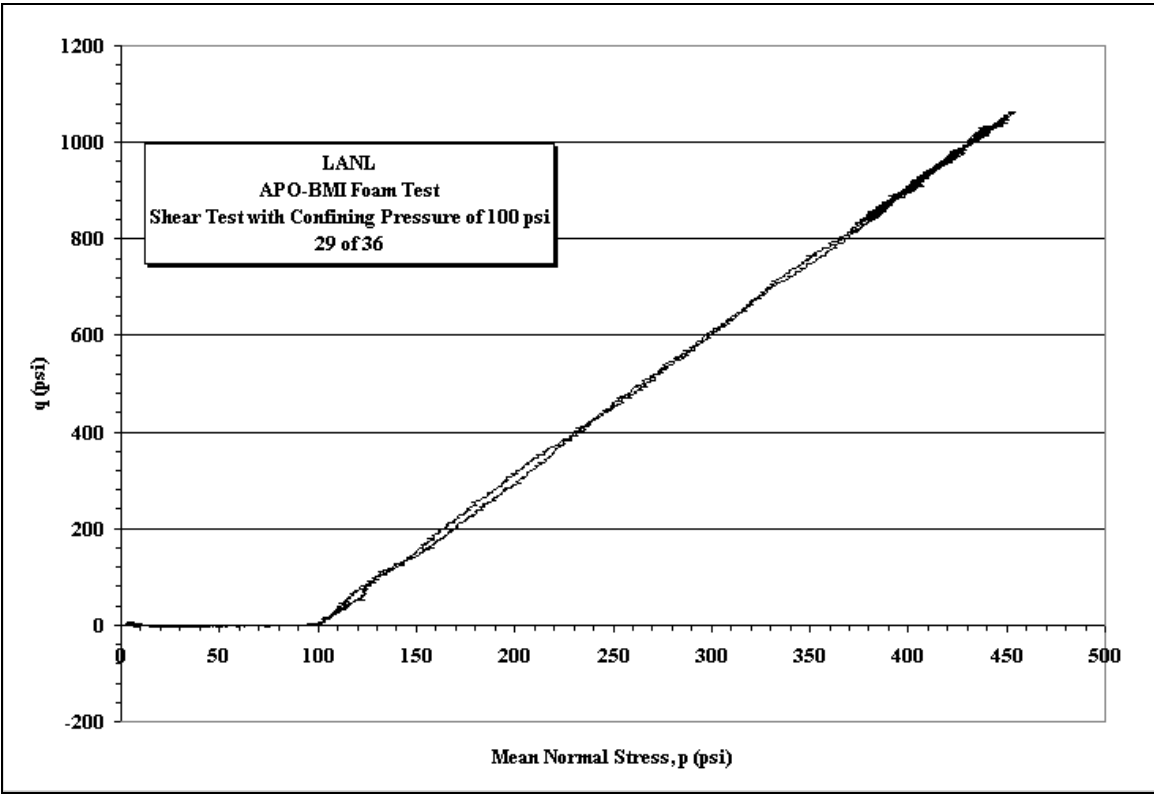
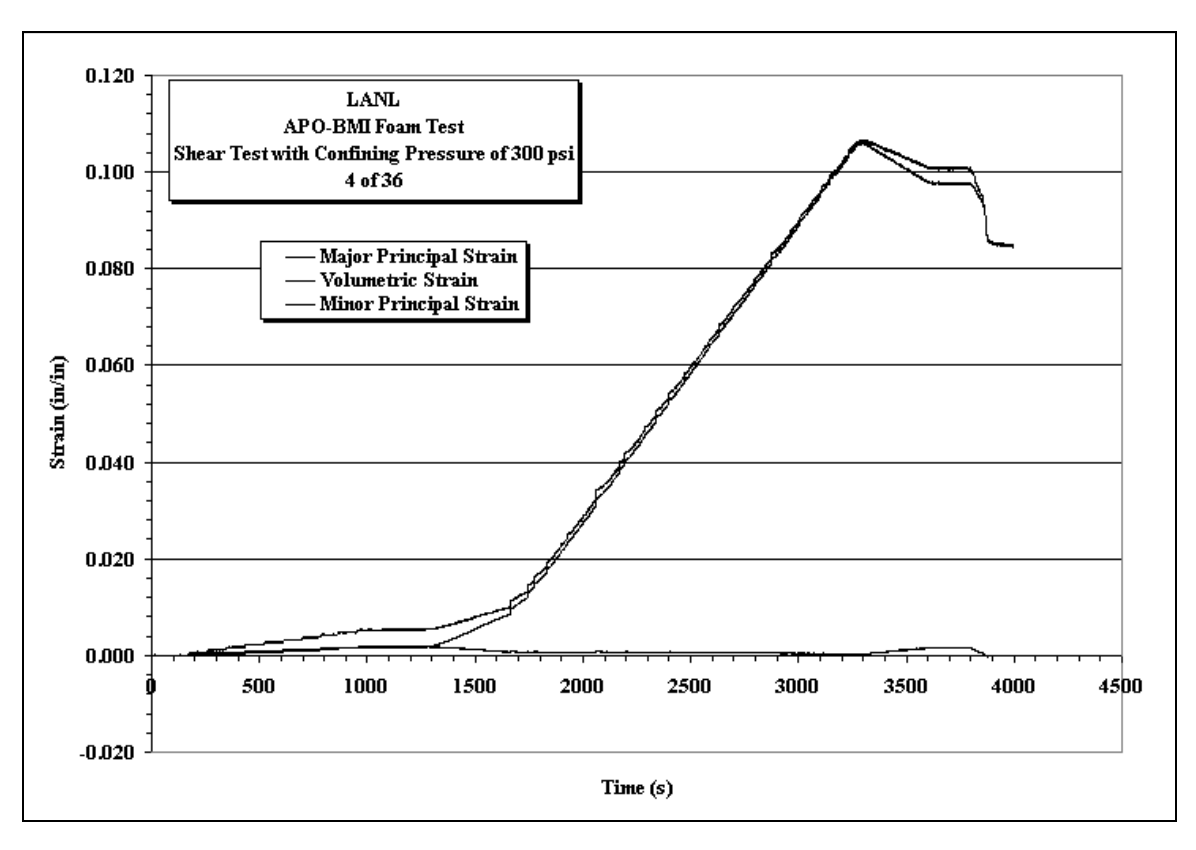


Figure A40. Minor Principle Strain vs. Major Principle Strain and Deviatoric Stress vs. Mean Stress plots for Sample 29of36 with a constant confining pressure of 100 psi.



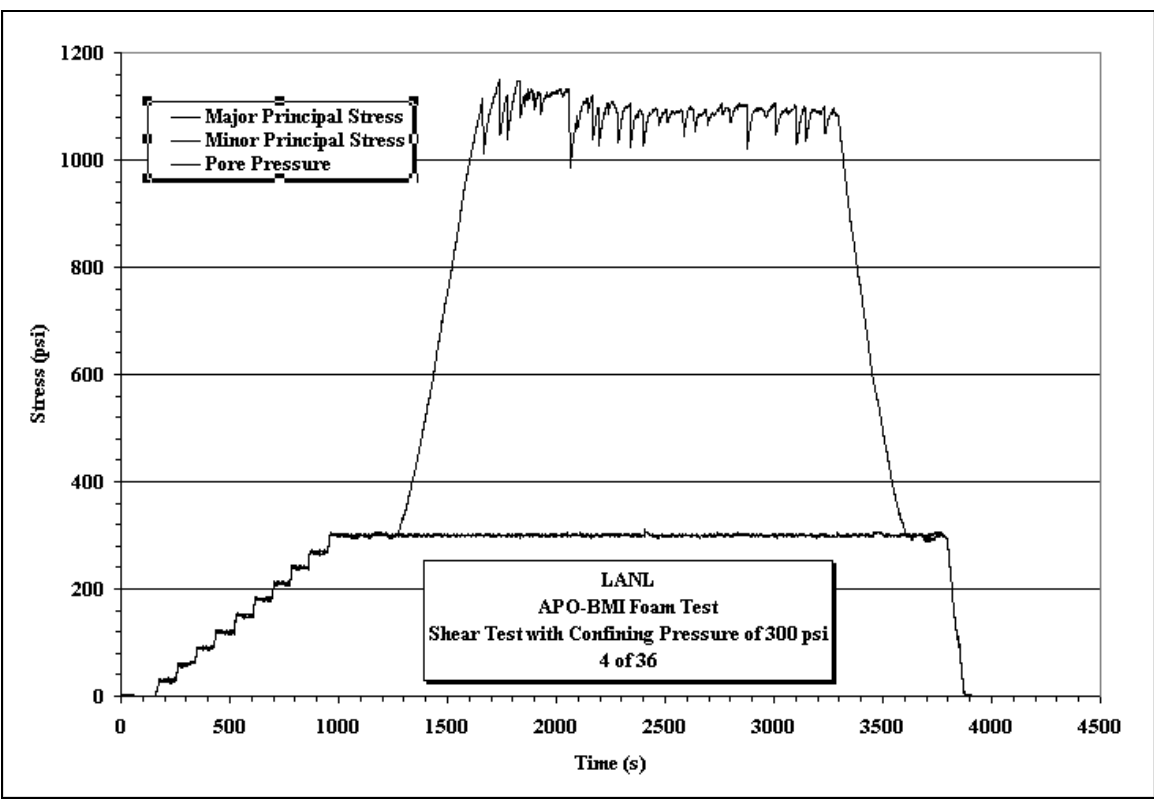
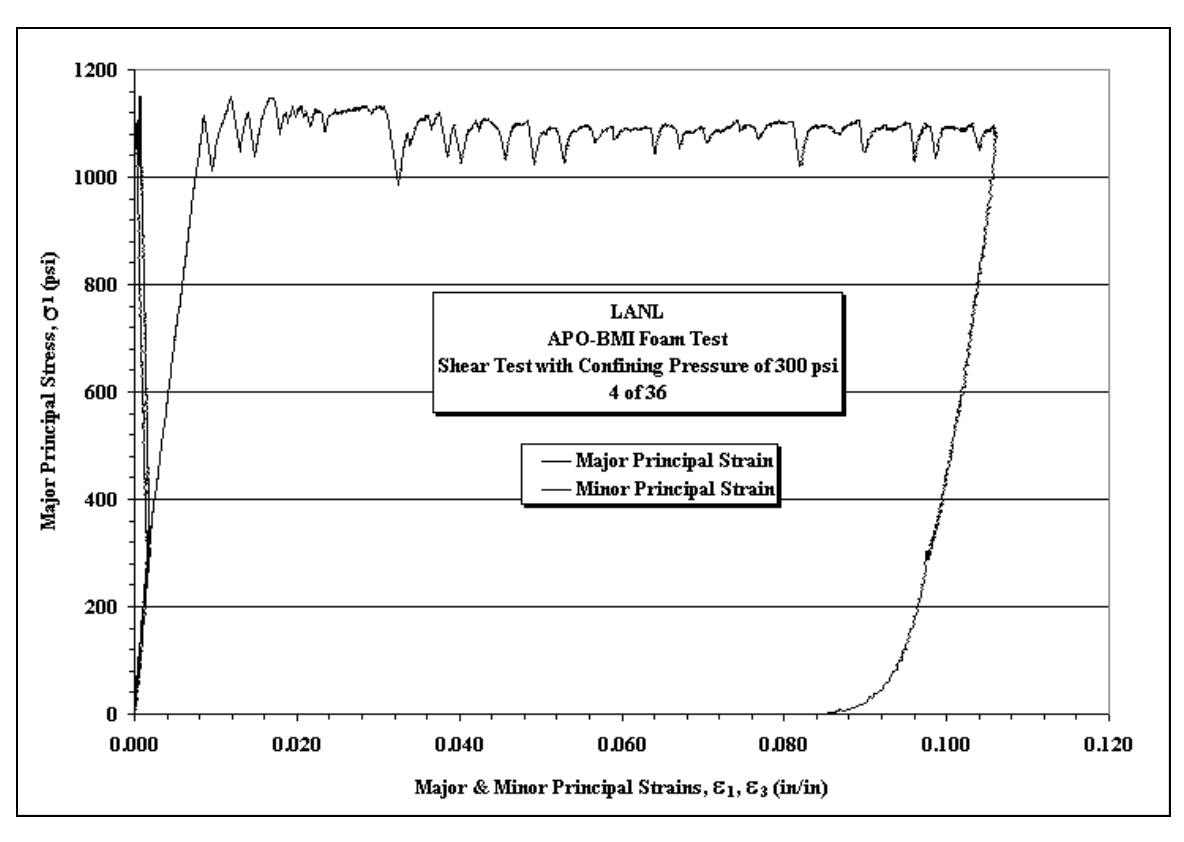


Figure A41. Minor Principle Strain vs. Major Principle Strain and Deviatoric Stress vs. Mean Stress plots for Sample 4of36 with a constant confining pressure of 300 psi.



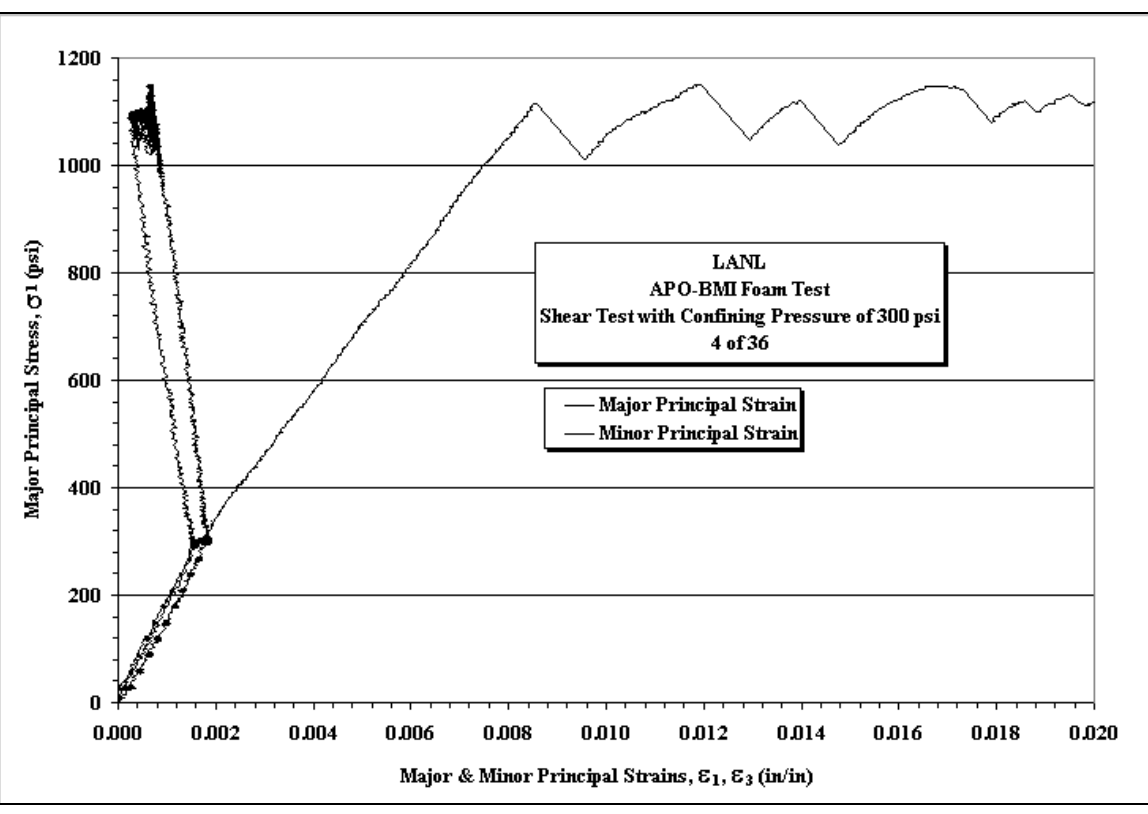
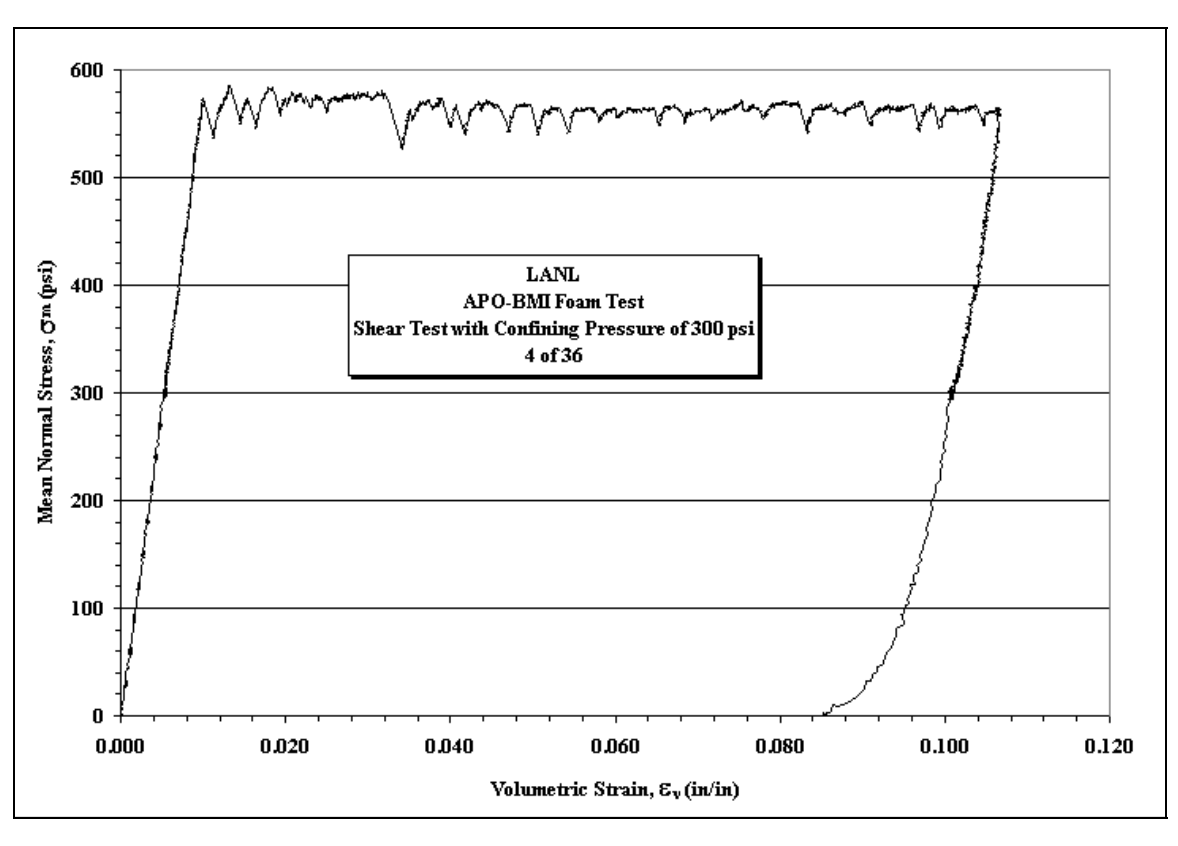


Figure A42. Stress vs. Strain plots for Sample 4of36 with a constant confining pressure of 300 psi.



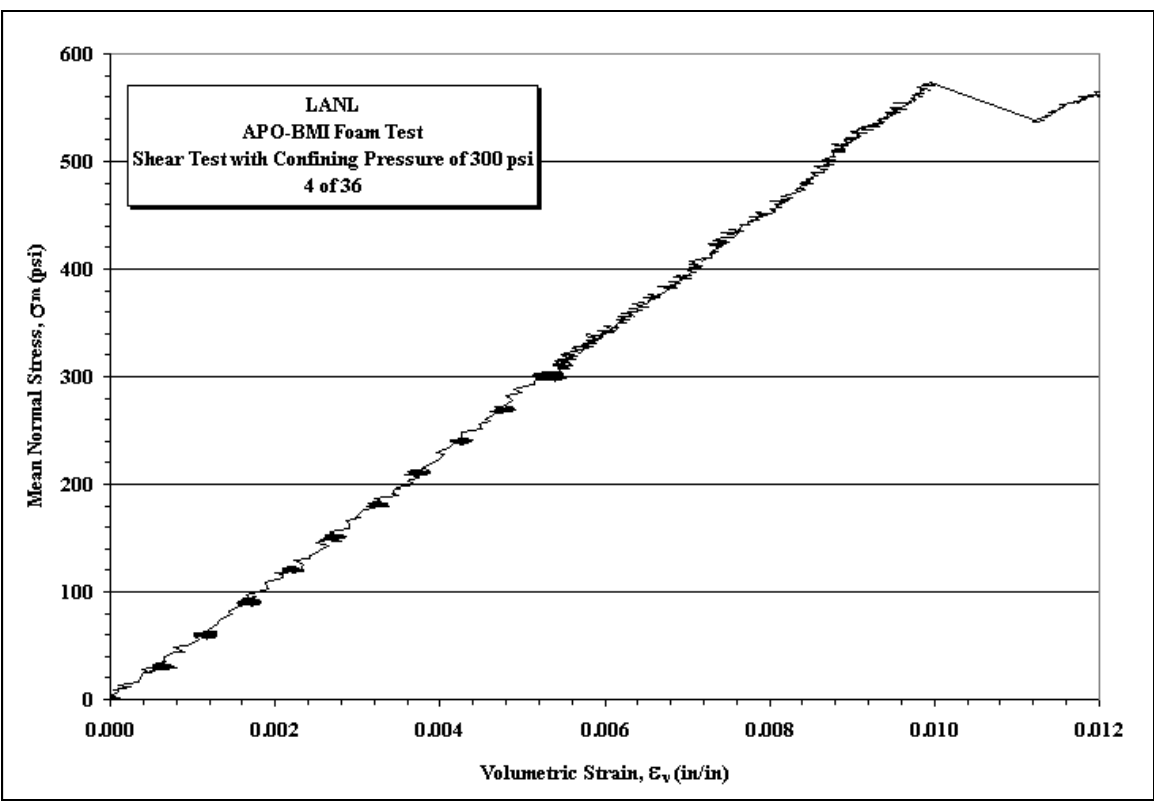
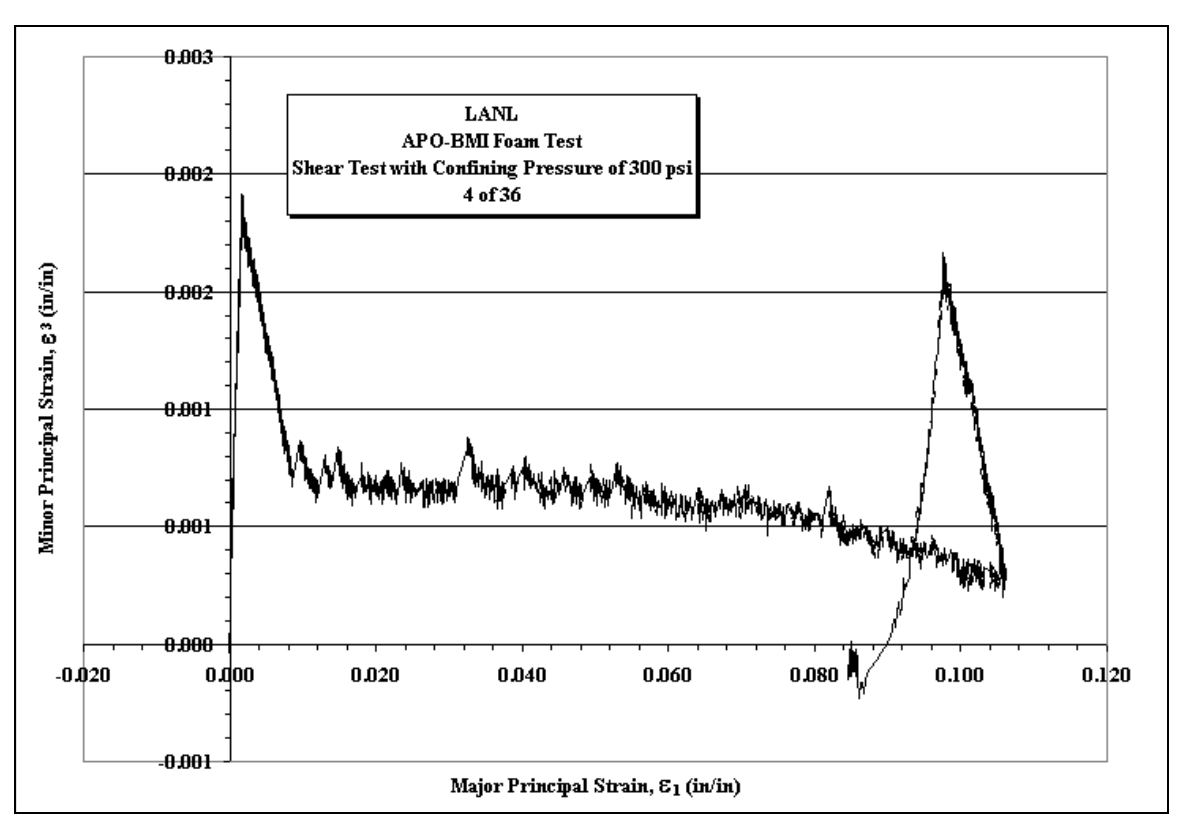


Figure A43. Mean Stress vs. Volumetric Strain plots for Sample 4of36 with a constant confining pressure of 300 psi.



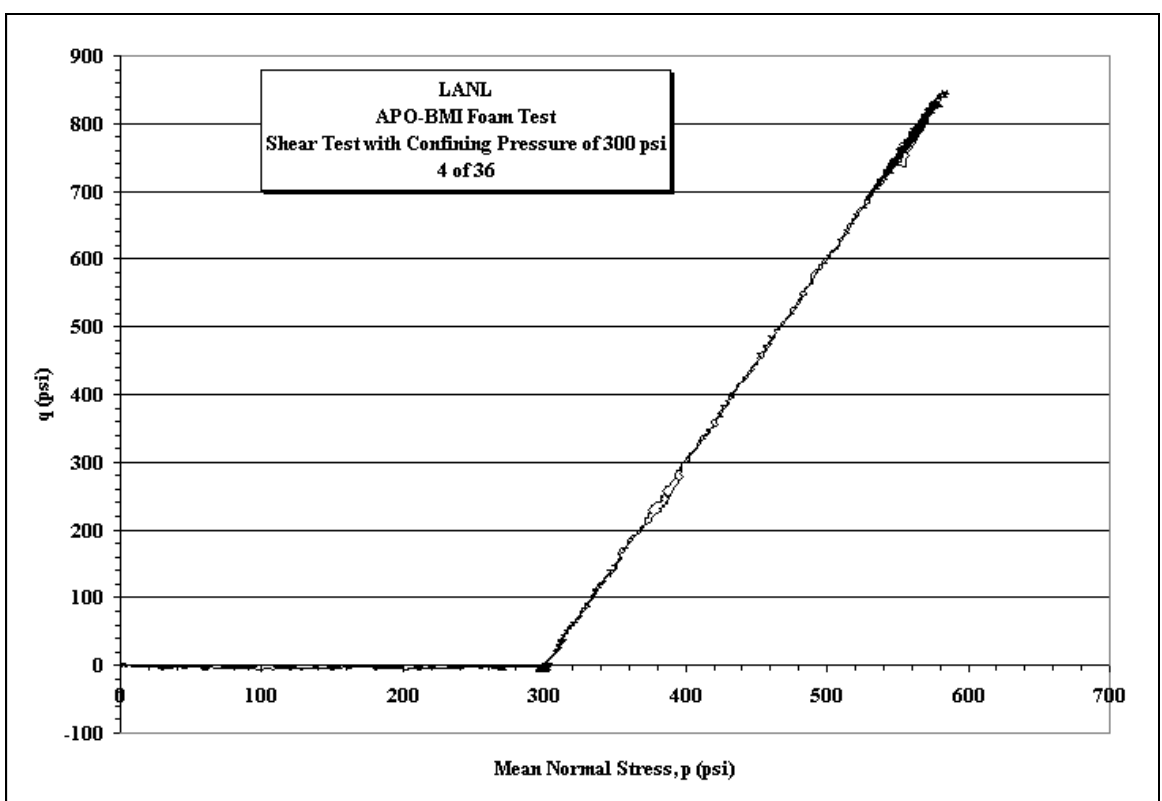
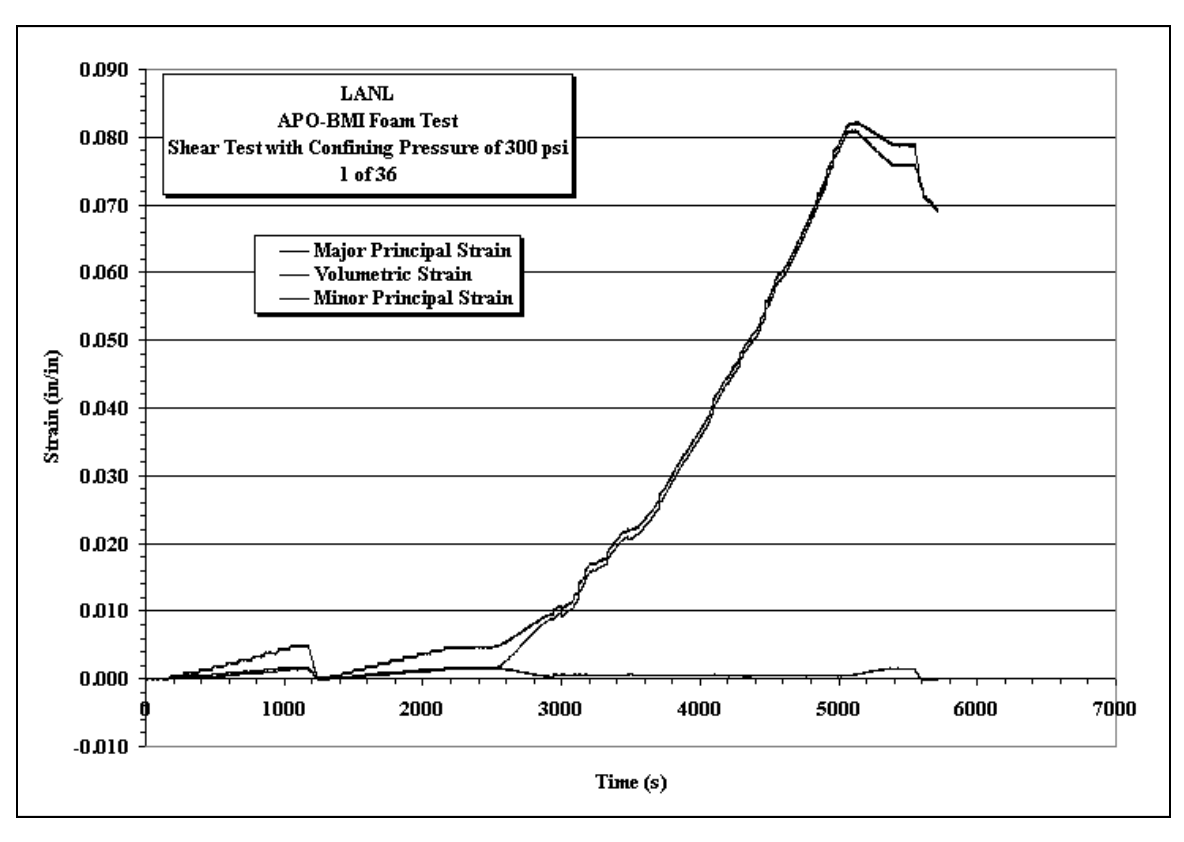


Figure A44. Minor Principle Strain vs. Major Principle Strain and Deviatoric Stress vs. Mean Stress plots for Sample 4of36 with a constant confining pressure of 300 psi.



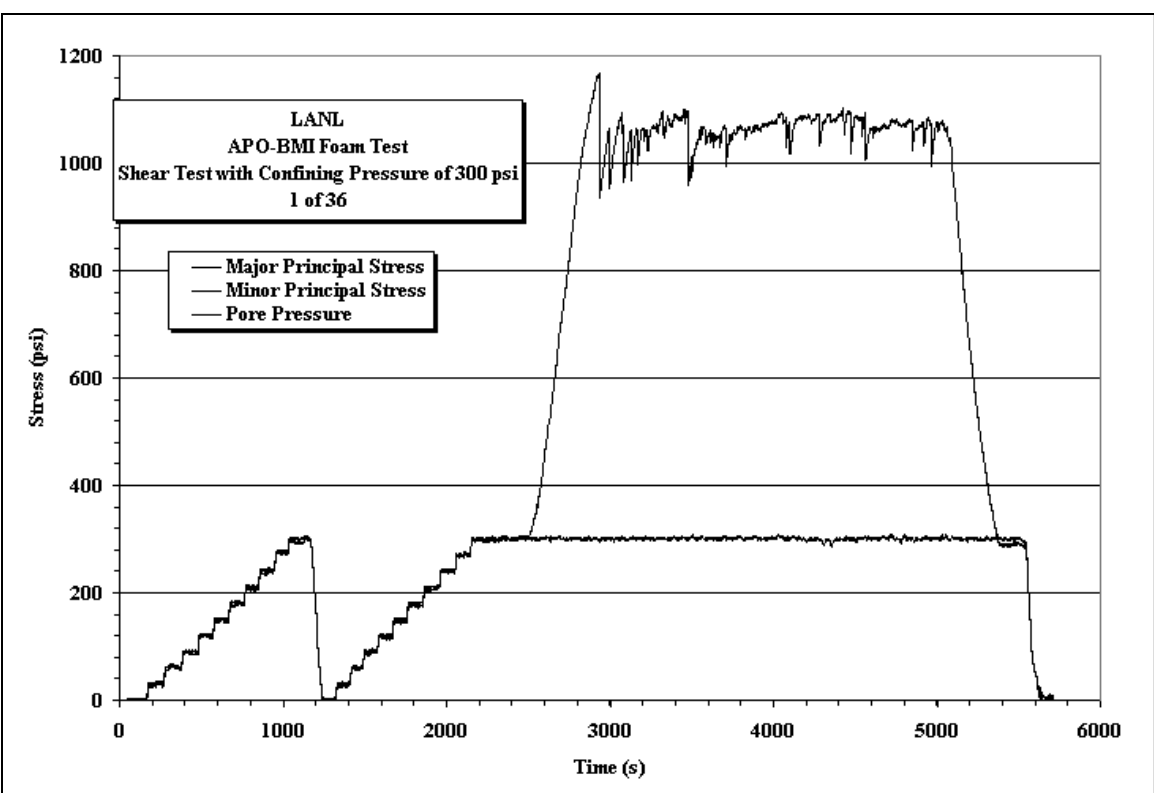
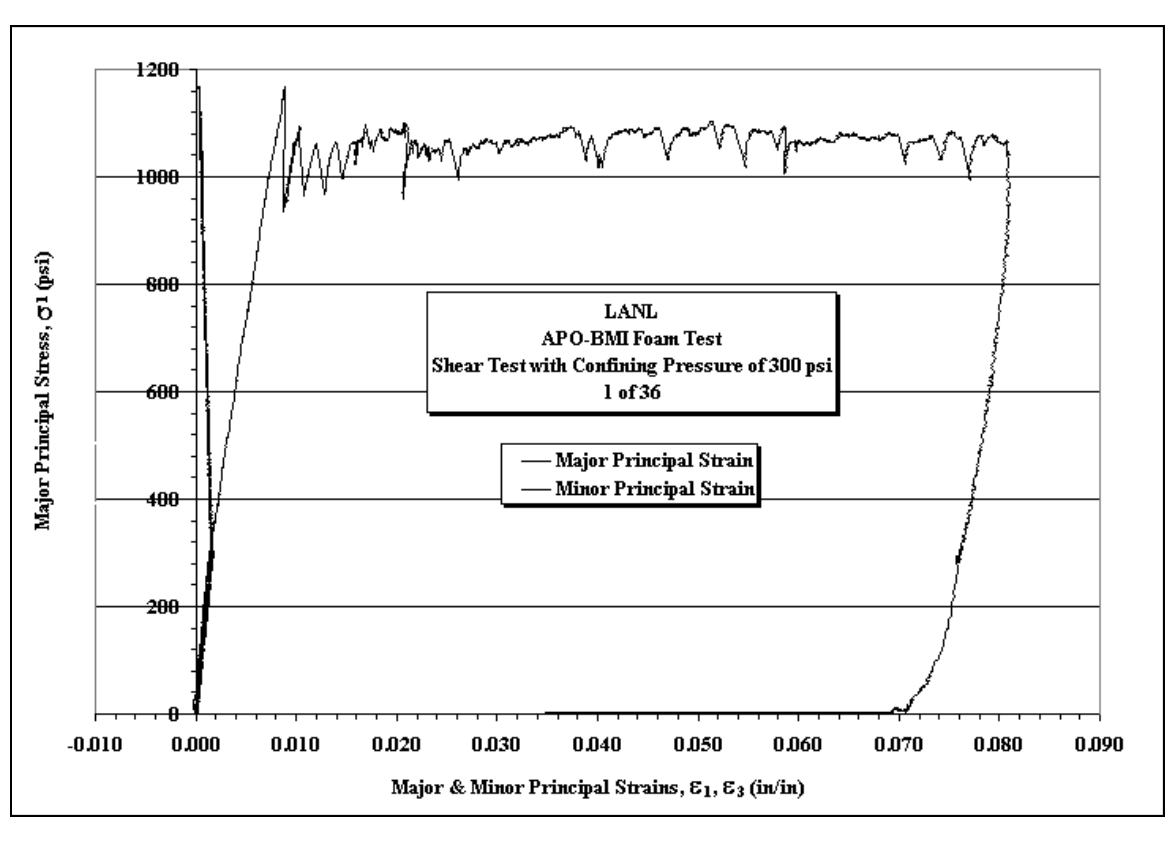


Figure A45. Minor Principle Strain vs. Major Principle Strain and Deviatoric Stress vs. Mean Stress plots for Sample 1of36 with a constant confining pressure of 300 psi.



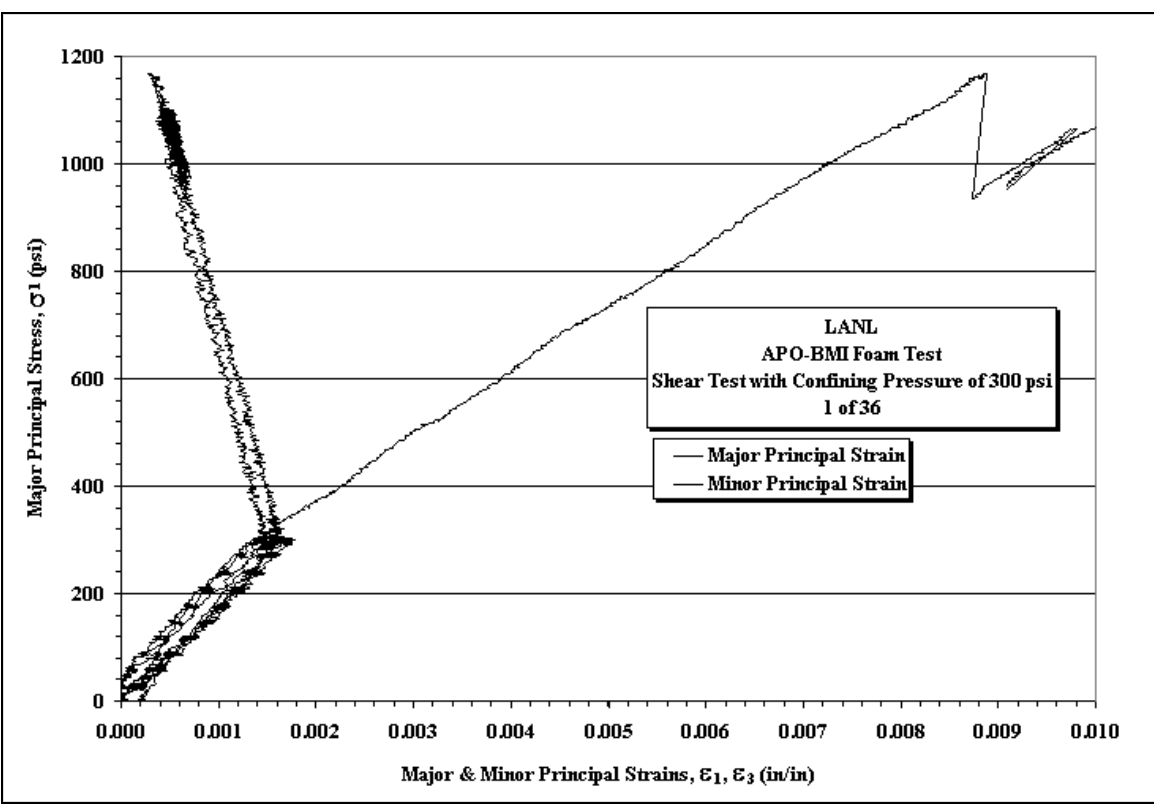
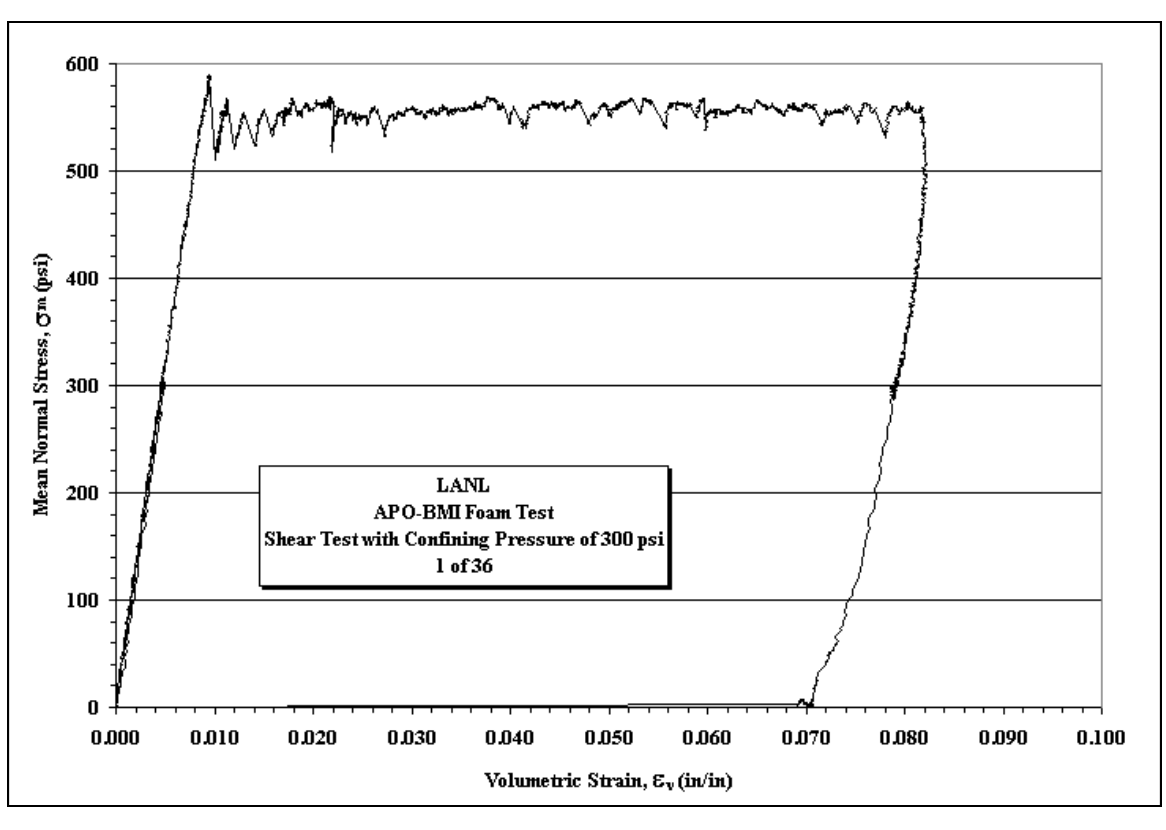


Figure A46. Stress vs. Strain plots for Sample 1of36 with a constant confining pressure of 300 psi.



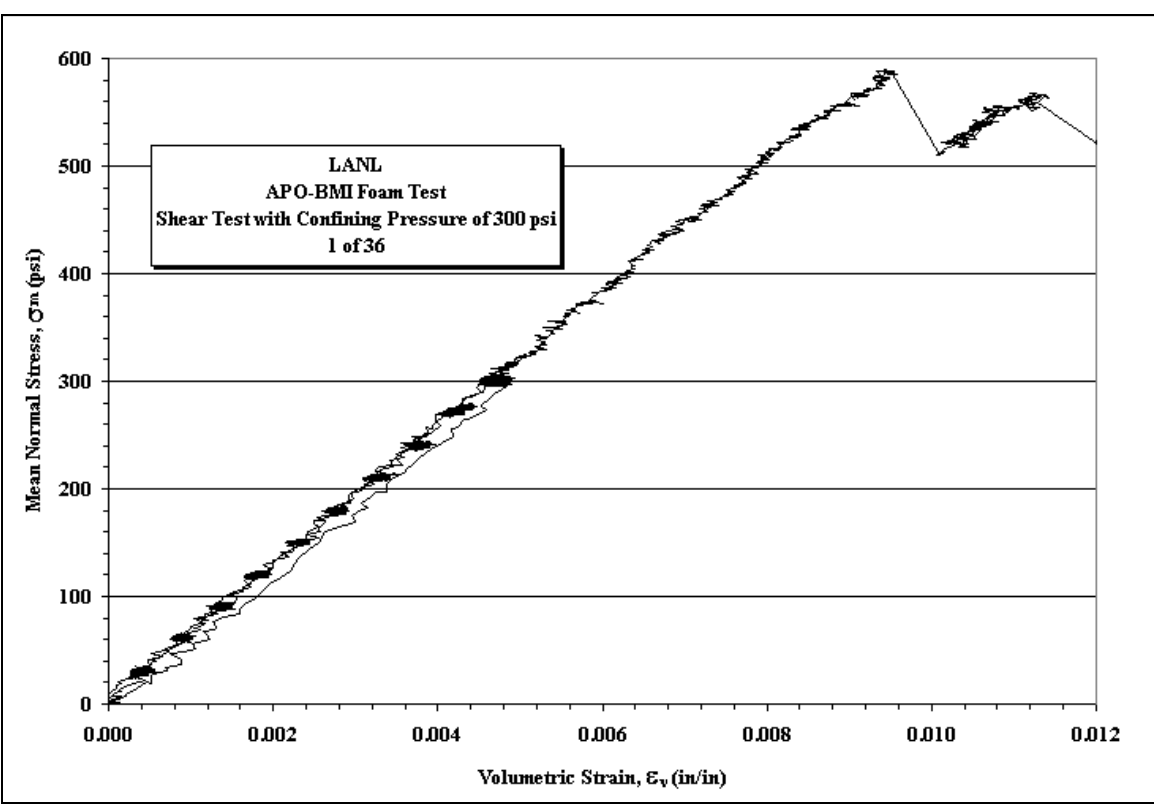
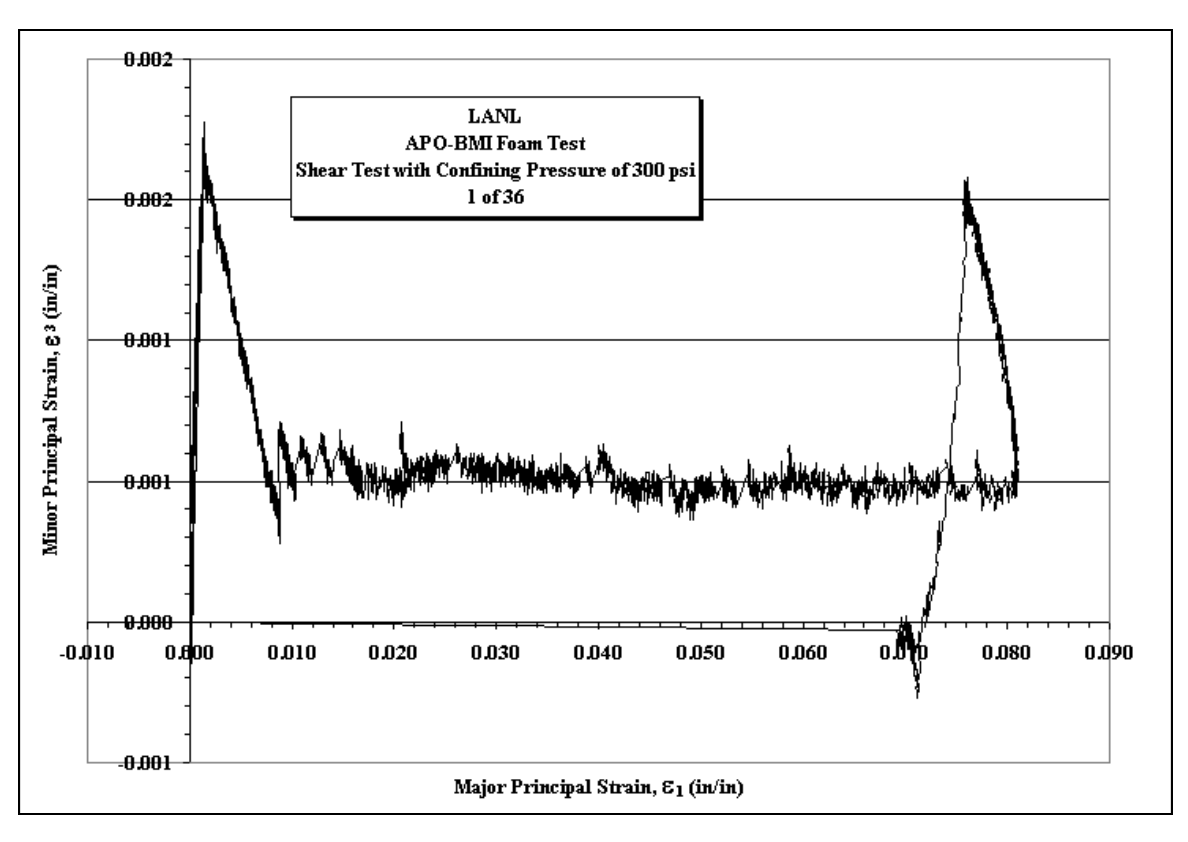


Figure A47. Mean Stress vs. Volumetric Strain plots for Sample 1of36 with a constant confining pressure of 300 psi.



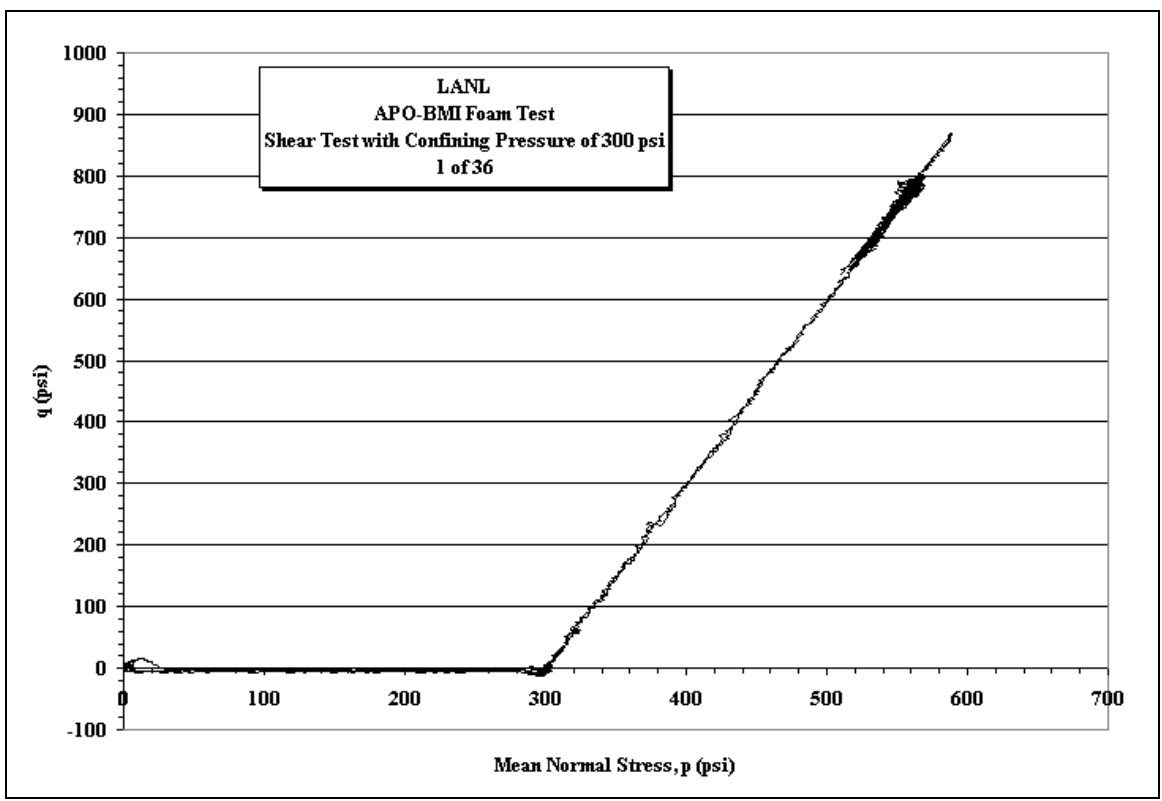
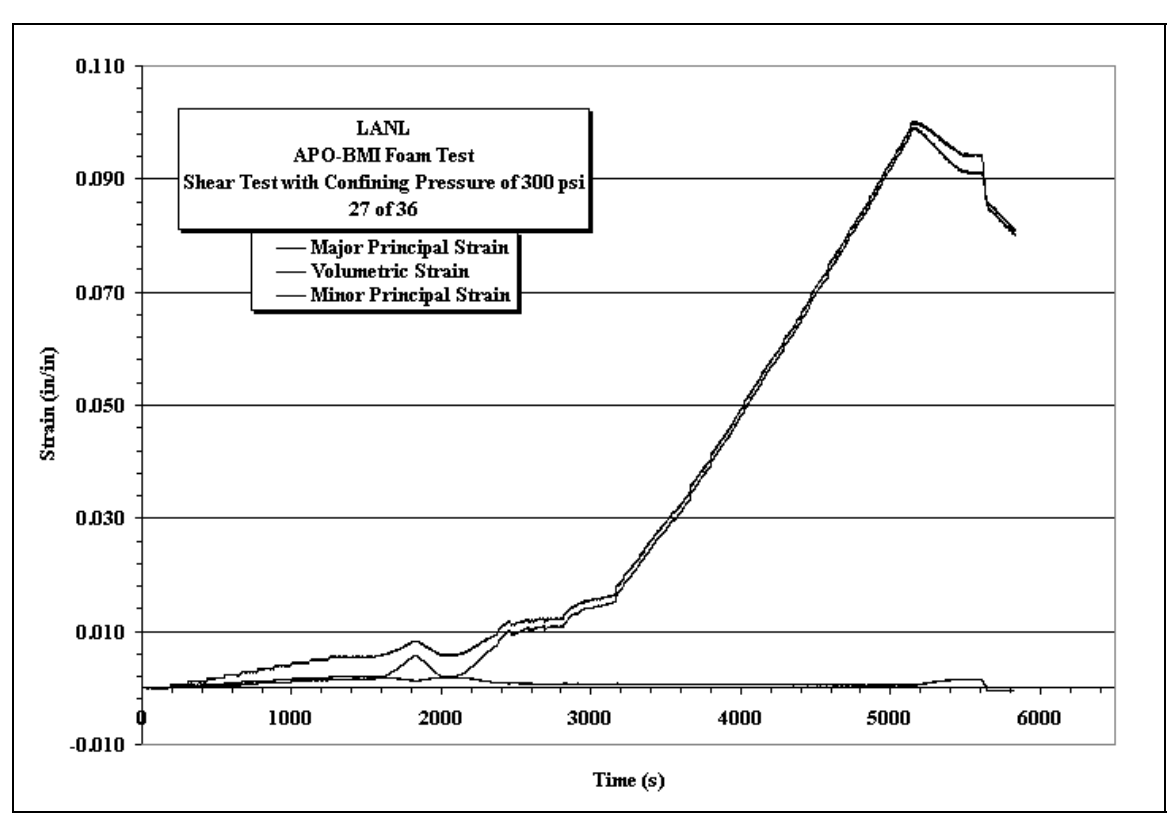


Figure A48. Minor Principle Strain vs. Major Principle Strain and Deviatoric Stress vs. Mean Stress plots for Sample 1of36 with a constant confining pressure of 300 psi.



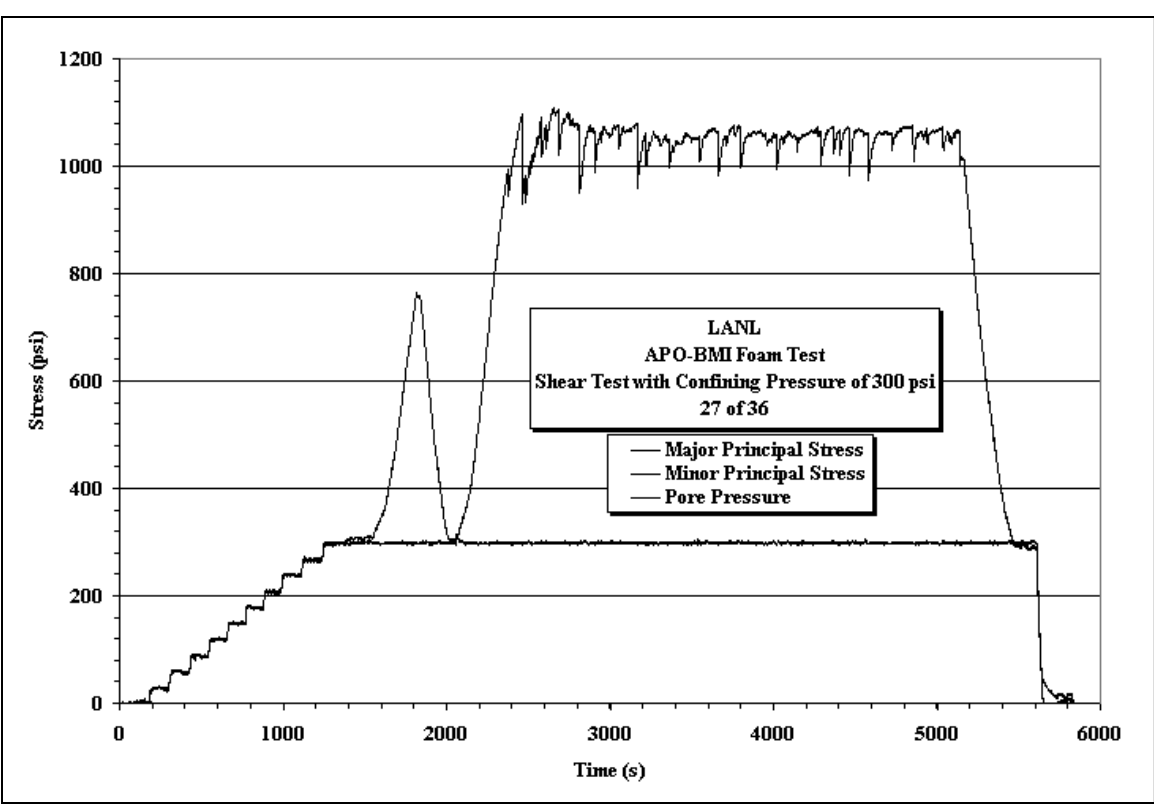
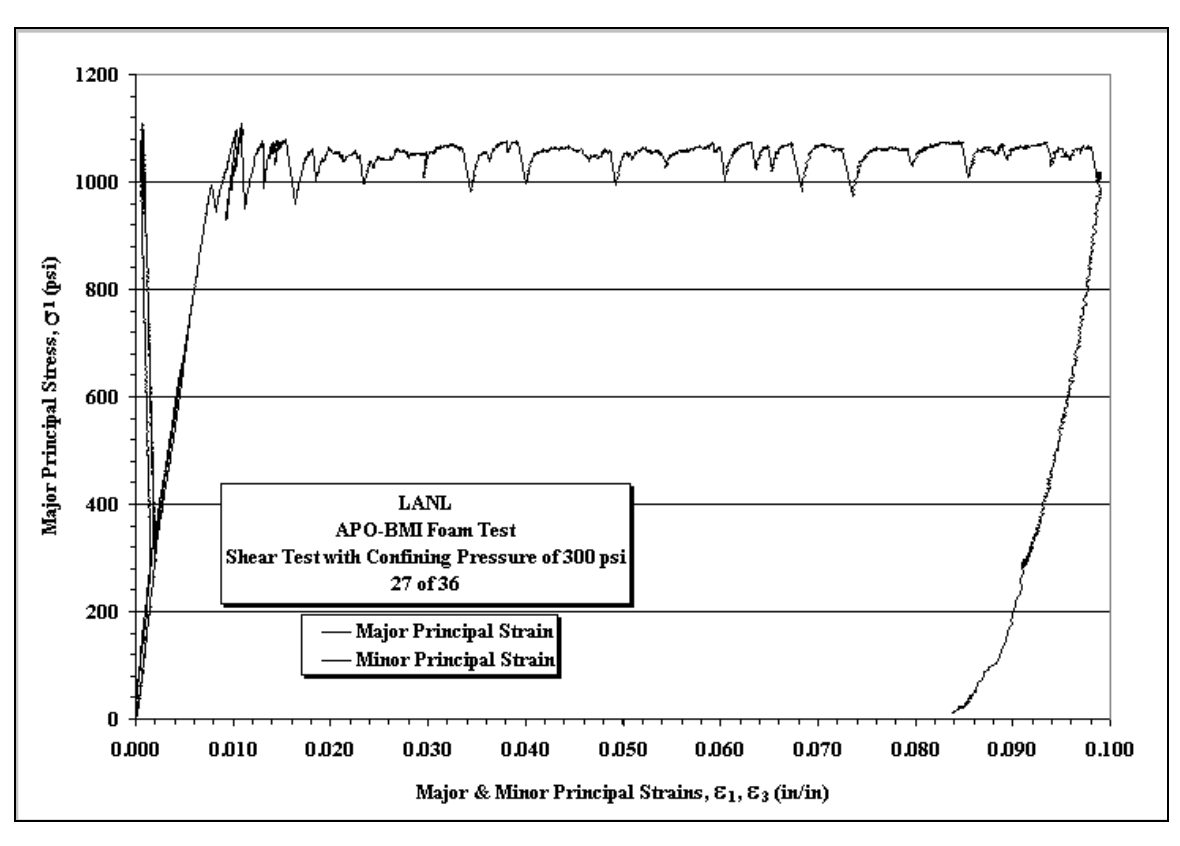


Figure A49. Minor Principle Strain vs. Major Principle Strain and Deviatoric Stress vs. Mean Stress plots for Sample 27of36 with a constant confining pressure of 300 psi.



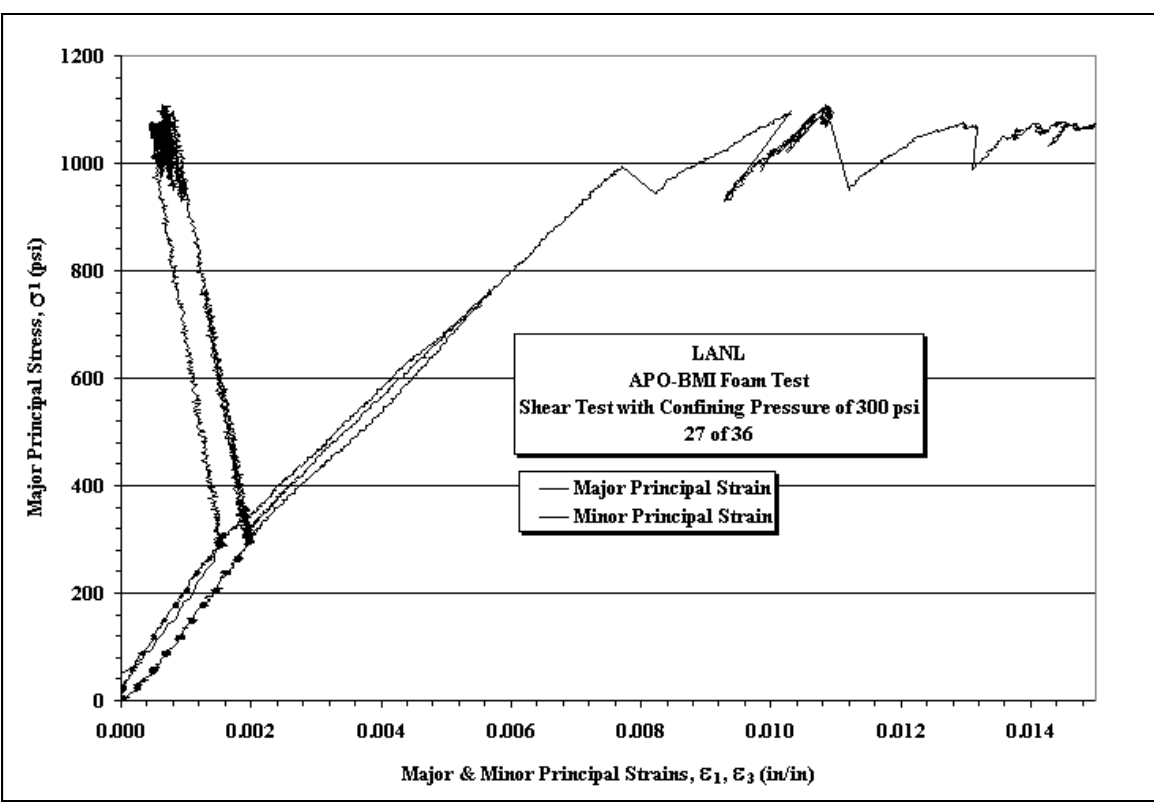
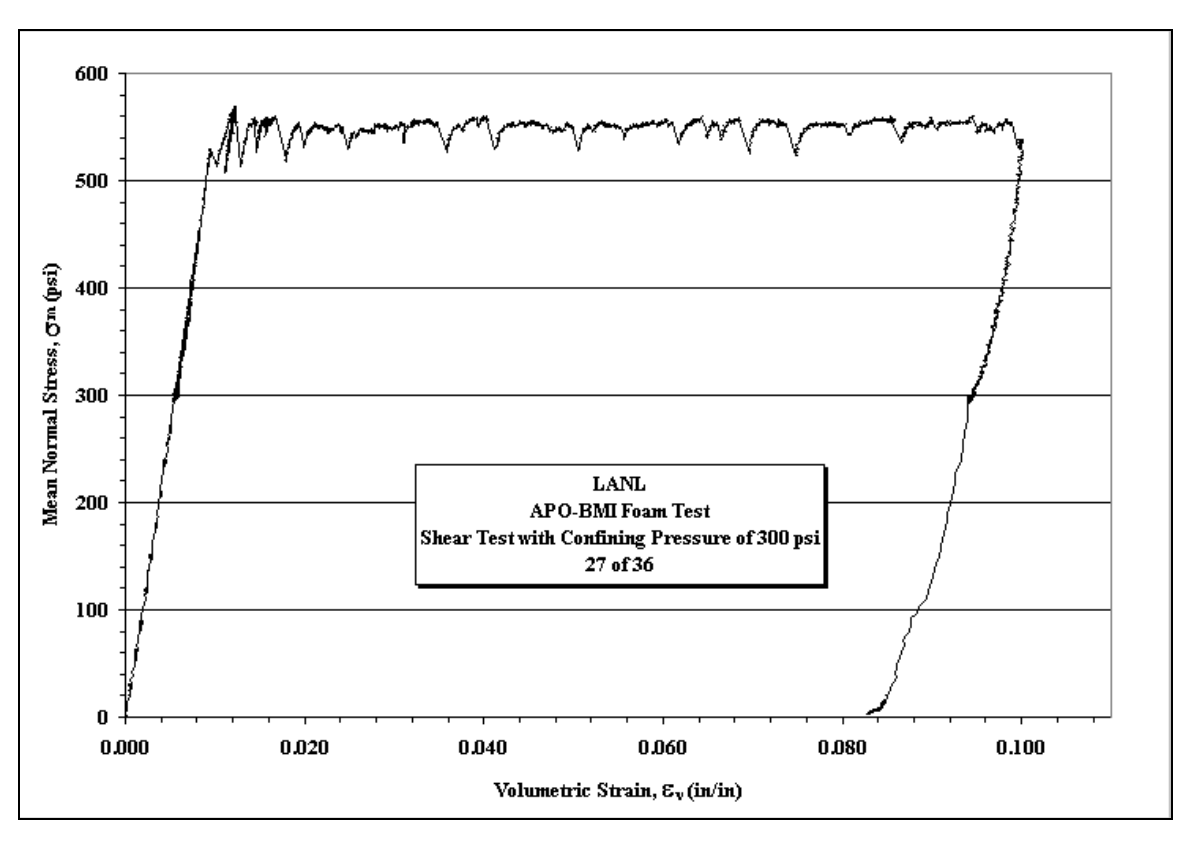


Figure A50. Stress vs. Strain plots for Sample 27of36 with a constant confining pressure of 300 psi.



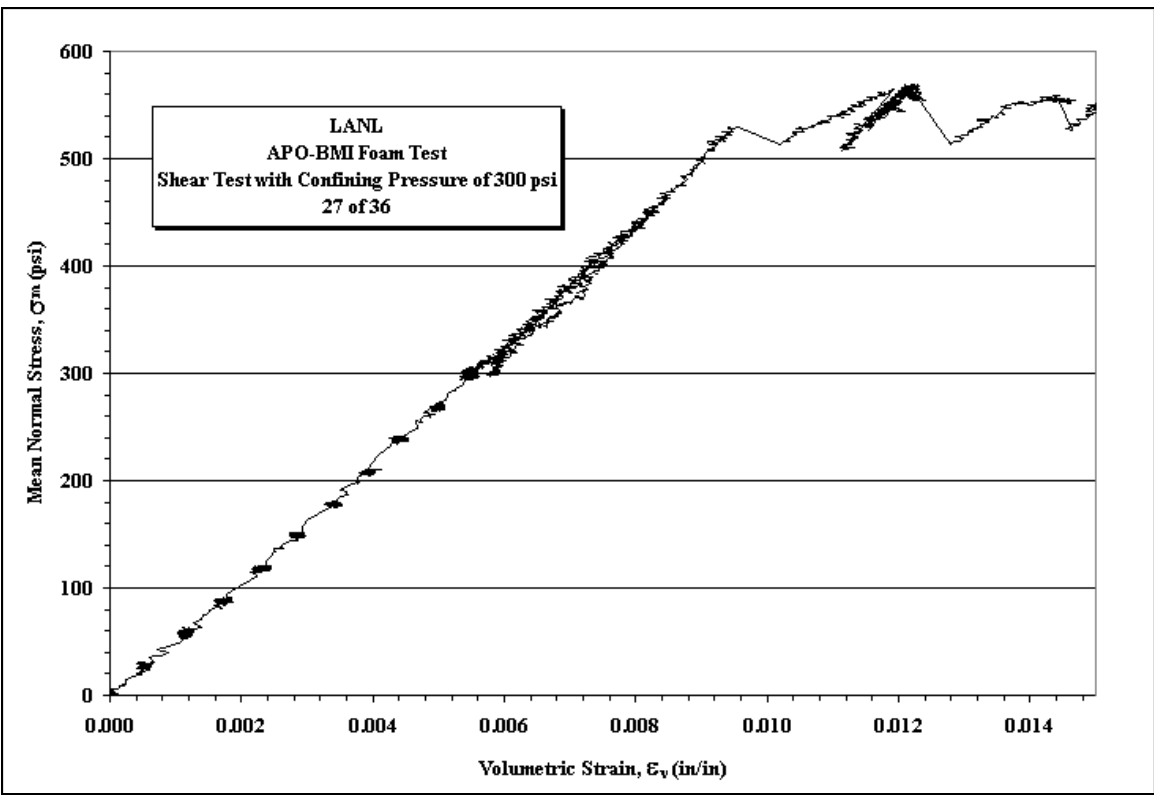
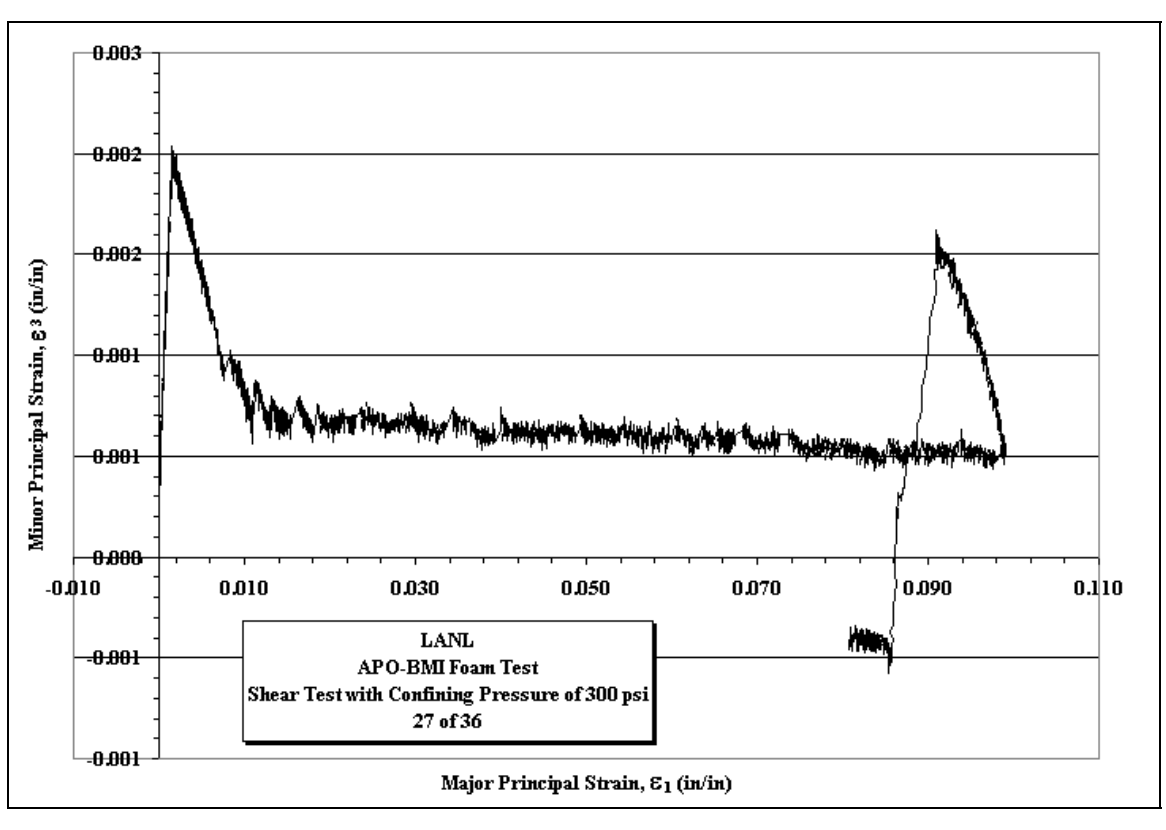


Figure A51. Mean Stress vs. Volumetric Strain plots for Sample 27of36 with a constant confining pressure of 300 psi.



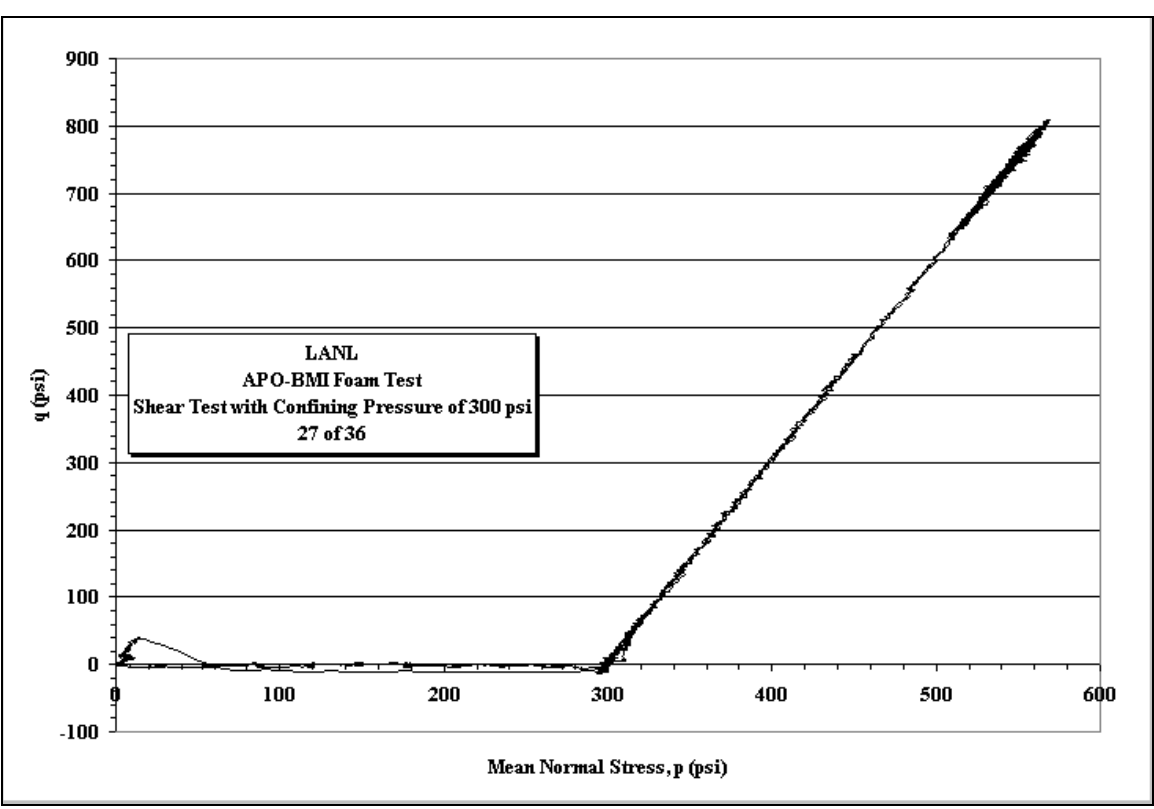
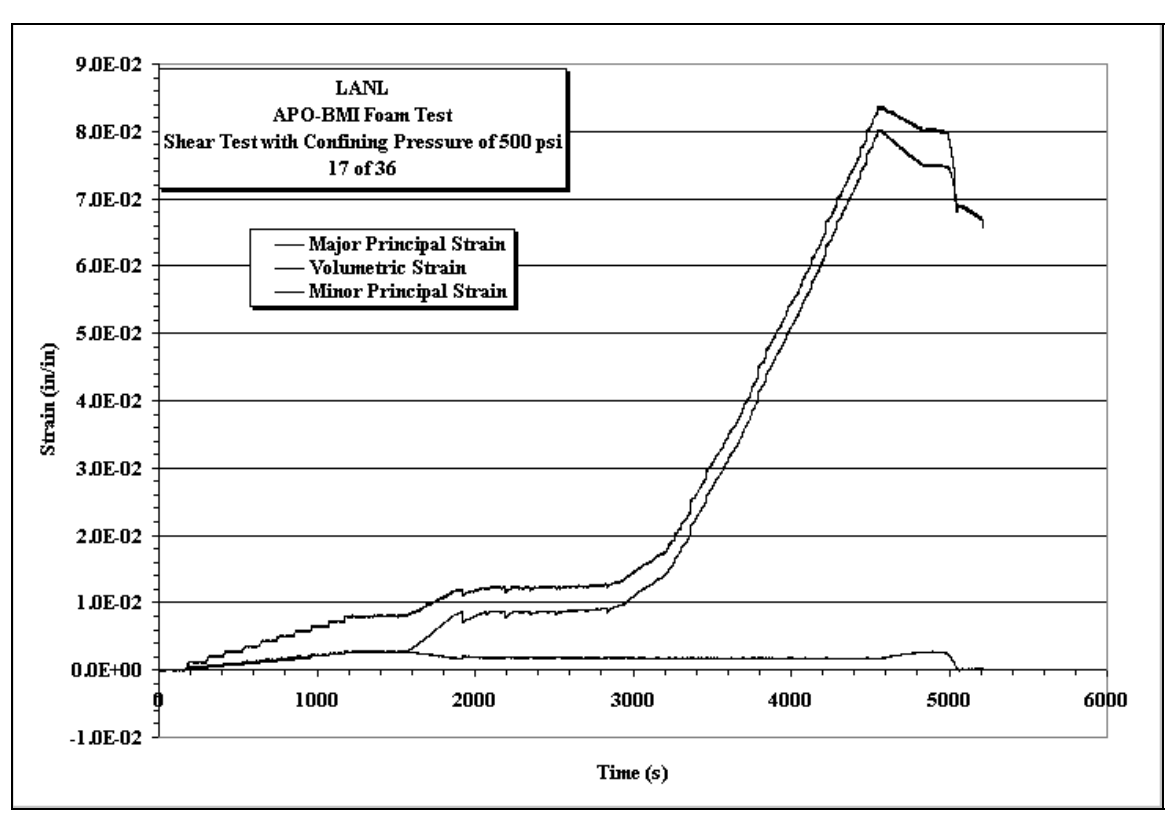


Figure A52. Minor Principle Strain vs. Major Principle Strain and Deviatoric Stress vs. Mean Stress plots for Sample 27of36 with a constant confining pressure of 300 psi.



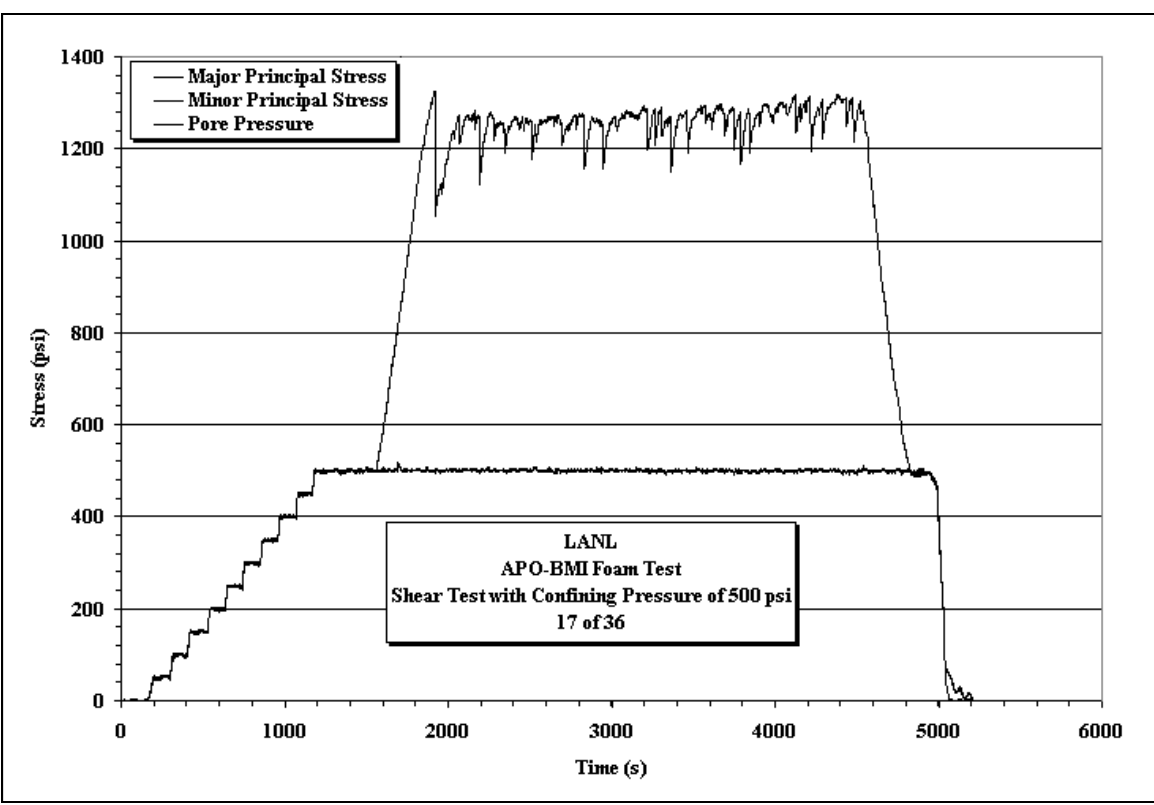
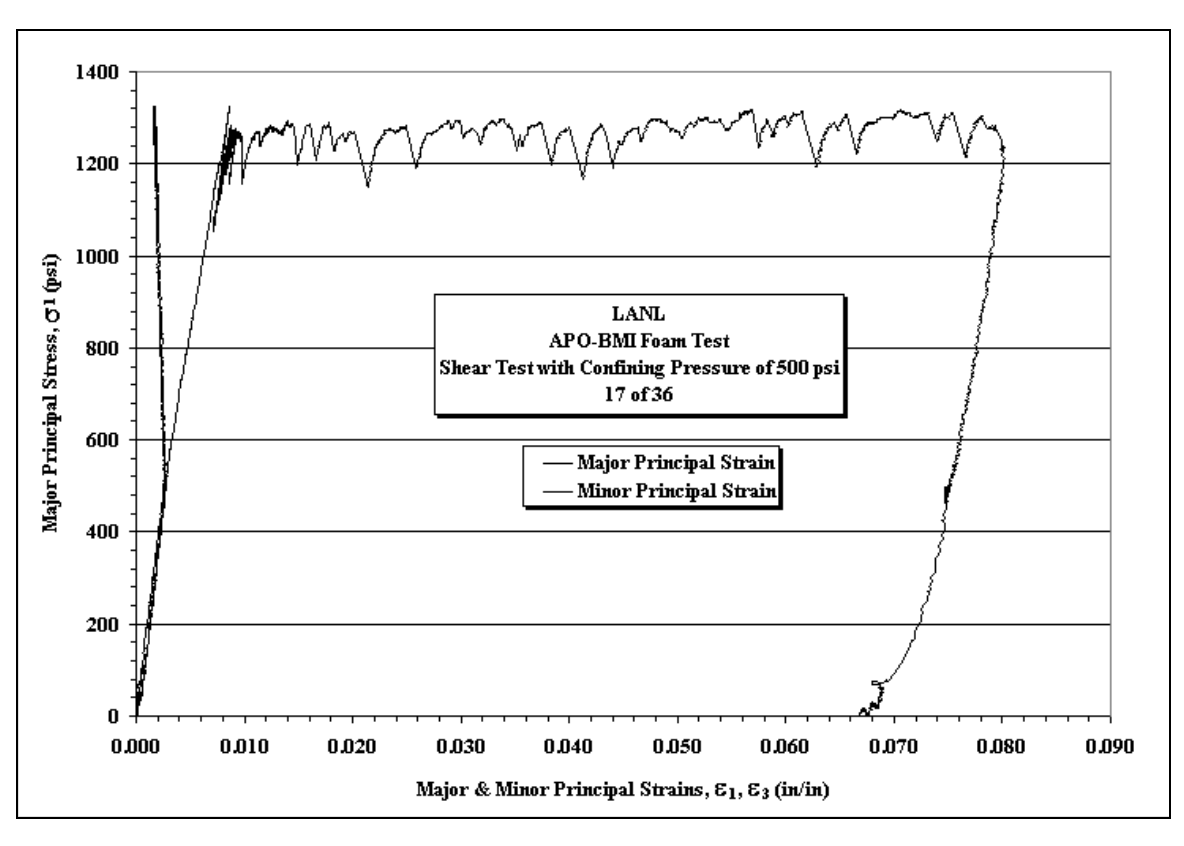


Figure A53. Minor Principle Strain vs. Major Principle Strain and Deviatoric Stress vs. Mean Stress plots for Sample 17of36 with a constant confining pressure of 500 psi.



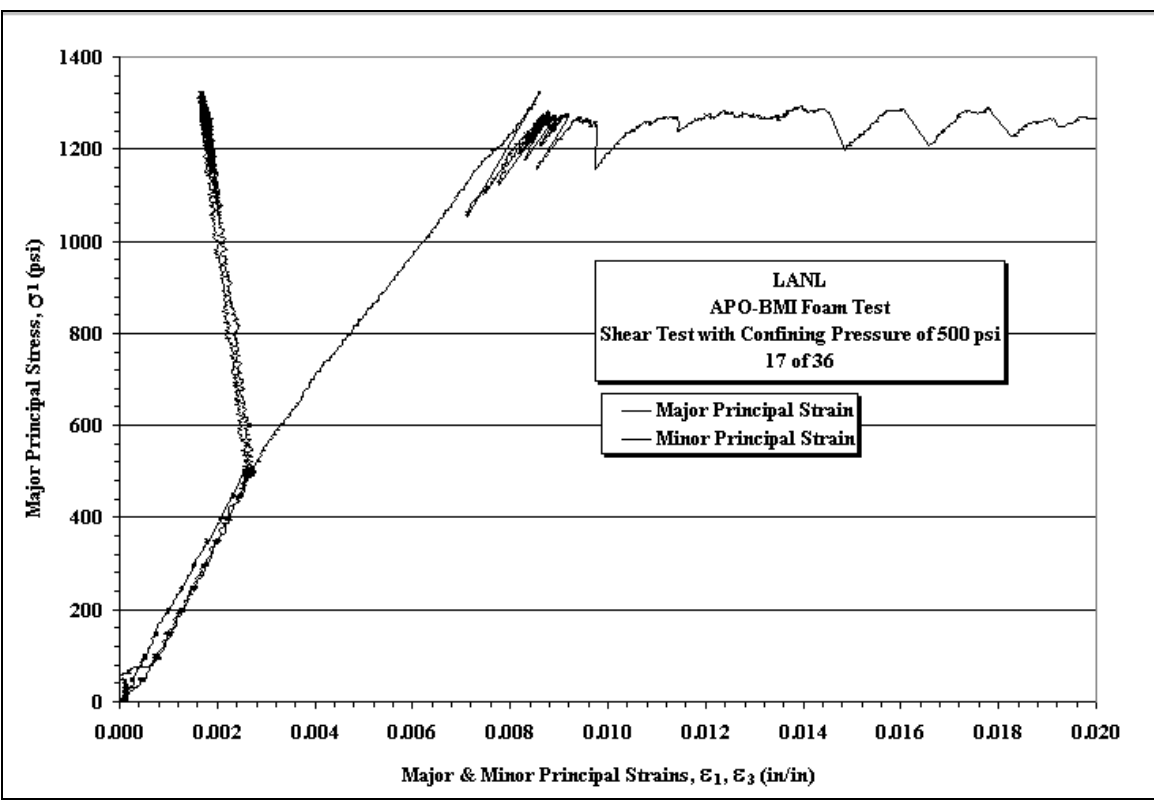
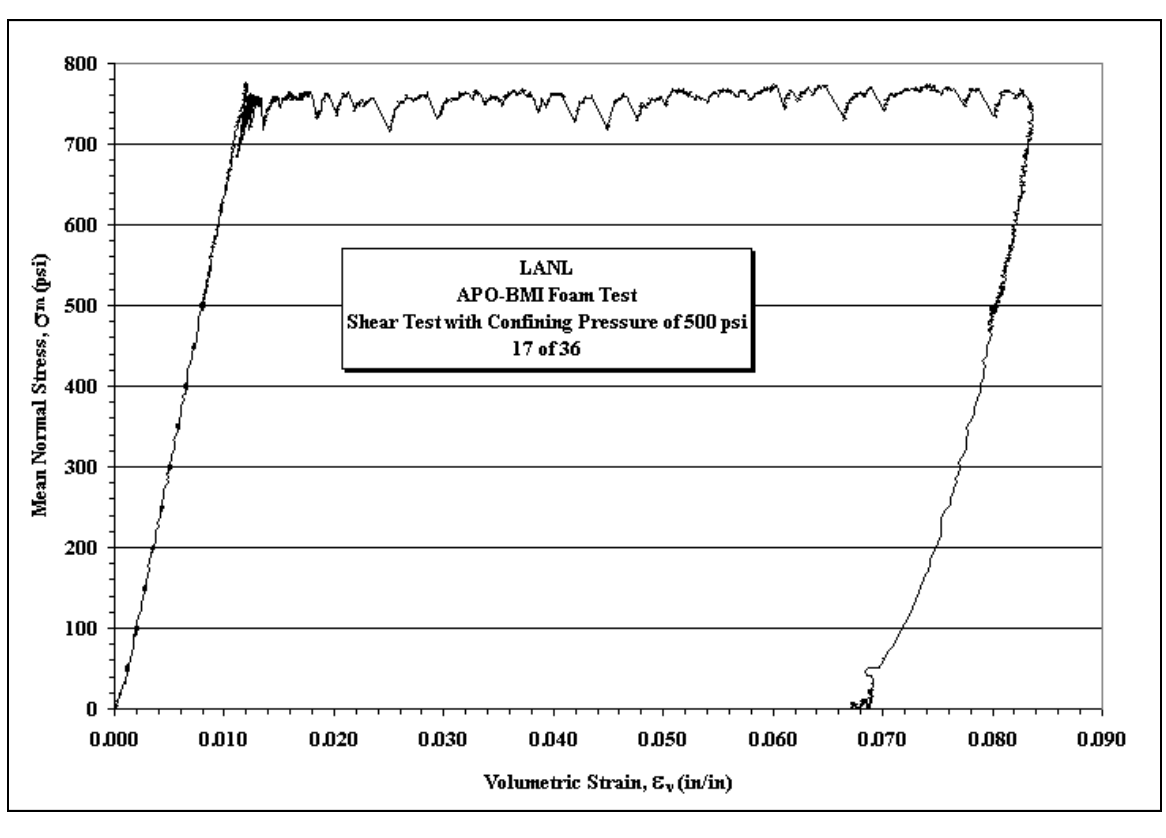


Figure A54. Stress vs. Strain plots for Sample 17of36 with a constant confining pressure of 500 psi.



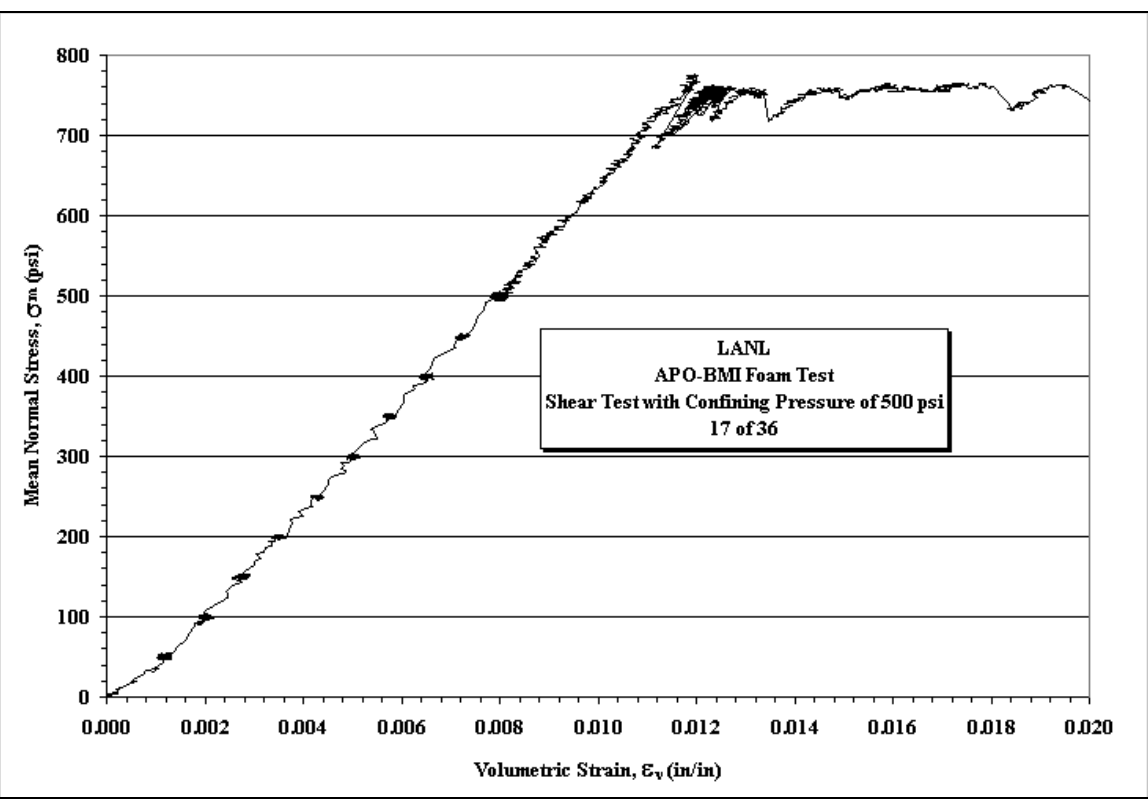
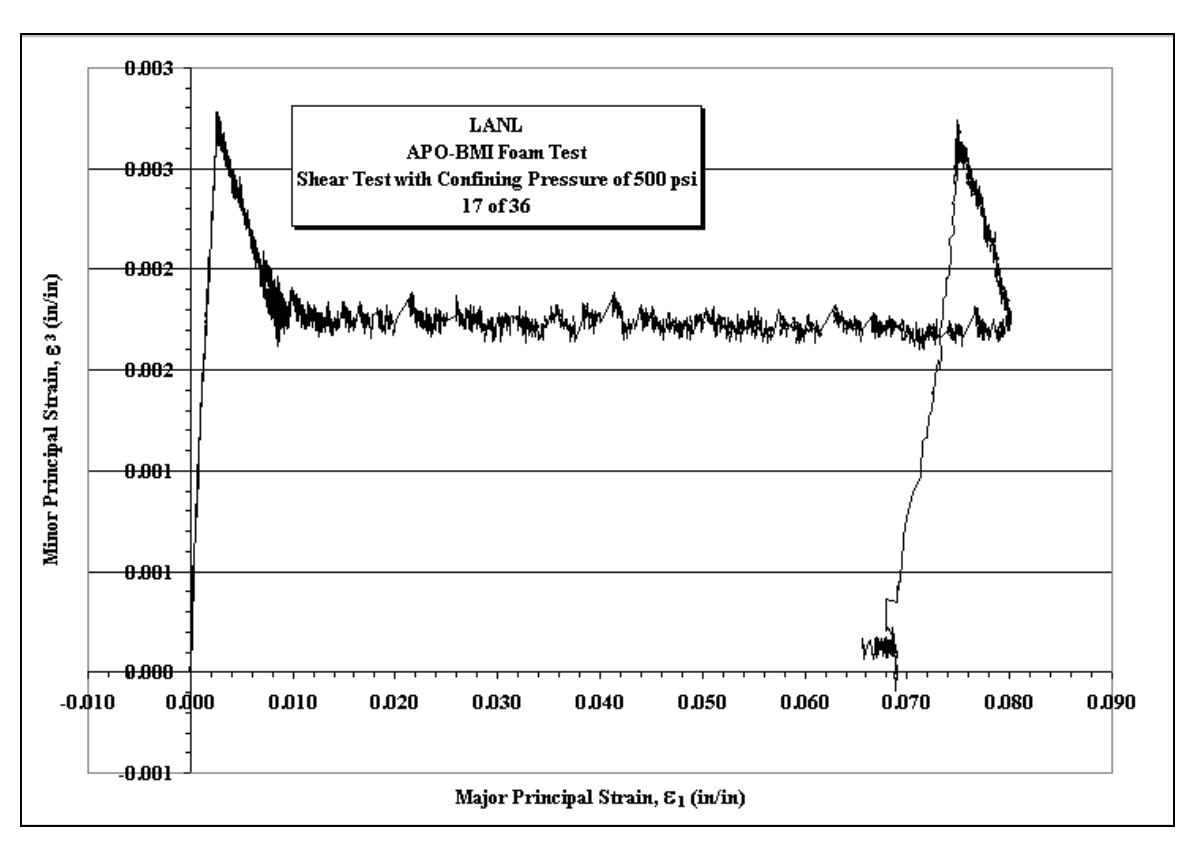


Figure A55. Mean Stress vs. Volumetric Strain plots for Sample 17of36 with a constant confining pressure of 500 psi.



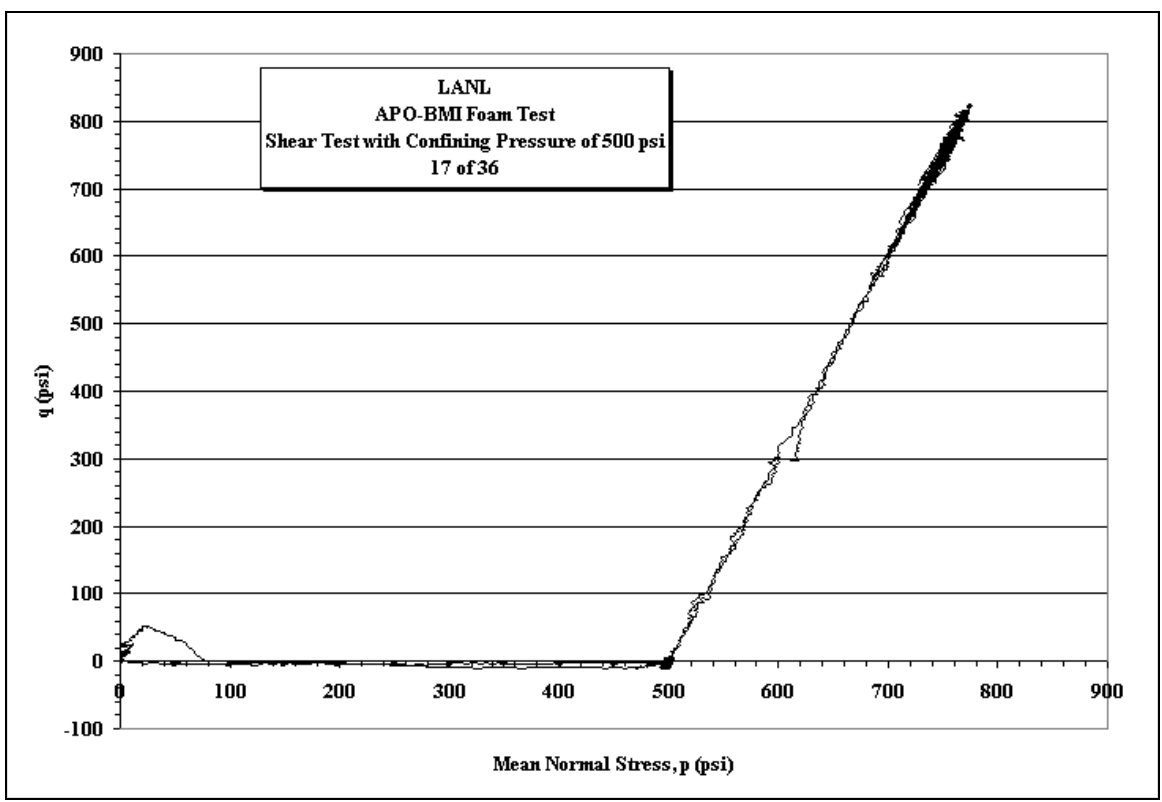
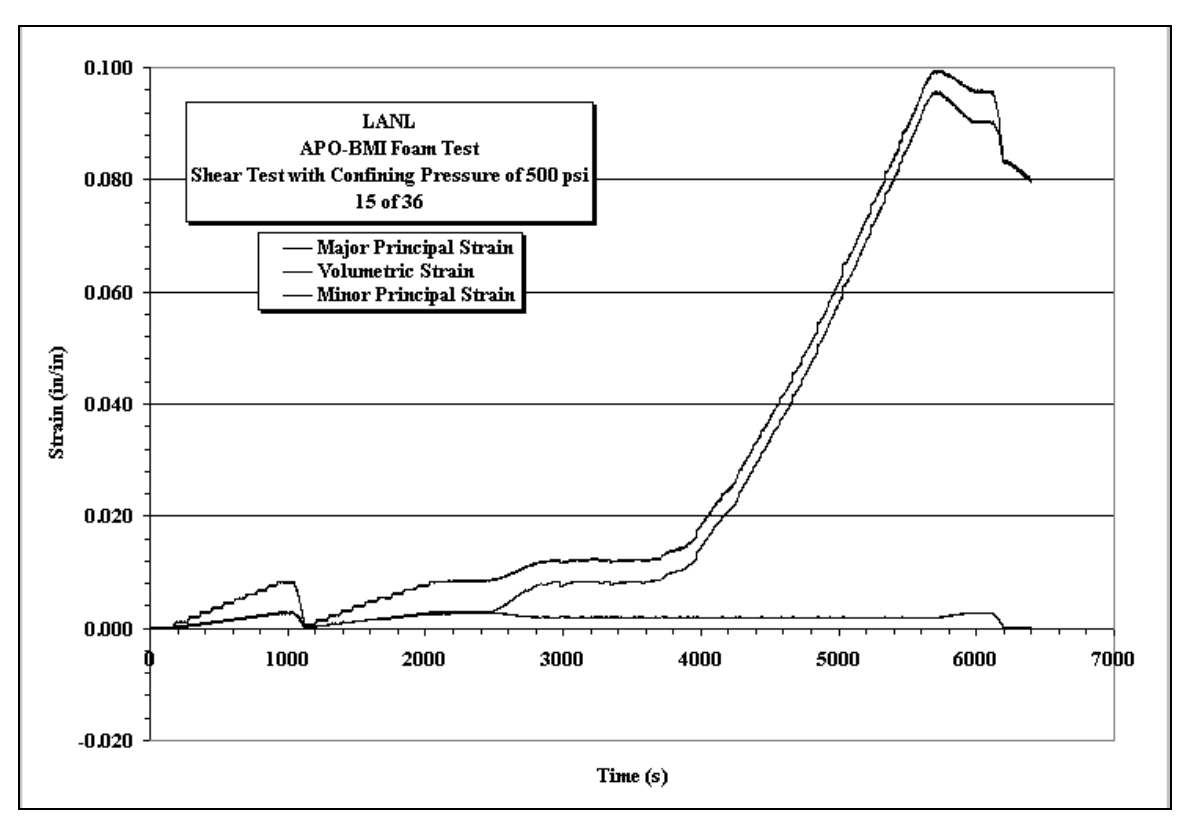


Figure A56. Minor Principle Strain vs. Major Principle Strain and Deviatoric Stress vs. Mean Stress plots for Sample 17of36 with a constant confining pressure of 500 psi.



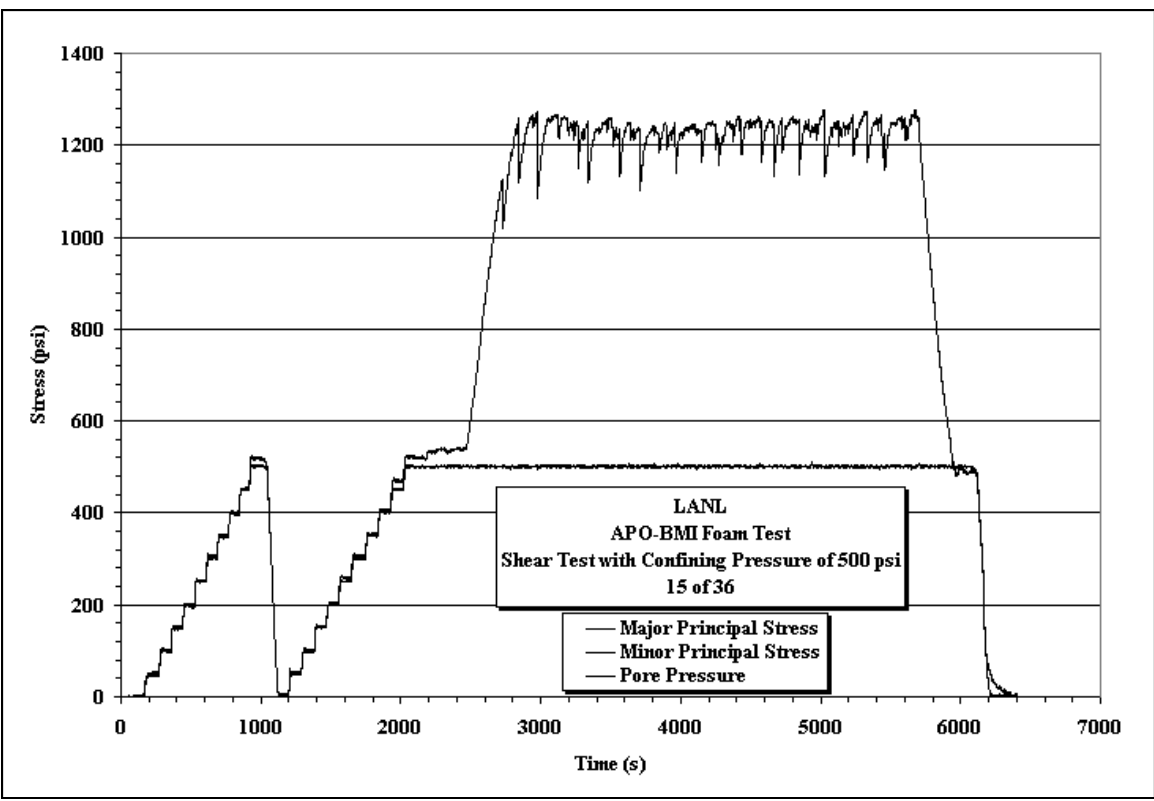
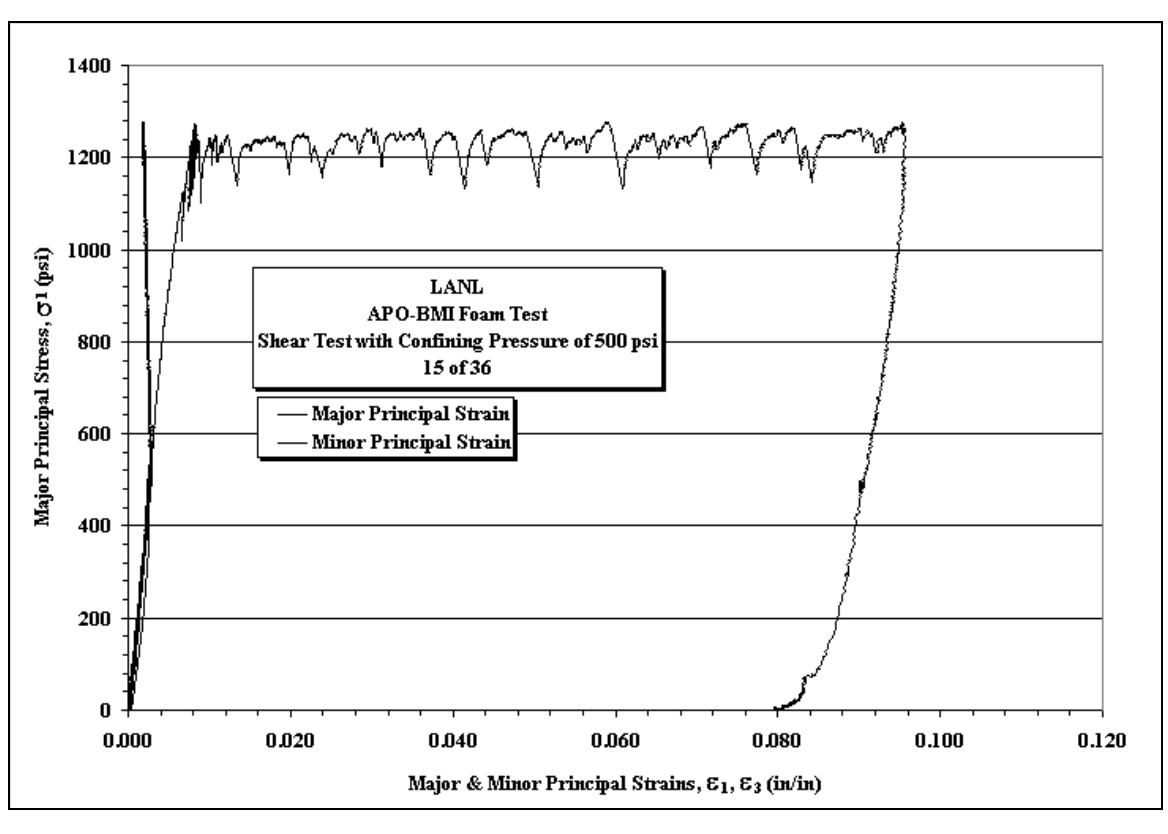


Figure A57. Minor Principle Strain vs. Major Principle Strain and Deviatoric Stress vs. Mean Stress plots for Sample 15of36 with a constant confining pressure of 500 psi.



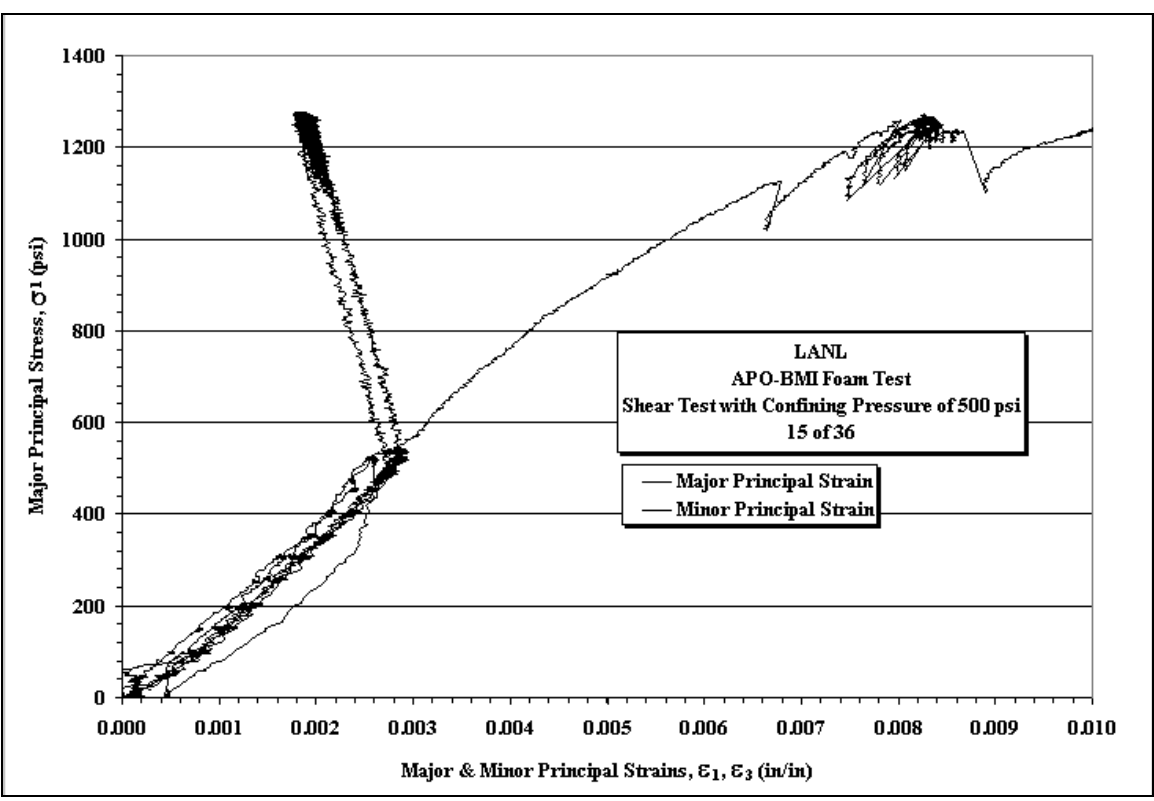
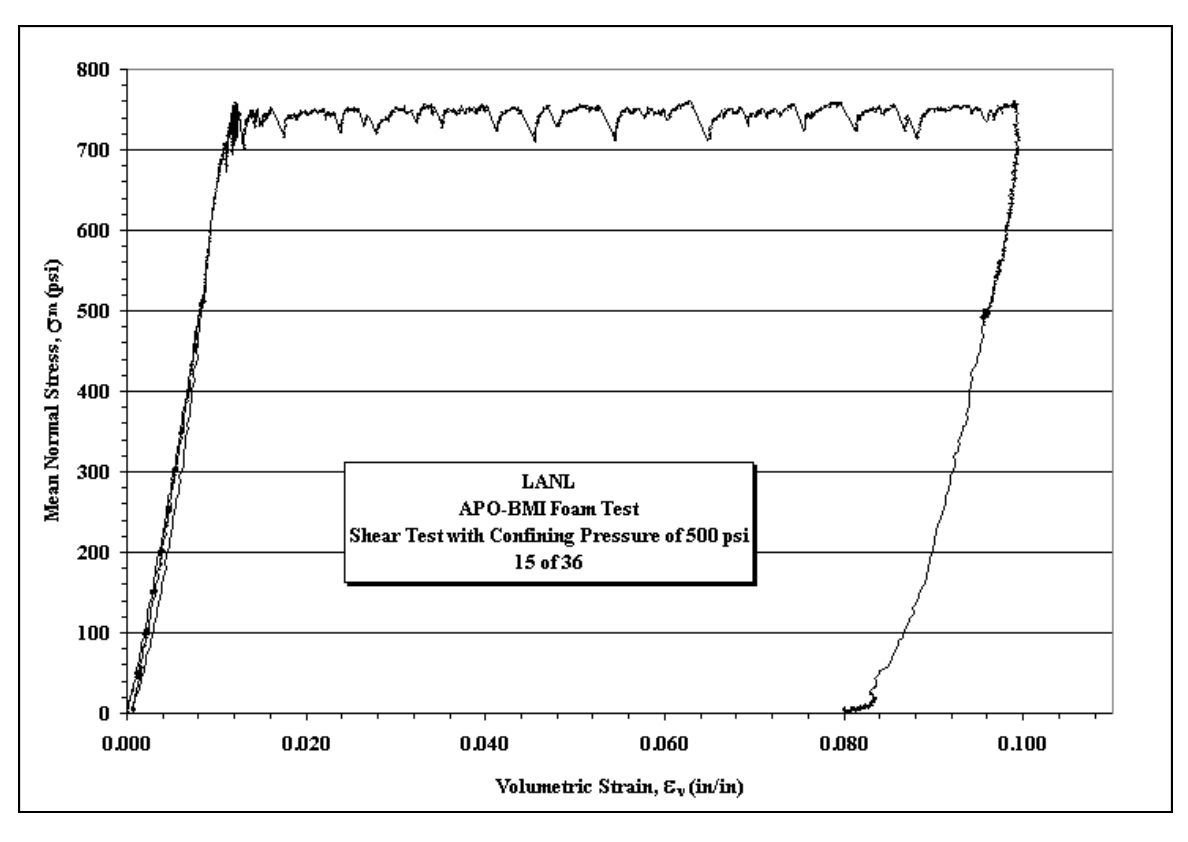


Figure A58. Stress vs. Strain plots for Sample 15of36 with a constant confining pressure of 500 psi.



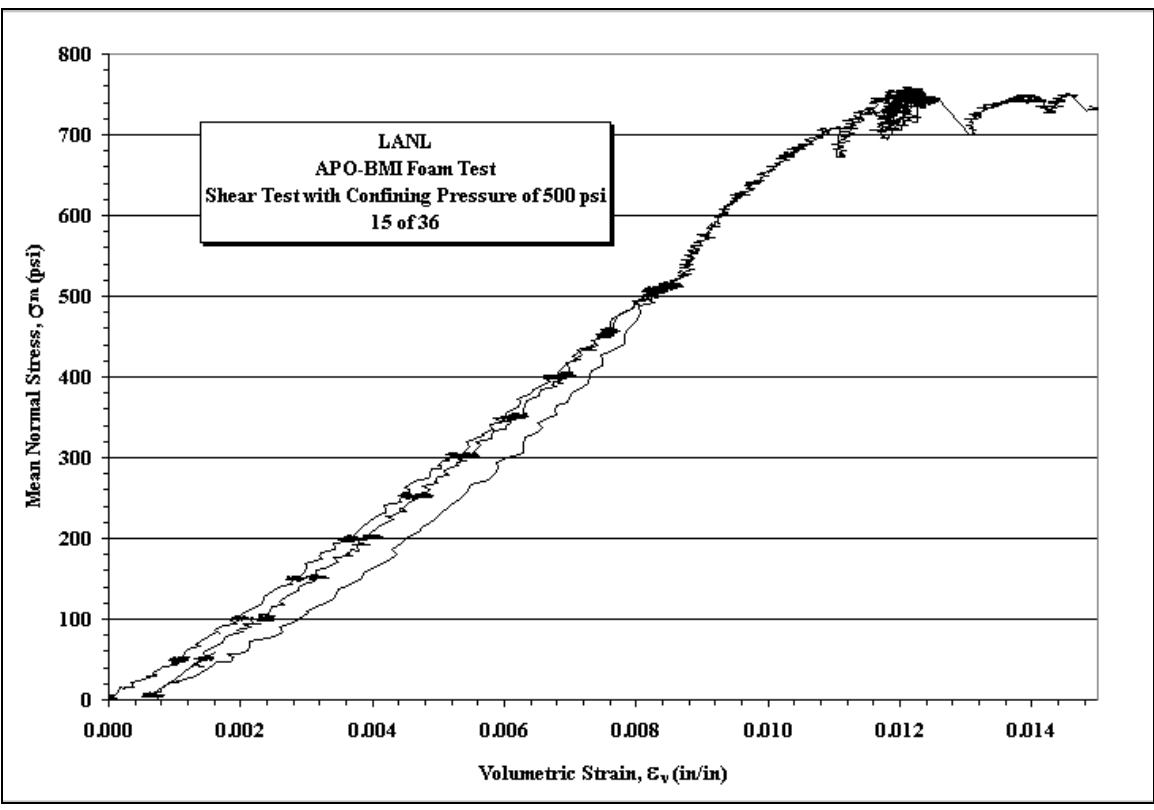
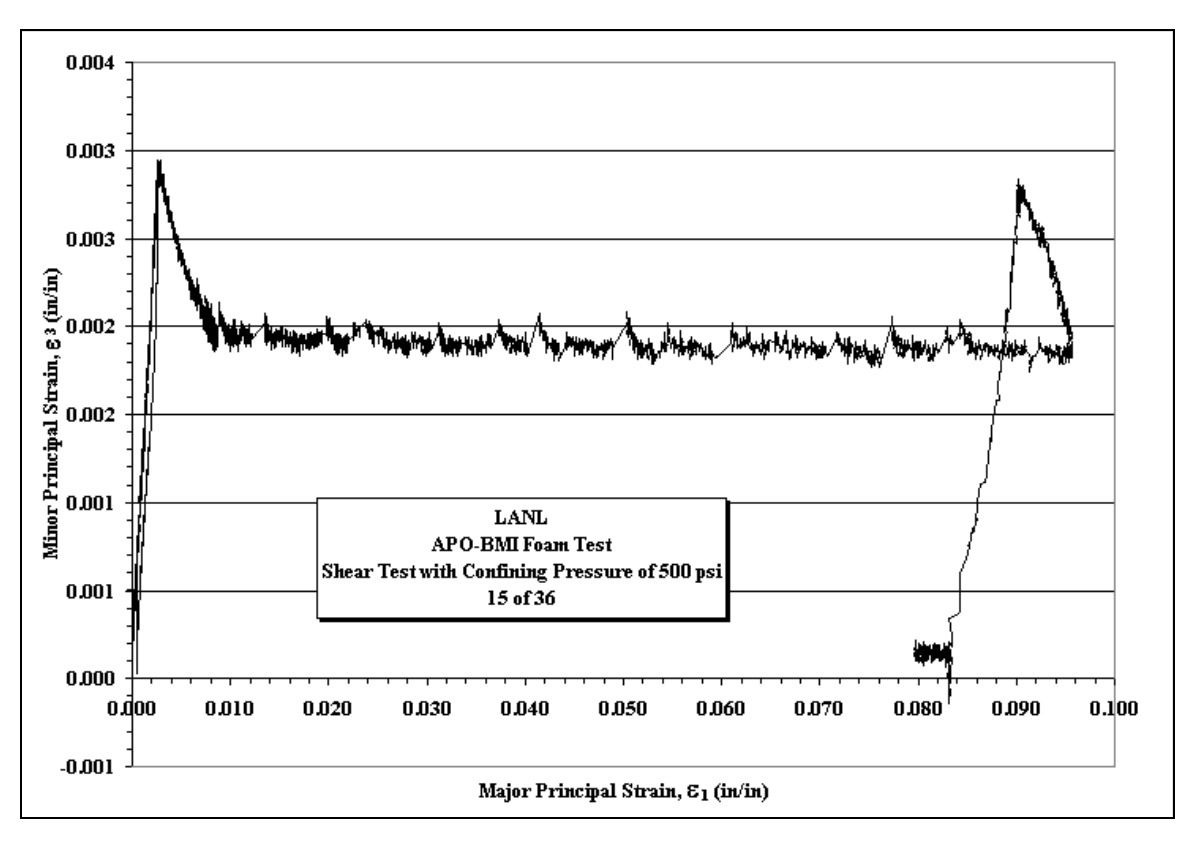


Figure A59. Mean Stress vs. Volumetric Strain plots for Sample 15of36 with a constant confining pressure of 500 psi.



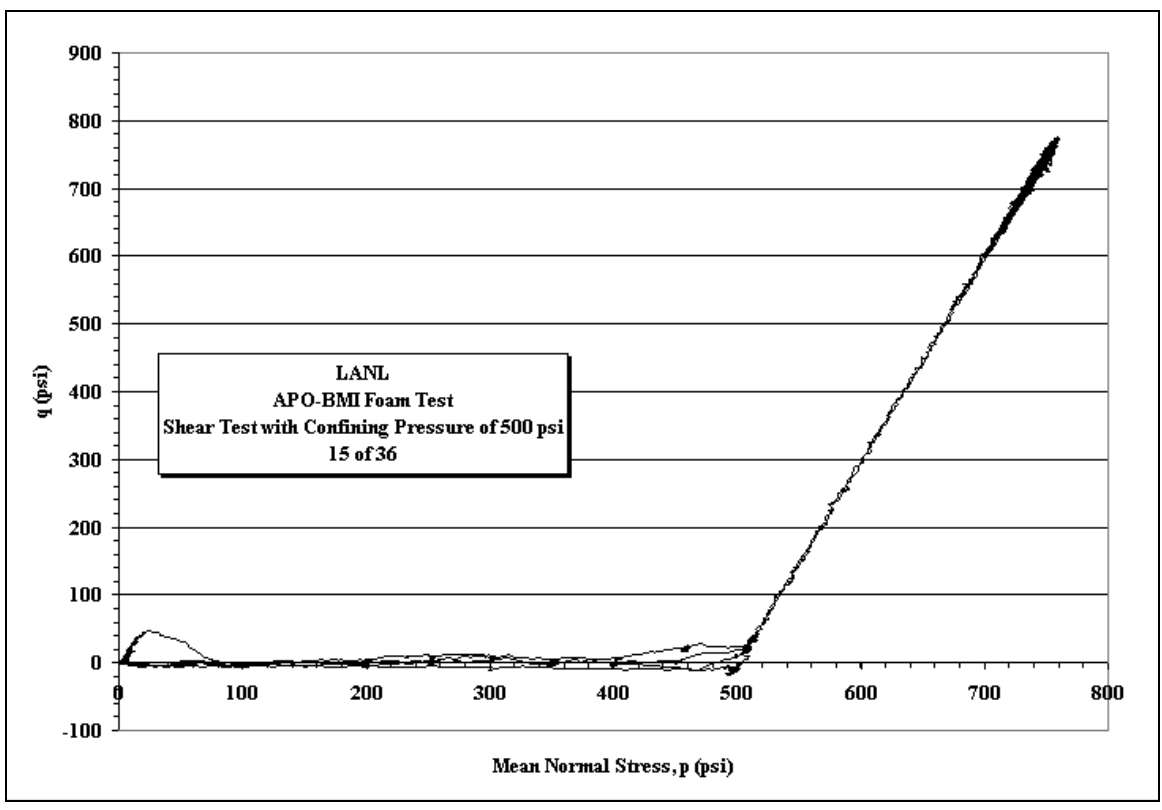
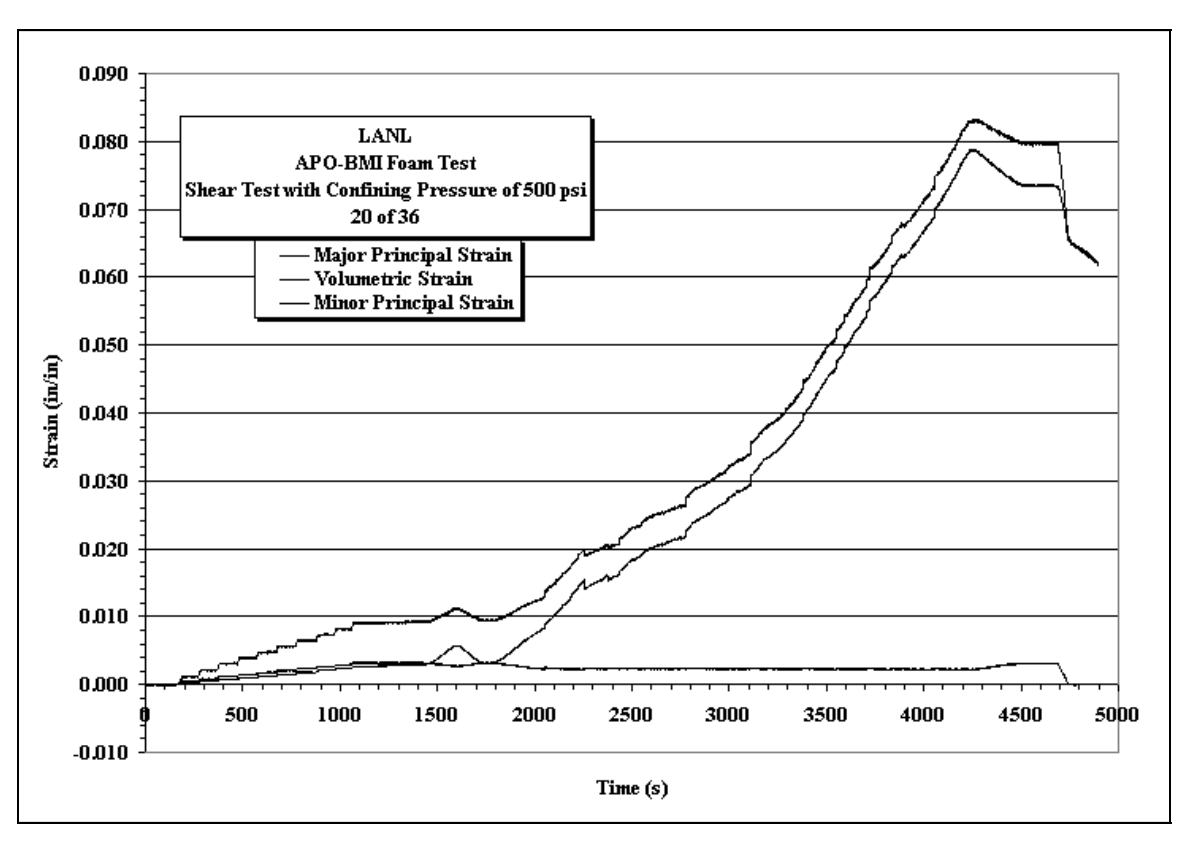


Figure A60. Minor Principle Strain vs. Major Principle Strain and Deviatoric Stress vs. Mean Stress plots for Sample 15of36 with a constant confining pressure of 500 psi.



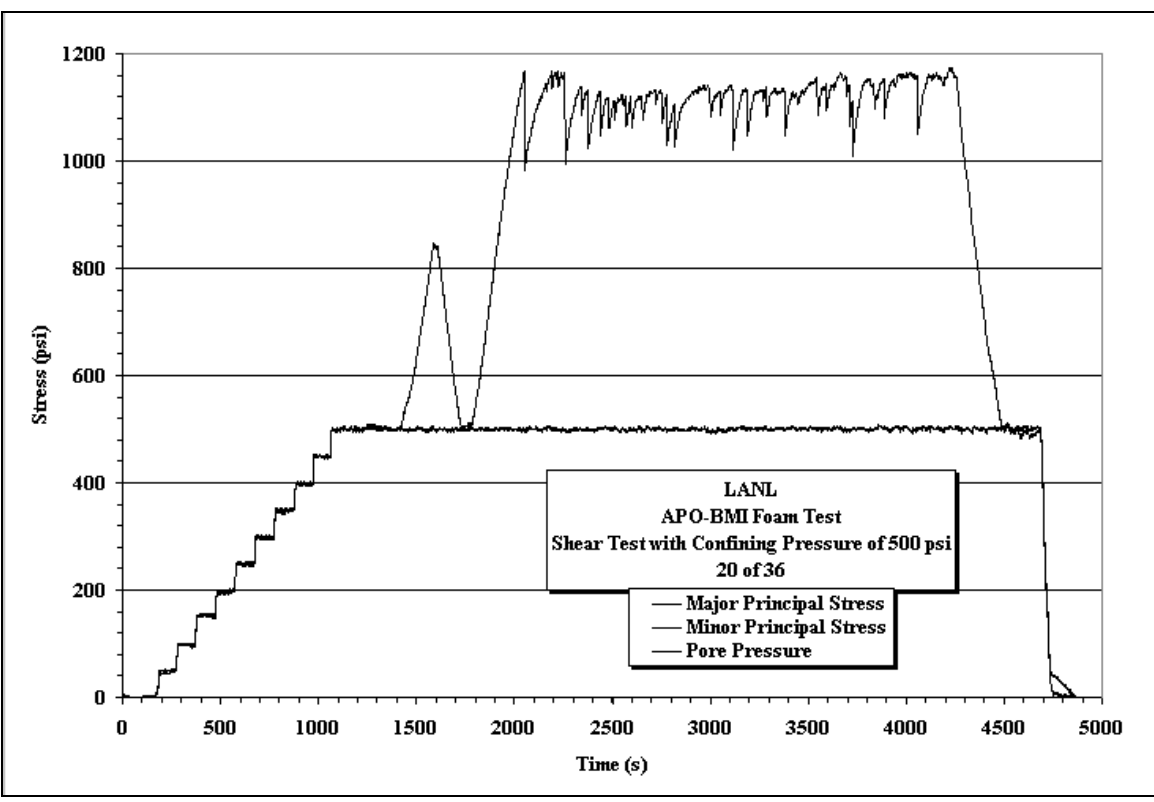
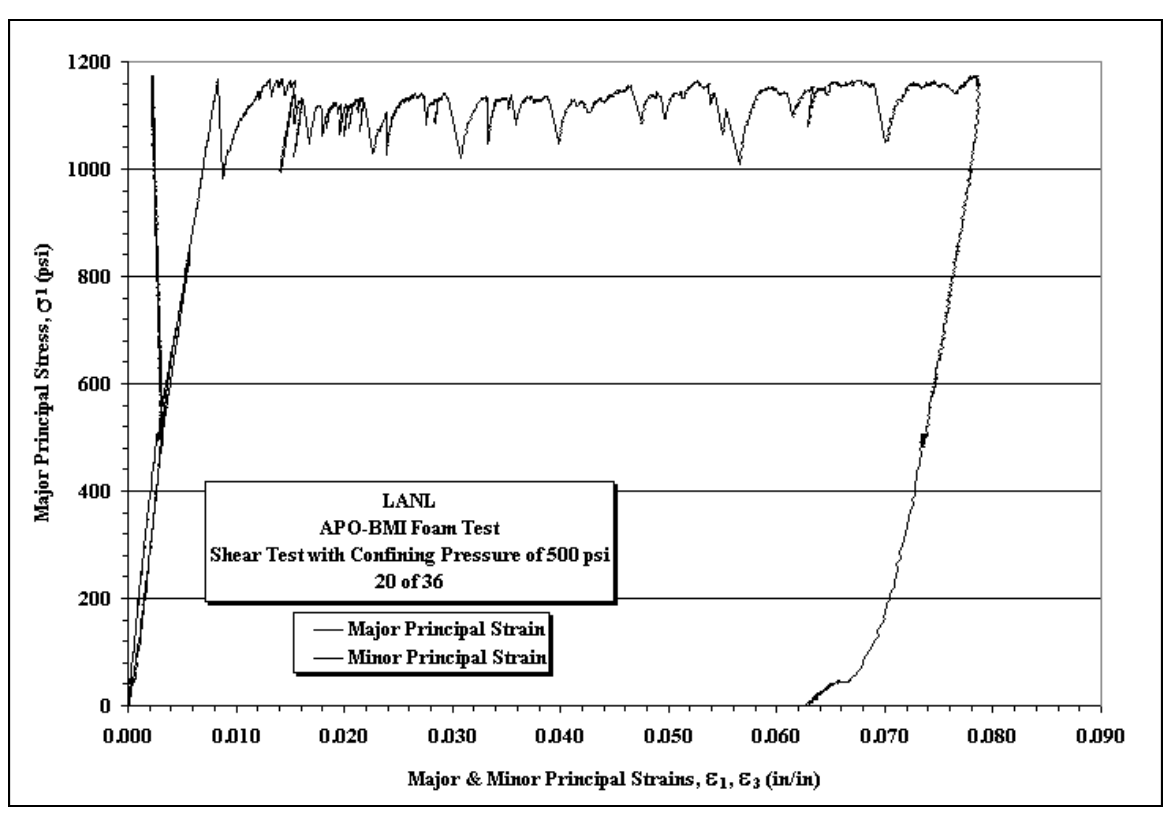


Figure A61. Minor Principle Strain vs. Major Principle Strain and Deviatoric Stress vs. Mean Stress plots for Sample 20of36 with a constant confining pressure of 500 psi.



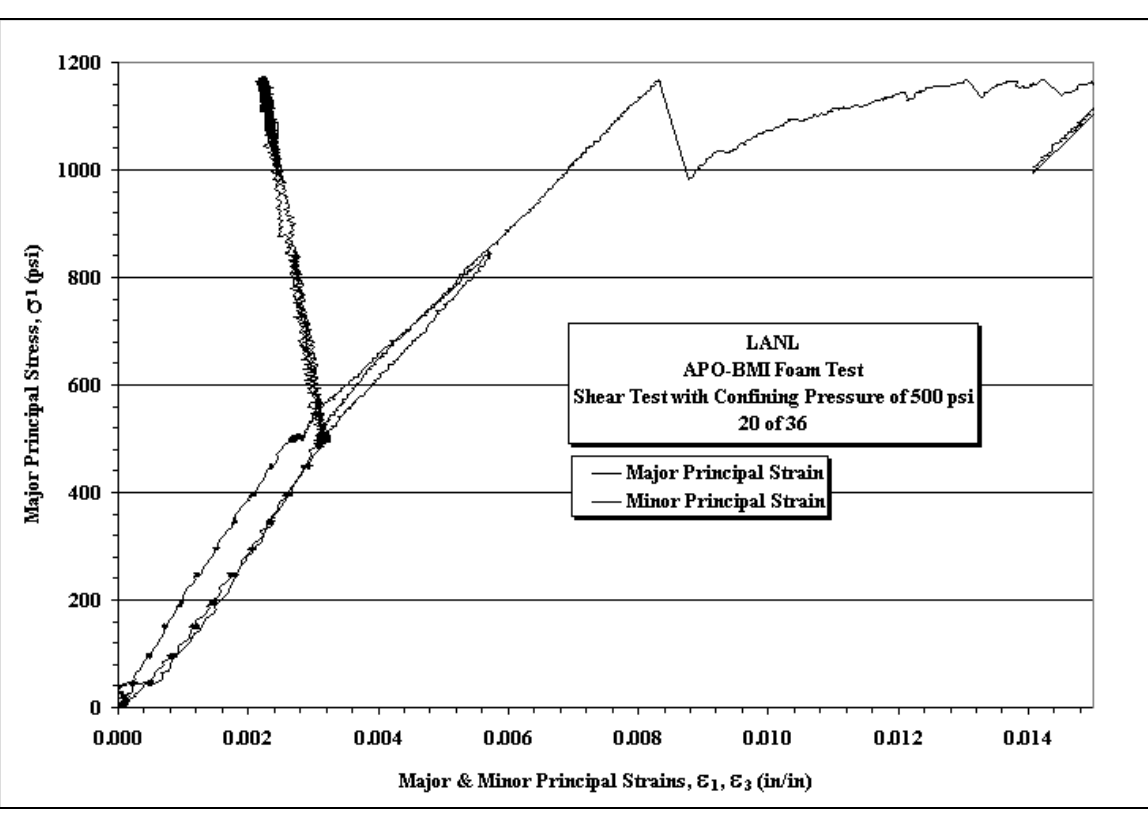
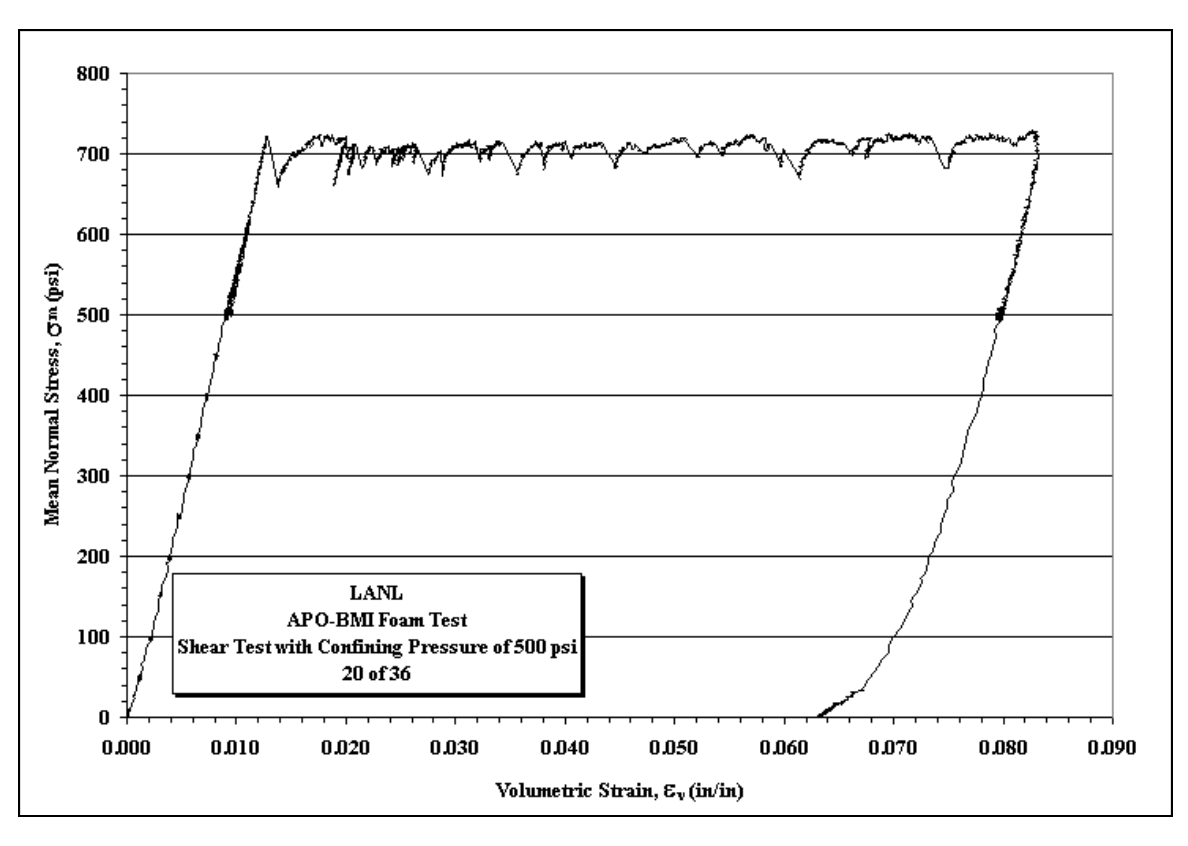


Figure A62. Stress vs. Strain plots for Sample 20of36 with a constant confining pressure of 500 psi.



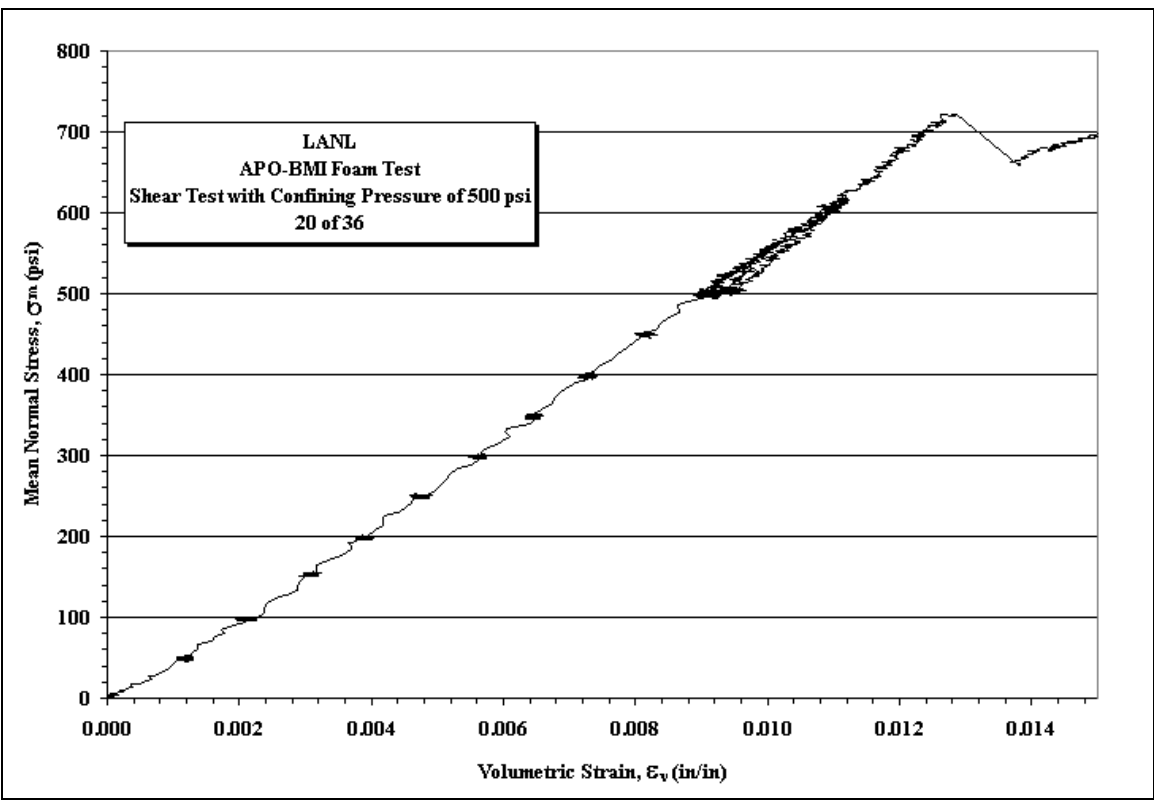
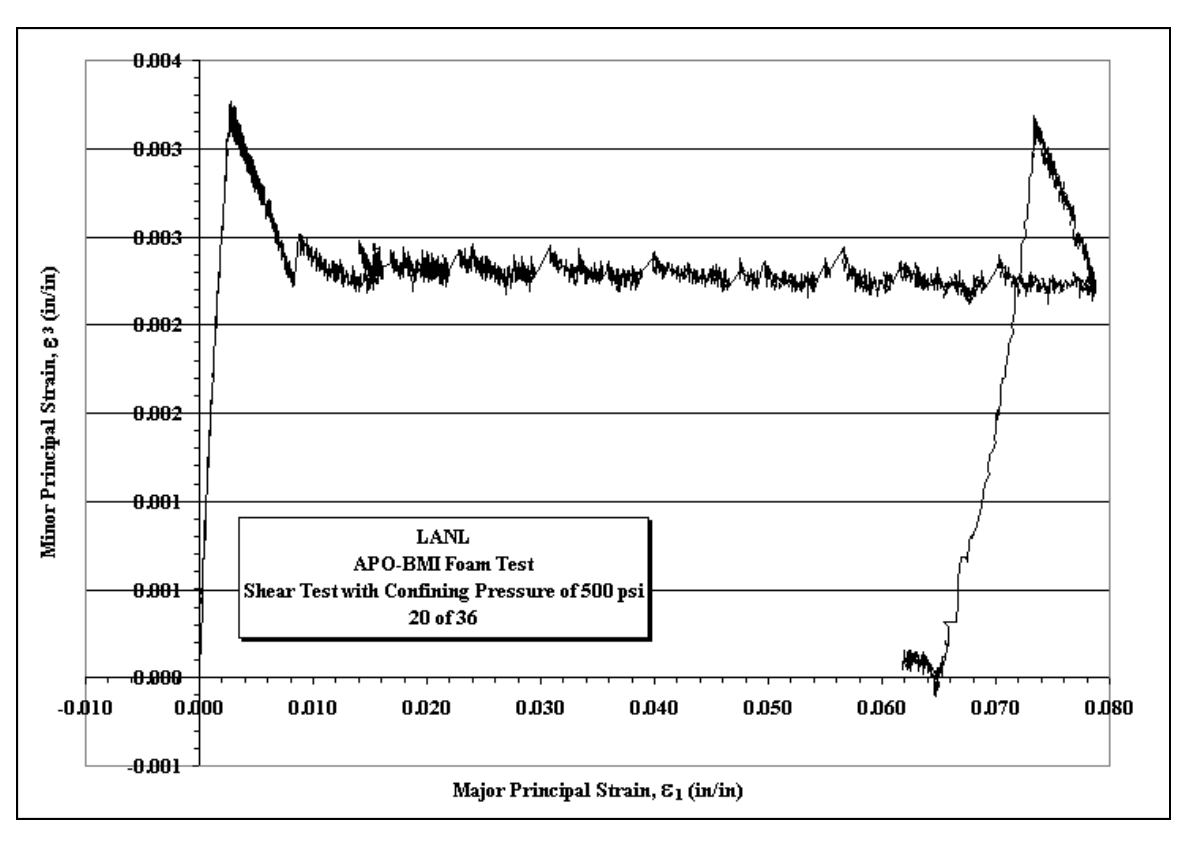


Figure A63. Mean Stress vs. Volumetric Strain plots for Sample 20of36 with a constant confining pressure of 500 psi.



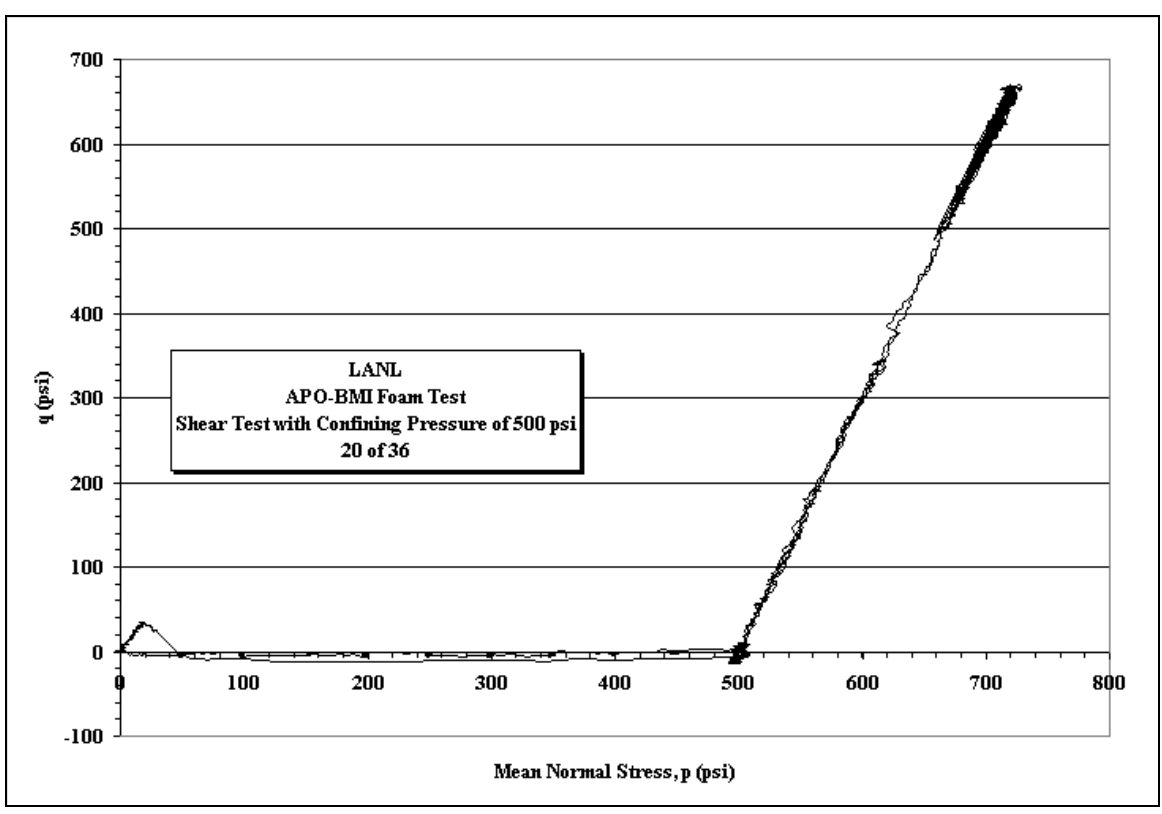
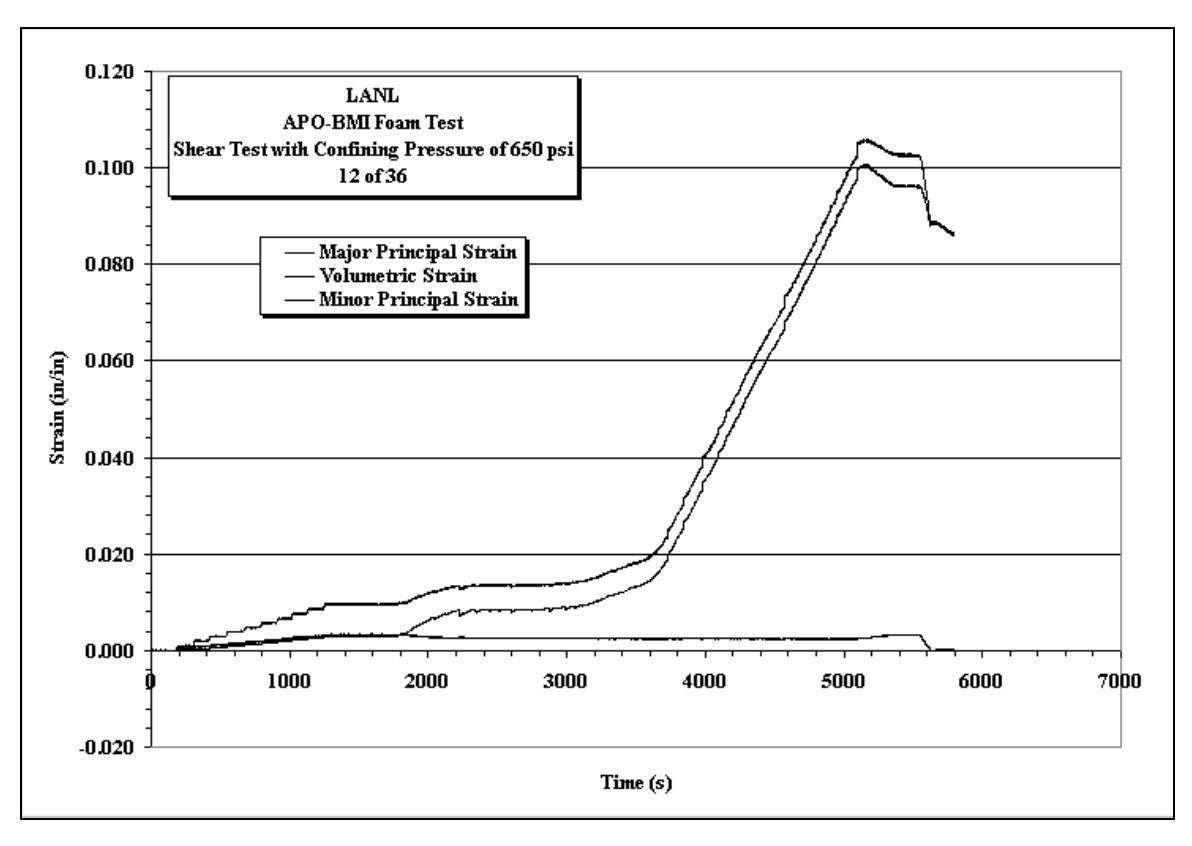


Figure A64. Minor Principle Strain vs. Major Principle Strain and Deviatoric Stress vs. Mean Stress plots for Sample 20of36 with a constant confining pressure of 500 psi.



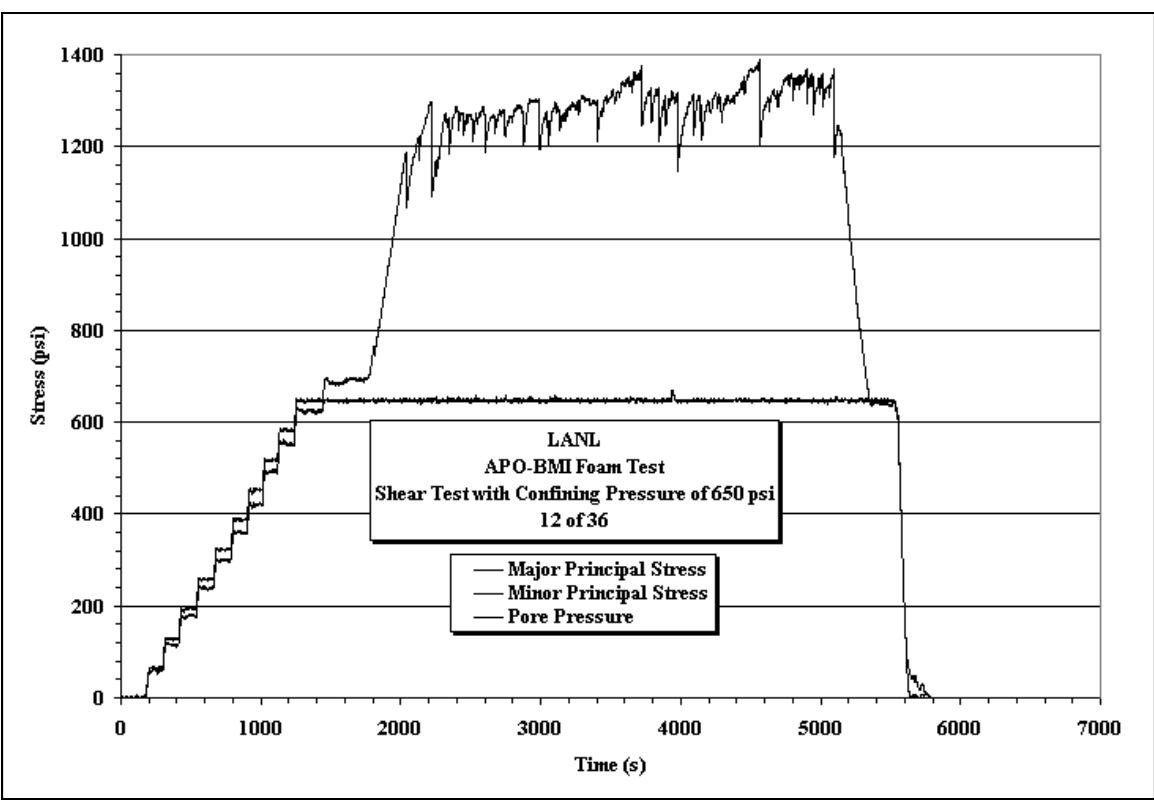
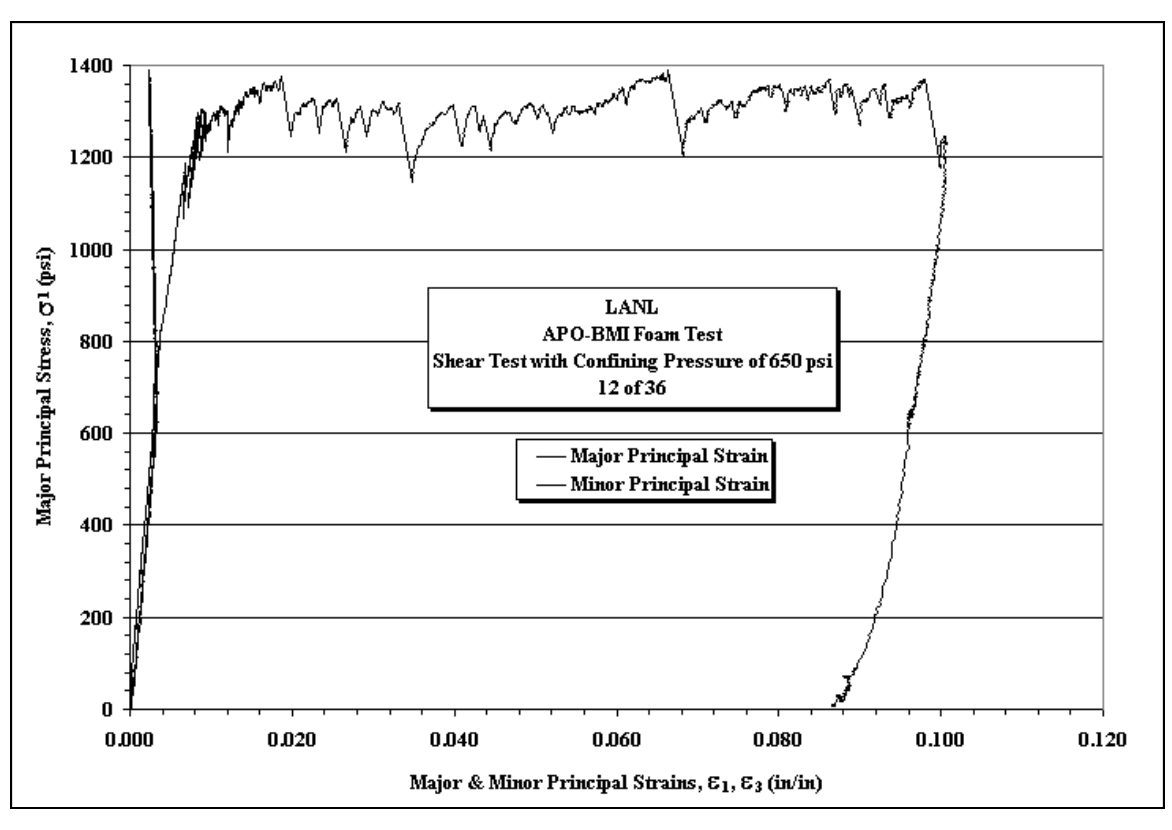


Figure A65. Minor Principle Strain vs. Major Principle Strain and Deviatoric Stress vs. Mean Stress plots for Sample 12of36 with a constant confining pressure of 650 psi.



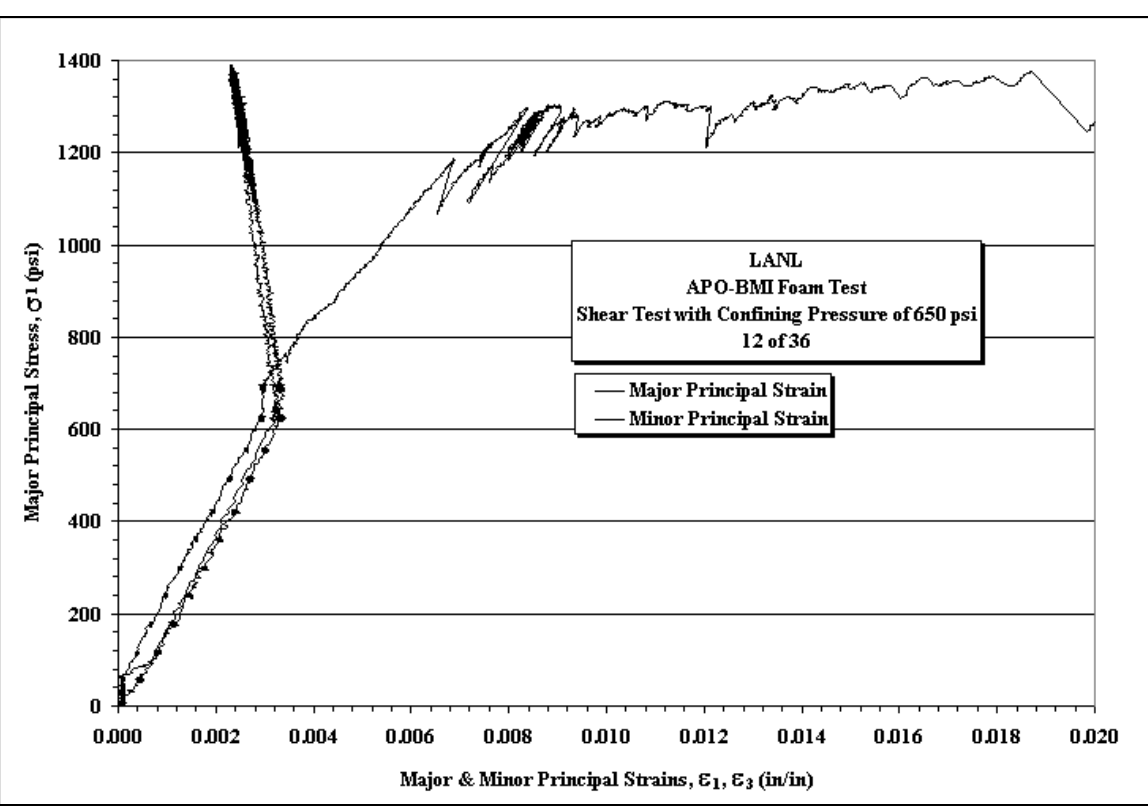
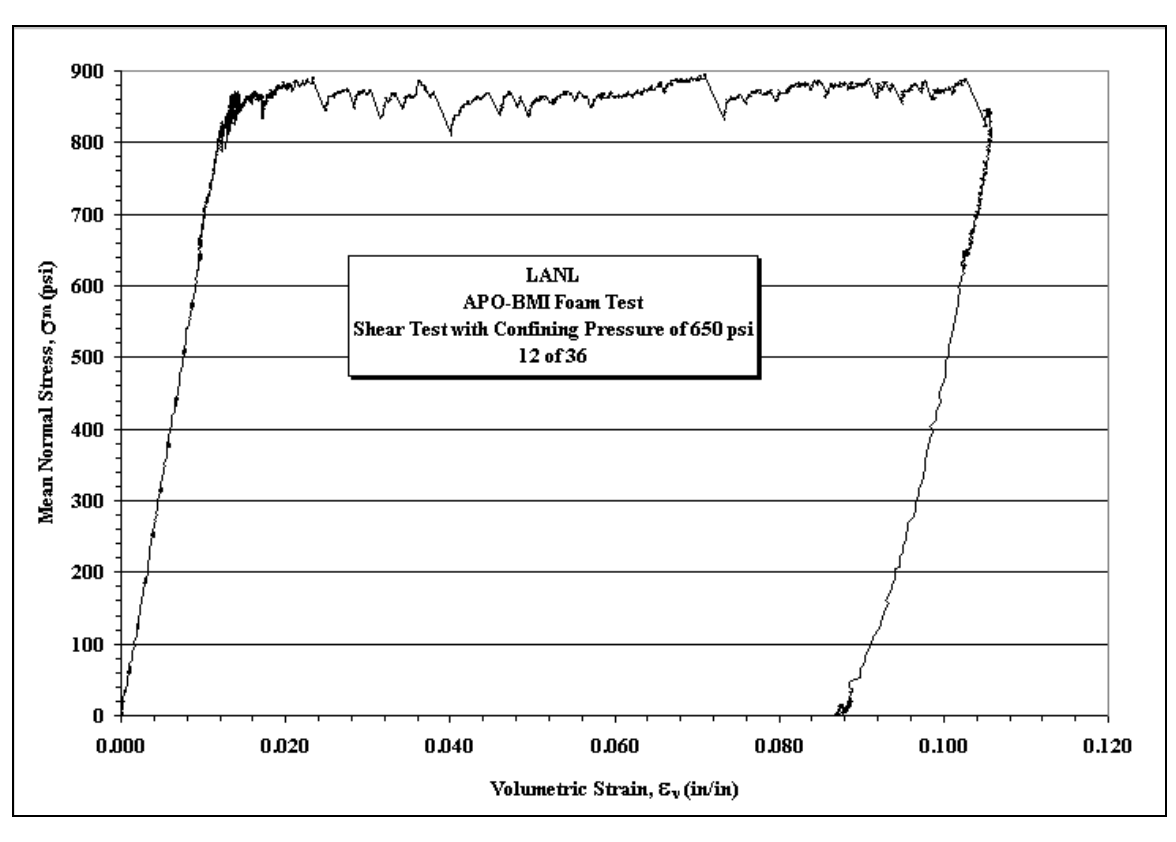


Figure A66. Stress vs. Strain plots for Sample 12of36 with a constant confining pressure of 650 psi.



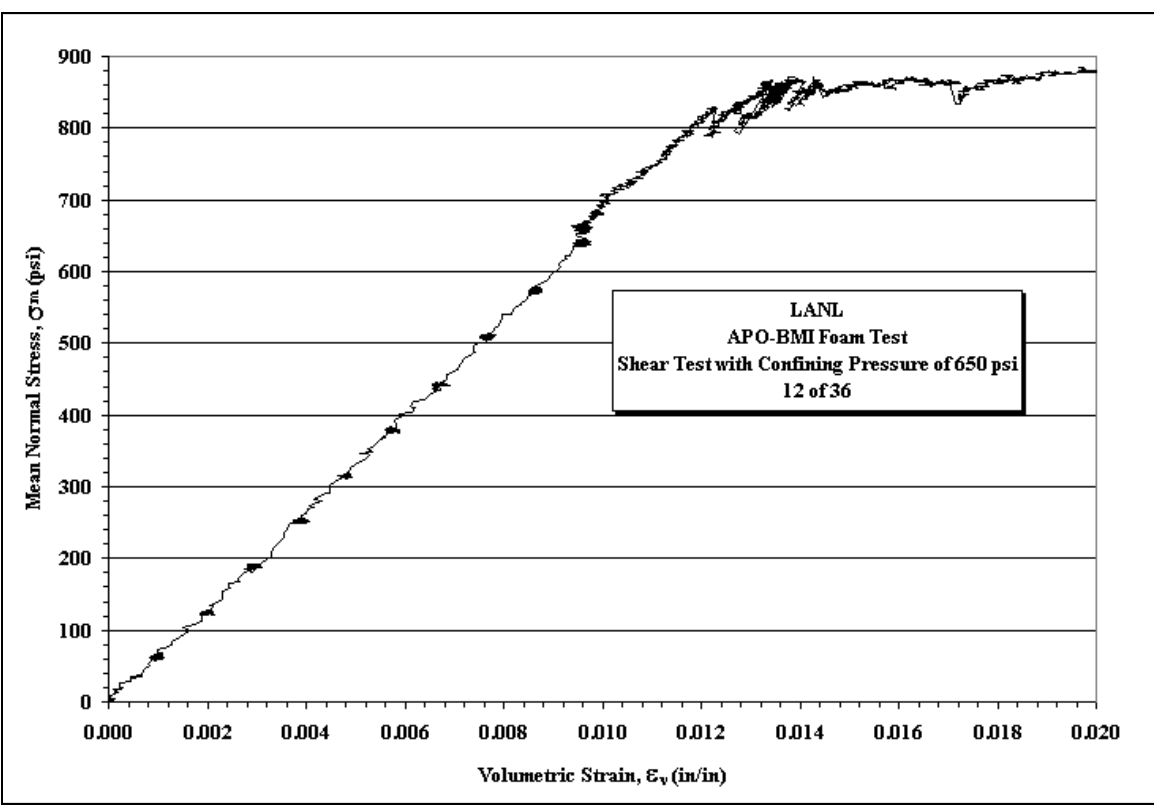
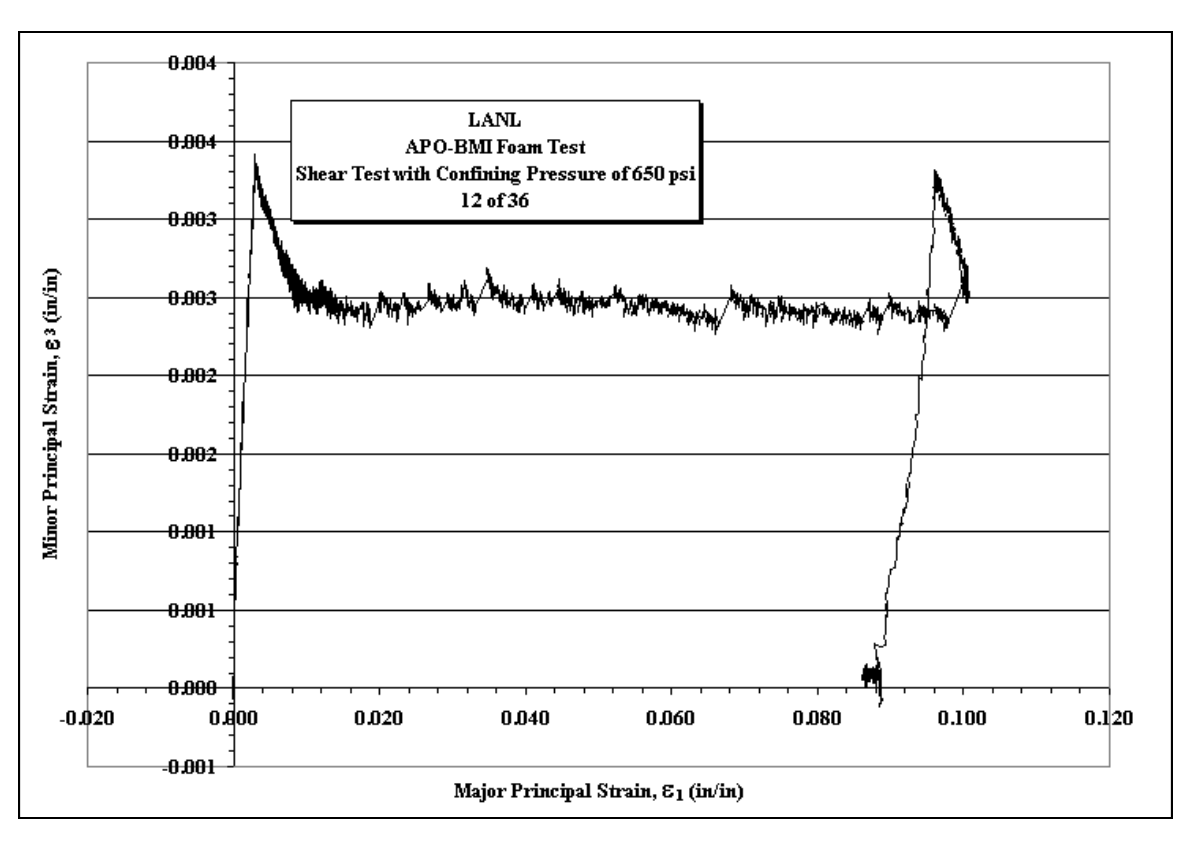


Figure A67. Mean Stress vs. Volumetric Strain plots for Sample 12of36 with a constant confining pressure of 650 psi.



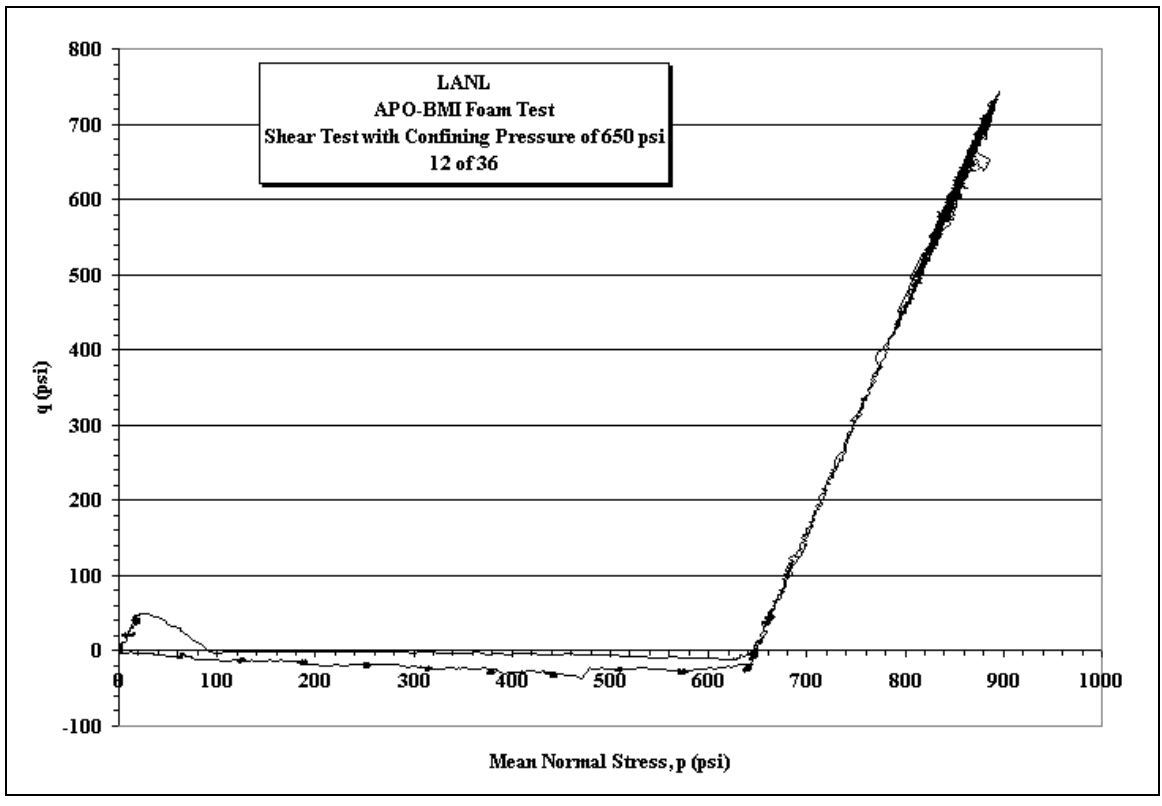
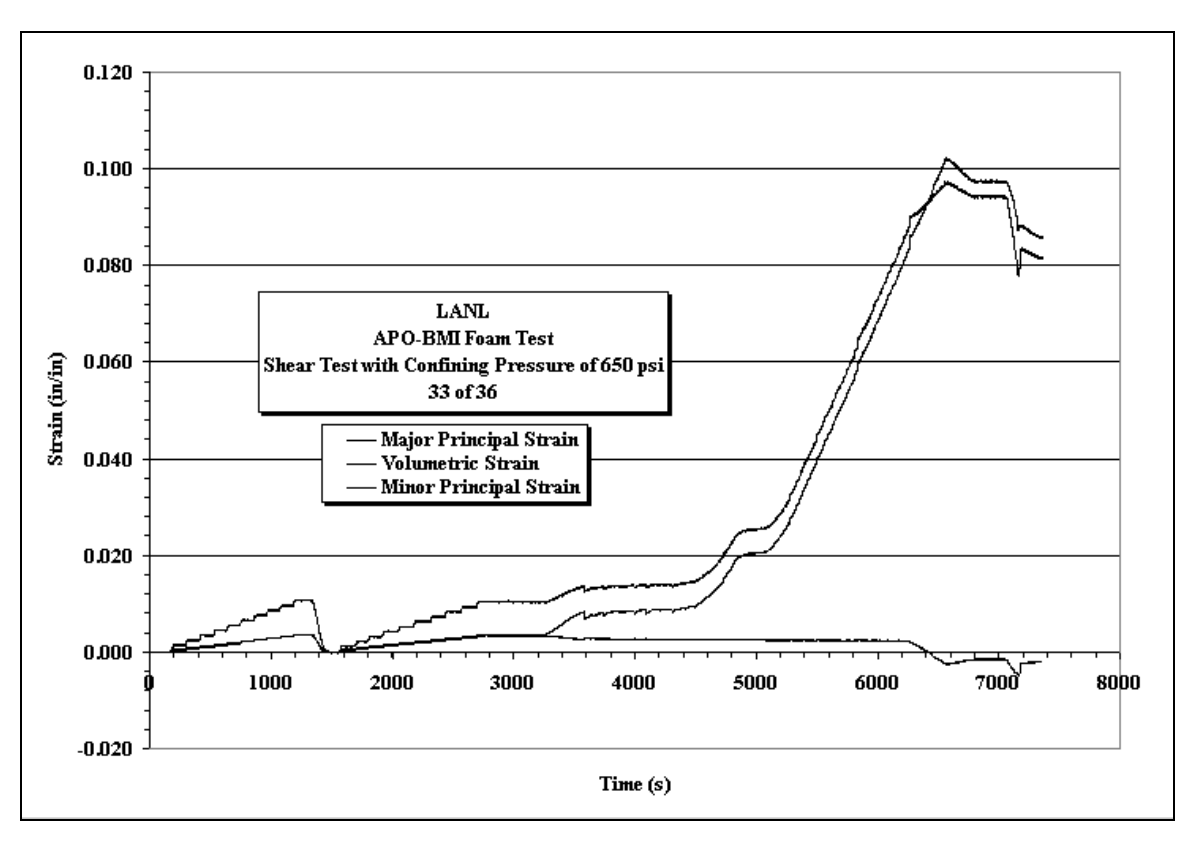


Figure A68. Minor Principle Strain vs. Major Principle Strain and Deviatoric Stress vs. Mean Stress plots for Sample 12of36 with a constant confining pressure of 650 psi.



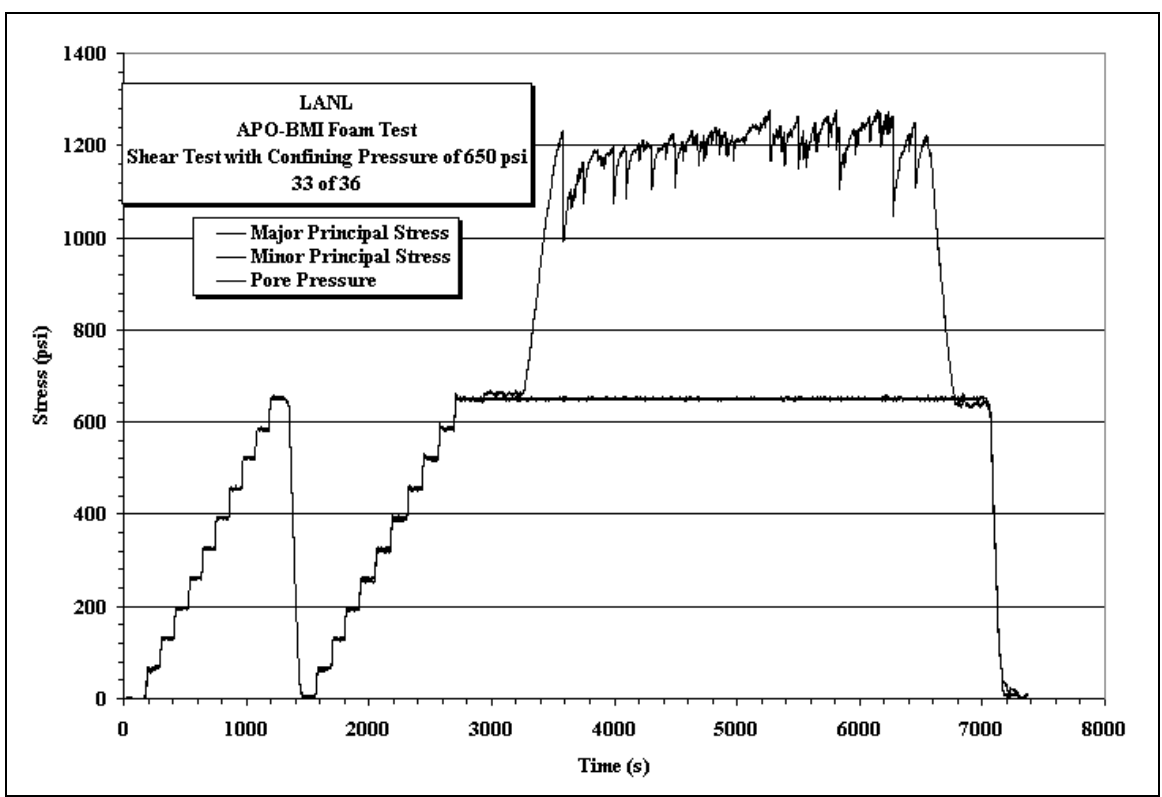
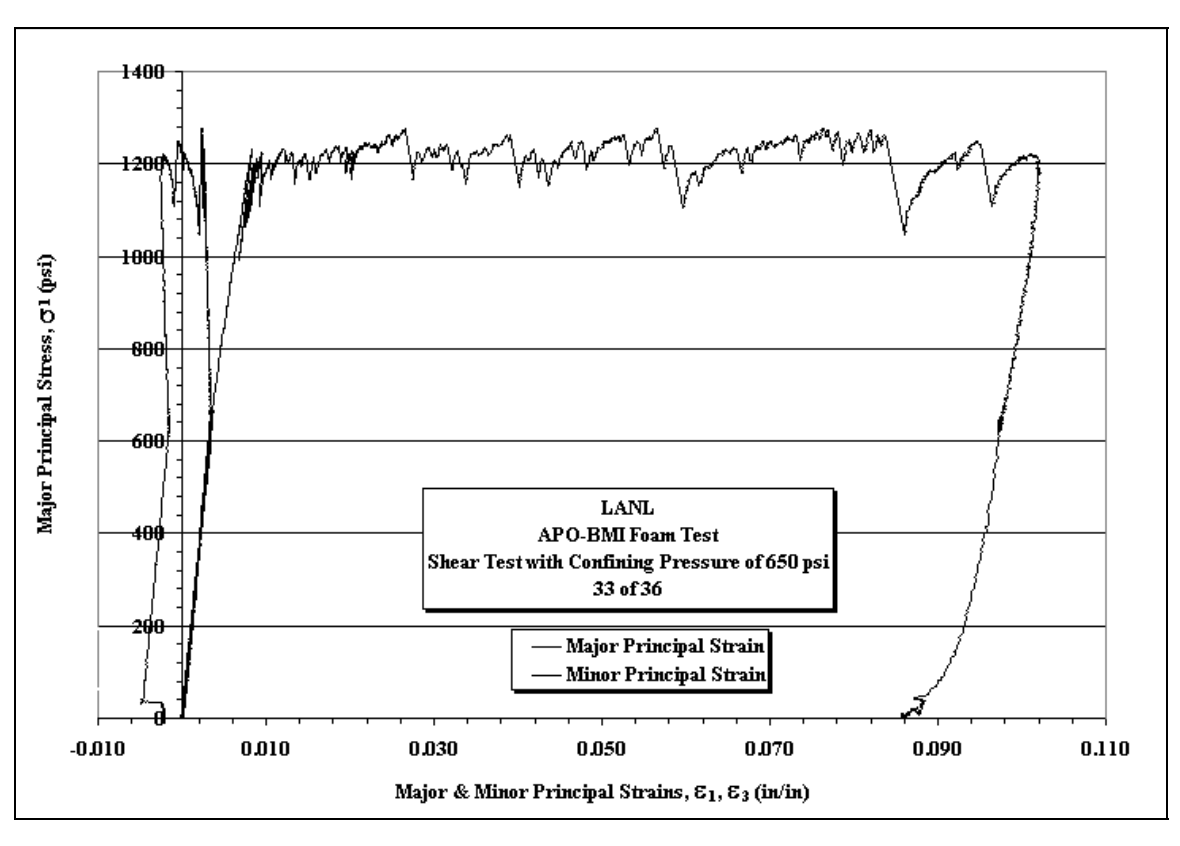


Figure A69. Minor Principle Strain vs. Major Principle Strain and Deviatoric Stress vs. Mean Stress plots for Sample 33of36 with a constant confining pressure of 650 psi.



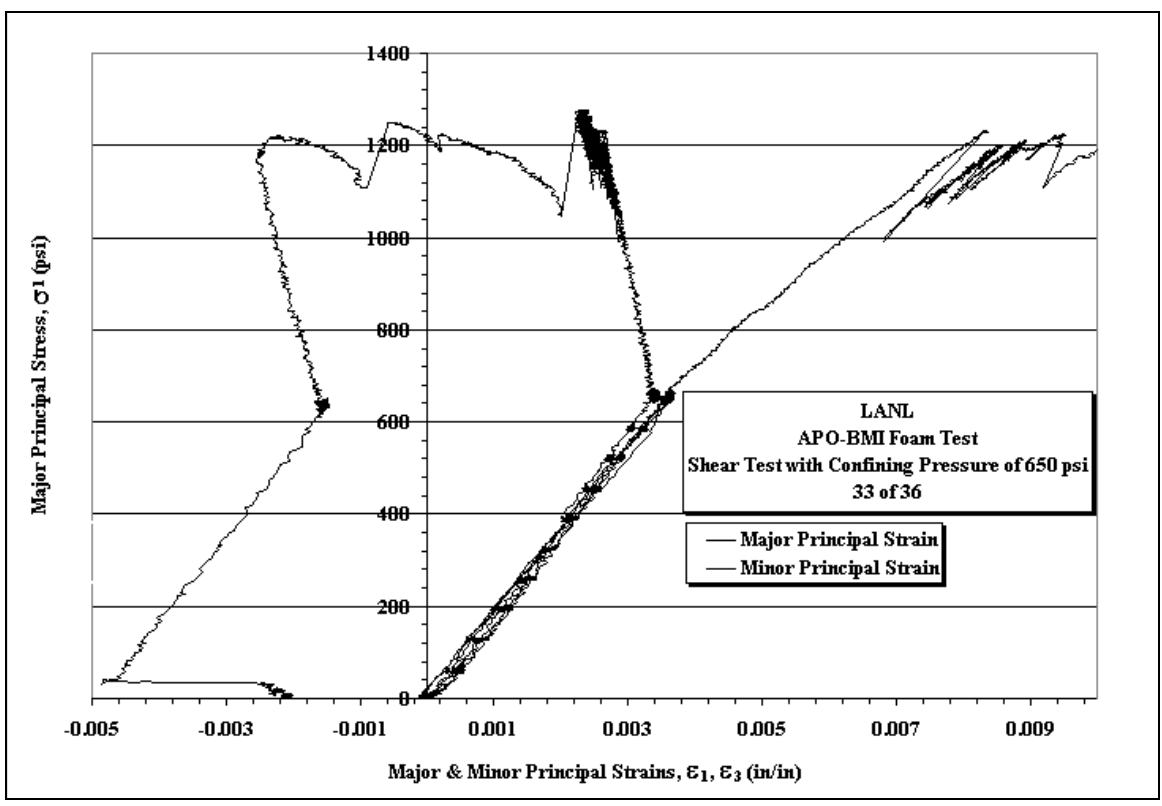
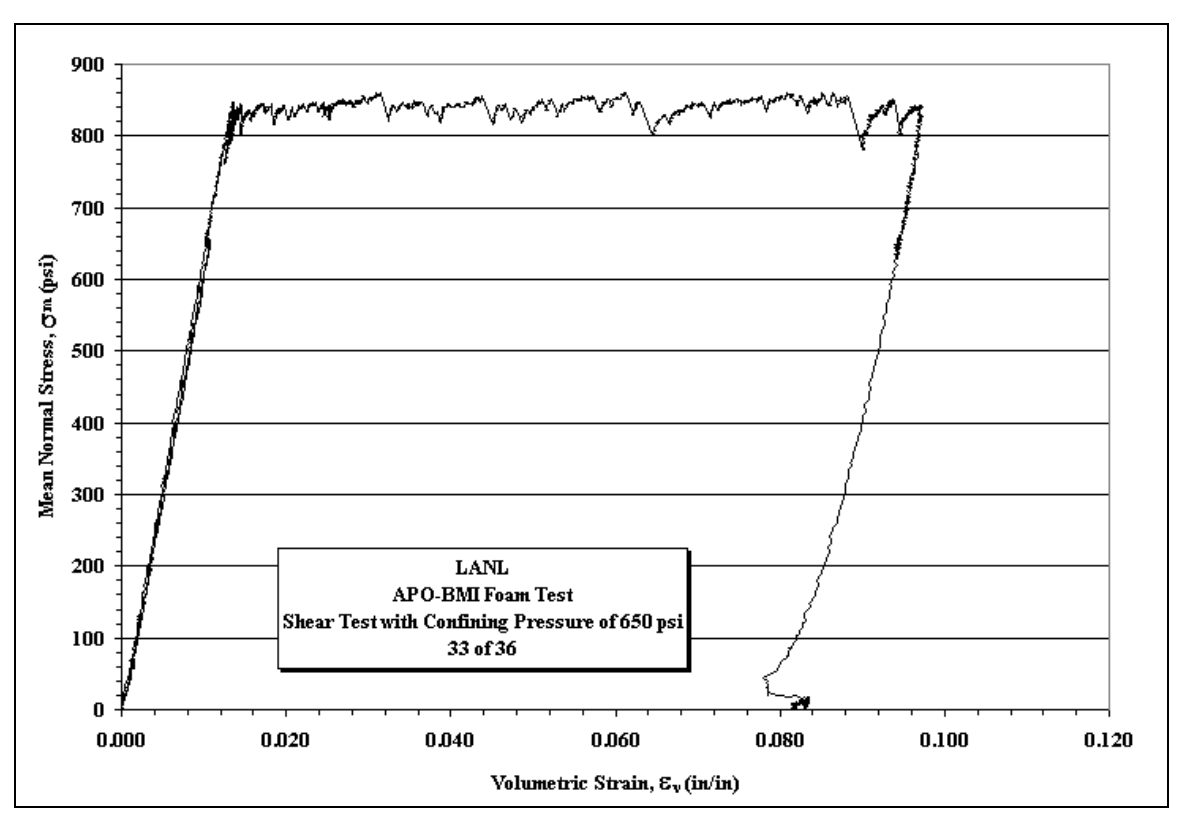


Figure A70. Stress vs. Strain plots for Sample 33of36 with a constant confining pressure of 650 psi.



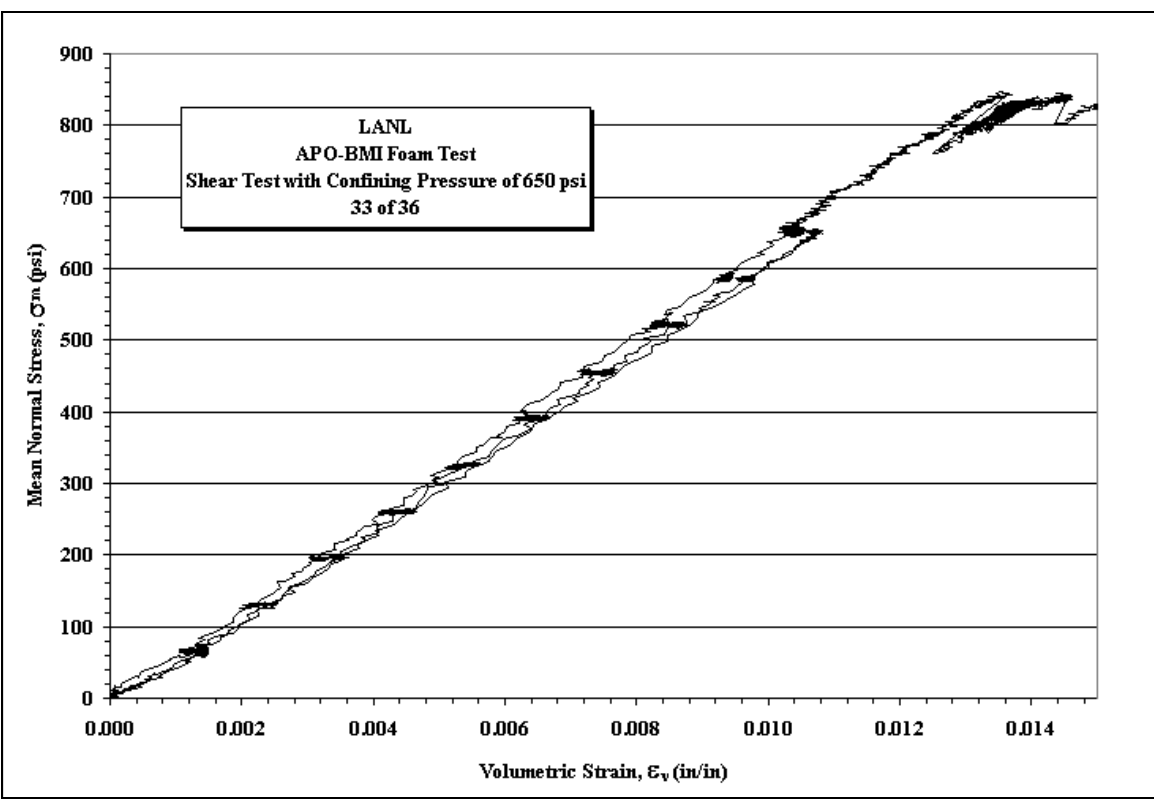
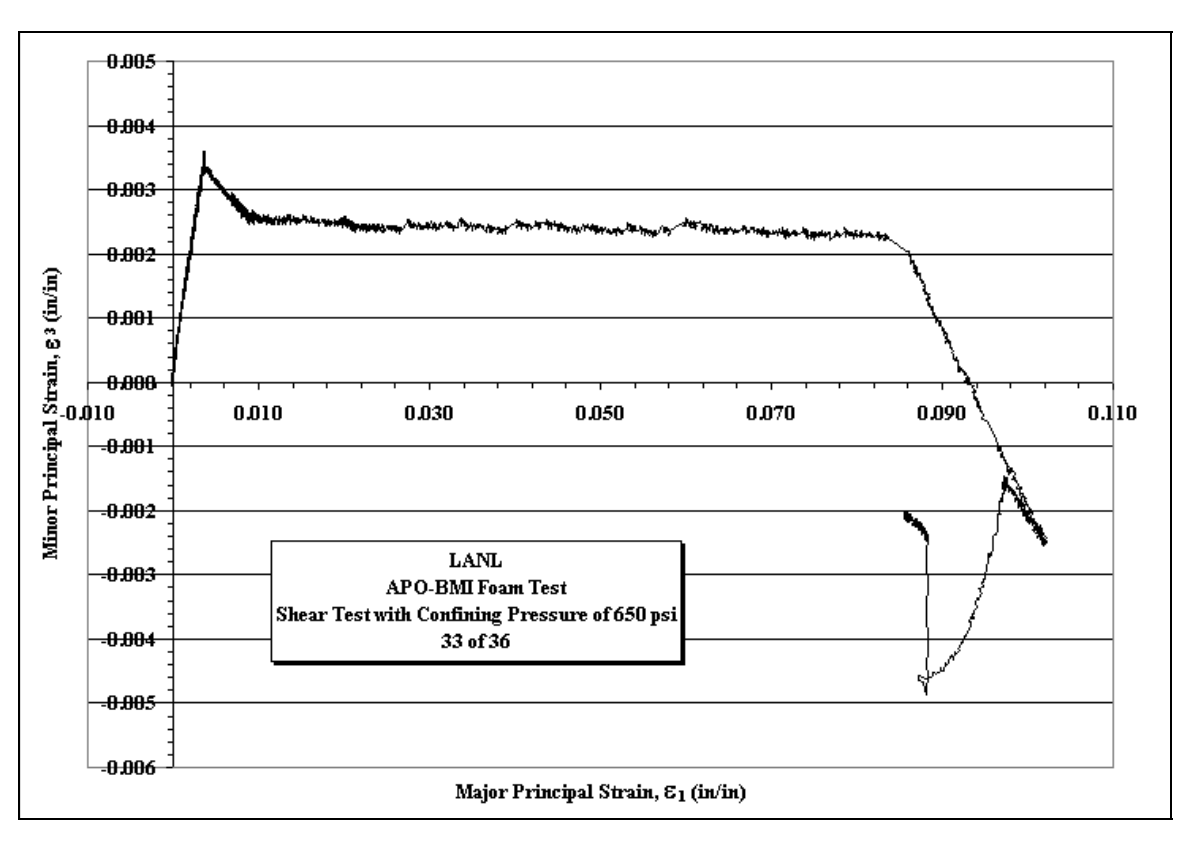


Figure A71. Mean Stress vs. Volumetric Strain plots for Sample 33of36 with a constant confining pressure of 650 psi.



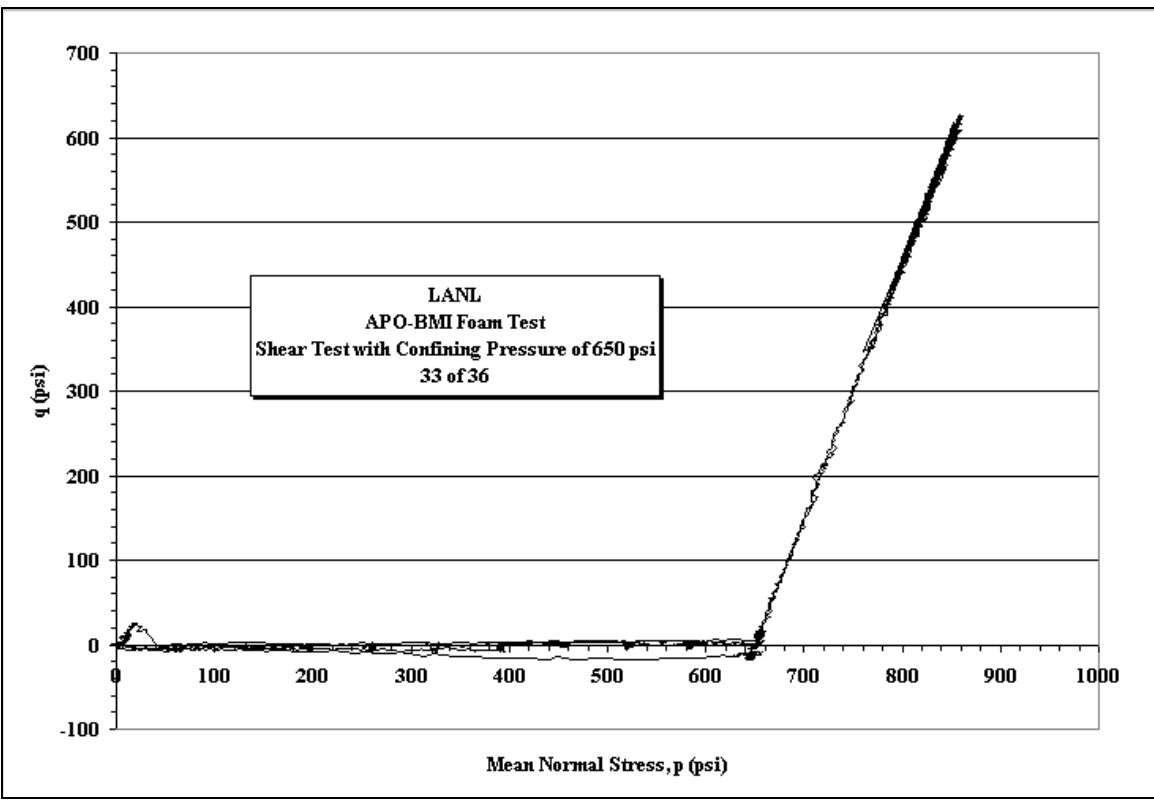
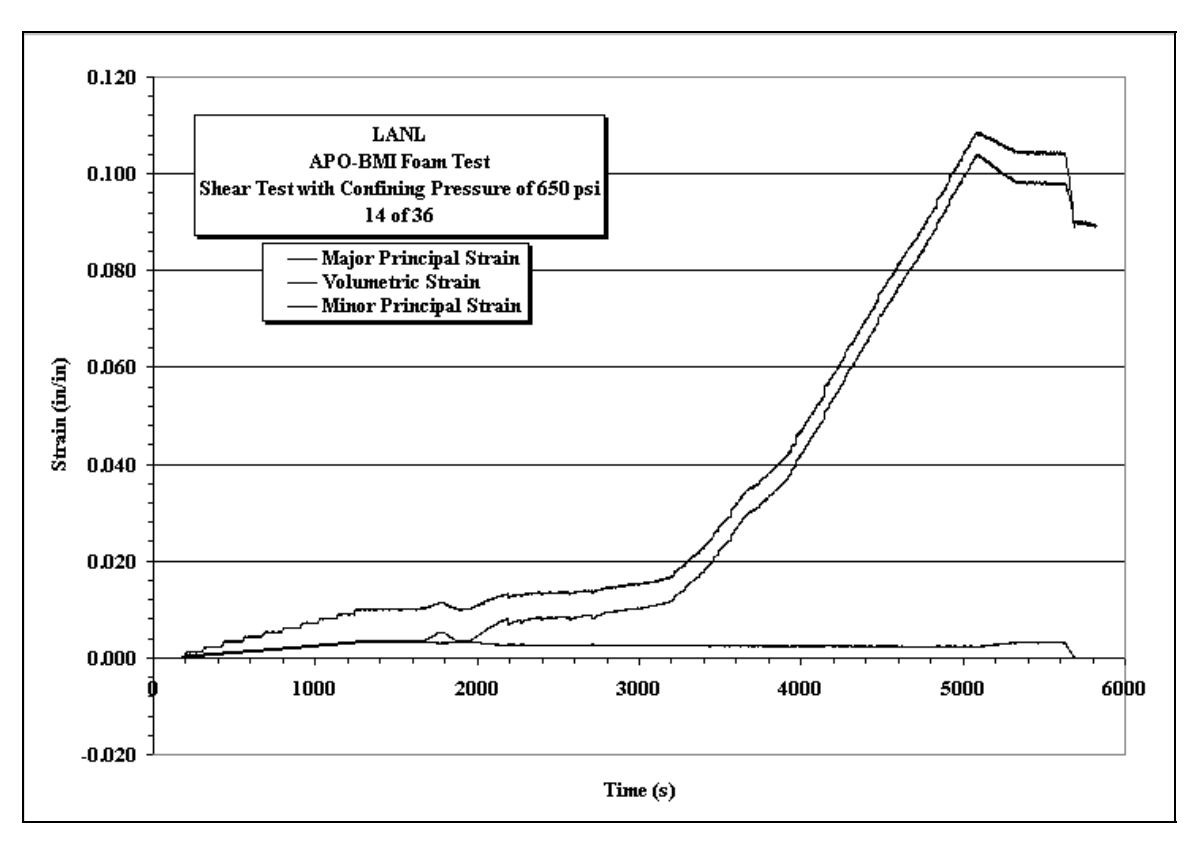


Figure A72. Minor Principle Strain vs. Major Principle Strain and Deviatoric Stress vs. Mean Stress plots for Sample 33of36 with a constant confining pressure of 650 psi.



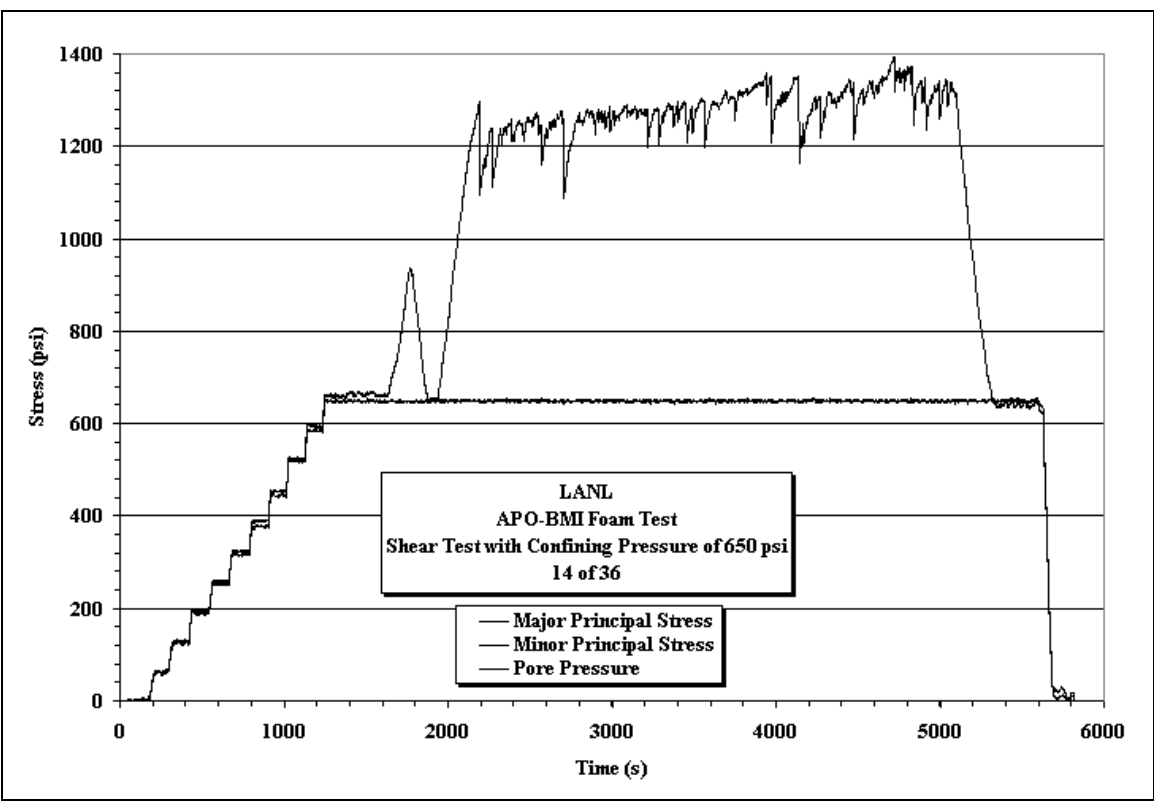
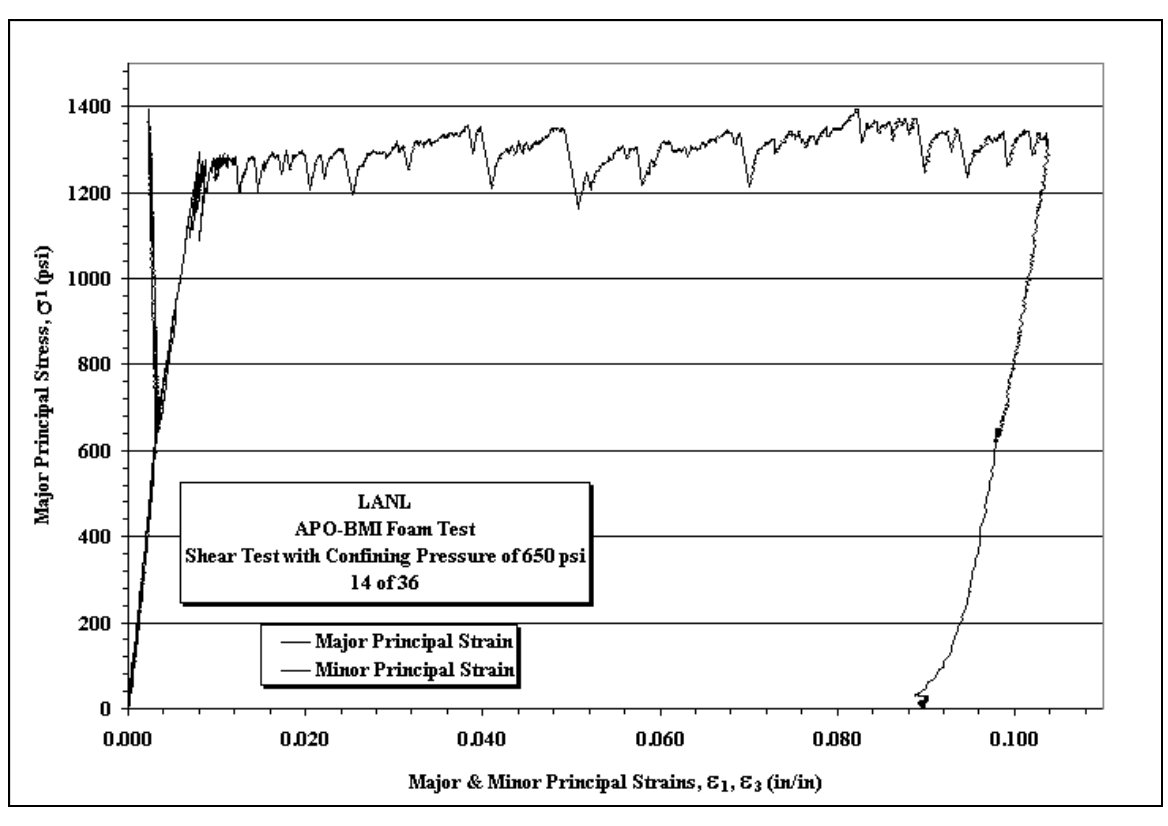


Figure A73. Minor Principle Strain vs. Major Principle Strain and Deviatoric Stress vs. Mean Stress plots for Sample 14of36 with a constant confining pressure of 650 psi.



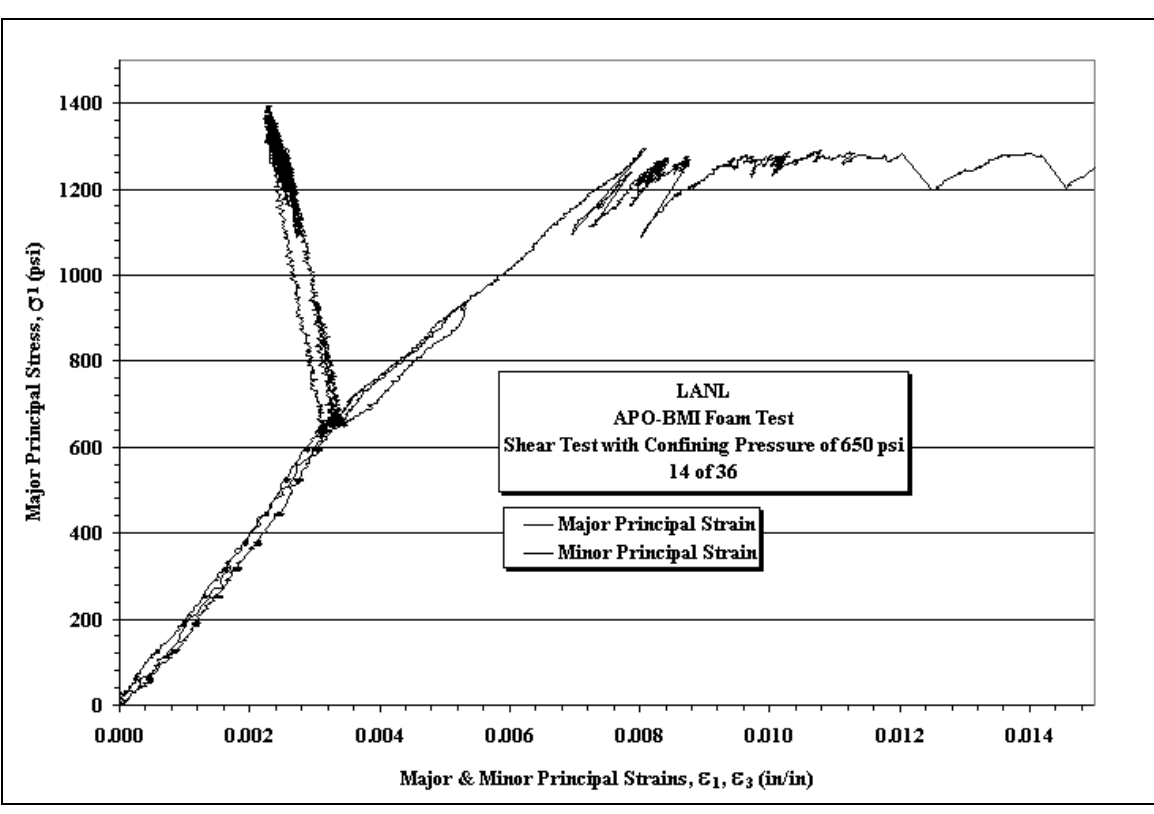
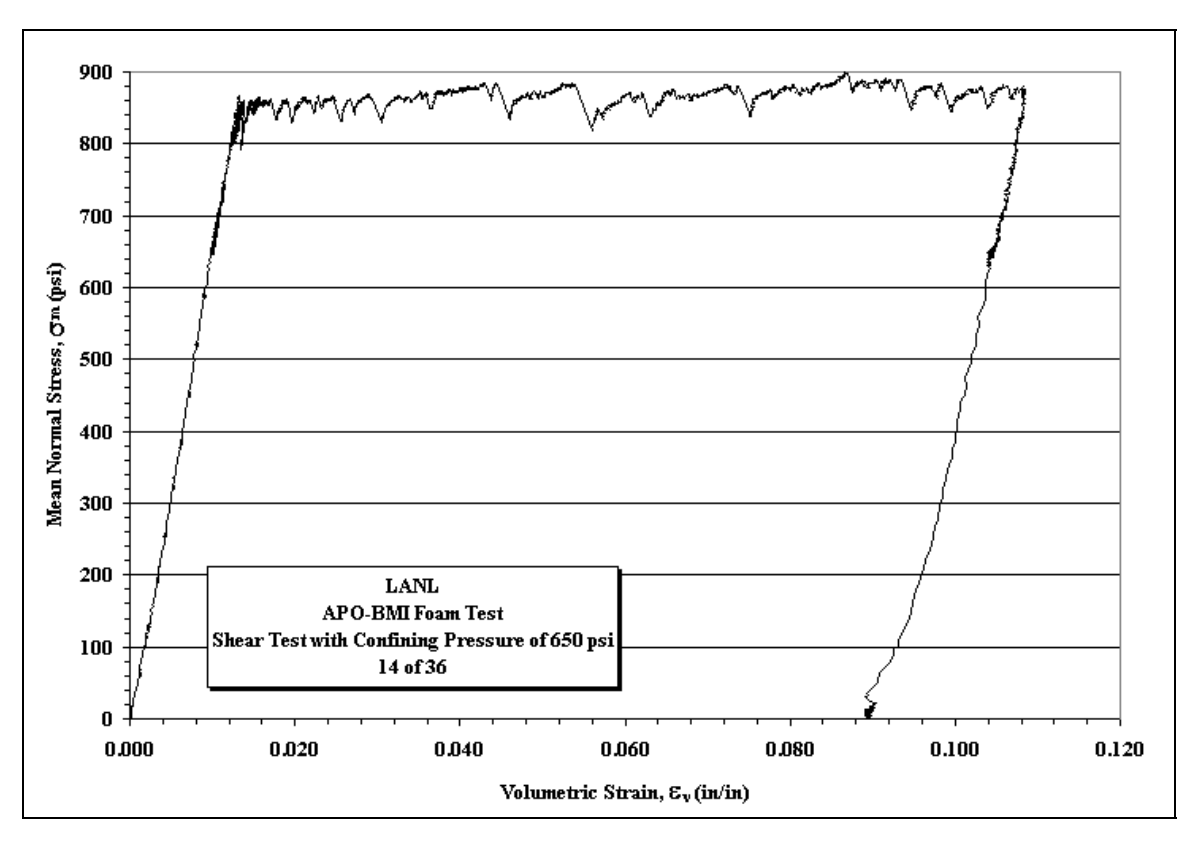


Figure A74. Stress vs. Strain plots for Sample 14of36 with a constant confining pressure of 650 psi.



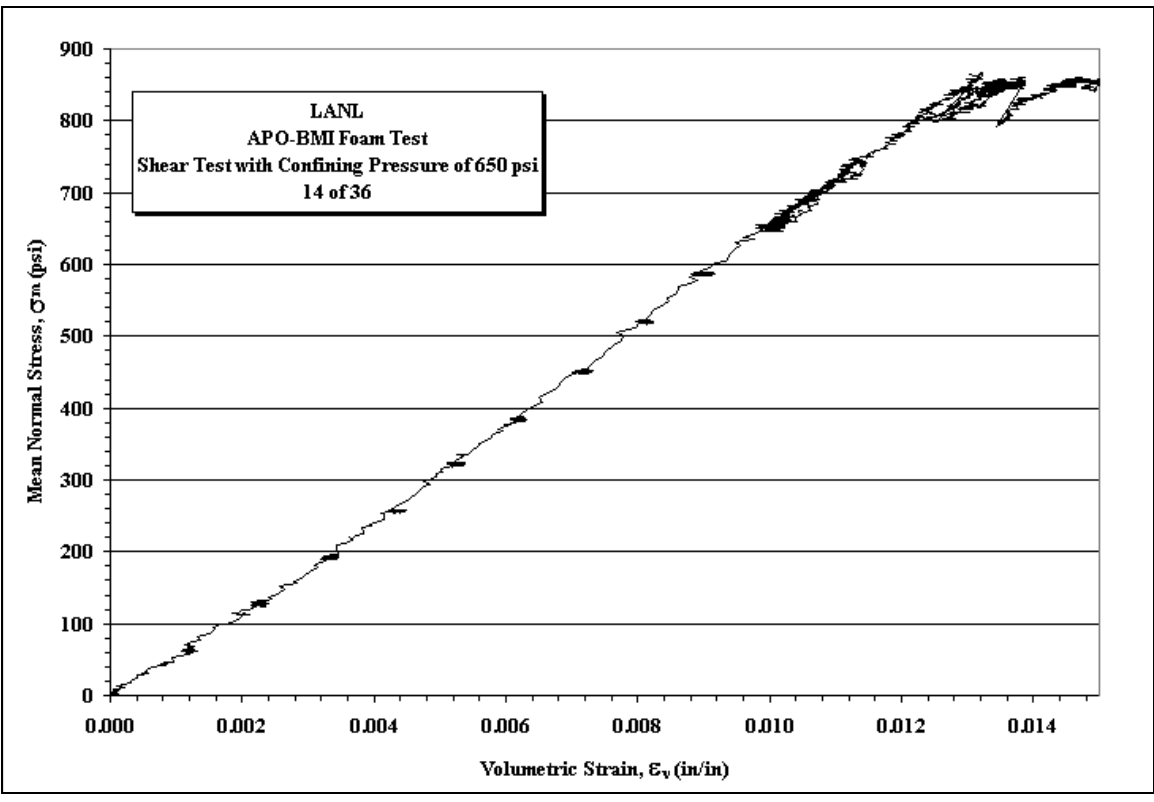
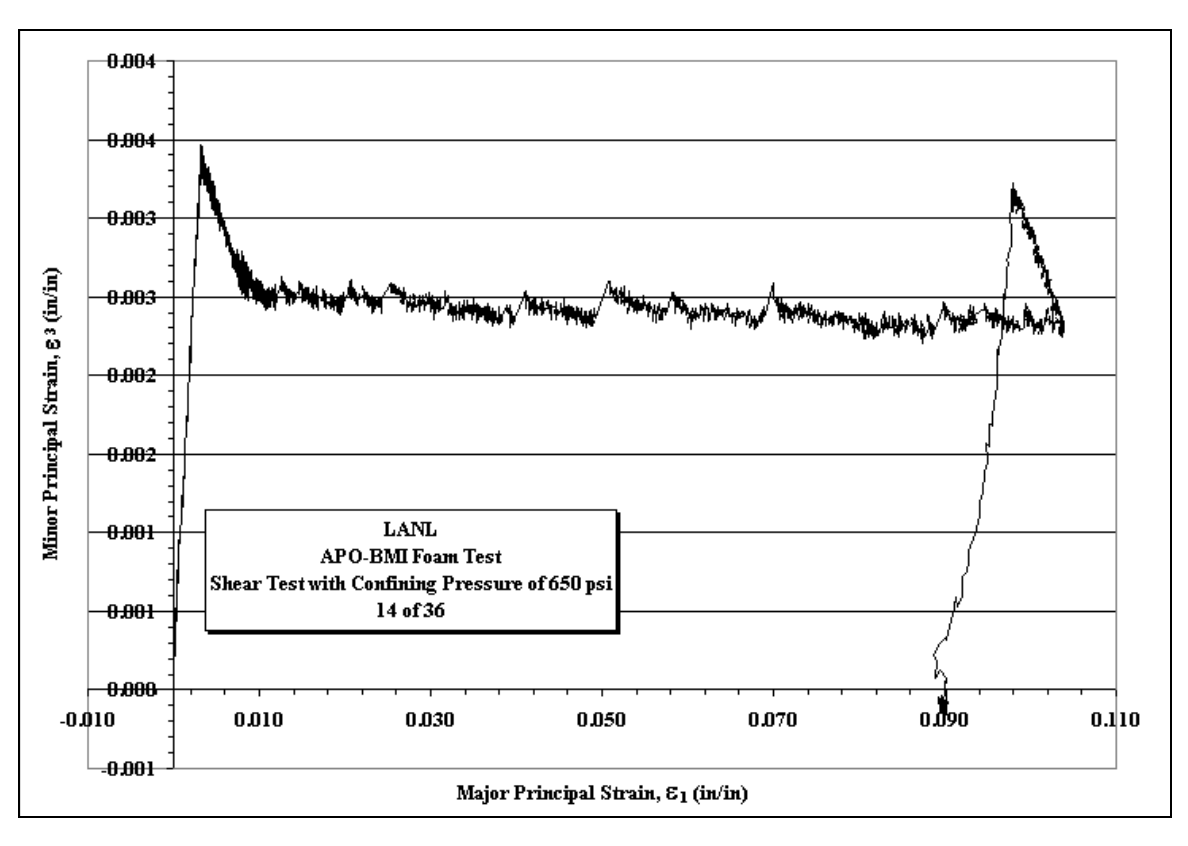


Figure A75. Mean Stress vs. Volumetric Strain plots for Sample 14of36 with a constant confining pressure of 650 psi.



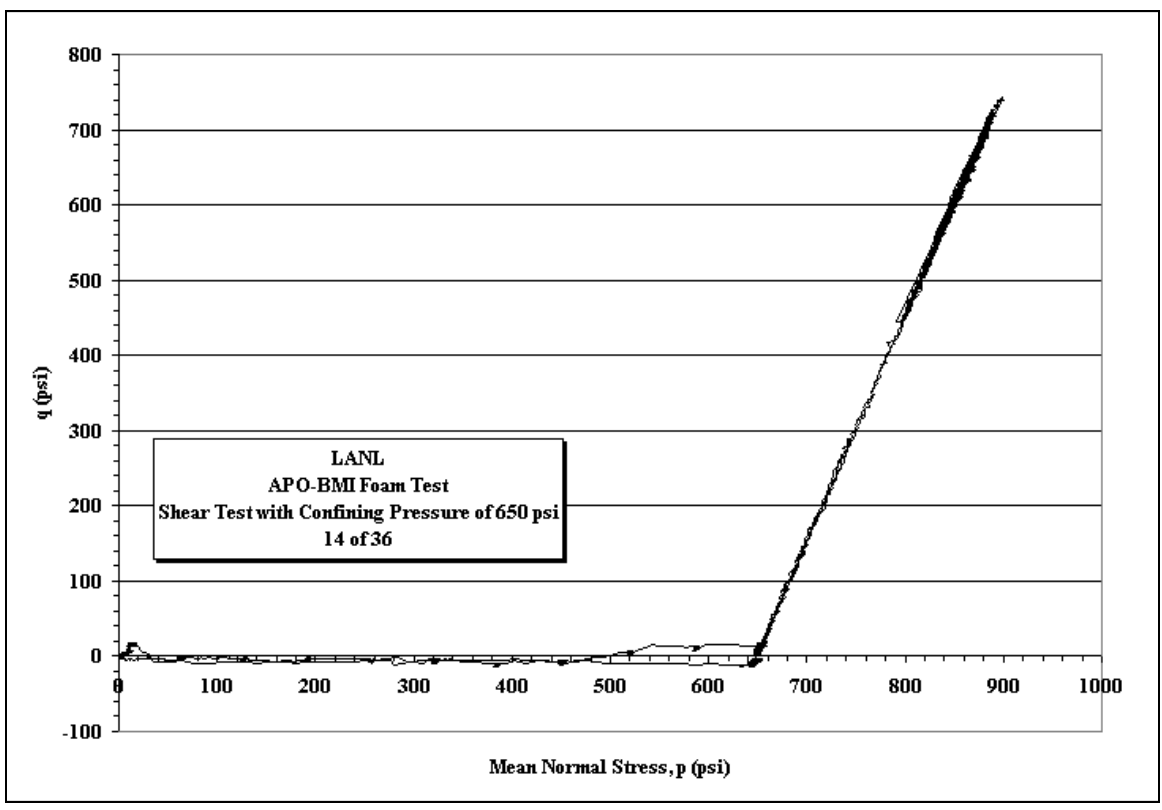
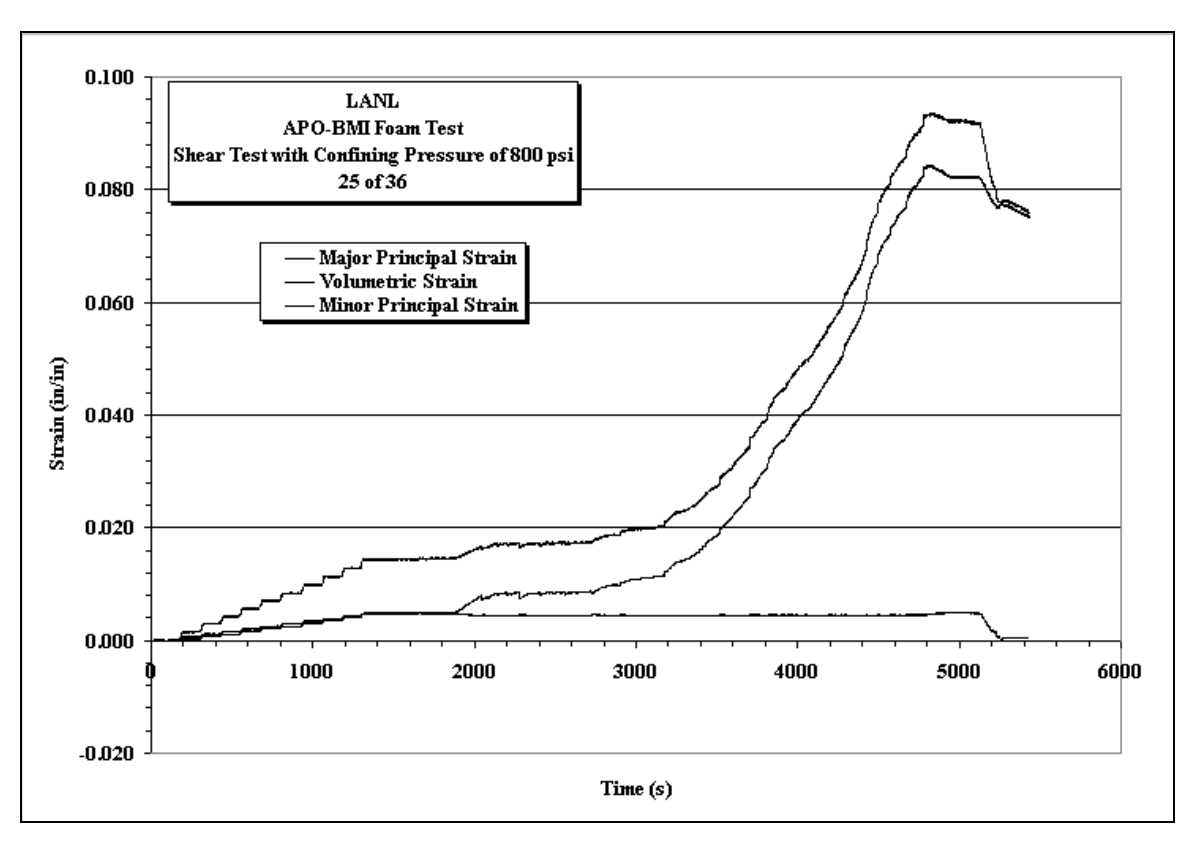


Figure A76. Minor Principle Strain vs. Major Principle Strain and Deviatoric Stress vs. Mean Stress plots for Sample 14of36 with a constant confining pressure of 650 psi.



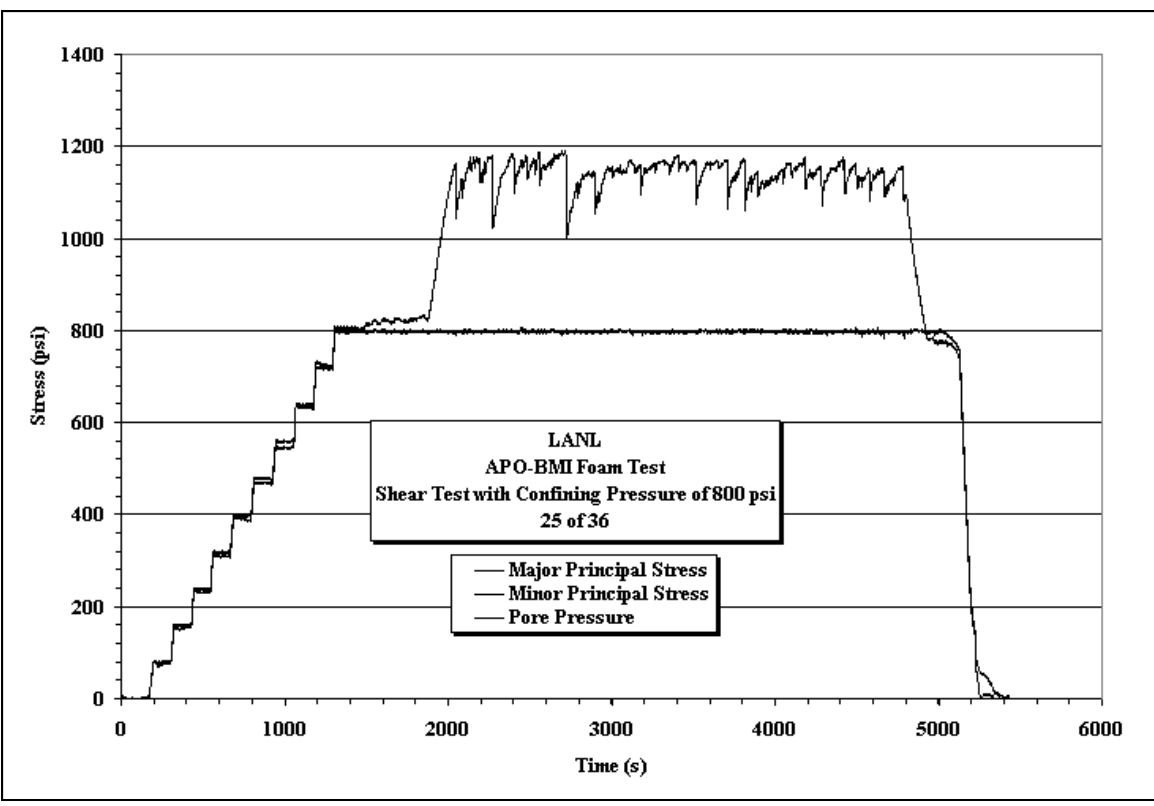
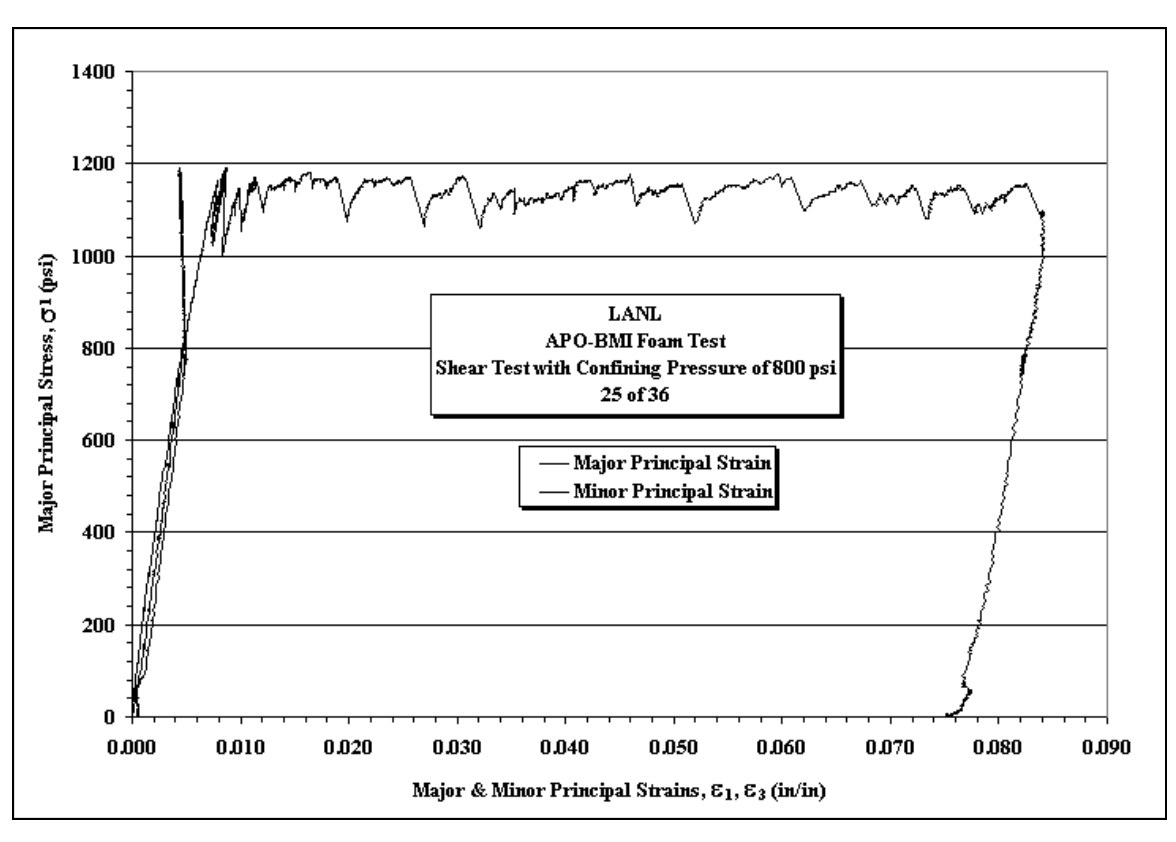


Figure A77. Minor Principle Strain vs. Major Principle Strain and Deviatoric Stress vs. Mean Stress plots for Sample 25of36 with a constant confining pressure of 800 psi.



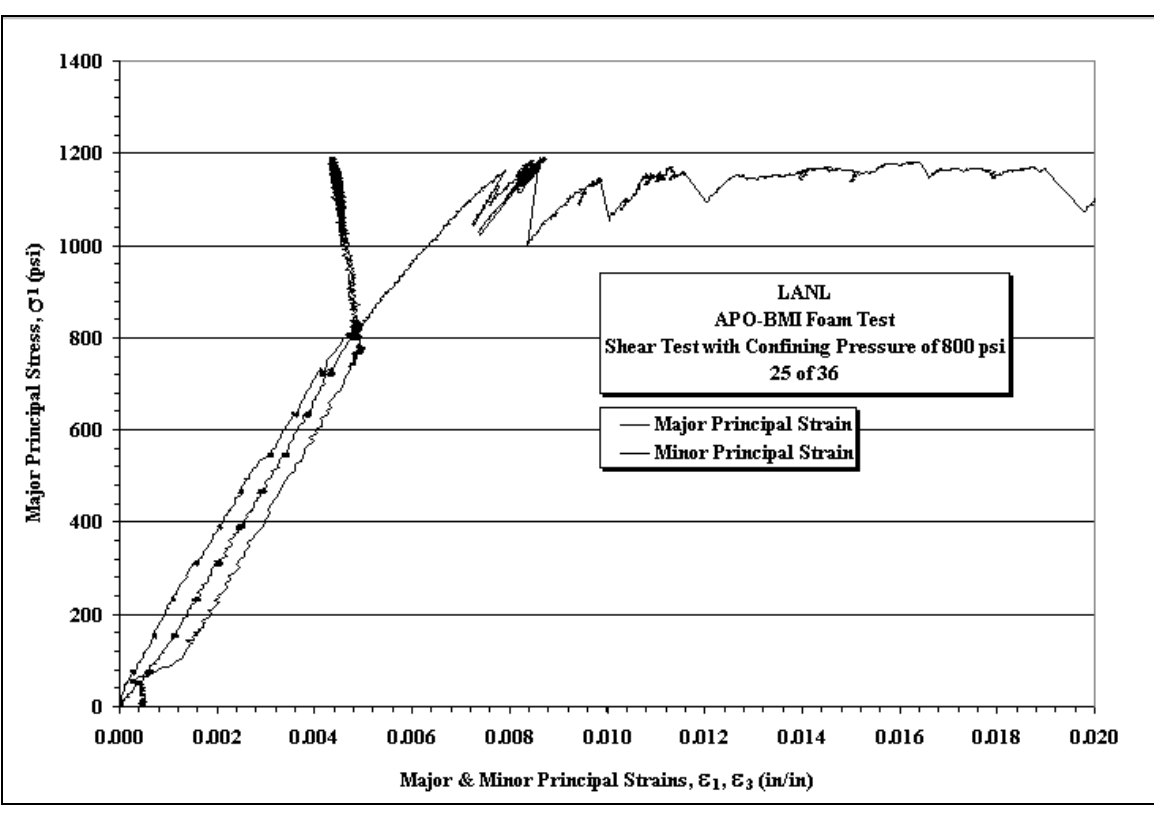
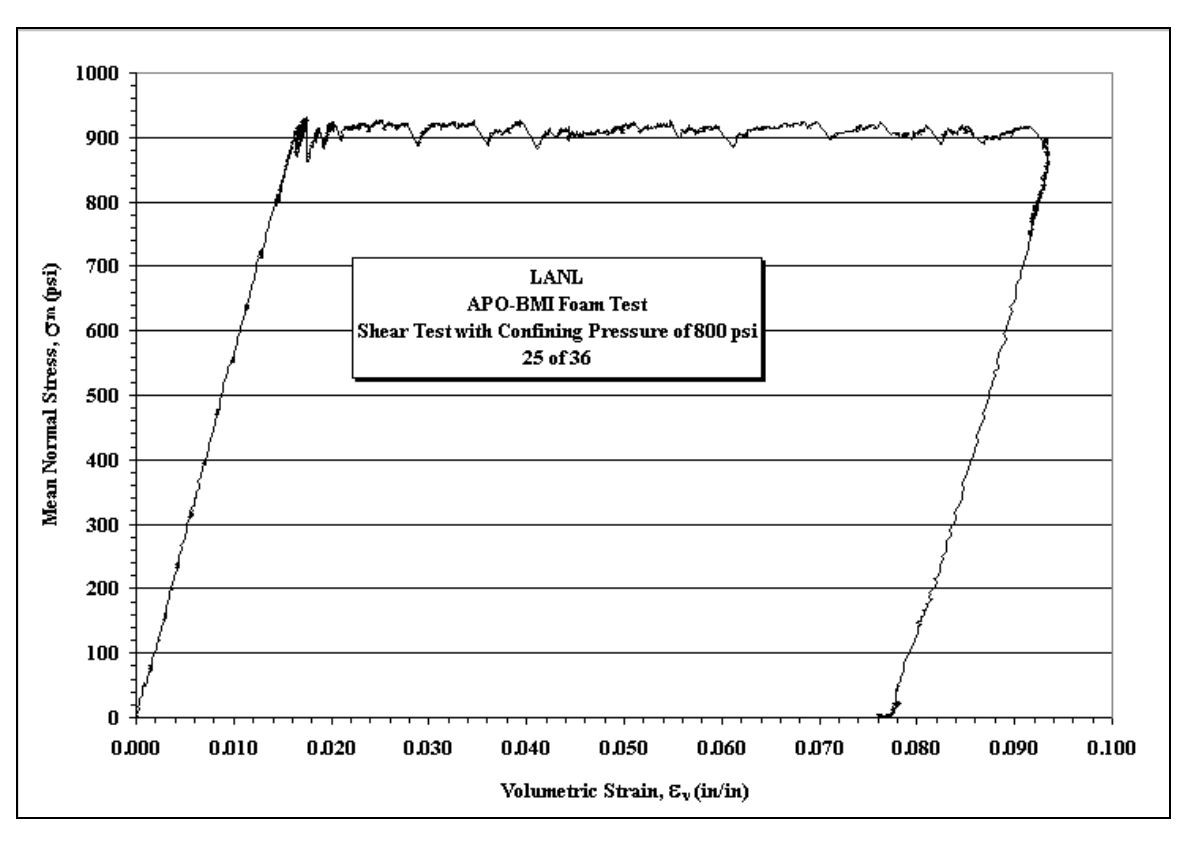


Figure A78. Stress vs. Strain plots for Sample 25of36 with a constant confining pressure of 800 psi.



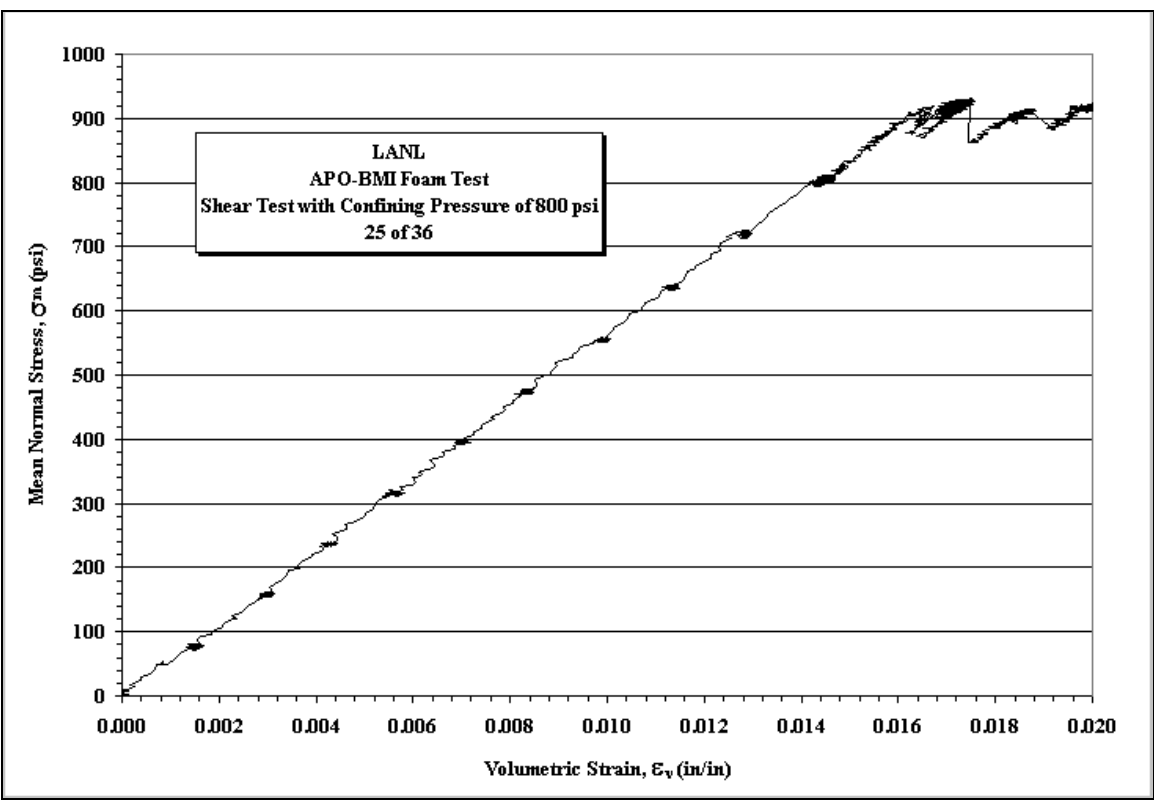
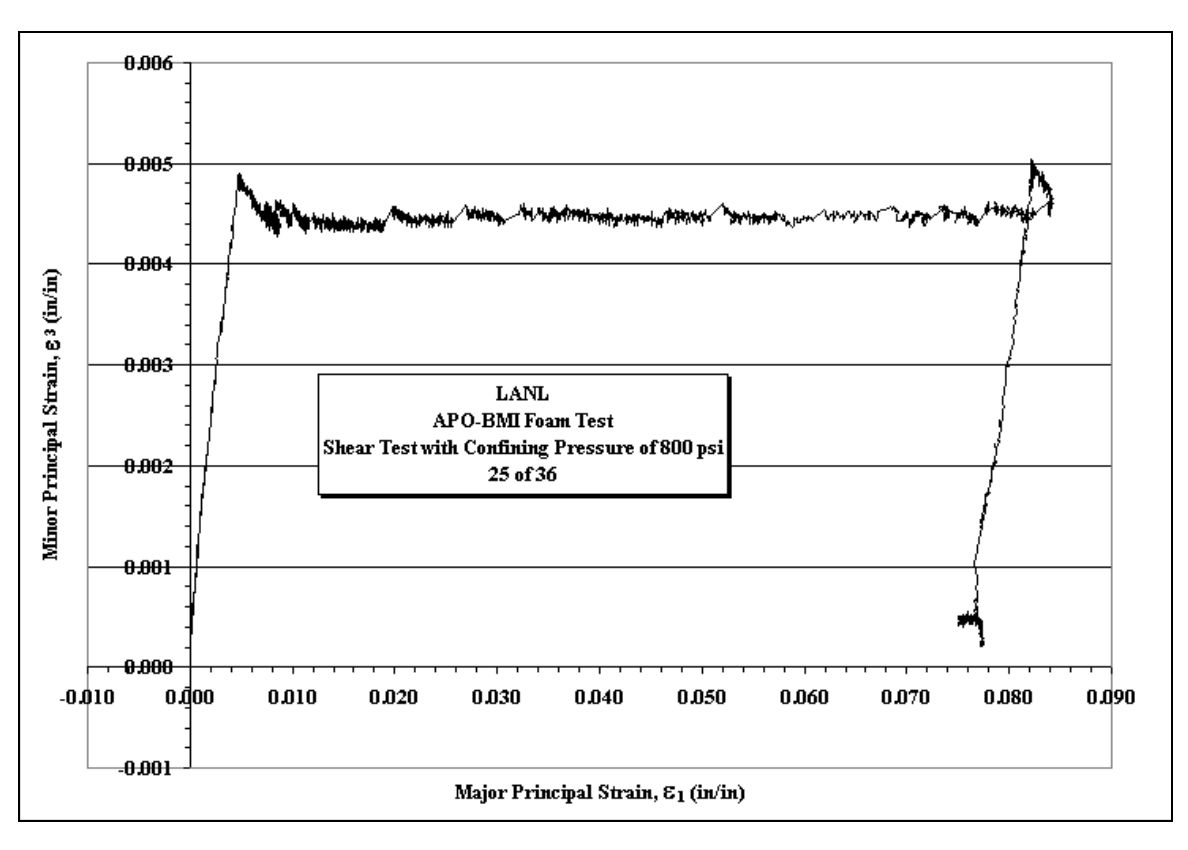


Figure A79. Mean Stress vs. Volumetric Strain plots for Sample 25of36 with a constant confining pressure of 800 psi.



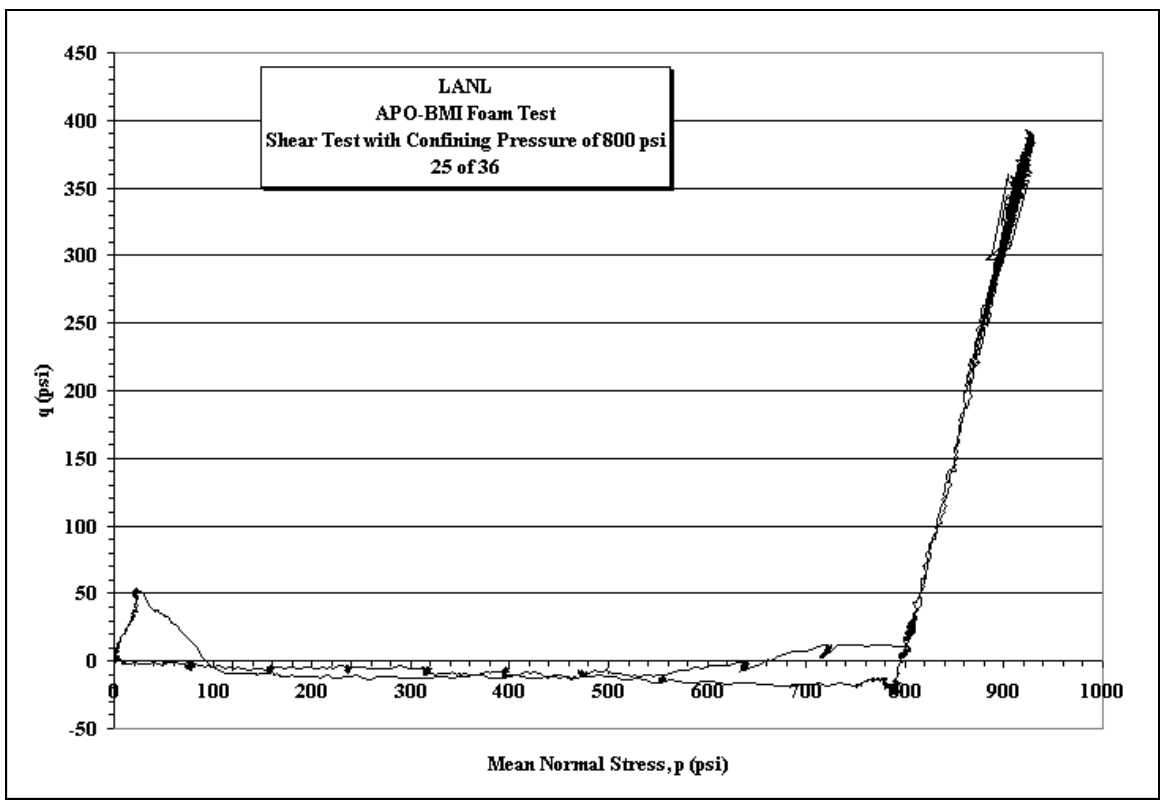
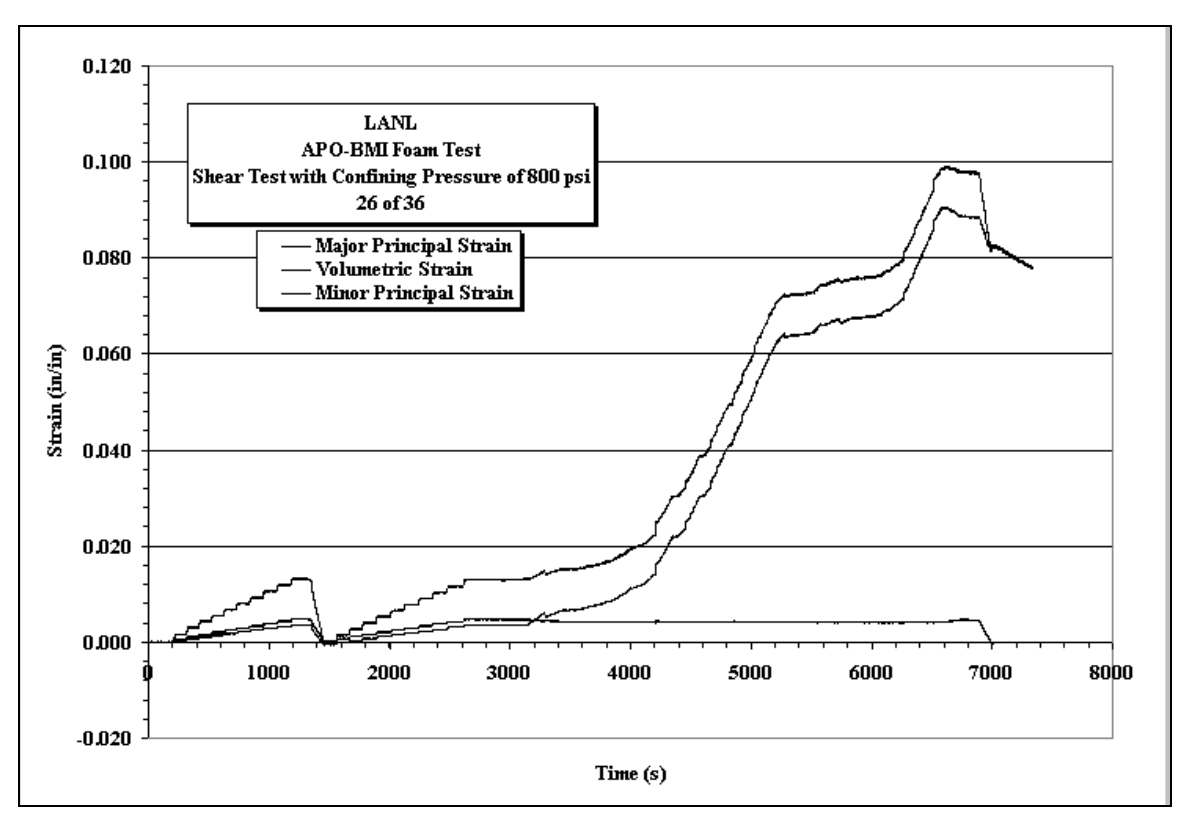


Figure A80. Minor Principle Strain vs. Major Principle Strain and Deviatoric Stress vs. Mean Stress plots for Sample 25of36 with a constant confining pressure of 800 psi.



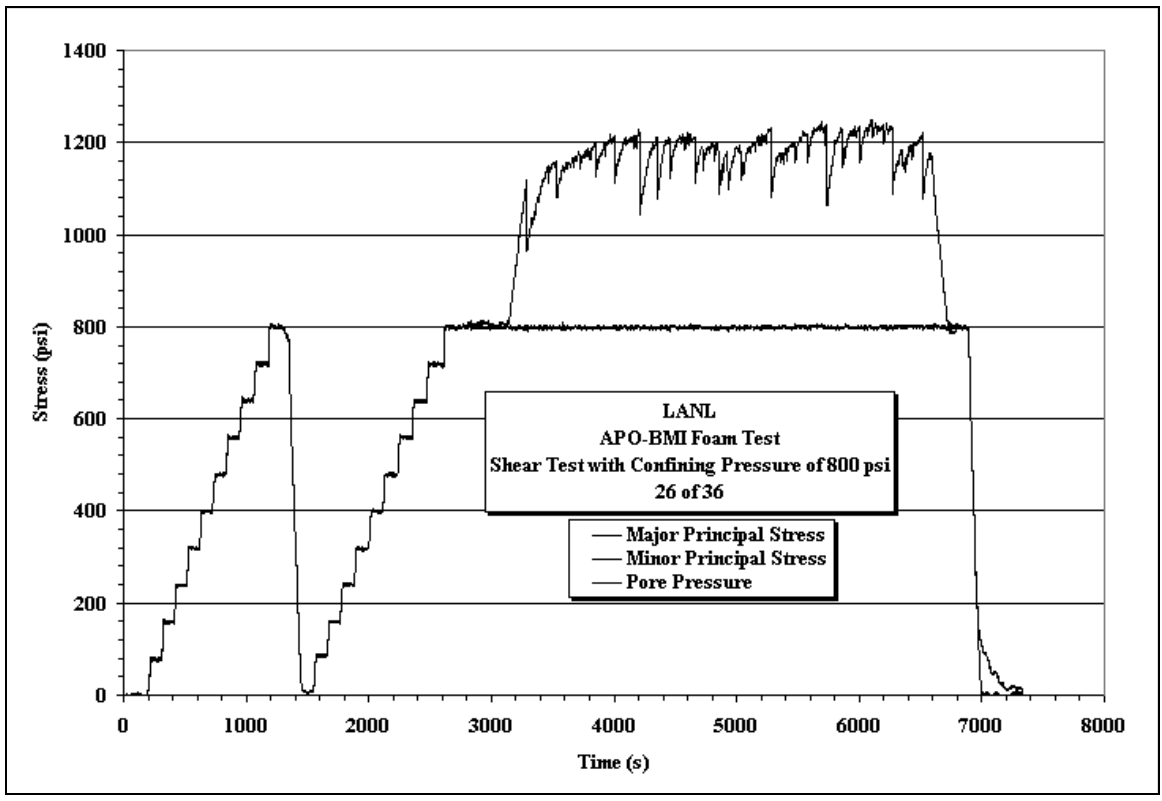
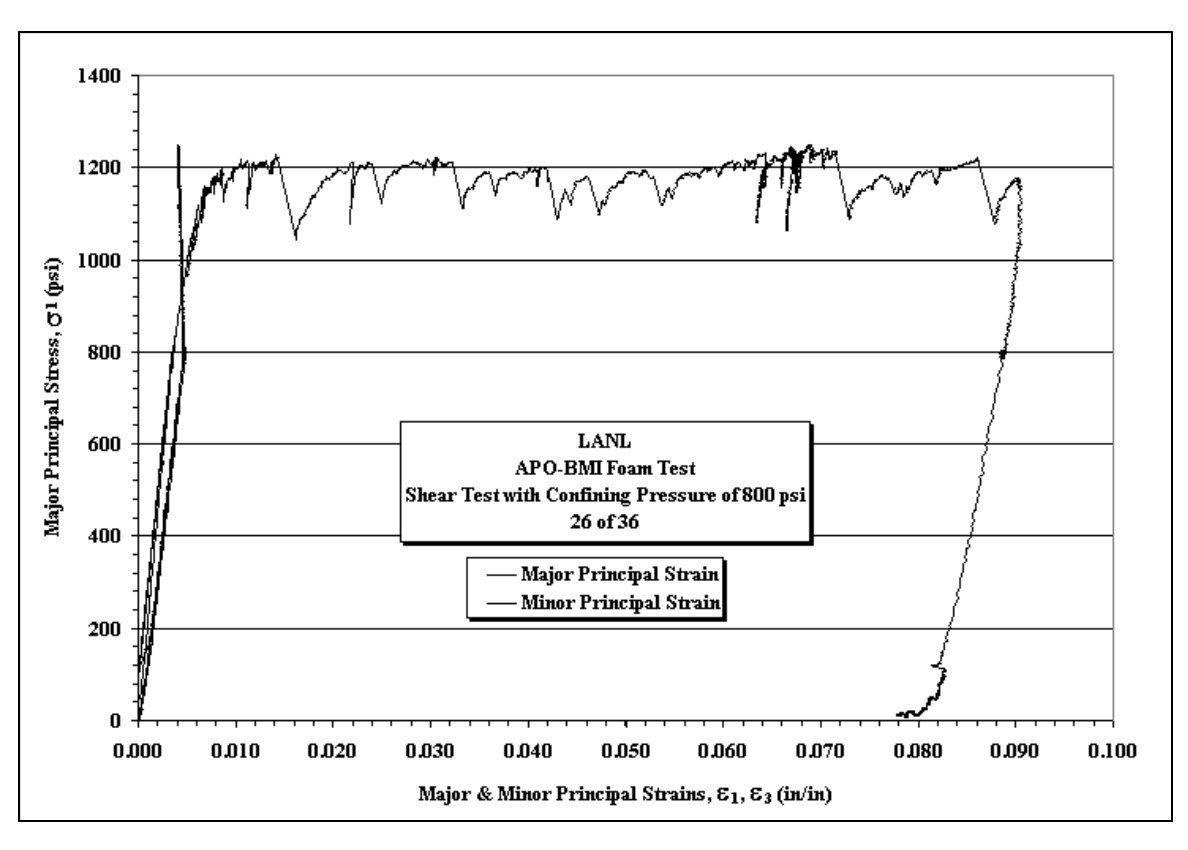


Figure A81. Minor Principle Strain vs. Major Principle Strain and Deviatoric Stress vs. Mean Stress plots for Sample 26of36 with a constant confining pressure of 800 psi.



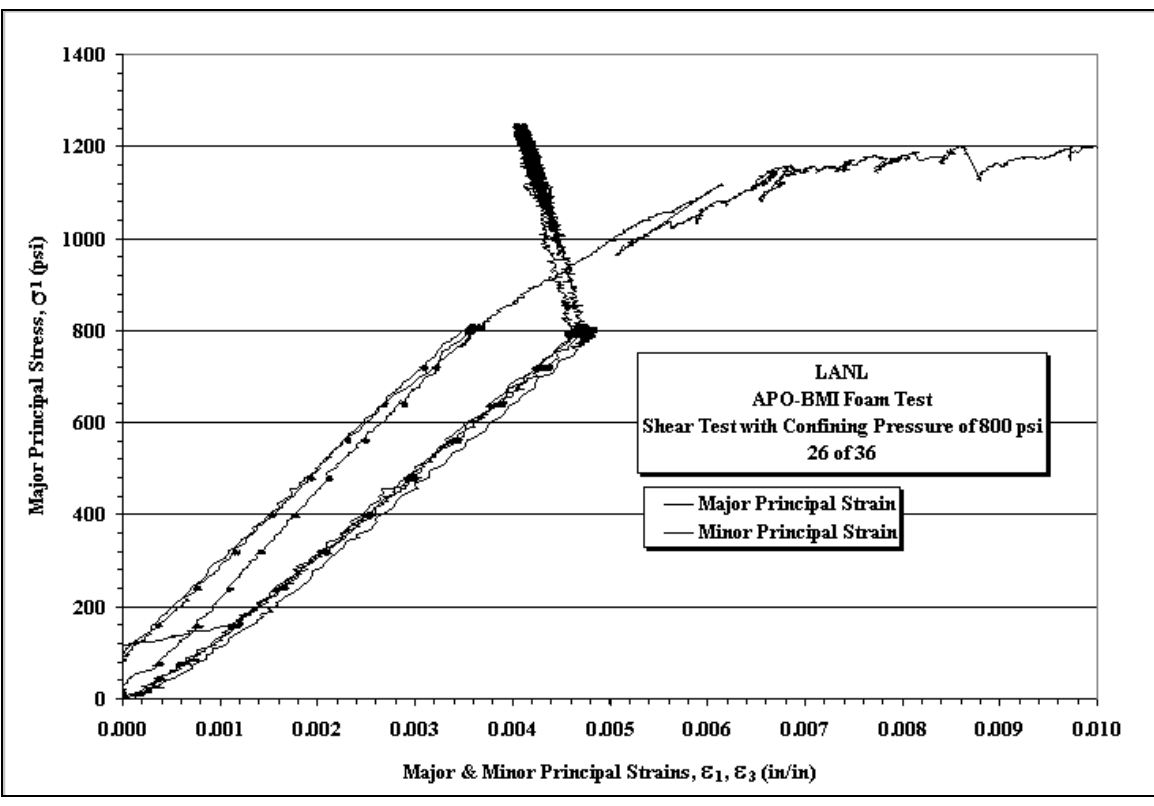
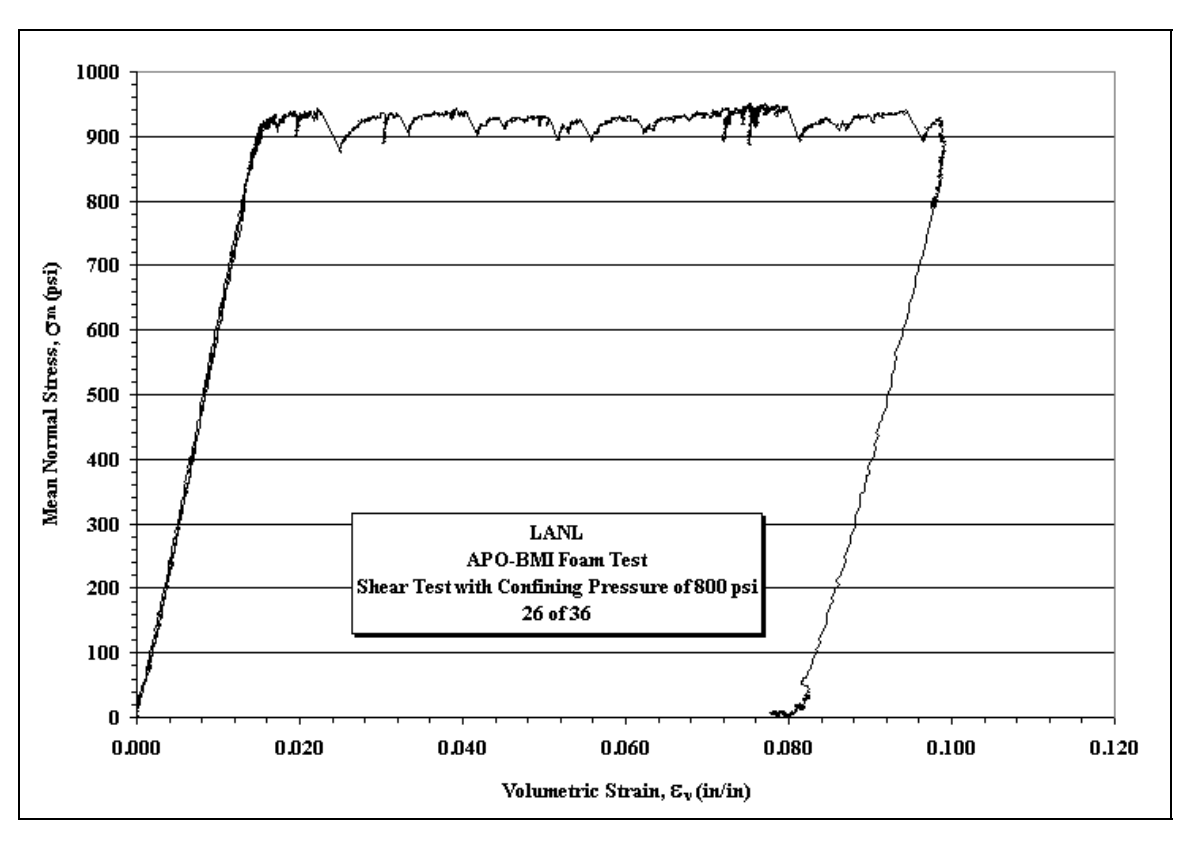


Figure A82. Stress vs. Strain plots for Sample 26of36 with a constant confining pressure of 800 psi.



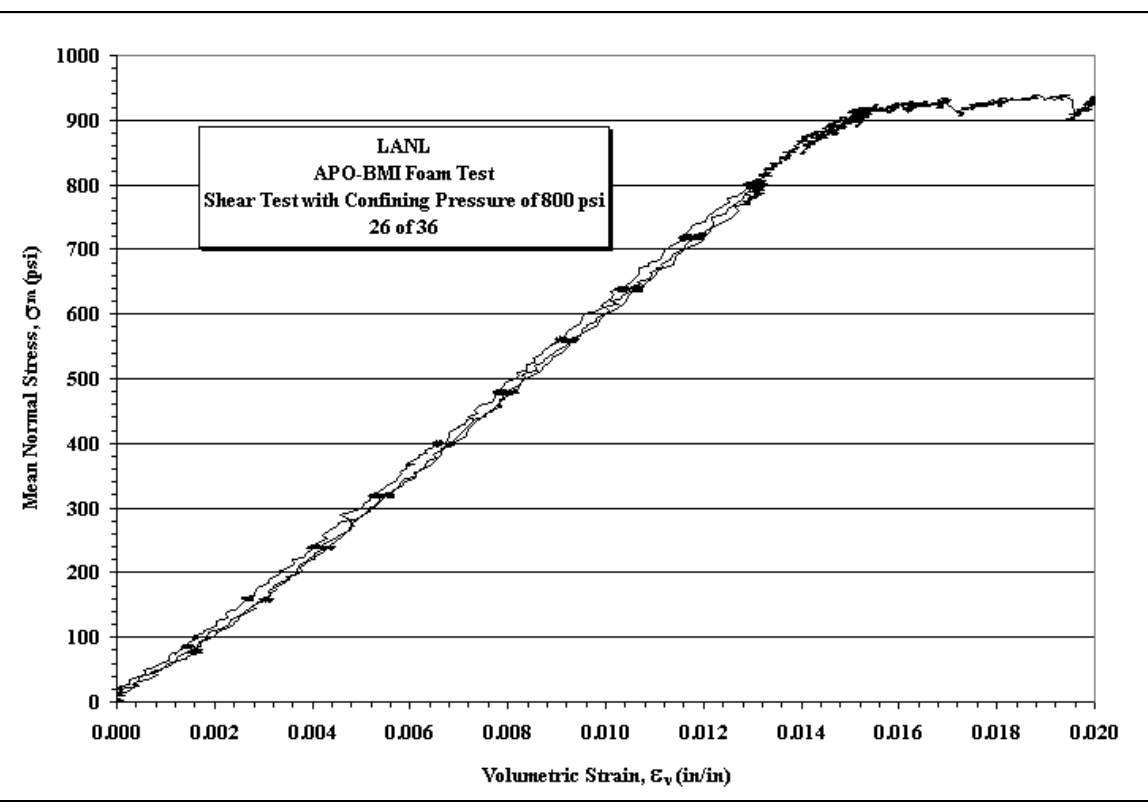
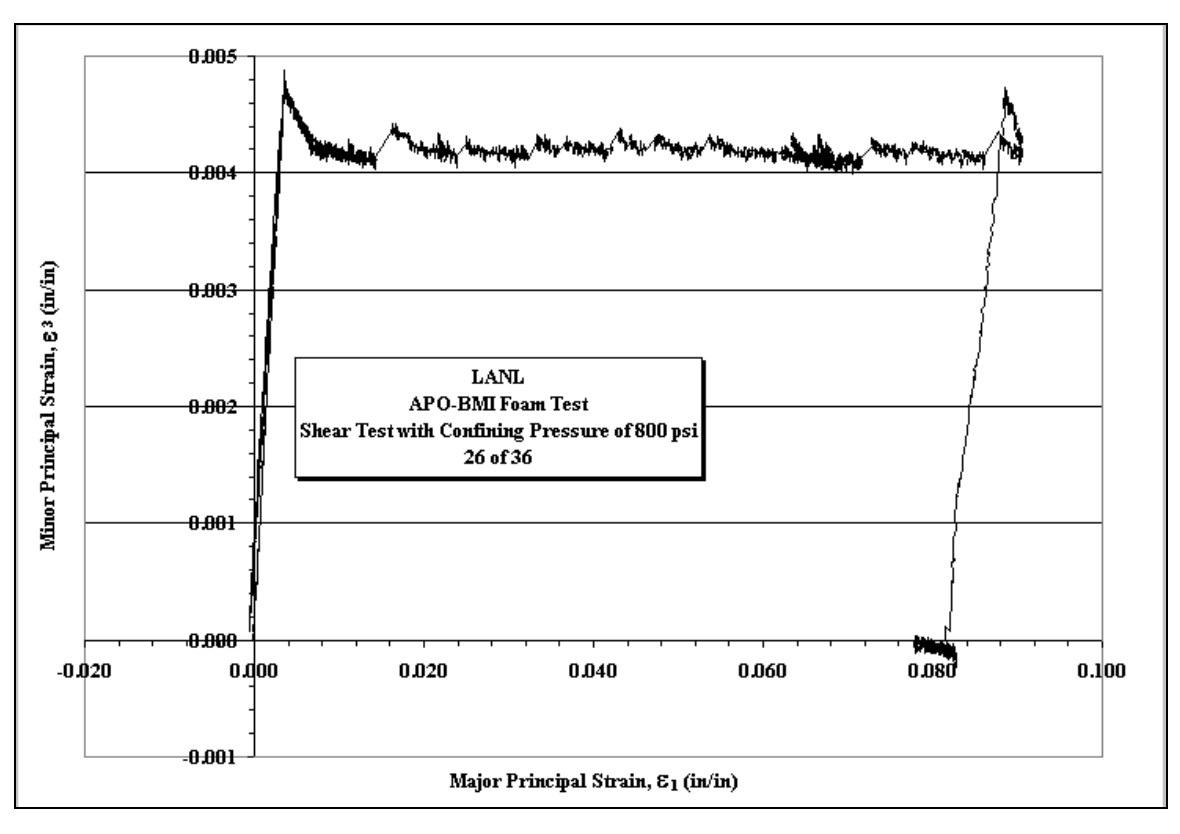


Figure A83. Mean Stress vs. Volumetric Strain plots for Sample 26of36 with a constant confining pressure of 800 psi.



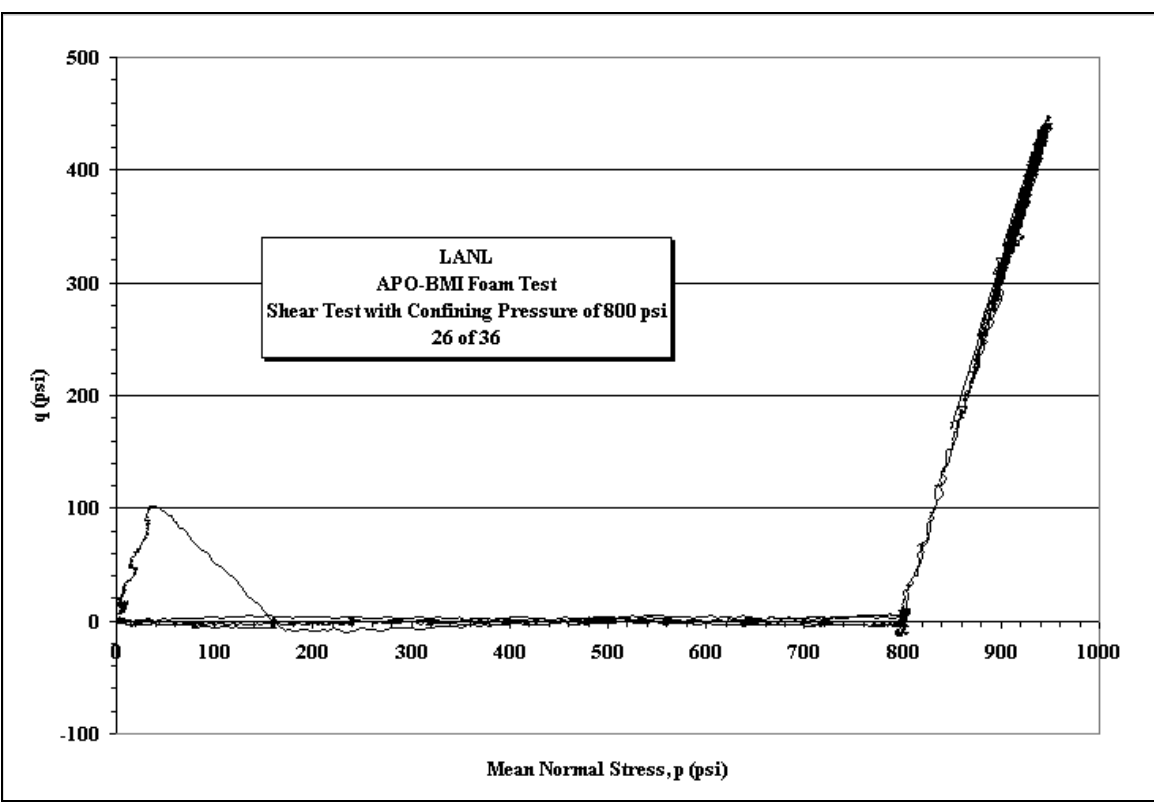
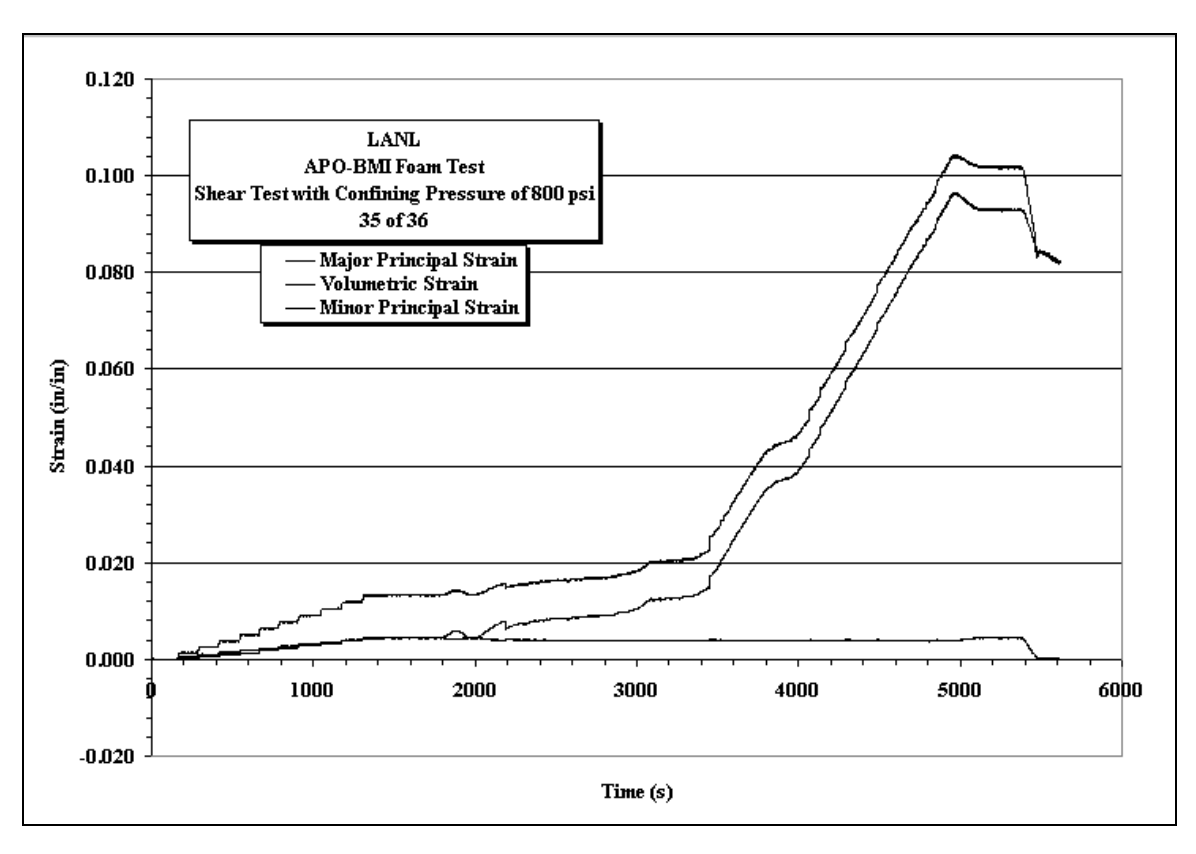


Figure A84. Minor Principle Strain vs. Major Principle Strain and Deviatoric Stress vs. Mean Stress plots for Sample 26of36 with a constant confining pressure of 800 psi.



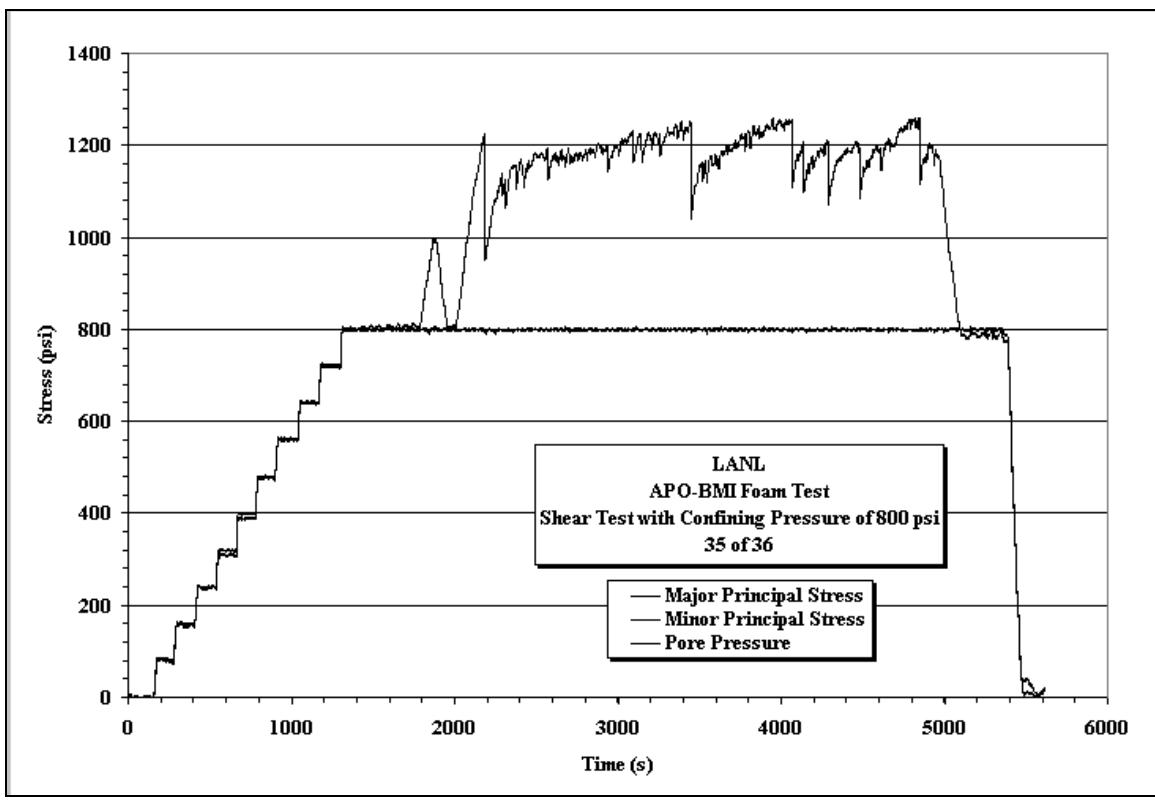
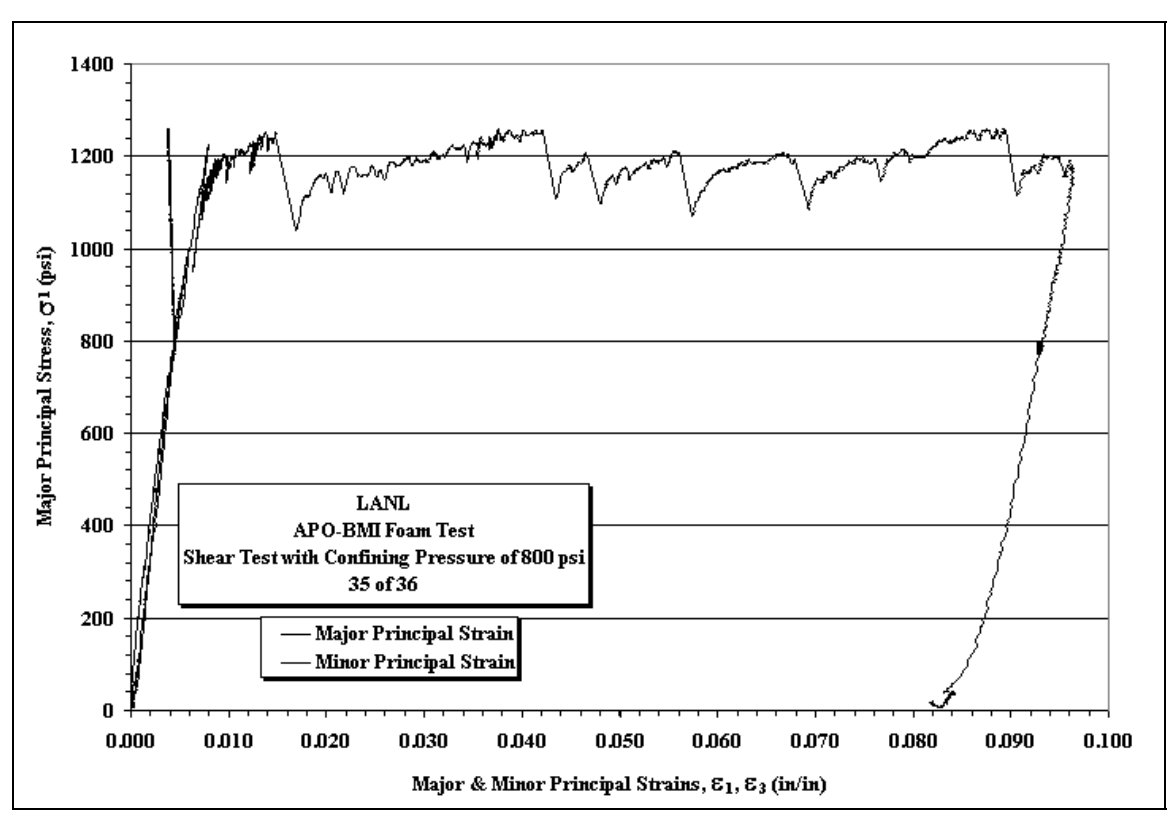


Figure A85. Minor Principle Strain vs. Major Principle Strain and Deviatoric Stress vs. Mean Stress plots for Sample 35of36 with a constant confining pressure of 800 psi.



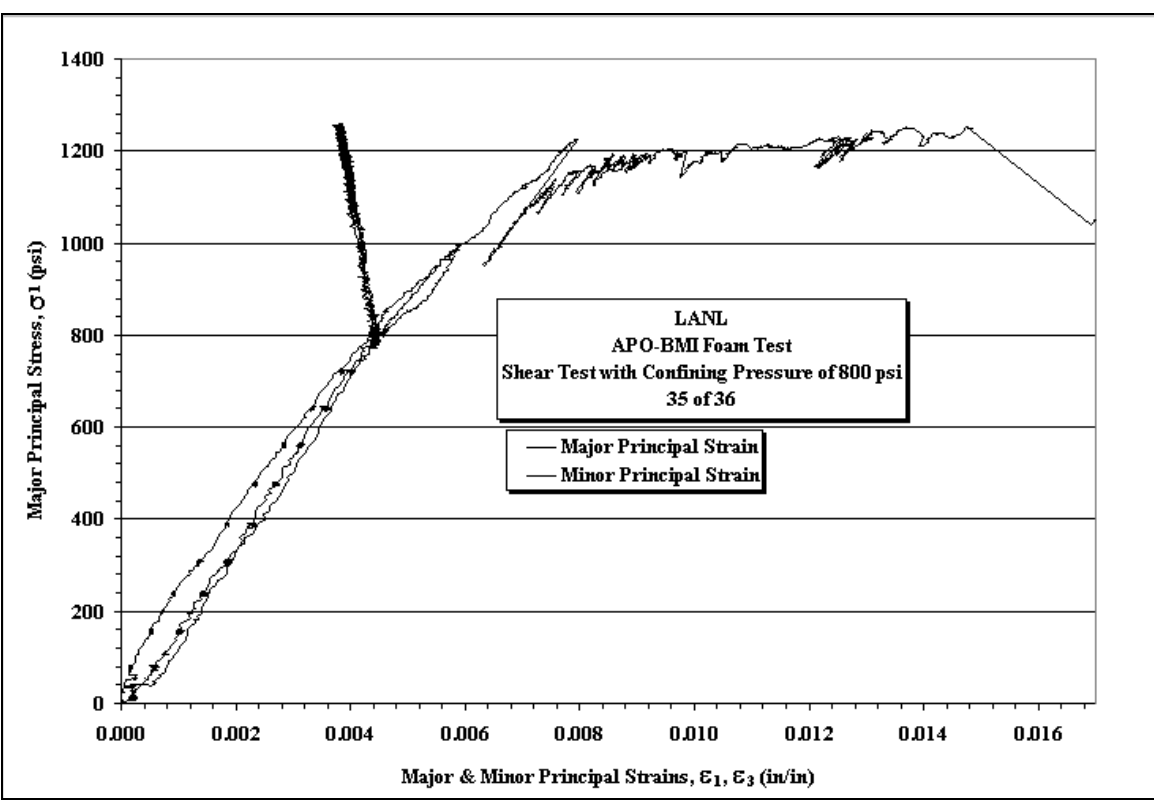
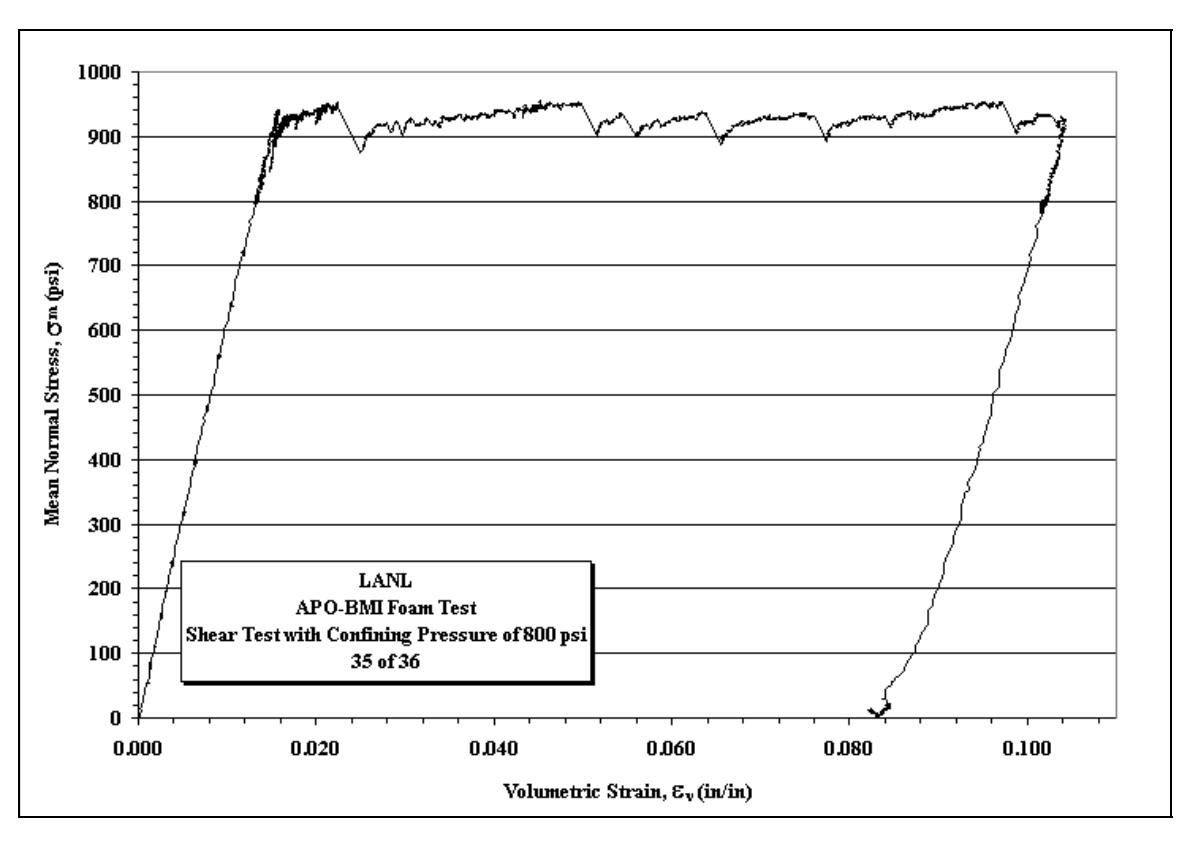


Figure A86. Stress vs. Strain plots for Sample 35of36 with a constant confining pressure of 800 psi.



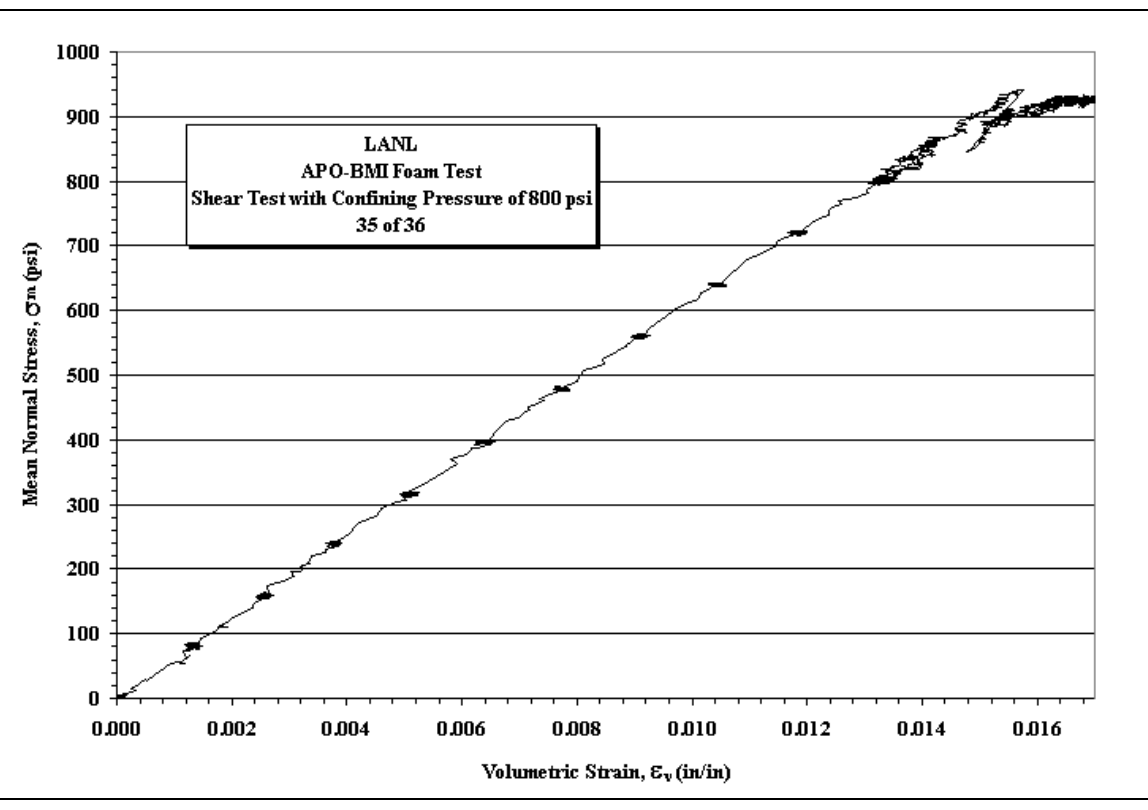
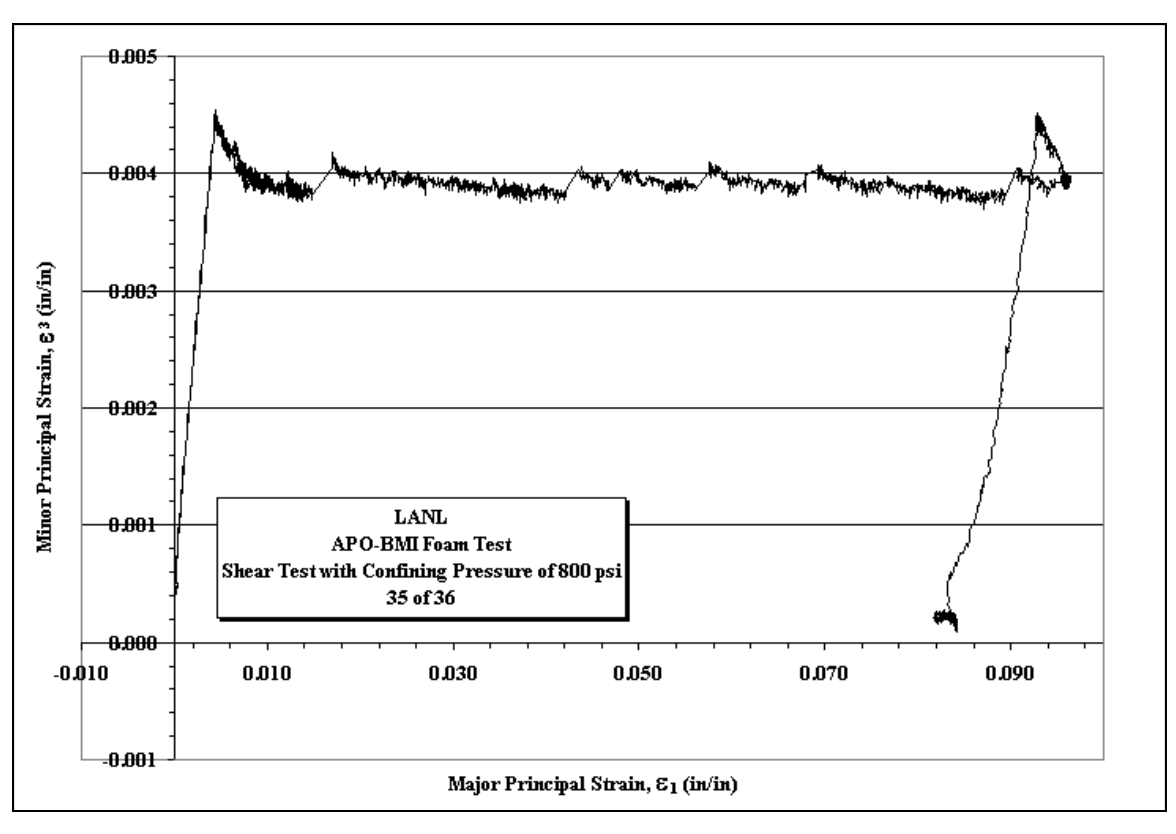


Figure A87. Mean Stress vs. Volumetric Strain plots for Sample 35of36 with a constant confining pressure of 800 psi.



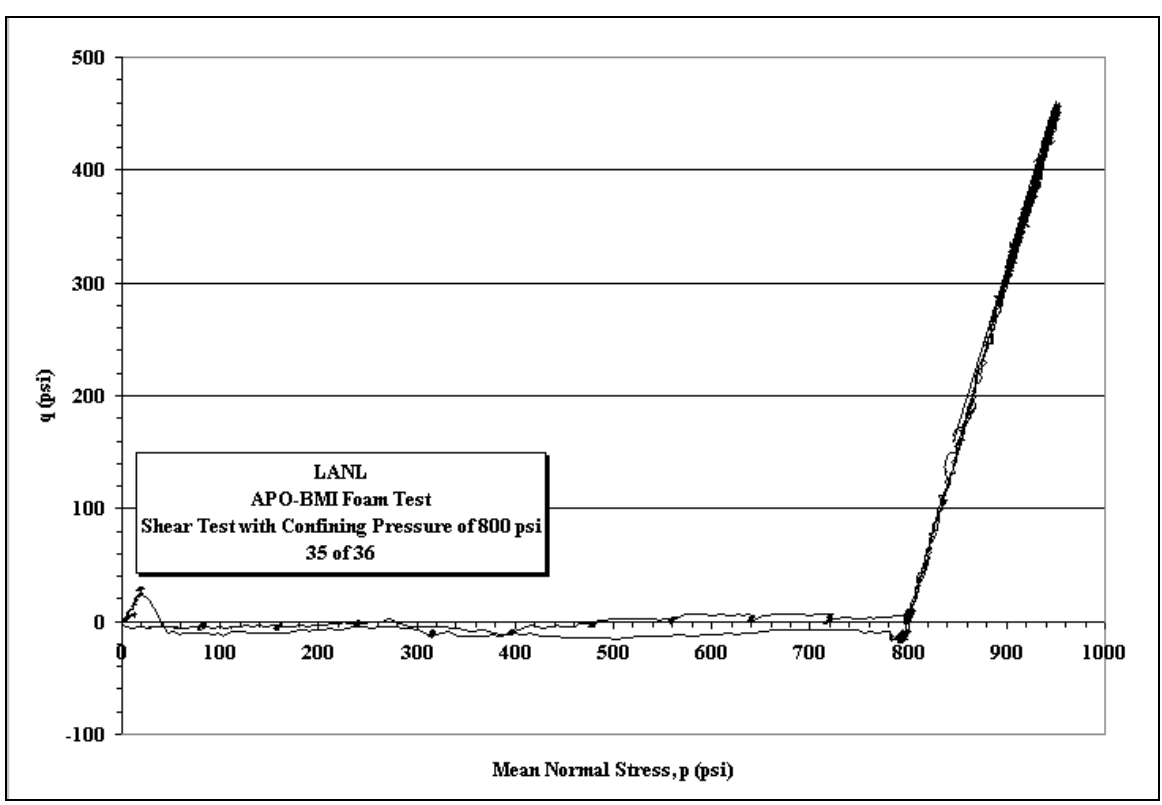
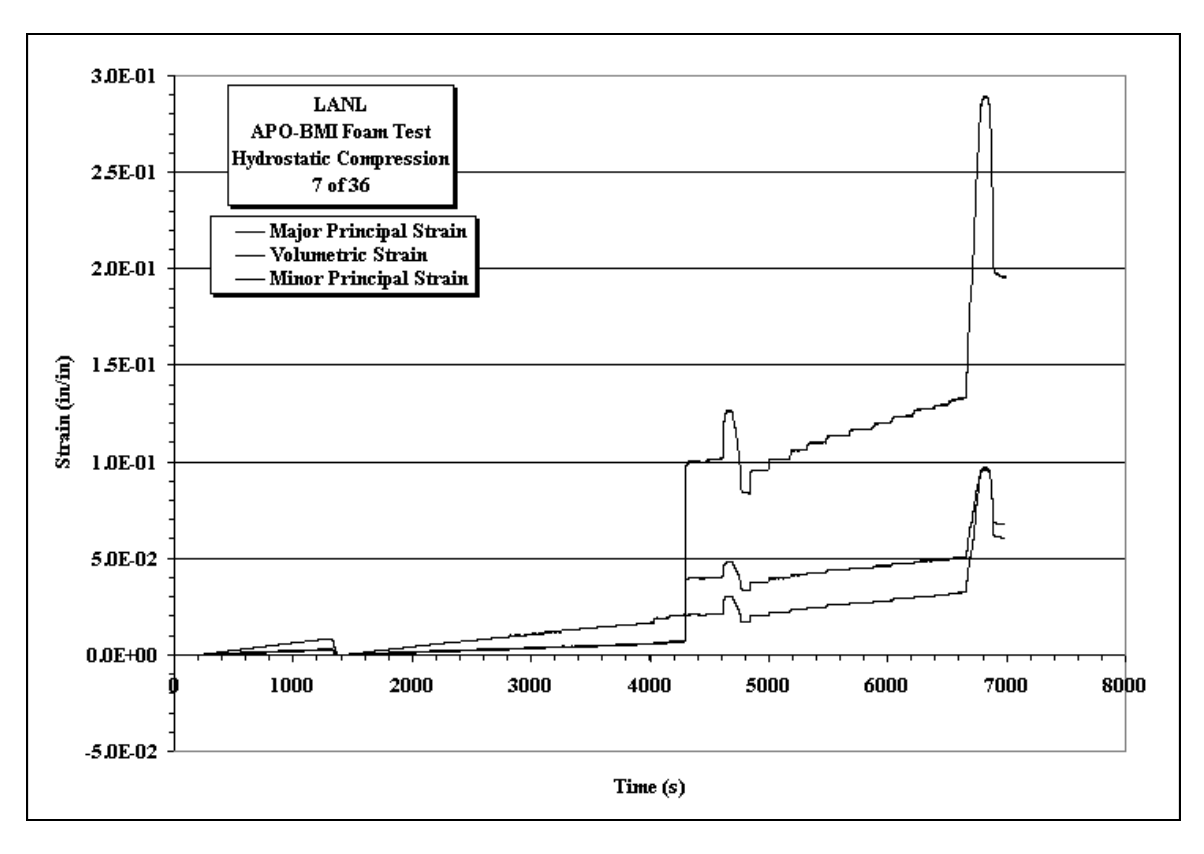


Figure A88. Minor Principle Strain vs. Major Principle Strain and Deviatoric Stress vs. Mean Stress plots for Sample 35of36 with a constant confining pressure of 800 psi.



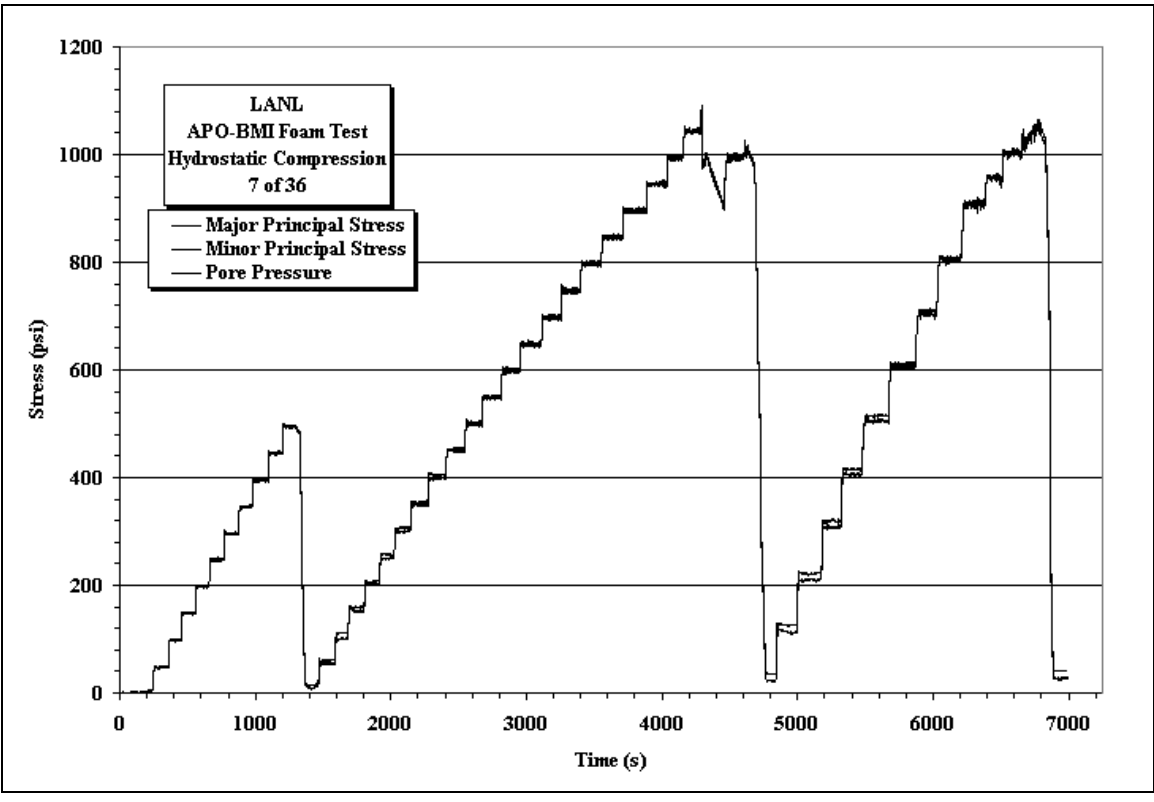
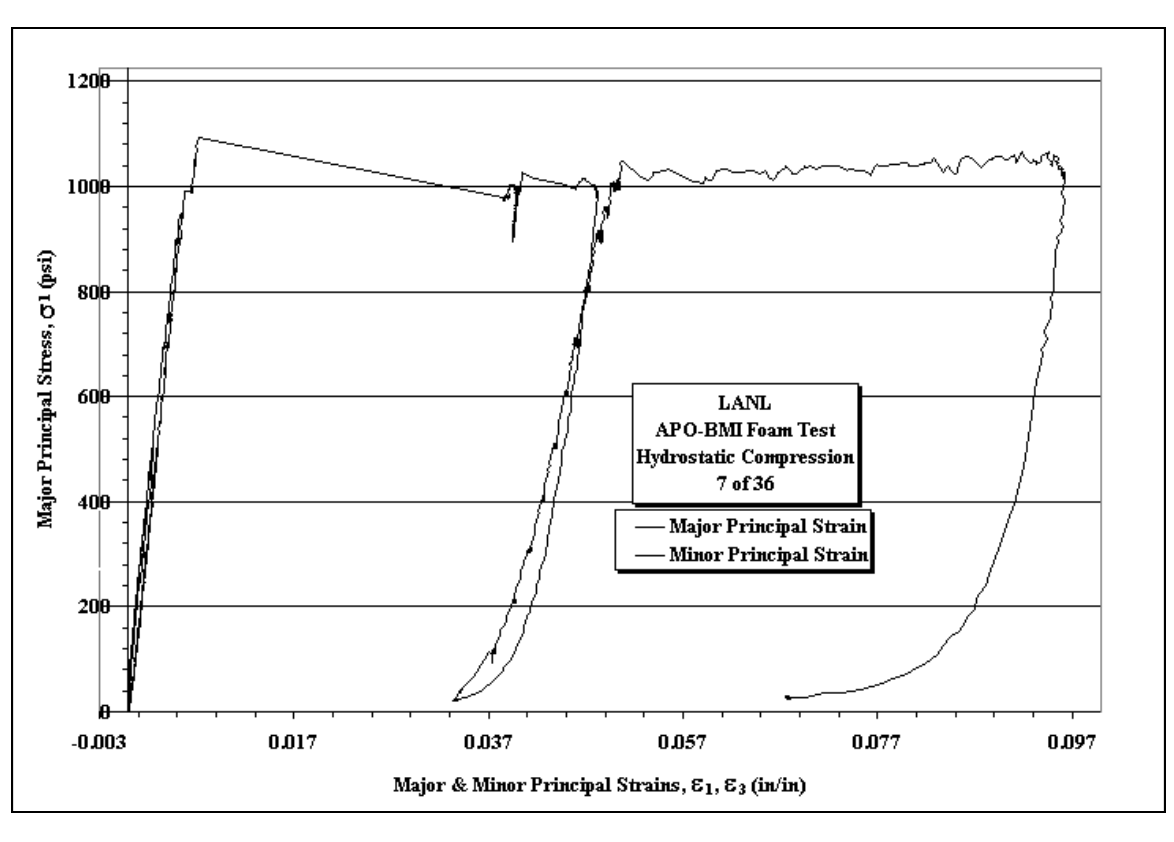


Figure A89. Strain vs. Time and Stress vs. Time plots for Sample 7of36 under an equivalent pressure applied in all directions.



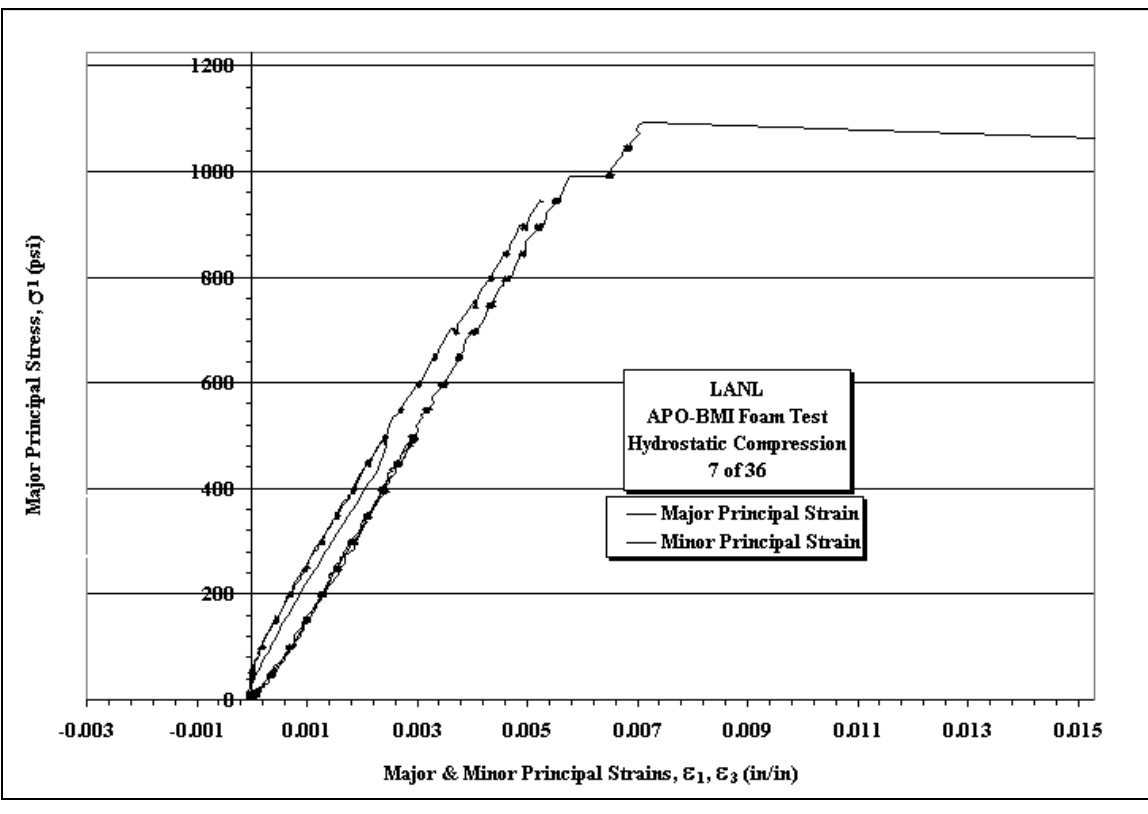
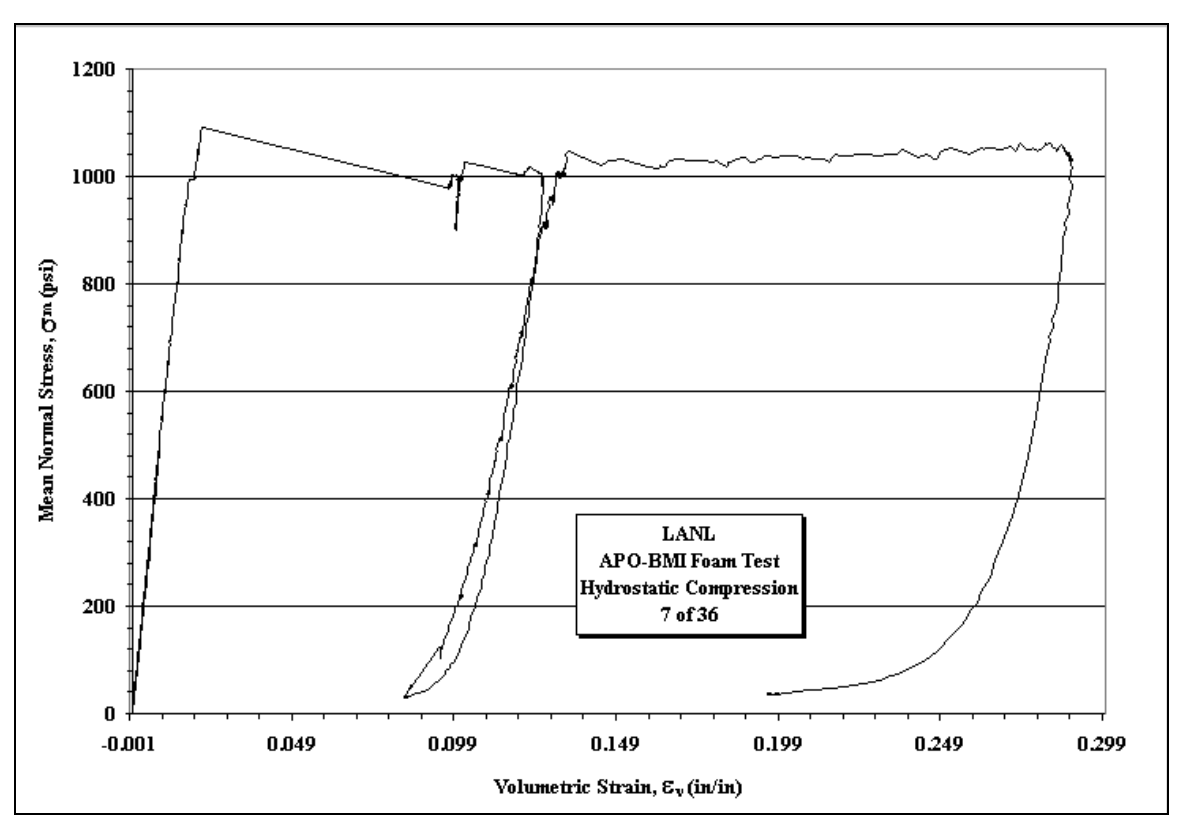


Figure A90. Stress vs. Strain plots for Sample 7of36 under an equivalent pressure applied in all directions.



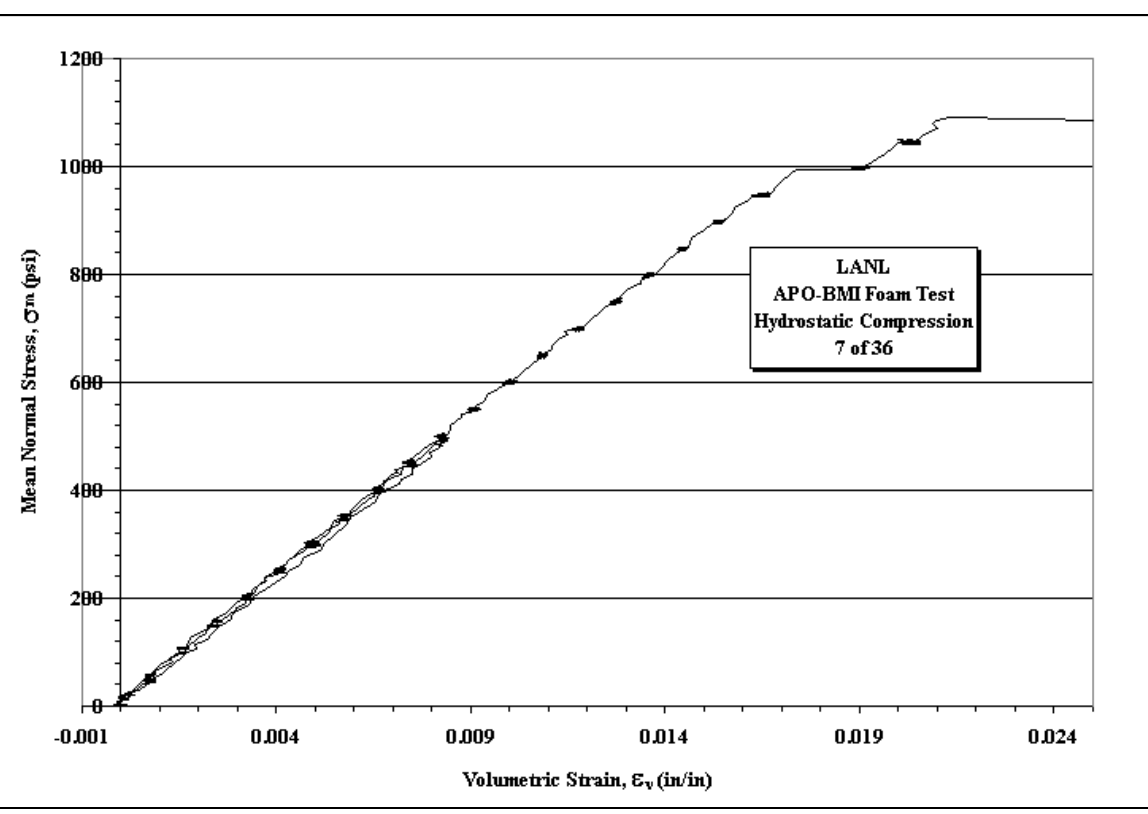
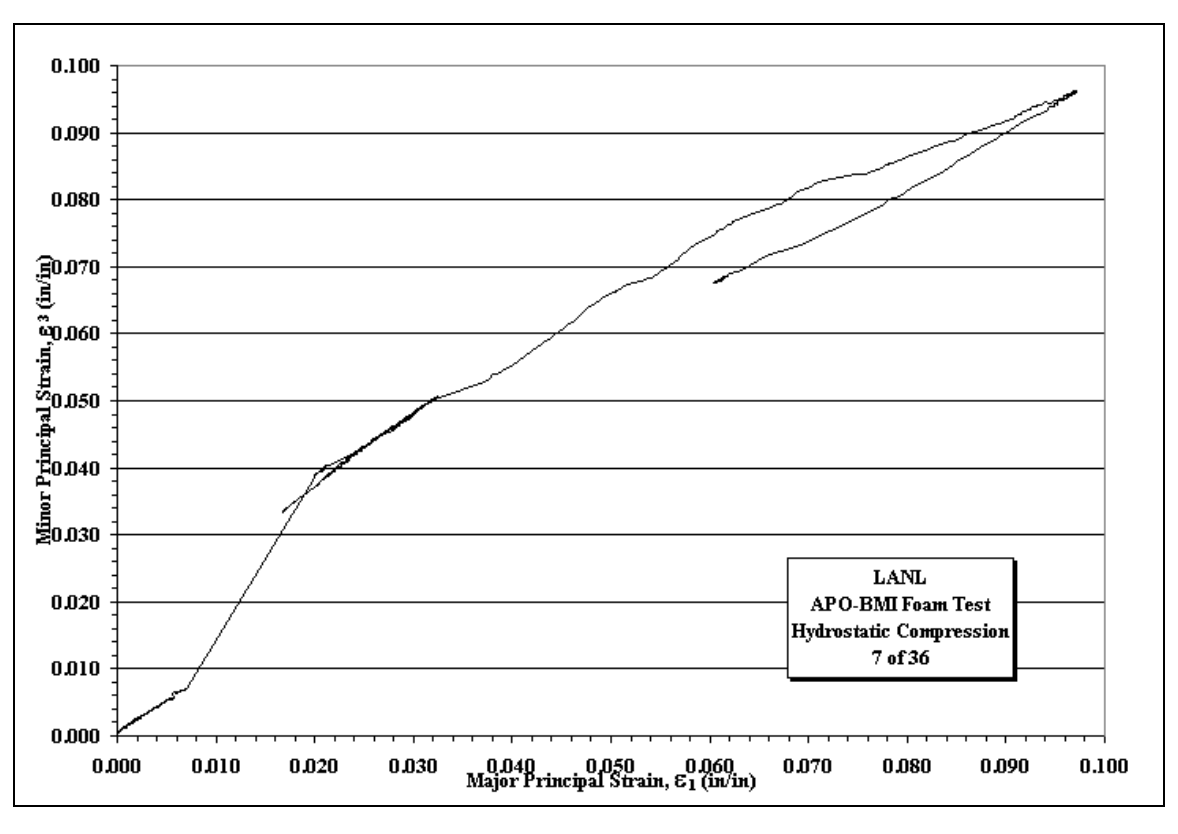


Figure A91. Mean Stress vs. Volumetric Strain plots for Sample 7of36 under an equivalent pressure applied in all directions.



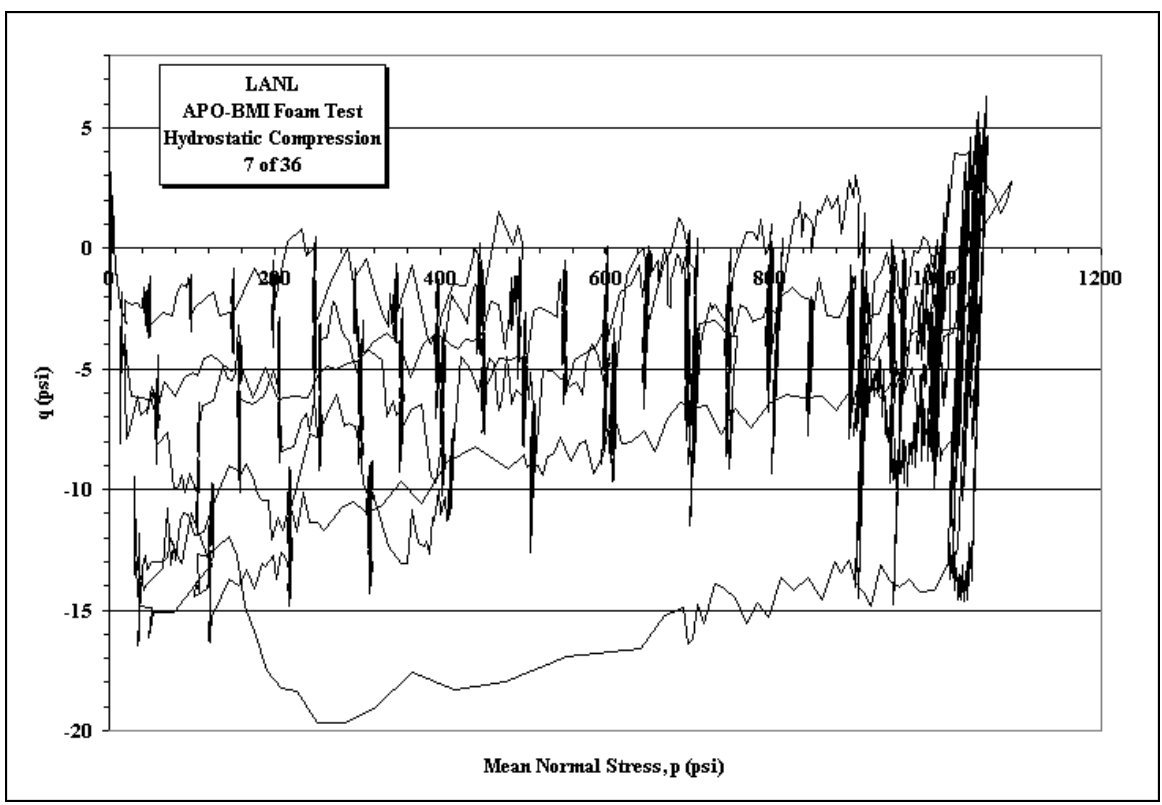
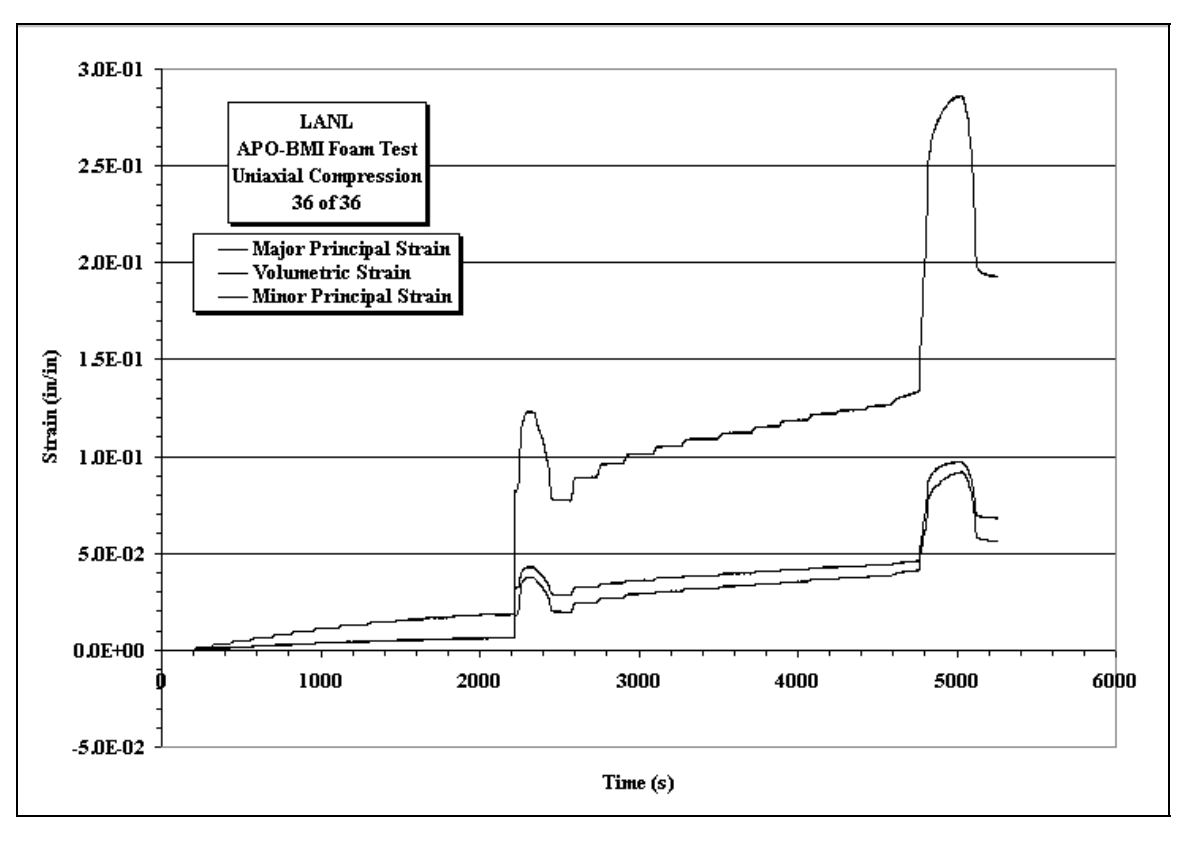


Figure A92. Minor Principle Strain vs. Major Principle Strain and Deviatoric Stress vs. Mean Stress plots for Sample 7of36 under an equivalent pressure applied in all directions.



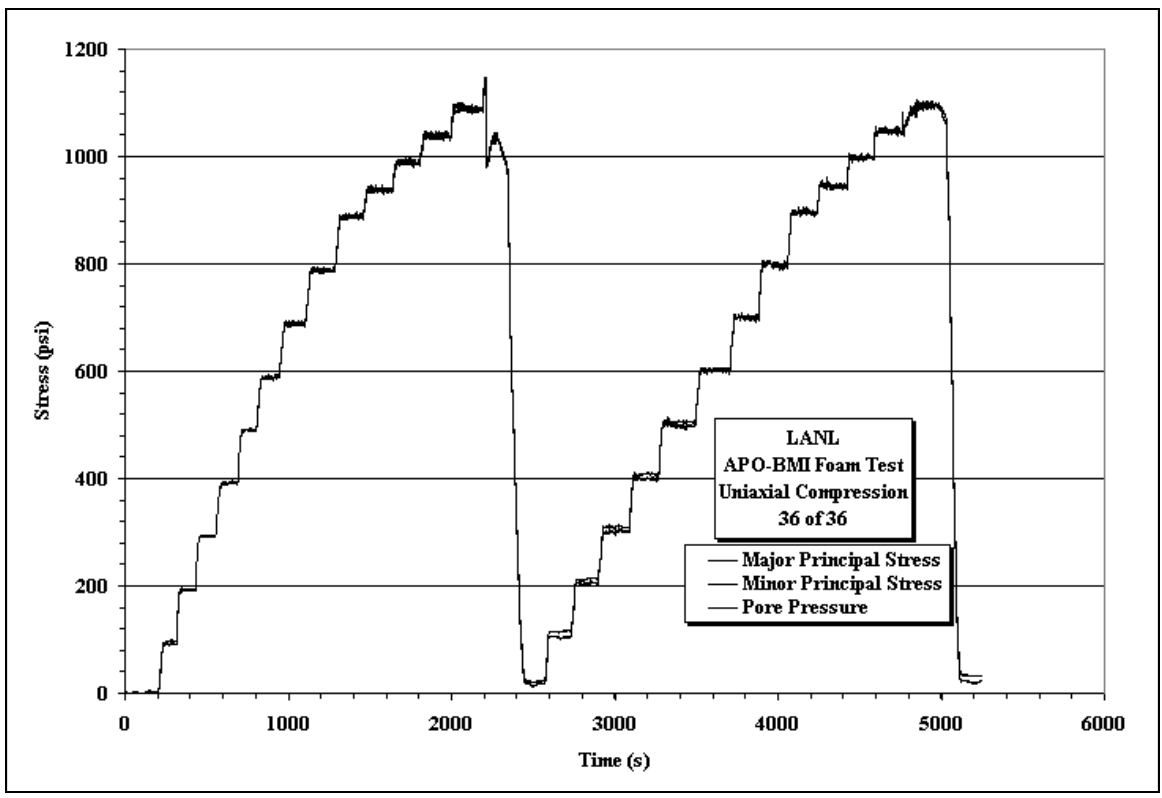
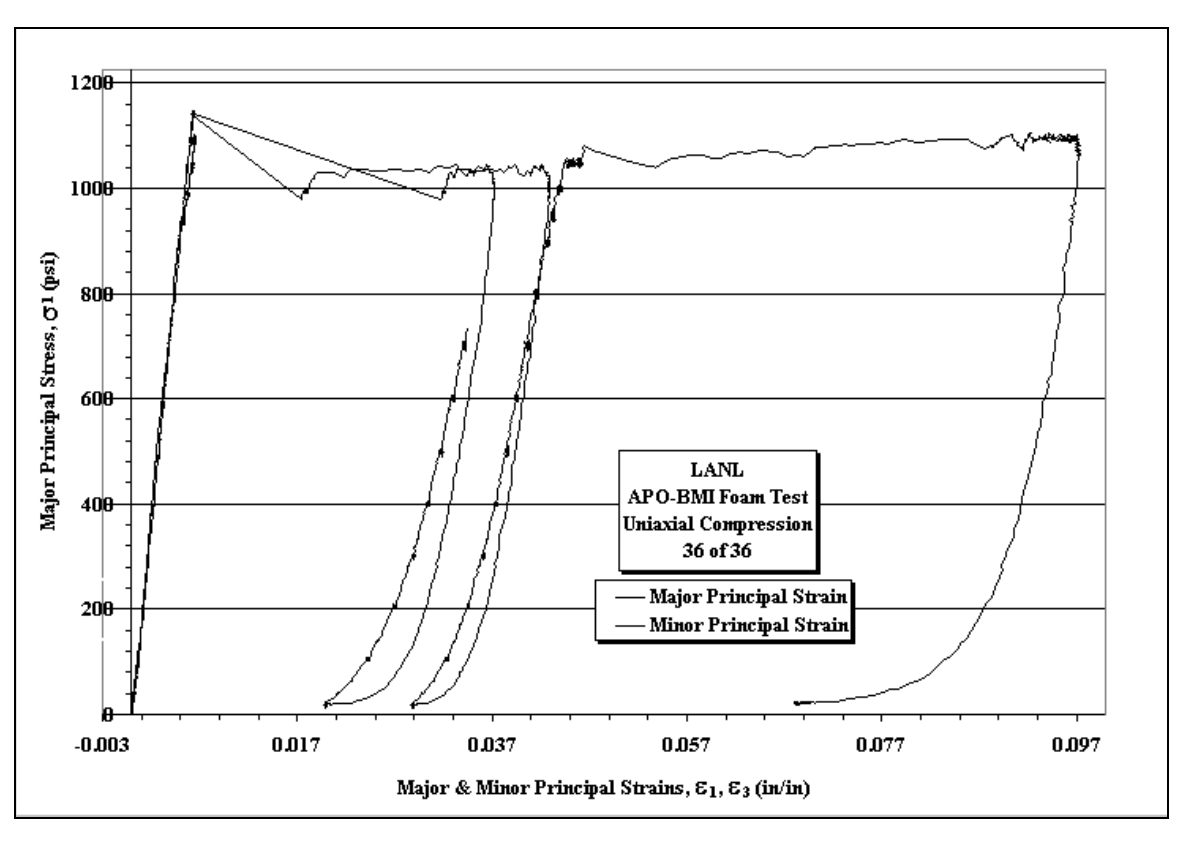


Figure A93. Strain vs. Time and Stress vs. Time plots for Sample 36of36 under an equivalent pressure applied in all directions.



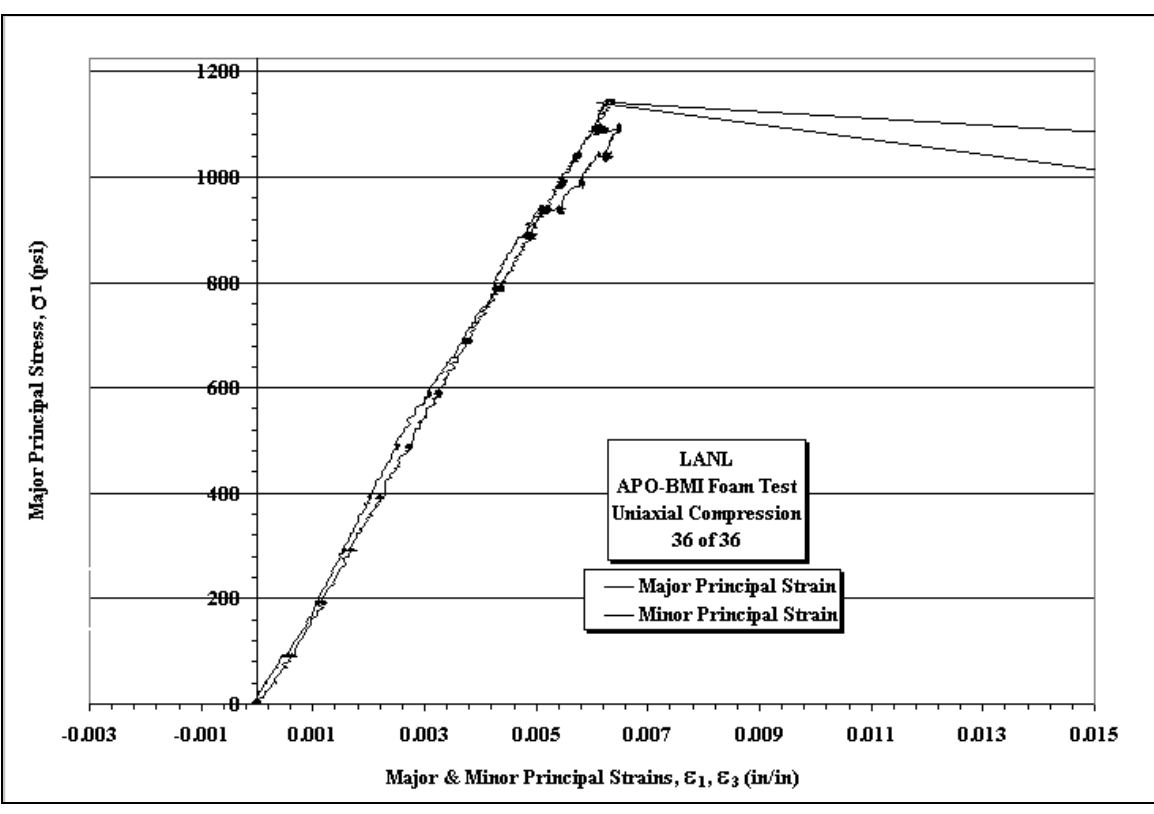
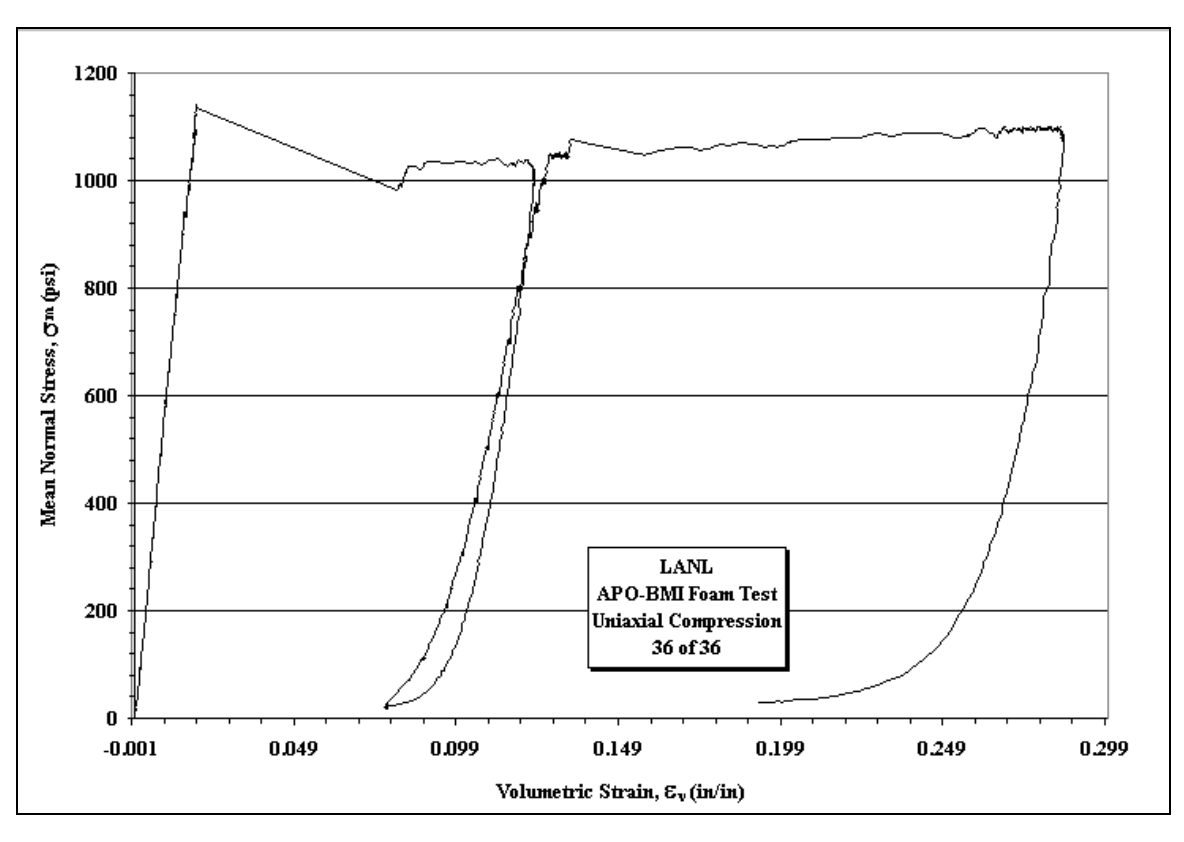


Figure A94. Stress vs. Strain plots for Sample 36of36 under an equivalent pressure applied in all directions.



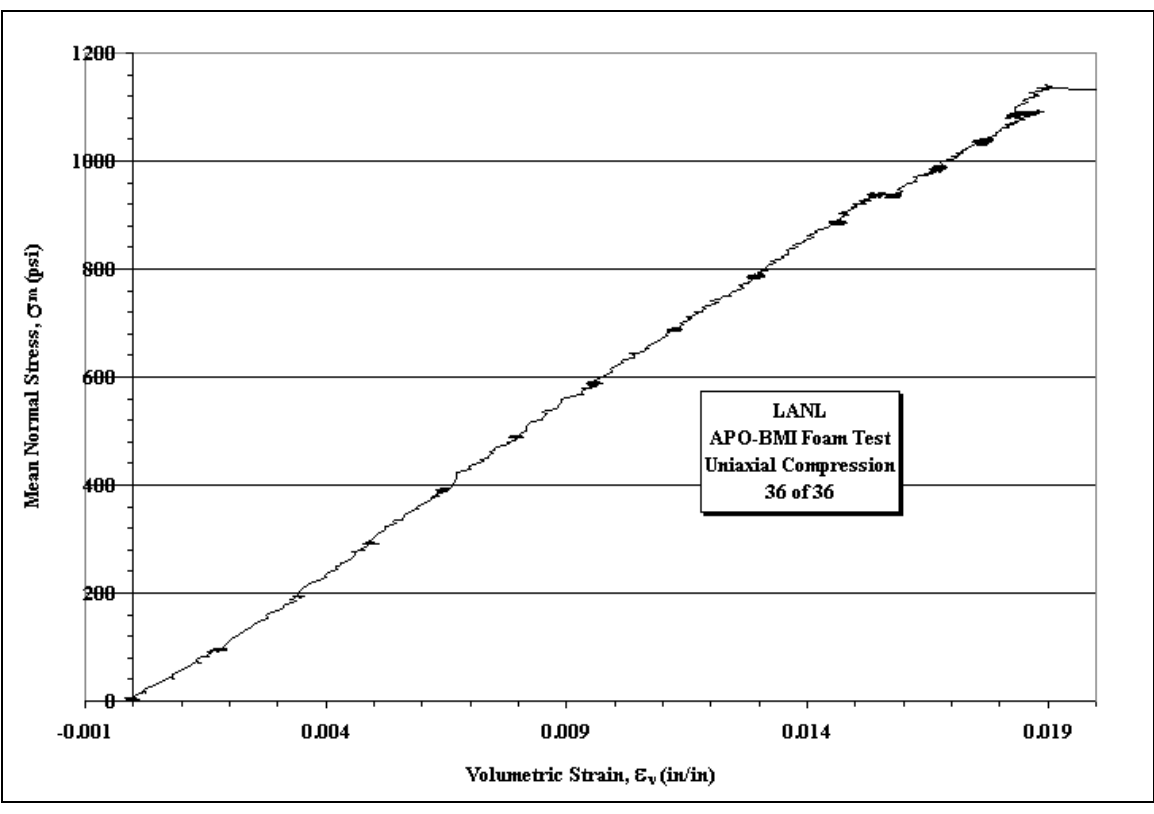
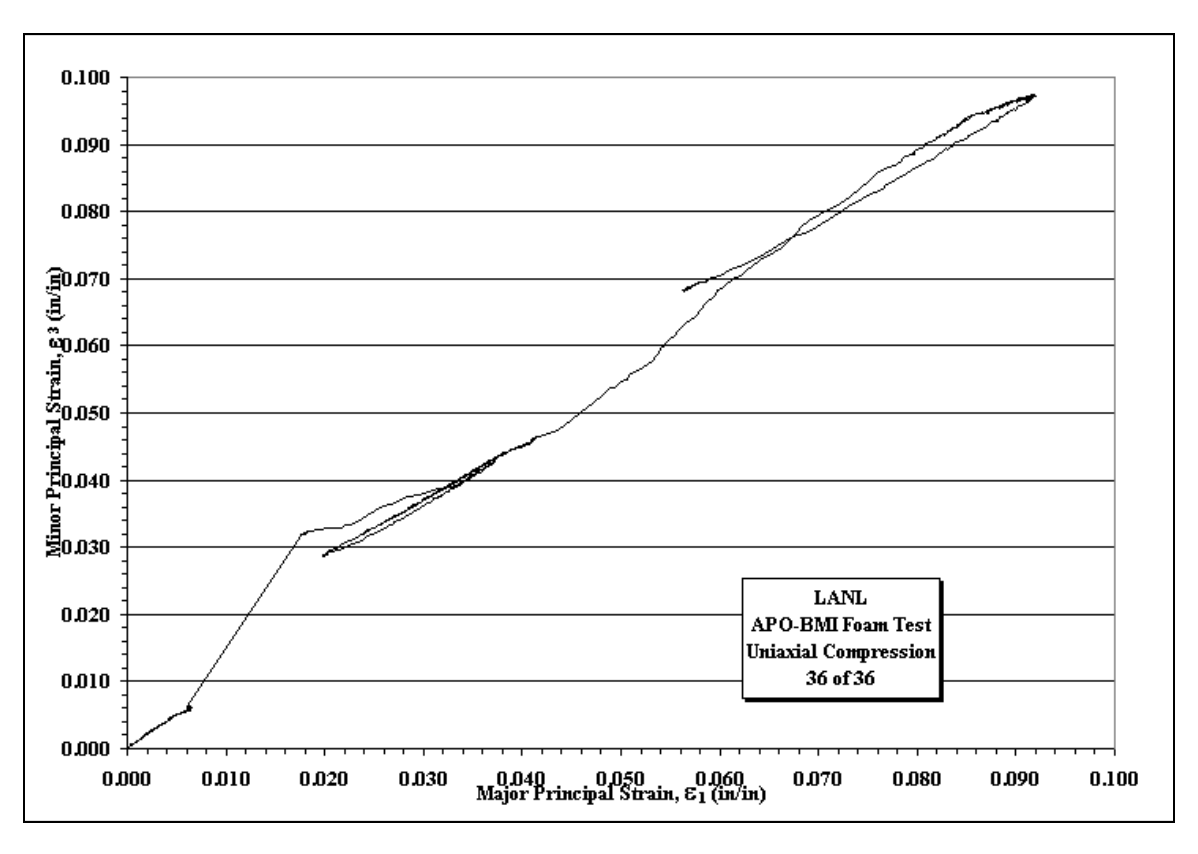


Figure A95. Mean Stress vs. Volumetric Strain plots for Sample 36of36 under an equivalent pressure applied in all directions.



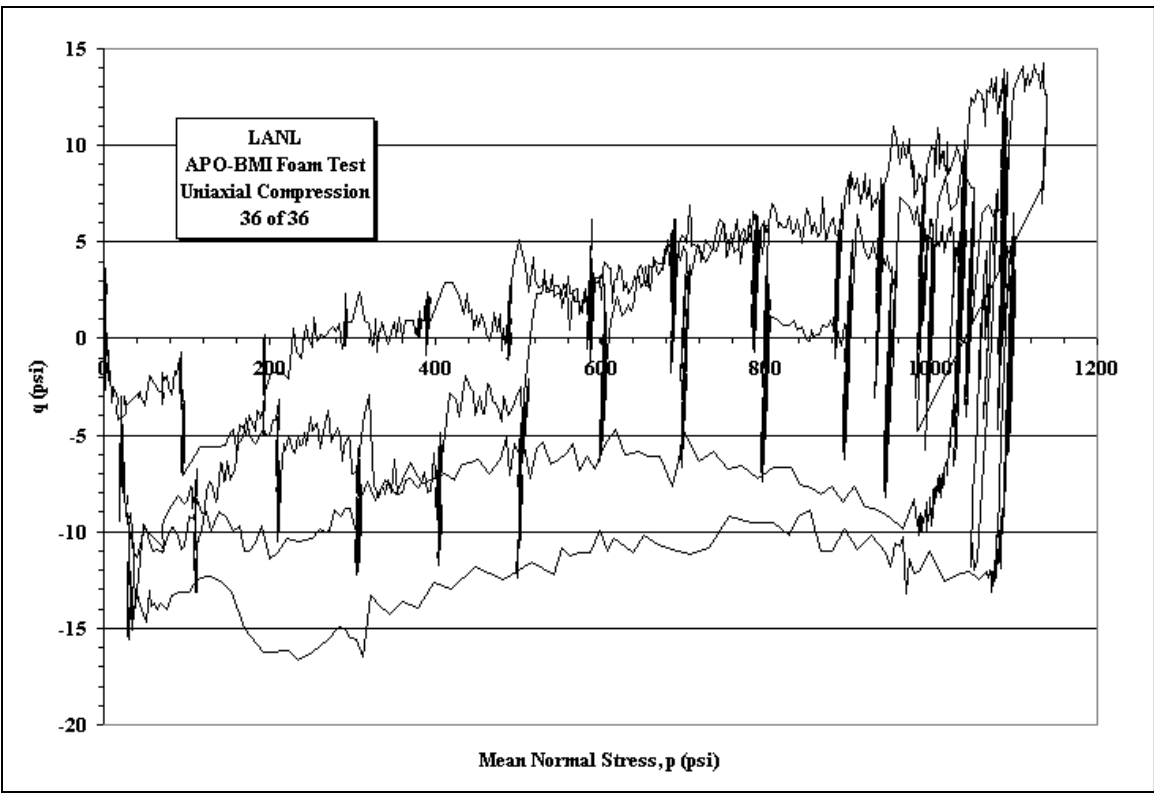
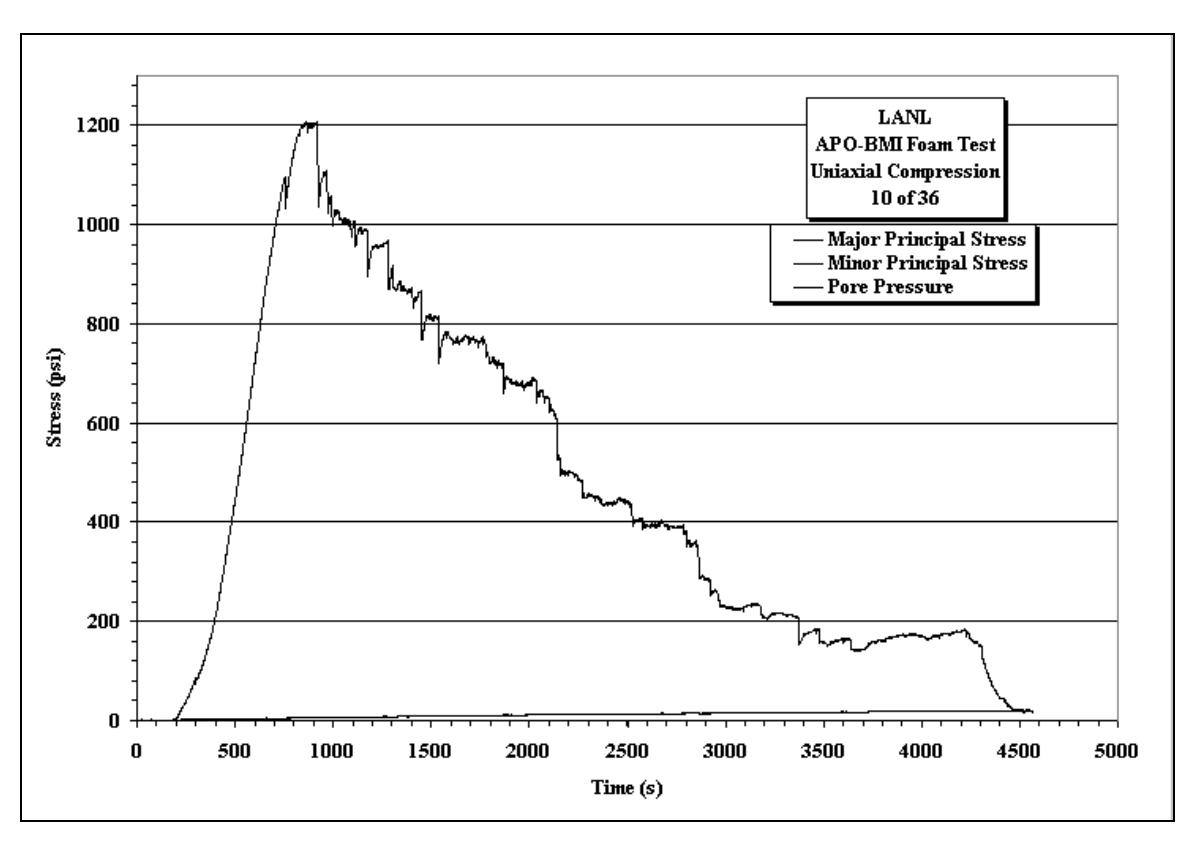


Figure A96. Minor Principle Strain vs. Major Principle Strain and Deviatoric Stress vs. Mean Stress plots for Sample 36of36 under an equivalent pressure applied in all directions.



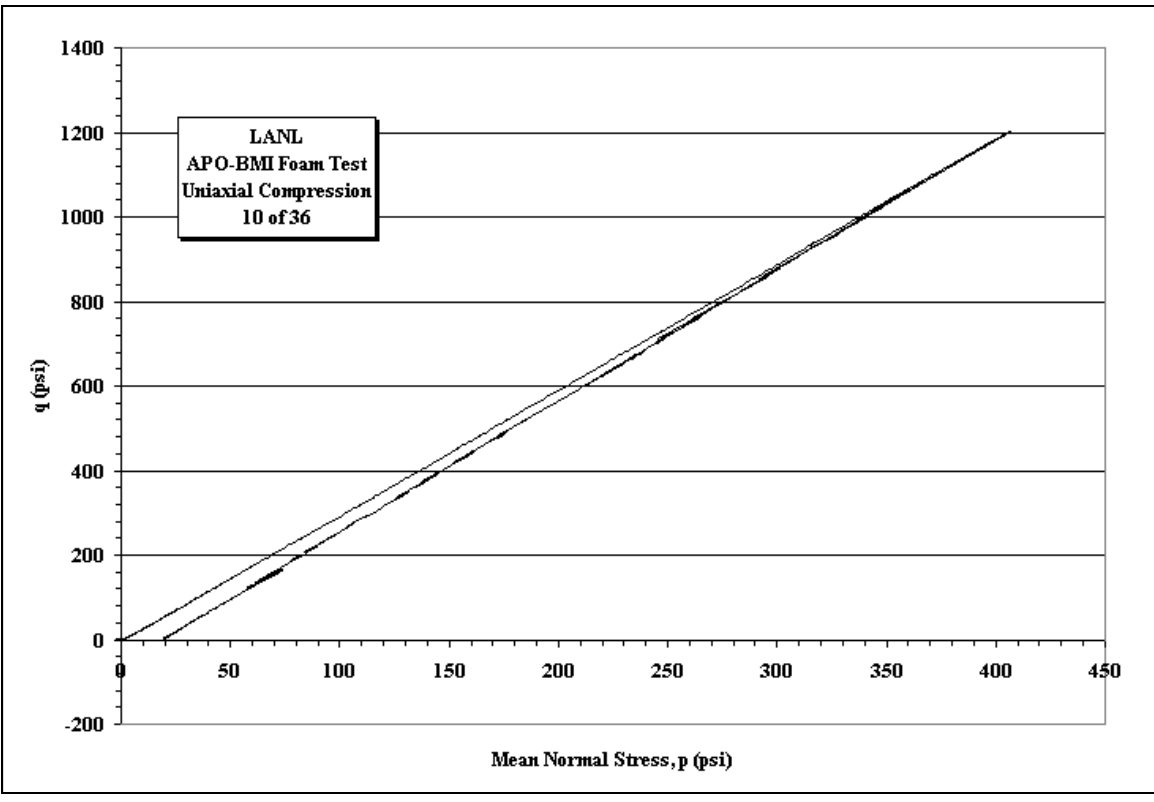
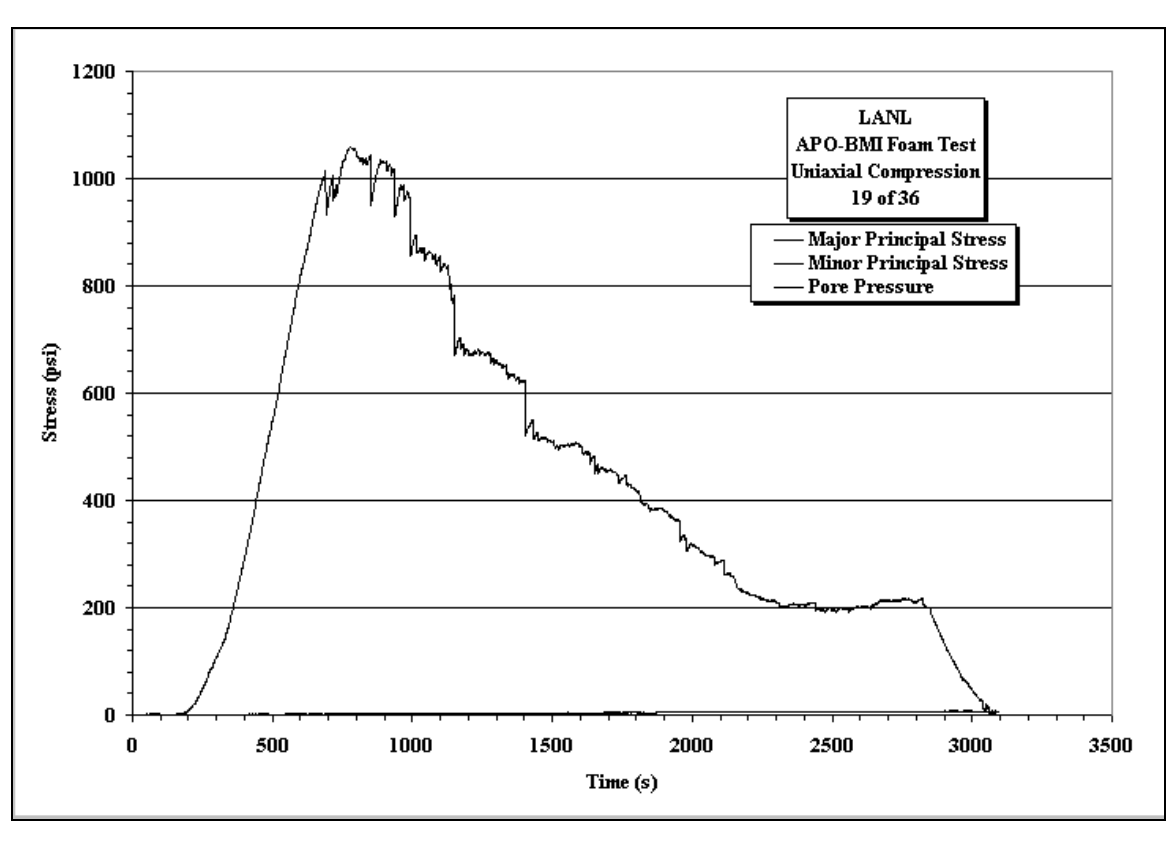


Figure A97. Stress vs. Time and Deviatoric Stress vs. Mean Stress plots for Sample 10of36 under a uniaxial pressure applied longitudinally on sample.



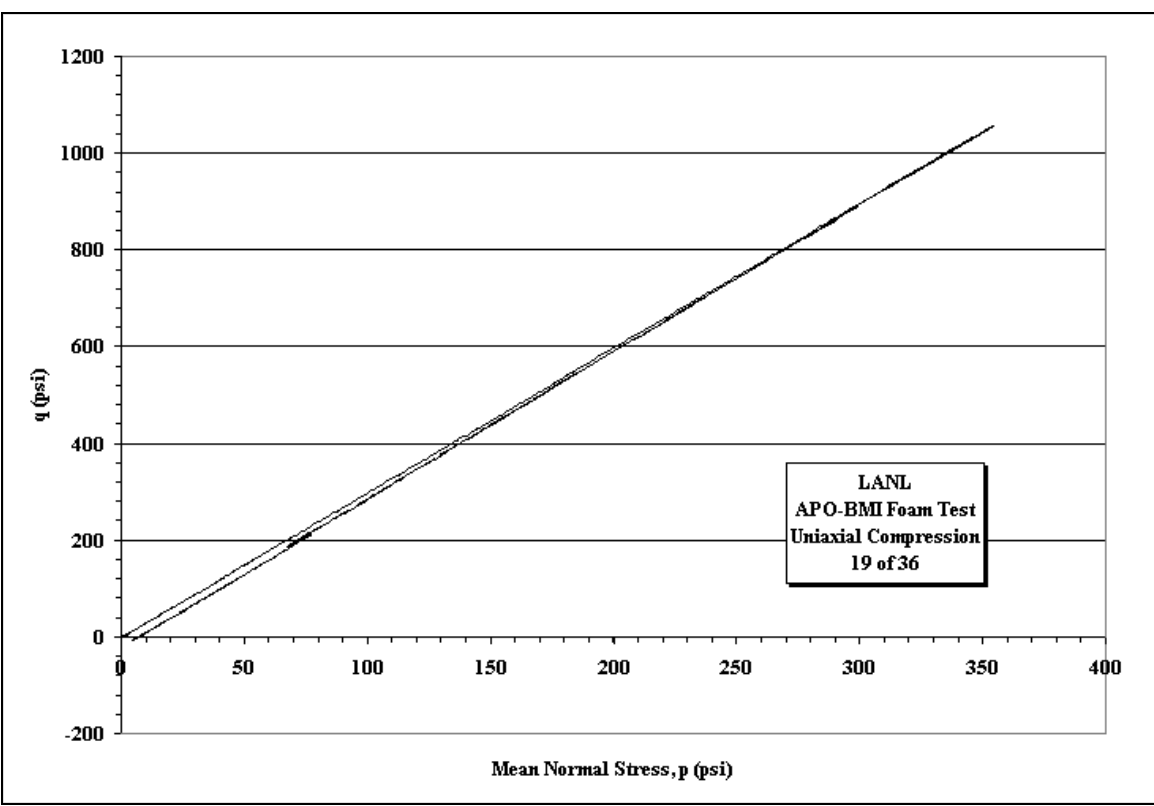
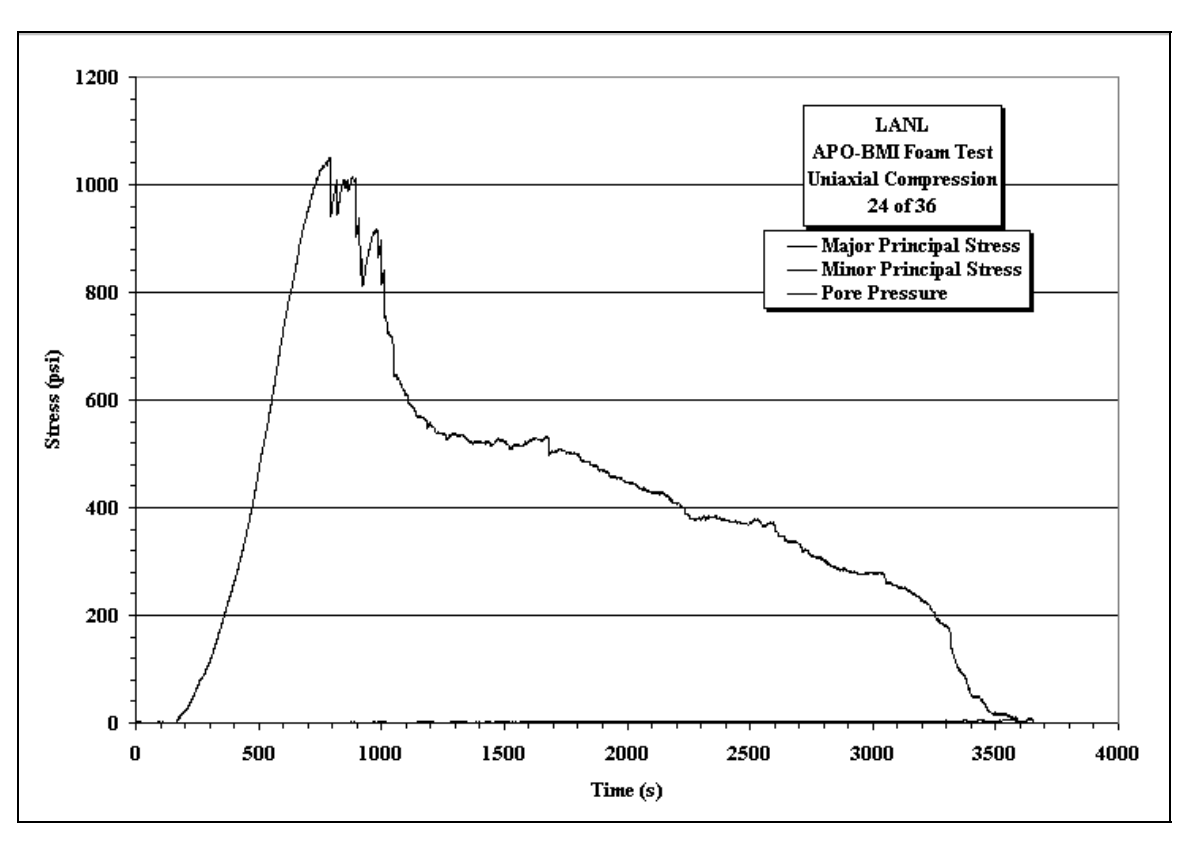


Figure A98. Stress vs. Time and Deviatoric Stress vs. Mean Stress plots for Sample 19of36 under a uniaxial pressure applied longitudinally on sample.



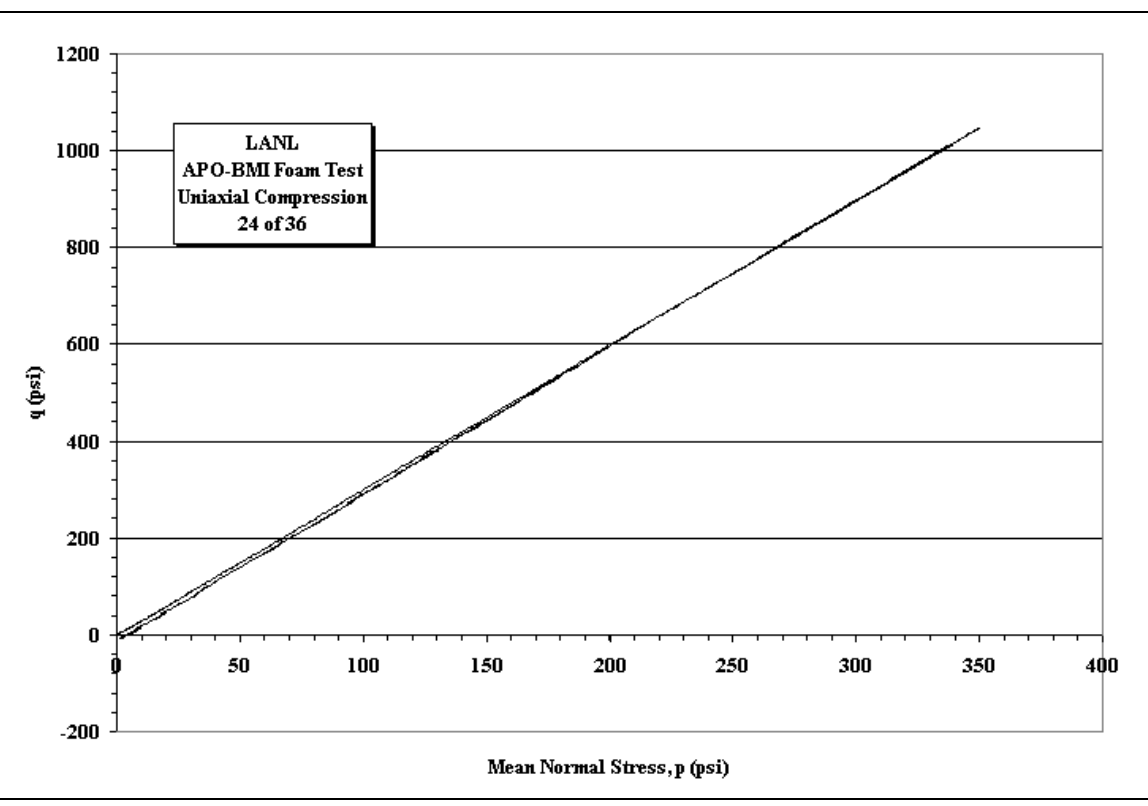
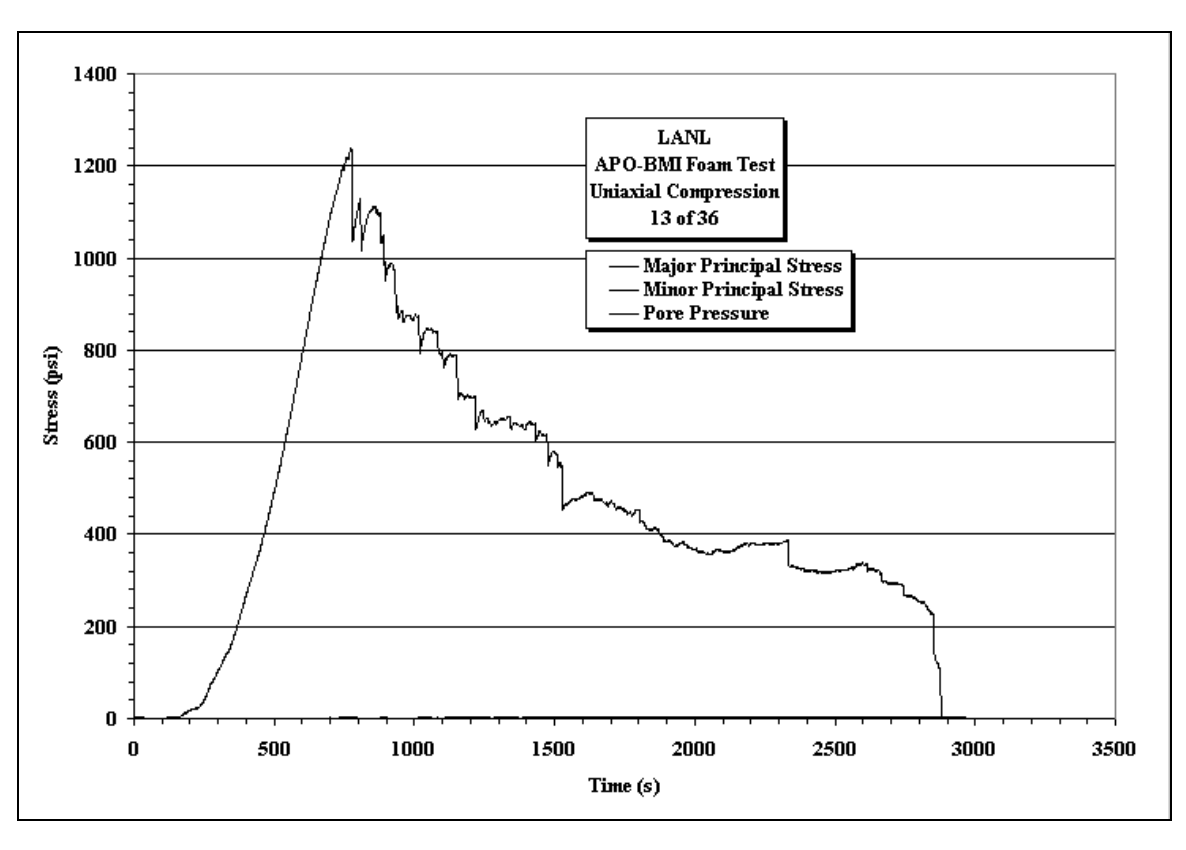


Figure A99. Stress vs. Time and Deviatoric Stress vs. Mean Stress plots for Sample 24of36 under a uniaxial pressure applied longitudinally on sample.



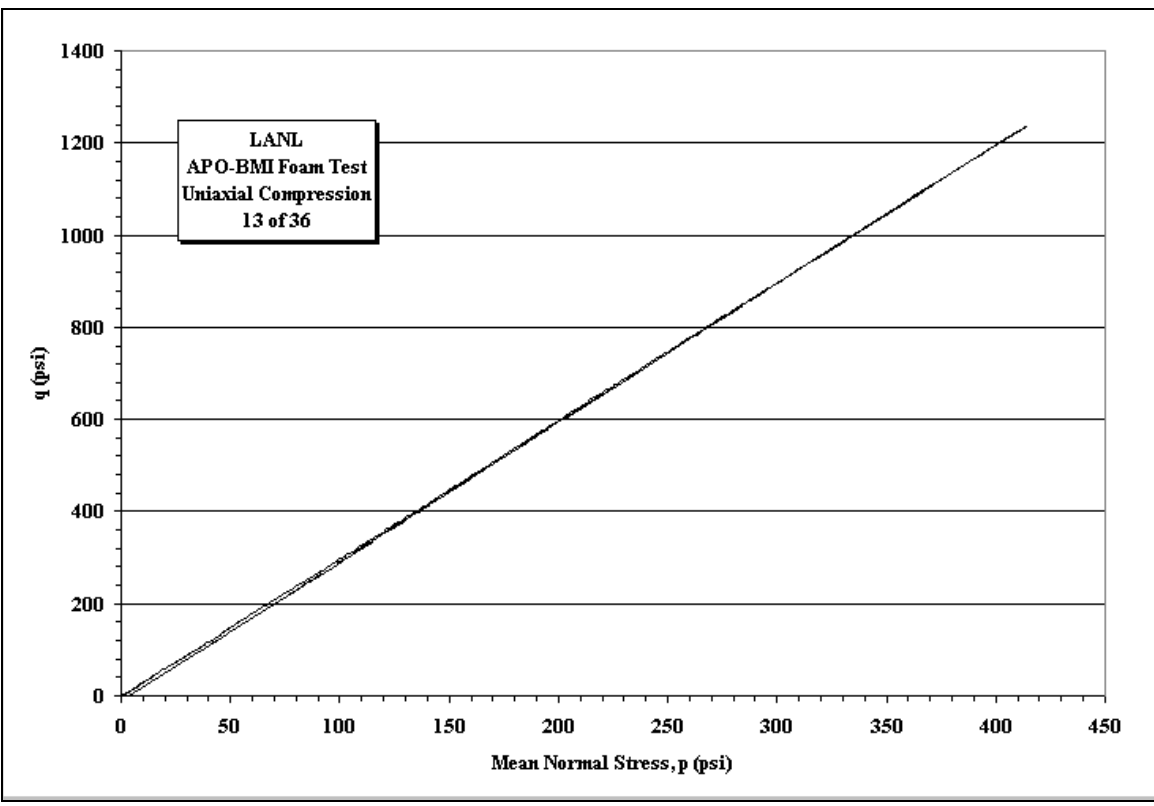
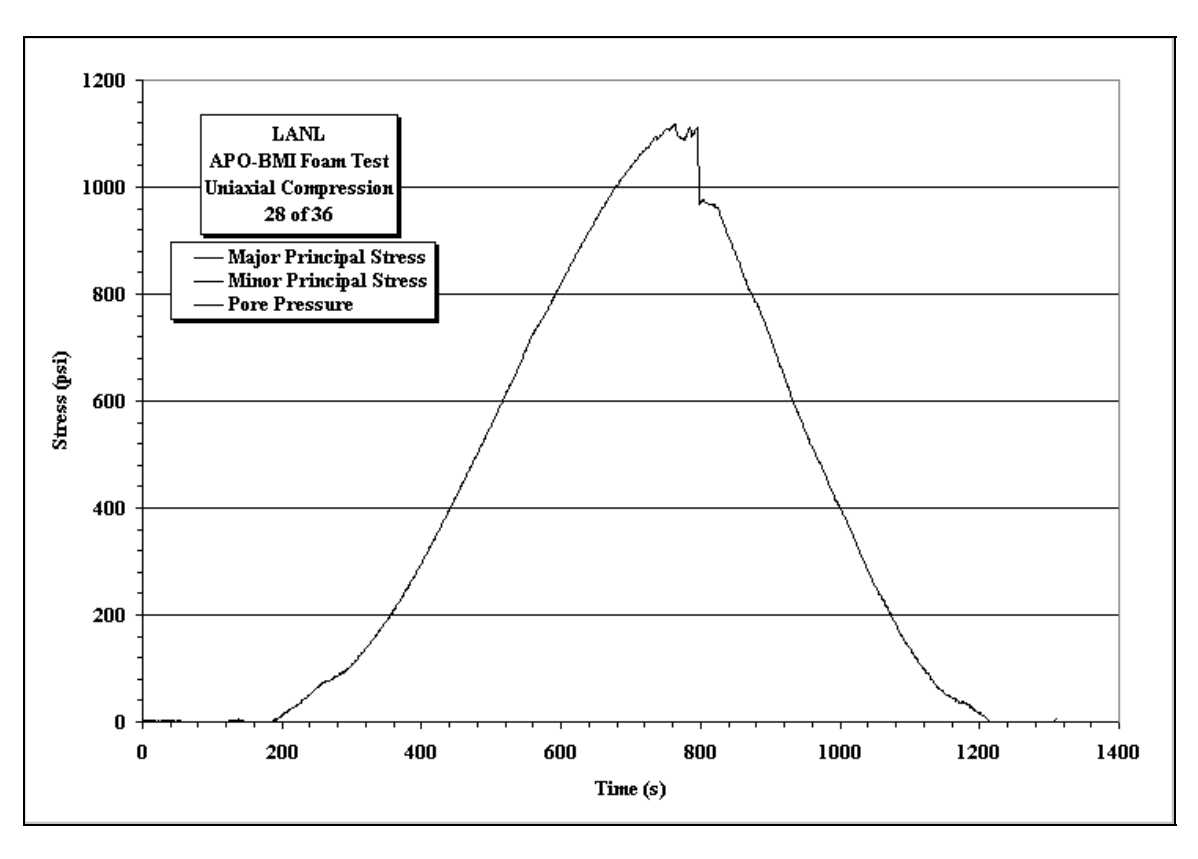


Figure A100. Stress vs. Time and Deviatoric Stress vs. Mean Stress plots for Sample 13of36 under a uniaxial pressure applied longitudinally on sample.



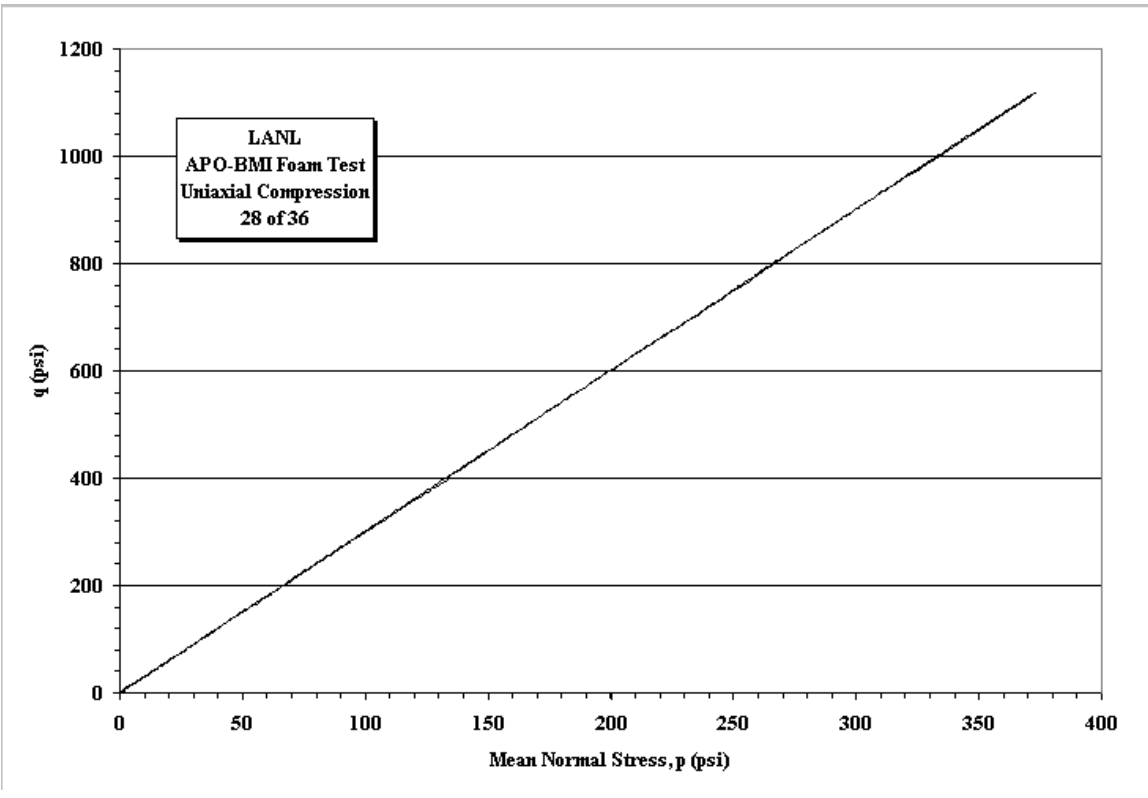
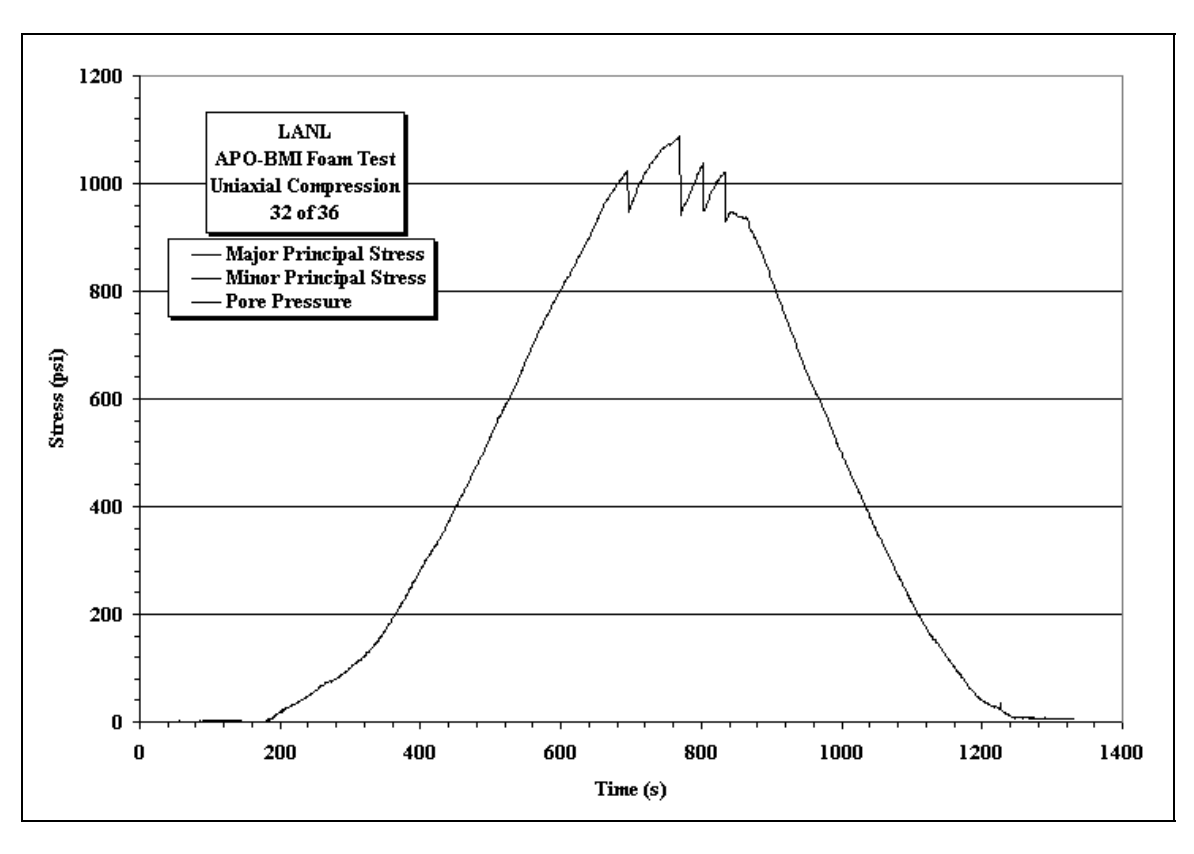


Figure A101. Stress vs. Time and Deviatoric Stress vs. Mean Stress plots for Sample 28of36 under a uniaxial pressure applied longitudinally on sample.



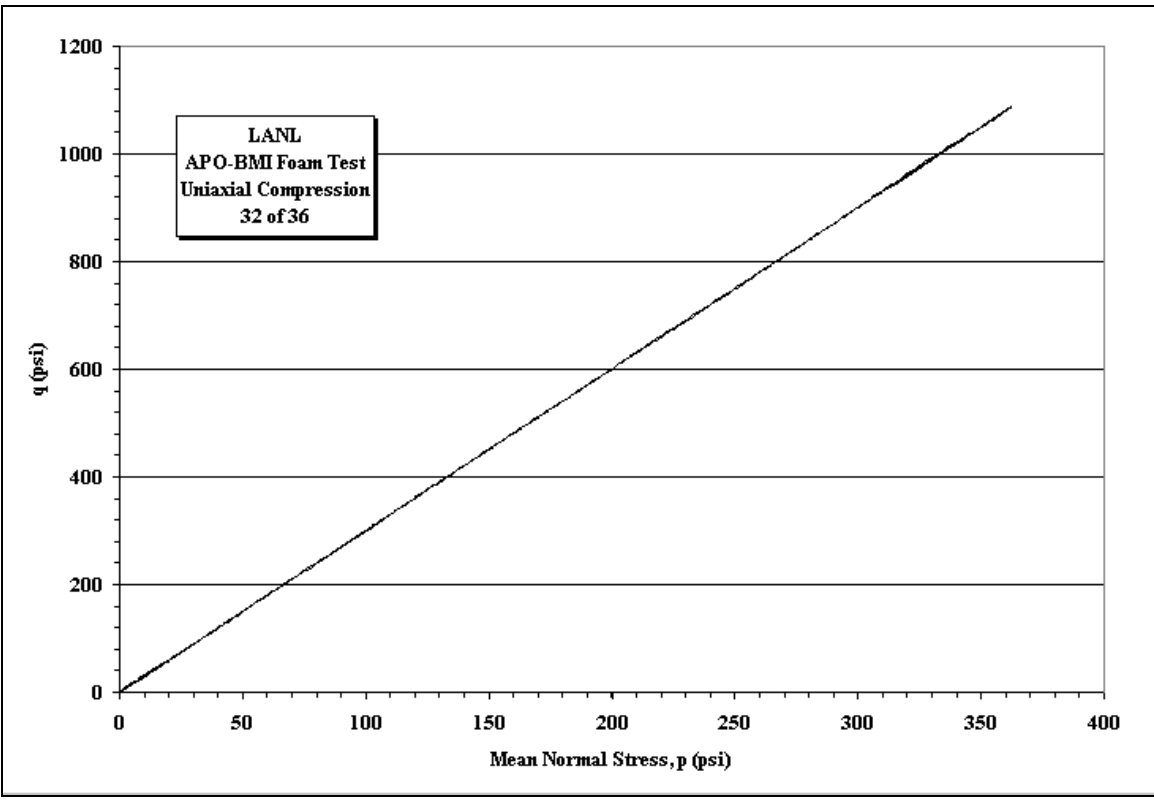
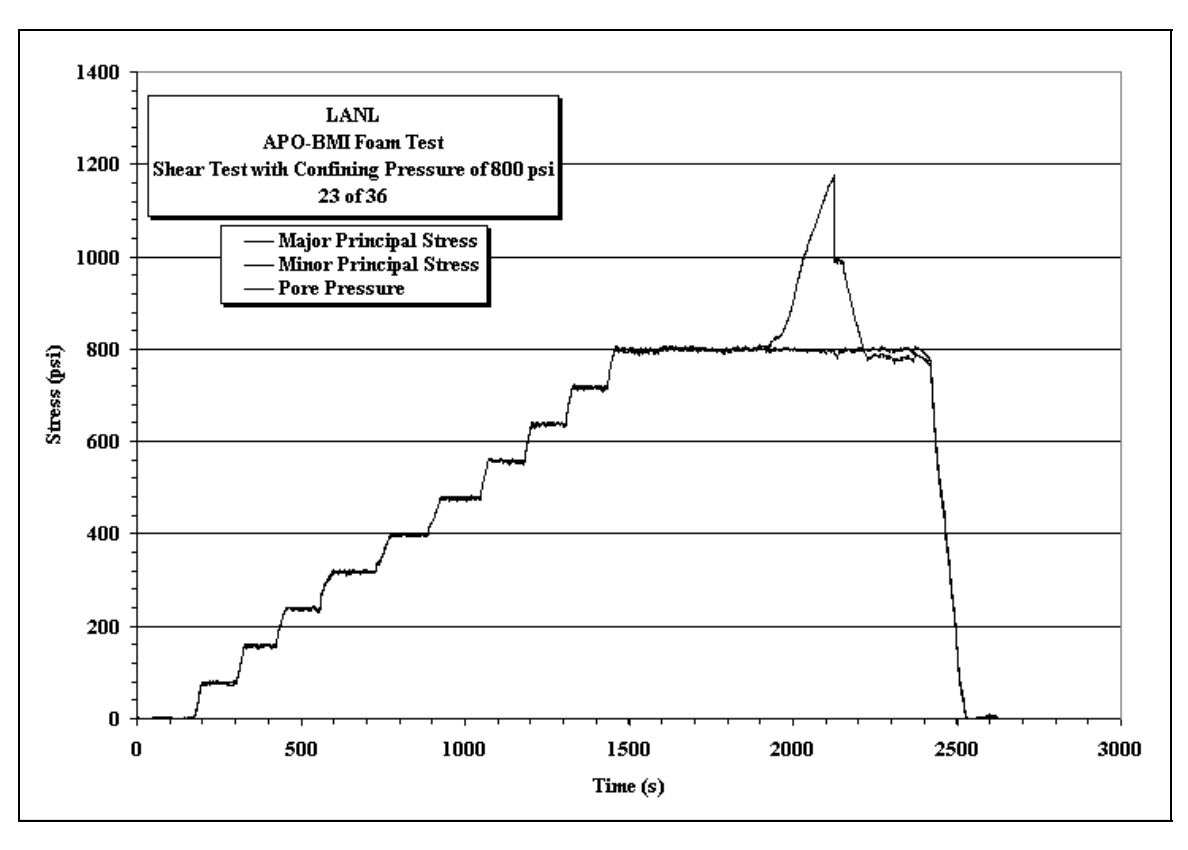


Figure A102. Stress vs. Time and Deviatoric Stress vs. Mean Stress plots for Sample 32of36 under a uniaxial pressure applied longitudinally on sample.



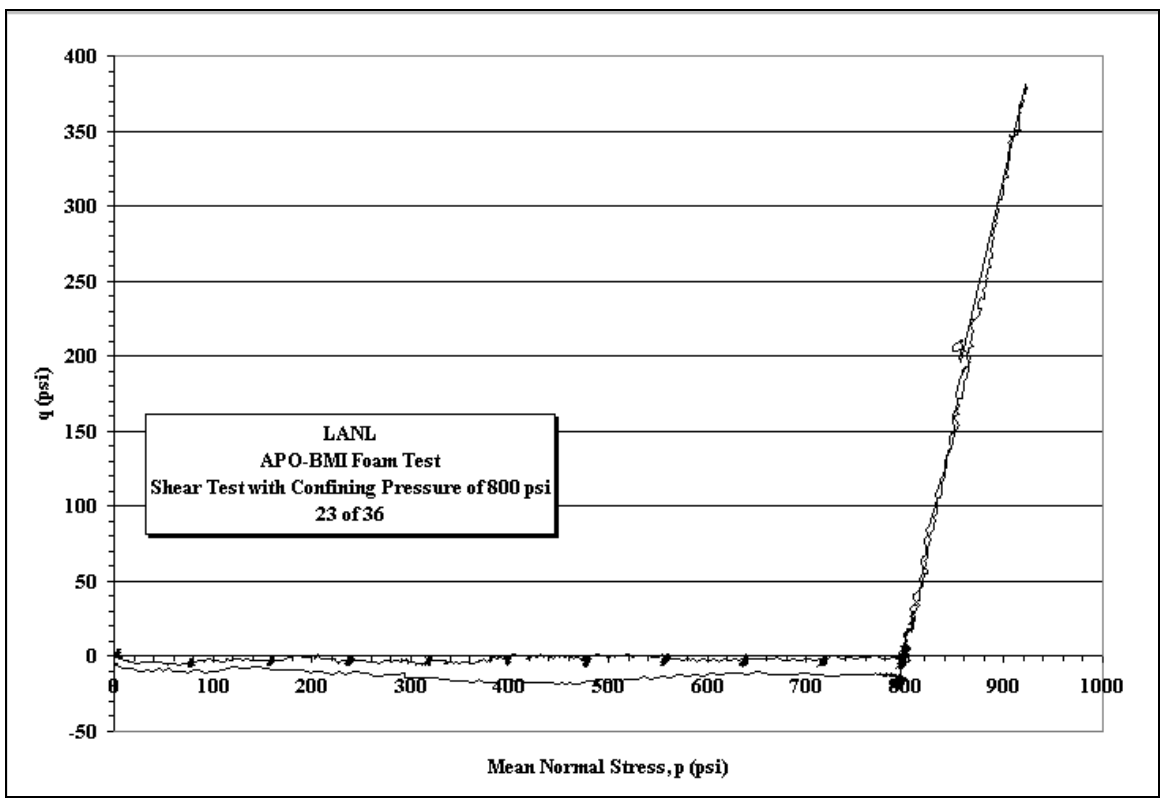


Figure A103. Stress vs. Time and Deviatoric Stress vs. Mean Stress plots for Sample 23of36 with a constant confining pressure of 800 psi.